Nutrient Removal and Fouling Reduction

in Electrokinetic Membrane Bioreactor

at Various Temperatures

By

Chunliang Wei

A Thesis
Submitted to the Faculty of Graduate Studies in Partial Fulfillment of the
Requirements for the Degree of

Doctor of Philosophy

Department of Civil Engineering
University of Manitoba
Winnipeg, CANADA

ABSTRACT

With the aim of mitigating membrane fouling, an electrocoagulation (EC) based electrokinetic membrane bioreactor (EMBR) was developed and operated with real municipal wastewater under low temperatures. Both batch tests and continuous EMBR experiments demonstrated the significant advantages in membrane fouling reduction over the conventional antifouling strategies, ushering its potential applications as an attractive hybrid MBR technology for decentralized wastewater treatment in remote cold regions. The main research observations and findings could be summarized as follows: (1). Effective membrane fouling mitigation at low temperatures was due to destruction of extracellular polymeric substances (EPS) and subsequent reduction of the biocake resistance. The transmembrane pressure (TMP) increased at a much slower rate in EMBR and the filtration resistance was about one third of the control MBR prior to chemical cleaning cycle; (2). A new membrane parameter, the specific fouling rate (SFR) was proposed, relating the fouling rate with permeate flux and temperature-dependent viscosity. Pore clogging and biocake resistances were quantified for the first time with the same membrane module and operating conditions as in regular MBR, rather than resorting to the use of batch filtration setups; (3). The floc size in EMBR did not increase as a result of the air scouring shear force and decrease in the extracellular polymeric substances (EPS); (4). When current intensity was less than 0.2 A, polarity reversal had minimal impact on electrode passivation reduction due to insignificant hydrogen yield, however, if current intensity was above 0.2 A, frequent polarity reversal (< 5 min per cycle) was detrimental to electrode passivation if no sufficient mixing was provided; (5). Viability of the microorganisms in the EMBR system was found to be dependent on duration of the current application and current density. The bacterial viability was not

significantly affected when the applied current density was less than 6.2 A/m^2; (6). Significant

abiotic ammonification was found in electrocoagulation (EC). DO in the treated liquid was

depleted within an hour, under the anaerobic condition in EC, nitrate was chemometrically

reduced to ammonium following a two-step first order reaction kinetics. Aeration (DO > 2 mg/L)

was shown effective in suppressing abiotic ammonification; (7). Magnetic resonance imaging

(MRI) technology was used for the first time as an in-situ non-invasive imaging tool to observe

membrane fouling status in an EMBR.

To My Mother, My late Father and My Late Brother

ACKNOWLEDGEMENTS

First of all I would like to express my greatest gratitude to my doctoral advisor Professor Jan Oleszkiewicz and co-advisor Professor Maria Elektorowicz for offering me the opportunity to conduct this research, for their far-reaching scientific insights, tireless guidance and persistent encouragement during this long journey. They are not only my academic supervisor, but also my life mentors. I am profoundly benefitted by their enduring research enthusiasms and respectful scientific spirits.

I am deeply grateful to Professor Nazim Cicek for his valuable instructions, suggestions and discussions during this thesis work. I would also like to thank all of the examination committee members for their time to review and comment on my thesis.

I wish to express my sincere gratitude and appreciation to the former and present heads of the Civil Engineering Department Professor Peter Rasmussen and Professor Ahmed Shalaby for allowing me to do the research work while working full time.

Thanks also go to the staff in the Civil Engineering Dept. and graduate students in the Environmental Engineering Laboratory for their help.

THE UNIVERSITY OF MANITOBA
FACULTY OF GRADUATE STUDIES

*****

COPYRIGHT PERMISSION

Nutrient Removal and Fouling Reduction in Electrokinetic Membrane Bioreactor at Various Temperatures

By

Chunliang Wei

A Thesis/Practicum submitted to the Faculty of Graduate Studies of The University of Manitoba in partial fulfillment of the requirement of the degree

of

Doctor of Philosophy

(c) 2016

TABLE OF CONTENTS

LIST OF TABLES

Table 2.1 Comparison of various membrane module configurations

Table 2.2 Comparison of external and submerged MBR

Table 2.3 Impacting factors of EPSs in MBR process

Table 2.4 Membrane fouling features and cleaning approaches

Table 2.5 Operating costs of the EC process

Table 2.6 Some of the recent applications of EC in the industrial and municipal wastewater treatment

Table 2.7 Some applications of electrophoresis in the control of membrane fouling

Table 2.8 Examples of membrane fouling reduction in electrokinetically enhanced MBRs

Table 2.9 Examples of Nitrate Removal in the Electrocoagulation Process

Table 3.1 Specifications and operating conditions of ZW-1 membrane module

Table 3.2 Experimental parameters for electrochemical fundamentals

Table 3.3 Feed composition

Table 4.1 Particle size distribution of ASP biomass after electrocoagulation

Table 4.2 Average floc size of another ASP biomass after electrocoagulation

Table 4.3 The production rates of hydrogen gas at various experimented current intensities

LIST OF FIGURES

LIST OF APPENDICES

ABBREVIATIONS AND NOMENCLATURE

$\emptyset$	the electric potential of flat plate electrode (V)
$\emptyset_i$	the electric potential at the inner electrode (V)
$\emptyset_o$	electric potential at the outer electrode (V)
μ_T	the viscosity of permeate (Pa.s),
A_{ox}	activity of the oxidizing agent
A_{re}	activity of the reducing agent
ASP	activated sludge process
BOD	biological oxygen demand
C	the floc strength co-efficient

C_b	concentration of the EPS in the bulk solution (kg/m^3)
C_e	equilibrium concentration of the EPS at the interface (kg/m^3)
CF	crossflow
CIP	cleaning in place
COD	chemical oxygen demand (mg/L)
CST	capillary suction time (s)
d	floc diameter (m)
D	the distance between the electrode plates (m)
DE	dead-end
DEP	dielectrophoresis
DO	dissolved oxygen (mg/L)
DOC	dissolved organic carbon
E	electric field intensity (N/C)
E^0	standard potential of a specific oxidation reduction reaction (V)
E1	estrone
E2	17β-estradiol
E2-Eq	17β-estradiol equivalence
EA	estrogenic activity
EC	electrocoagulation
ED	electrodialysis
EDCs	endocrine disrupting compounds or chemicals
EE2	17α-ethinylestradiol
EF	electroflotation

EMBR	electrokinetic membrane bioreactor
EPS	extracellular polymeric substances
F	Faraday constant
F/M	food to microorganism ratio
F_e	the electrostatic force (N)
F_f	the float (N)
F_g	the gravity (N)
F_h	the hydrodynamic resistance force (N)
FIA	flow injection analyzer
FS	flat sheet
FTIR	Fourier transform infrared spectroscopy
G	the average velocity gradient (s^{-1})
HF	hollow fiber
HRT	hydraulic retention time
HVI	high voltage impulse
I	Electric current
J	Flux ($L/(m^2h)$) or m/s
K	particle collision factor
m	mass of VSS of biocake (per unit surface area), kg/m^2
MBR	membrane bioreactor
MF	microfiltration
MLSS	mixed liquor suspended solids
MLVSS	mixed liquor volatile suspended solids

MRI	magnetic resonance imaging
n	order of reaction for the overall deposition process, respectively, dimensionless
N	the mixing blade speed (rps)
NF	nanoflitration
Nitritation	partial nitrification of ammonia to nitrite
ORP	redox potential (V)
OT	open tubular
P_0	power number of the mixing blade
PE	polyethylene
PES	ployethylsulphone
PP	ployproylene
PVDF	ployvinylidene difluoride
QS	quorum sensing
r	the particle's hydrodynamic radius (m)
R	gas constant
R_b	floc size breakage rate
R_c	membrane surface cake layer resistance
R_{cg}	concentration gradient resistance
R_{ck}	resistance caused by the cake layer
RD	rotary disk
R_f	the net floc size growth rate
R_g	floc size growth rate due to collision
r_i	radius of the inner electrode (m)

R_m	the intrinsic membrane resistance (/m)
r_o	radius of the outer electrode (m)
RO	Reverse osmosis
R_p	the inner membrane pore blockage resistance (/m)
R_{pb}	pore blocking resistance (/m)
R_t	the total filtration resistance (/m),
SCOD	soluble chemical oxygen demand
SEM	scanning electron microscopy
SMEBR	submerged membrane electro-bioreactor
SMP	soluble microbial products
SOUR	specific oxygen uptake rate (mg O_2/g MLVSS. h)
SRF	specific resistance to filtration (/m)
SRT	solid retention time (d)
SVI	specific volume index
SW	spiral wound
T	absolute temperature (K)
t	time, s
TEP	transparent exopolymer particles
TMP	the trans-membrane pressure (Pa),
TN	total nitrogen
TOC	total organic carbon
TP	total phosphorus
TSS	total suspended solids (mg/L)

UF	ultrafiltration
V	volume of the coagulation tank (m^3)
v_e	colloidal particle's electrophoretic velocity
VSS	volatile suspended solids (mg/L)
XRD	X-ray Diffraction
YES	yeast estrogen-screening
γ	the steady state floc size exponent
ε	the energy dissipation rate per unit mass of fluid (Nm/(s. kg^{-1}))
ε_d	dielectric permittivity of water and
κ	fluid conductivity (mho/m)
ξ	zeta potential (V)
ρ_f	density of the particle at 20 ^{0}C
ρ_t	density of the influent at 20 ^{0}C (998.2 kgm^{-3})
ϵ_m	complex dielectric constant of the suspended particle
ϵ_p	complex dielectric constant of the suspending medium
v	kinematic viscosity (m/s)

CHAPTER 1: INTRODUCTION AND OBJECTIVES

1.1 Background and Research Needs

1.1.1 Applications and challenges of the membrane bioreactor in wastewater treatment

Of many challenges facing society today, global water resource crisis is unarguably one of the most imminent ones due to rapid population growth, urbanisation, industrialization and global warming tendency. Clean and fresh water is of vital importance to humanity, however, water scarcity affects the lives of about 40% of people on earth and 1.2 billion of them are suffering from lack of access to clean drinking water today [UNESCO report, 2014]. Increasingly stringent government regulations regarding drinking water quality and wastewater discharge limits drive the demand for efficient water/wastewater treatment and reuse technologies. Membrane filtration and membrane bioreactors (MBR) are among technologies used to address the world-wide water shortage issue.

Membrane separation is a physical process that uses porous membranes as a barrier to retain the particulates in a suspension through size exclusion. Before the 1970s, it was mainly used for water purification such as seawater desalination. In the last three decades membrane filtration has been extended to wastewater treatment first as an alternative to a secondary clarifier and then directly integrated into the conventional activated sludge tank, called submerged MBRs.

Compared to a typical activated sludge process (ASP), MBRs offers advantages such as smaller footprint, reduced sludge production, operating flexibility or automation and most importantly, consistent and superior effluent quality including higher removal efficiency for emerging

26

chemicals such as endocrine disrupting compounds (EDCs). In addition to the water demand and regulatory drivers, continuously decreasing membrane costs, process maturity and suitability for retrofit of existing wastewater treatment plants collectively contribute to broadening application of MBR today [Judd, 2011]. Global membrane market value has increased at an annual rate of 12% in the last twenty years and is expected to grow at an accelerating annual rate of 15.28% and to reach US$ 2.9 billion by the year of 2019 [PRNewswire, 2015].

In spite of increasing world-wide MBR applications, membrane fouling remains the major challenge. Membrane fouling, a phenomenon due to pore clogging or cake formation on the membrane surface, leads to decrease in permeate flux or increase in transmembrane pressure(TMP), and consequently, shortens the intervals for membrane cleaning cycles and lifetime of membrane modules. The ultimate effect of fouling is the higher operating cost in comparison to the conventional ASP, which is usually the main concern of industry. Therefore, MBR research has focused on fouling control strategies since the onset of this technology [Gkotsis et al., 2014].

According to Judd [2011], membrane fouling develops in three progressive stages resulting from pore blocking and cake filtration, i.e. conditioning fouling, slow/steady fouling and finally TMP jump. In the stage of initial conditioning fouling, the small particles or colloids in the fluid are adsorbed or sucked into the membrane pores, the extent and initial conditioning fouling rate are associated with the membrane characteristics such as pore size and chemical polarity etc. and concentration of extracellular polymeric substances (EPS). The steady fouling starts when the filtration cake layer is formed on the membrane surface. The growth of the cake layer is a

dynamic process and requires certain time to reach the maximum cake thickness, during this period of time membrane fouling increases steadily. Finally, when the biocake covers the entire membrane surface and the local flux is higher than the critical flux, the fouling suddenly aggregates and causes the sudden TMP increase.

It is widely accepted that EPS in the filtration medium are the main foulants [Meng et al., 2009; Judd et al., 2011; Potvin and Zhou, 2011]. EPS are the polymeric compounds including carbohydrates, proteins, nucleic acids present on or outside the cellular surface and in the microbial aggregates such as biofilms, flocs and sludge. It is vital for the survival of microorganisms because it glues the cells together and protects them from external invasion. EPS are rich in negatively charged groups such as carboxyl, phenolic, alcoholic, hydroxyl, phosphoric and sulfhydryl as well as nonpolar radicals such as aromatics and aliphatics, carbohydrate chains etc., the duality of hydrophilic and hydrophobic structures make EPS capable of wetting and cross-linking both hydrophilic and hydrophobic surfaces. It is widely agreed that EPS concentration positively affects membrane fouling through the following mechanisms: (1). EPS as a highly hydrated gel covers the membrane surface and prevents water from permeating membrane. Polysaccharide-like foulants are neutral in terms of the electric charge. Interaction between EPS molecules and membranes include dipole-dipole attraction and hydrogen bonding etc; (2). Higher EPS cause quicker formation of biocake on the membrane surface. EPS bind the microbes together and are embedded in the deep layers of biocake, which not only contribute to formation and growth of the biocake, but also assist in strengthening the mechanical stability of biocake.

In the last three decades, numerous studies have been conducted to prevent or mitigate

membrane in MBR operation [Meng et al. 2009; Jiang et al., 2005; Wu et al., 2006; Monclùs et

al., 2010; Ramos et al., 2014]. Strategies include: membrane material modification, MBR

configuration optimization, feed pretreatment [Kraume et al., 2009], control of MBR operating

conditions including hydraulic retention time (HRT), solid retention time (SRT) and air scouring

intensity etc., coagulation addition into the biomass [Citulski et al., 2008; Chen et al., 2012;

Vanysacker et al., 2014], the application of ozone [Wu et al., 2010], electric field [Bani-Melhem

et al., 2010; Bani-Melhem et al., 2011; Wei et al., 2012; Liu et al., 2012; Akamatsu et al., 2010]

and ultrasound [Sui et al., 2008; Xu et al., 2009]. In spite of varying successes with those fouling

mitigation technologies, more effective antifouling strategies are sought for industrial MBR

applications.

1.1.2 Electrokinetic technologies in MBR wastewater treatment

Electrokientic technologies, including electrophoresis-based electrofiltration, dielectrophoretic

flux enhancement and electrocoagulation (EC), have been increasingly investigated as promising

membrane fouling control strategies in the recent years. Electrophoresis and dielectrophoresis

(DEP) function through an electrokinetic mechanism, i.e. relying on uniform or non-uniform

electric field to distract fouling particles away from the membrane surface [Yang et. al., 2002].

In EC, the electrochemical functionalities will be multilateral: i.e. simultaneous chemical /

biological oxidation and reduction, coagulation and flotation, consequently a variety of

contaminants such as heavy metal, oil, suspended solid and phosphorus etc. may be removed.

Due to in situ generation of high valence metal ions and the resulting hydroxides through

hydrolysis, the colloidal particles are aggregated to form larger flocs, which subsequently

increases the porosity of biocake and thus improves the membrane flux. Furthermore, the freshly

generated coagulants adsorb the EPS, the major suspected membrane foulant in bulk media,

which in turn affect the growth kinetics and structural characteristics of biocake on the

membrane surface. Compared to various afore-mentioned membrane fouling control approaches,

the electrokinetic technologies are applicable to a variety of industrial and municipal wastewater

treatment of all scales. Their simple and compact configurations require small space, making

installation and scale-up easy and highly flexible. In addition, the electrophoretic behavior and

electrochemical reactions are quantifiable, which means consistent treatment outcomes are

usually predictable. Electrokinetic technologies require no chemicals and produce less sludge

compared to conventional coagulant based fouling control methods. Finally, automation of the

electrokinetic technologies is easy to implement with low capital investment and operating costs.

In electrofiltration, a direct current field is applied in the direction of filtration flow, the

negatively charged colloidal particles are subjected to the electrophoretic force and have a

tendency to overrun the hydrodynamic resistance force and move against the fluid flow or away

from the membrane surface. As a result, formation of the membrane surface cake can be

eliminated or significantly mitigated under sufficient electrical field strength. The filtration

resistance is thus decreased and permeation flux is increased accordingly.

The fundamental physical mechanism underlying DEP is the interaction of induced dipoles of

colloidal particles with a spatially non-uniform electric field. When subjected to an external

electric field, a neutral suspension particle and the surrounding medium in a colloidal solution

tend to be polarized and the colloidal particle therefore becomes a dipole. In the presence of a

non-uniform external electric field the colloidal particles are subjected to a dielectrophoretic force, which drives the particles to move in the direction of the electric field and away from the membrane.

A new type of hybrid MBR called Submerged Membrane Electro-bioreactor (SMEBR) was developed and extensively studied in recent years [Bani-Melhem et al., 2010; Bani-Melhem et al., 2011; Ibeid et al., 2013; Hasan et al., 2012; Ibeid et al., 2013; Hasan et al., 2014]. The membrane module of SMEBR is encircled by a pair of cylindrical meshed electrodes, consequently various physical, chemical and biological processes occur simultaneously in the reactor. The main physical phenomenon is electrokinetic migration of the biomass flocs away from the membrane surface. The chemical processes include in situ releasing of metal ions as efficient coagulant and precipitation of phosphate. Finally, the core SMEBR is still an activated sludge reactor, where biological nitrification and organic matter mineraliztion process occurs.

Electrokinetic processes including EC have been reported to be effective antifouling technologies for membrane filtration [Ibeid et al., 2013; Hasan et al., 2014]. However, there are two drawbacks for the electrophoretic and dielectrophoretic methods. Because of the weak repelling electrophoretic force between fine particles in the biomass and membrane surface, usually electric fields at a magnitude of 10K v/cm need to be applied to obtain a significant biocake prevention effect. Such a high voltage will cause substantial water hydrolysis and produce explosive hydrogen gas, generate high joule heat and most importantly, will inactivate microorganisms critical to the biological process. Second, the electrophoretic and dielectrophoretic antifouling technologies require relatively stationery fluid, but in MBRs aeration is indispensable for aerobic biological process and membrane surface scouring.

Therefore, it is impractical to apply the electrophoretic and dielectrophoretic antifouling technologies to MBRs in the wastewater treatment. In fact, all of the published works were conducted in bench scale for membrane filtration in water treatment.

The EC based SMEBR technology is the most promising electrokinetic technology for MBR antifouling [Bani-Melhem et al., 2010; Ibeid et al., 2013; Hasan et al., 2014]. The sporadic studies (1 to 2 papers per year) in the last five years leave some fundamental and application issues to be addressed, such as fouling reduction mechanisms, impact of electric current on bacterial viability, electrochemical reduction of nitrate into ammonium and electrokinetic effect on EDC destruction or attenuation. With respect to application, no work has been reported about whole nutrient removal including denitrification, and especially on MBR performance at low temperatures which is a typical challenge for a conventional MBRs due to acceleration of fouling mechanisms.

1.1.3   Fundamental issues to be addressed in the electrokinetic technologies

Due to increasing application of electro technologies in processes involving microorganisms, impact of electrical current on the microbial metabolism and viability has been investigated over the past two decades [Jass et al., 1995; Jackman et al., 1999; Sethuraman et al., 2008; Wei et al., 2012; Dong et al., 2015]. The proposed mechanisms of the antibacterial activity include: (1) damage on cell membranes leading to irreversible permeabilization and leakage of essential cytoplasmic constituents; (2) electrochemically generated biocides or antimicrobial agents (e.g., H_2O_2, oxidizing radicals, ozone, and chlorine molecules); (3) pH elevation in a non-buffered

system due to cathodic reductive electrolysis, which inhibits microbial metabolism, especially in the localized vicinity of the electrodes; (4) direct oxidation of enzymes or coenzymes essential to bacterial viability; and (5) accretion of metal ions on or in bacterial cells interferes with the physiology of microbes [Davis et al., 1991]. The previous bacterial viability studies mostly focused on pure cultures of specific strains in synthetic cultivation media. Few investigations have explored the influence of electric current on bacterial growth and survivability in mixed cultures, especially for the microorganisms in an MBR system.

Apart from the biologically negative impact on microbes, the chemical side effects of electric application on the treatment performance are usually neglected or overlooked, e.g. reversal of nitrification or electrochemical reduction of nitrate into ammonium. Electrochemical treatment of nitrate has been applied to industrial wastewater such as low-level nuclear wastes, and effluent from regeneration of ion exchangers [Hansen et al., 1996; Bouzek et al., 2001; Chen et al., 2004]. It has also been used for denitrification of groundwater [Hofmann et al., 2006; Lacasa et al., 2011; Hossini et al., 2014]. Selective reduction of nitrate to nitrogen is difficult to achieve due to the chemical valence complexity of elemental nitrogen and the potential for substantial amount of nitrate that may be converted to ammonium. In spite of the coexistence of electrokinetic technologies and electrochemical nitrate removal processes for years, they were studied or operated independently with different objectives and consequently. Electrochemical generation of ammonium from nitrate was largely ignored in the electrokinetic processes such as electrofiltration, electroosmosis, electro-dewatering and electrocoagulation. Therefore, the underlying kinetics leading to ammonium yield still remains to be elucidated and the strategies to prevent abiotic ammonification need to be explored.

33

Temperature is an important factor, significantly affecting microbial activity and growth rate in the activated sludge process (ASP). Low temperature can be directly related to intensified de-flocculation, poor biomass settleability, reduced solubility and deteriorating treatment efficiency. In MBRs, the adverse influence of low temperature becomes more intolerable because the increase in the liquid viscosity and EPS concentration significantly aggravate membrane fouling making this technology less applicable in cold regions. Canada is a vast high latitude country with thousands of sparsely populated small communities remotely located in the north of the continent, with about 6 million people living in communities with population less than 5000. Geographical isolation, wide population scattering and harsh climatic conditions make extensive sewer networks uneconomical, so exploration of MBR for decentralized wastewater treatment is attractive for discharge compliance and water environmental protection in small communities.

1.2 Objectives of the thesis

Membrane fouling remains the major challenge for broader MBR application in practical wastewater treatment, especially at low temperatures. The recently emerged electrokinetic technology such as SMEBR provided a new approach to mitigate membrane fouling; however, it was only tested at ambient temperatures. Based on the Global Membrane Bioreactor Market 2014-2018 research report [PRNewswire, 2015], application of "green" MBR is becoming an increasing trend globally. The green MBR is characterized by high energy efficiency, easy installation / maintenance and enhanced phosphorus removal. The research aims to lay a foundation for such a green MBR, with the following objectives:

1. Investigate the fundamentals of the electrically enhanced membrane bioreactor (EMBR) with regard to impacts of electric current on (a) pH; (b) zeta potential; (c) EPS; (d) capillary suction time (CST); (e) membrane filtration enhancement; (f) electric efficiency; (g) generation and oxygen dependence of the metal cationic species; (h) suppression of precipitation on the electrode surface; and (i) bacterial viability;

2. Determine and quantify electrochemical reduction of nitrate into ammonium and find strategies to mitigate that effect;

3. Develop an EMBR system for total nutrient removal at ambient temperature;

4. Optimize an EMBR system fed with synthetic wastewater for membrane fouling suppression at ambient temperature;

5. Develop principles of membrane fouling retardation in an EMBR system fed with real municipal wastewater at low temperatures;

6. Determine the technical feasibility of using an EMBR as an alternative decentralized wastewater treatment system with improved nutrient removal and reduced membrane fouling in cold regions.

1.3 Thesis organization

This thesis presents the fundamentals of the electrokinetic technology and its application as a preventive strategy for the MBR fouling at low temperatures. There are six chapters in the thesis. This chapter outlines the project background, research needs, overall objectives and organization of this thesis.

In Chapter 2, the membrane separation technology and MBR in the wastewater treatment are described. Focus is on the nature, mechanism and inhibition /mitigation technologies of membrane fouling. This is followed by a review of development and application of various electrokinetic technologies including EC, especially the findings and theoretical foundation of membrane fouling suppression. The last part of Chapter 2 covers some of the electrochemical fundamentals which provide insight into the potential side effects of the electrokinetic technologies with emphasis on abiotic ammonification and antibacterial influence. Material and experimental methodologies are described in Chapter 3, including the multipurpose DC power supply unit, membrane module, instruments for analyses of CST, zeta potential, TMP, magnetic resonance imaging (MRI), X-ray Diffraction (XRD), Fourier transform infrared spectroscopy (FTIR), dissolved organic carbon (DOC), flow injection analyzer (FIA), particle size, and analytical methods for specific volume index (SVI), ammonium, nitrate, nitrite, phosphate, transparent exopolymer particles (TEP), EPS, pH, dissolved oxygen (DO), redox potential (ORP) and conductivities etc. In addition, the experimental setups and operations are chronologically presented for investigations on the fundamentals of EMBR, development of an EMBR system for total nutrient removal in synthetic wastewater, optimization of the EMBR system towards membrane fouling suppression at ambient temperature and demonstration of membrane fouling retardation with real municipal wastewater at low temperatures. In Chapter 4 the research results and findings are presented and illustrated with figures and tables. Also included in this chapter is discussion and interpretation of the experimental observations, challenges and solutions to the potential application problems. Chapter 5 presents the engineering significance of this research, with particular strategies addressing some of the key technical challenges for practical application of the electro kinetic technology in MBR process. The electrokinetically related

operating costs are briefly discussed and compared with the other electrokinetic technologies including EC. Lastly, Chapter 6 summarizes the main observations, findings and general conclusions from this research.

CHAPTER 2: LITERATURE REVIEW

2.1 Membrane Bioreactor (MBR)

2.1.1 Membrane separation technology

Membrane filtration can be tracked back into the 18th century, it is a separation process in which particulate substances are retained by a physical barrier called a membrane based on the principle of size exclusion [Judd, 2011]. Modern membrane technology emerged in the early 1960s when Loeb and Sourirajan pioneered seawater desalination with the invented cellulose acetate RO membrane [Mulder, 2000; Mastsuura, 2001]. Since then membrane technology has experienced continuous and accelerated development.

The driving force for membrane separation is a pressure gradient between the influent and effluent sides of the membrane module, called TMP, though it may also be assisted by electric potential gradient, temperature gradient or concentration gradient. Compared to the conventional phase separation methods such as vaporization, condensation and crystallization, membrane technology offers many prominent advantages, including greatly reduced energy consumption, less chemical use, reliable product quality, scale flexibility and potential for full automation [Aptel et al., 1993, Jacangelo et al., 1997; Bodzek and Konieczny; 1998]. In the past 40 years membrane filtration technologies have been widely used in surface water treatment for potable water supply, industrial wastewater treatment and disinfection [Bechtel et al., 1988; Roche et al., 1993; Madaeni et al., 1995; Le-Clech et al., 2006].

2.1.1.1 Membrane materials

Membranes used in water purification / wastewater filtration processes usually are composed of finely porous synthetic materials made of ceramics or polymers [Mulder, 1996; Le-Clech et al., 2006]. Ceramic membranes are produced from metal oxides such as zirconia oxide, aluminium oxide and titanium oxide, etc. Polymeric membrane materials generally include ployvinylidene difluoride (PVDF), ployethylsulphone (PES), polyethylene (PE) amd ployproylene (PP), etc. Ceramic membranes are chemically stable, mechanically stronger and have much longer lifetime, however they are much more expensive than the polymerics [Owen et al., 1995; Baker, 2000], which limits their broader use. As the particles in the feed water are usually negatively charged [Judd, 2006], hydrophilic membrane surfaces are typically preferred for reducing membrane fouling, which will be discussed further in the following sections.

2.1.1.2 Membrane configuration

The membrane is manufactured into modules for convenience of installation and maintenance. A module is generally an operational unit into which membranes are engineered [Judd, 2006; Bruggen et al., 2003] and typically includes elements such as membrane, support structure, feed inlet, permeate outlet and retentate outlet port etc. 5 major module configurations [Mallevaille, 1996; WEF, 2006] have been developed and employed in the membrane processes, i.e. plate and frame / flat sheet (FS), hollow fiber (HF), Open tubular (OT), spiral wound (SW) and rotary disk (RD). In the wastewater treatment processes, FS, HF and OT are the most used configurations, as shown in Fig. 2.1. FS and HF are basically the so called "outside in" filtration mode, i.e. the fluid

to be filtered is outside the membrane module, and permeate is driven by the suction pump to pass the membrane wall. On the other side, OT belongs to "inside out" filtration mode, meaning the fluid medium flows inside the tubular membrane module and penetrates the membrane wall outward typically driven by pressure gradient.
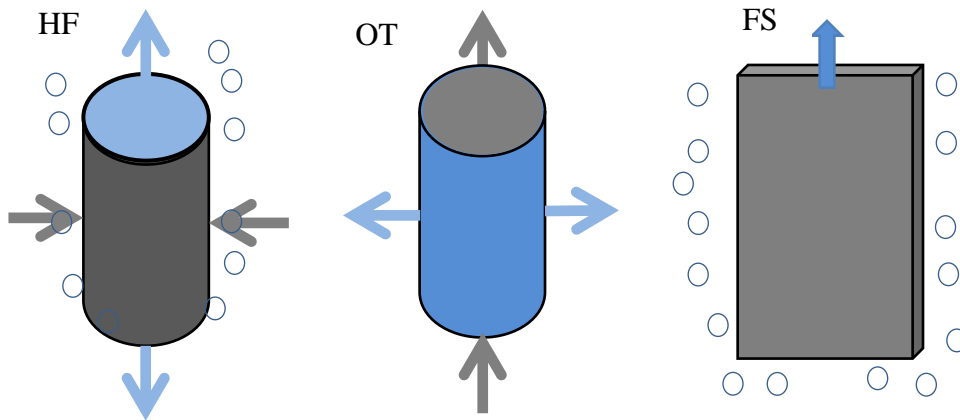
Fig. 2.1 Schematic of the most used membrane configurations

in wastewater treatment (dark grey: before treatment, blue: permeate)

The structural difference of the above membrane module configurations determines their operational characteristics, performance, cost as well as applicable areas [Ripperger et al., 2002; Laine et al., 2000]. Table 2.1 presents a systematic comparison of all module configurations in terms of packing density, turbulence enhancement, ease of cleaning, fouling resistance, cost and application.

Table 2.1 Comparison of various membrane module configurations
[Judd, 2006; WEF, 2006]

Configu-ration	Packing density	Turbulence enhancement	Ease of cleaning	Fouling resistance	Cost	Application
FS	Low	Fair	Fairly easy	High	High	ED, UF, RO
HF	High	Very poor	Difficult	Medium	Very low	MF/UF, RO

40

OT	Very low	Very good	Easy	High	Very high	CFMF/UF, NF
SW	High	Poor	Difficult	Medium	Low	RO/NF, UF
RD	Very low	Excellent	Fairly easy	Very high	High	Submerged MBR

Note: ED = electrodialysis   UF = ultrafiltration   RO = Reverse osmosis
       DE = dead-end   CF = crossflow   NF = nanoflitration
       MF = microfiltration

2.1.1.3 Dead end filtration and crossflow filtration

According to the feed flow direction, membrane operation in wastewater treatment applications can also be classified into dead-end filtration and crossflow filtration [Le-Clech et al., 2008; Cabassud et al., 2001]. In dead-end filtration, all of the filterable components (water molecules and soluble species) are forced to perpendicularly pass the membrane surface and the rest in the feed flow is left on or in it. In crossflow filtration, the feed flow travels in parallel with the membrane surface; a portion of the feed flow passes the membrane and forms a secondary flow on the other side of the membrane surface, which generates a shear force to avoid accumulation of particles on the membrane surface. Therefore, crossflow operation is superior to the dead-end filtration in terms of fouling tendency and tolerance, especially when the wastewater contains high concentration of solids. Examples of dead end filtration and crossflow filtration are flat sheet /hollow fiber and open tubular membrane, respectively, as shown in Fig. 2.1.

2.1.1.4 Membrane classification

According to the nominal pore size of membrane, membranes used in water and wastewater treatment can be categorized into four classes: microfiltration (MF), ultrafiltration (UF),

nanofiltration (NF) and reverse osmosis (RO). As shown in Fig. 2.2, the green arrow represents penetration of a component on the particular membrane class. E.g. ultrafiltration membranes allow only ions to pass but retain all of solids, colloids, virus and bacteria, they tend to be the most popular class of membrane used in the water and wastewater treatment processes.
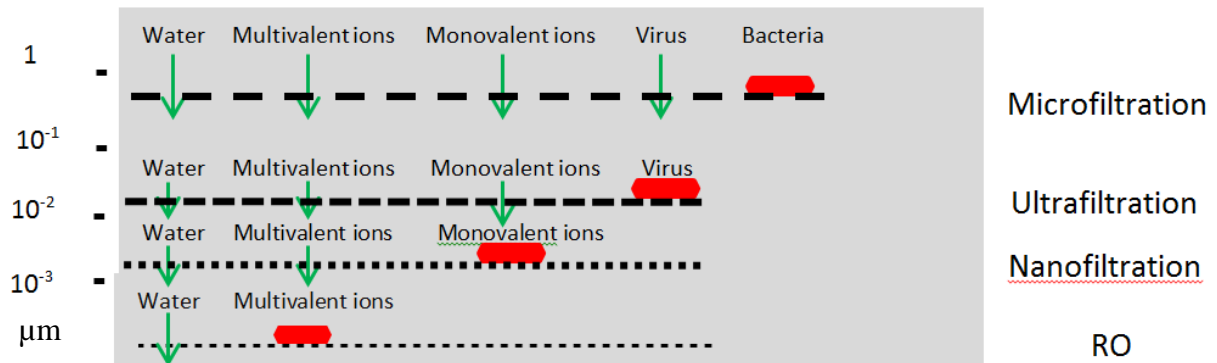
Fig. 2.2 Schematic representation of membrane classifications (adapted from Judd [2011])

2.1.2 MBR in wastewater treatment

2.1.2.1 Brief introduction

First introduced in late 1960s by Dorr-Oliver Inc., ultrafiltration (UF) and microfiltration (MF) were integrated into the conventional activated sludge wastewater treatment train to eliminate the seconady clarifier [Bemberis et al., 1971; Merlo et al., 2004; Judd, 2006; Yang et al., 2006; Mohammed et al., 2008]. As shown in the Fig. 2.3 (B) and (C), in comparison with the conventional activated sludge process, MBR offers prominent advantages such as smaller footprint, reduced sludge production, operating flexibility or automation and most importantly, consistent and superior effluent quality which is independent of MLSS [Han et al., 2005; Khor et al., 2006; Sun et al., 2007; Merz et al., 2007; Tian et al., 2009].

42
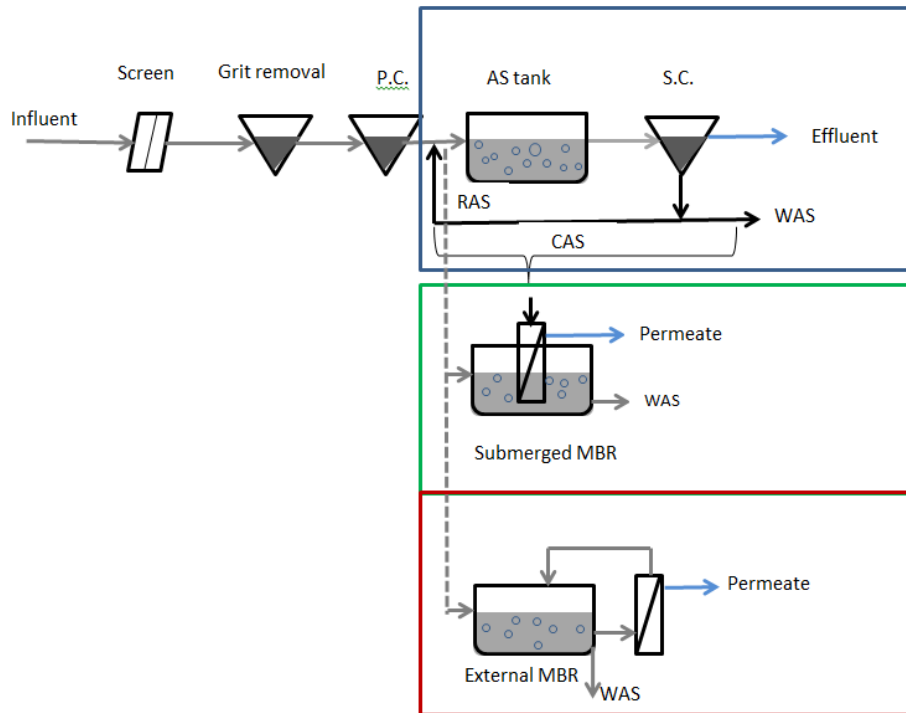
Fig. 2.3 Schematic of CAS, Submerged MBR and External MBR

2.1.2.2 Constant pressure and constant flux operating modes

In terms of the flux withdrawing characteristics there are two operating modes: constant TMP

mode and constant flux mode. In the constant TMP mode, filtration is driven by constant

pressure and permeate flow rate is the highest at the beginning but decreases gradually over time

due to membrane fouling, whereas in the constant flux mode, the permeate flow rate is generally

unchanged but TMP goes up over time. Constant TMP mode is mostly used in the water

treatment in which the sole objective is to achieve solid/liquid separation and a biological

process is absent. On the contrary the constant flux mode is more suitable for the biological

wastewater treatment for which the F/M ratio, HRT and effluent quality are easily controllable. If

the constant TMP mode is used for the biological wastewater treatment, then F/M ratio and HRT

vary over time and therefore, poorer effluent quality is expected at the initial operation stage of a new membrane module.

2.1.2.3 Two basic MBR application modes

There are two basic MBR application modes or operational configurations: "external" MBR and "submerged" MBR [Zanello et al., 2003; Yang et al., 2006], as shown in Fig. 2.3. In the external MBR mode which is in fact the configuration in the first generation of MBR, the membrane module is placed in a separate tank outside the bioreactor and the mixed liquor is pumped from the aeration tank into the membrane tank where the permeate is withdrawn and the suspended solids are retained. The concentrated biomass is then recirculated back to the aeration tank. The tubular membranes are generally used in this configuration and traditionally sweeping high fluid crossflow was used as a mean of fouling control.

In the submerged configuration, the membrane module is directly submerged in the bioreactor, instead of occupying an extra filtration tank, i.e. solid/liquid separation and biological process are effectively combined in a single container, which eliminates the necessity of sludge recirculation and thus is energy saving compared to the external MBR. Invention of the submerged MBR is an important breakthrough in the history of MBR development [Yamamoto et al., 1989] though conceptually it is a quite straightforward modification of the previous external MBR. In the submerged MBR, coarse bubble scouring, backflush and relaxation are the typical means for fouling mitigation. Hollow fibre or flat sheet membranes are typically used in the submerged MBR. Comparison of the typical external and submerged MBR is presented in Table 2.2 [Mulder, 1996; Judd, 2006; Lesjean et al., 2005].

44

Table 2.2 Comparison of external and submerged MBR

Parameter	External MBR	Submerged MBR
Footprint	Larger due to separate tank required	Smaller because tankage sharing of membrane and AS process
Permeate ($L/m^2.h$)	50 - 100	20 - 40
TMP (psi)	29 - 87	2.9 – 7.25
Filtration direction	Inside out	Outside in
Fouling tendency	Low	High
Sensitivity to influent	Less sensitive	Sensitive
Energy efficiency (kwh/m^3)	2 - 5	0.2 – 0.5
Application	Water treatment, industrial wastewater treatment	Municipal wastewater treatment

Twenty years ago the external MBR systems were limited to industrial wastewater treatment and water treatment processes [Morgan et al., 2006], however, in recent years with advent of air-lift-assisted cross flow pumping the external MBR is also increasingly applied in municipal wastewater treatment, with significantly reduced energy consumption of 0.2 kWh/m^3 [Futselaar et al., 2007].

2.1.2.4 Characteristic MBR operating parameters

Filtration resistance

Resistance is an inevitable phenomenon in filtration processes due to progressive clogging of the membrane pores or cake accumulation on the membrane surface. Filtration resistance is dependent on the membrane's physical and chemical properties as well as the wastewater characteristics; therefore it consists of the membrane's natural hydraulic resistance R_m as well as fouling induced resistance R_f:

$$R_T = R_m + R_f \qquad\qquad (2\text{-}1)$$

The membrane resistance R_m can be obtained according to the Hagen-Poisseuille law as following:

$$R_m = (8 \times \tau \times L)/(\pi \times D^2) \qquad\qquad (2\text{-}2)$$

where:

D = nominal membrane pore diameter (m)

τ = pore tortuosity

L = membrane thickness (m)

Flux

Being an important operational parameter in MBR process, flux is defined as the flow rate of permeate per unit of the membrane surface area. It can also be related to TMP, the membrane resistance and the viscosity of the filtration media through Darcy's law as the following:

$$J = Q/A = TMP/(\mu_t.R_T) \qquad\qquad (2\text{-}3)$$

Where:

J = flux, m/s or $L/m^2 \cdot h$

Q = wastewater flow rate, m^3/s,

A = membrane surface area, m^2

TMP = transmembrane pressure, Pa

R_T = total filtration resistance, m^{-1}

μ_t = viscosity of the permeate, Pa·s

The viscosity of the permeate μ_t is temperature dependent and it can be expressed as [Al-Shemmeri, 2012]:

$$\mu_t = 2.414 \text{ x } 10^{-5} \text{ x } 10^{247.8/(t-140)} \qquad (2\text{-}4)$$

Where t is temperature (Kelvin)

Permeability

Permeability P (m/s·Pa) is an indicator for a membrane's specific flux under the unit permeate driving pressure, i.e.

$$P = J / TMP = 1/(\mu_t * R_T) \qquad (2\text{-}5)$$

P can be used to compare the practical operation performances among various membrane modules.

2.1.3 Membrane fouling and control

This section systematically discusses the fundamental mechanisms and mitigation strategies of membrane fouling in MBR. As a way of filtration, fouling of the membrane or filter is an inevitable process, signified by flux decline, TMP increase and effluent quality deterioration due to fine particle deposition on and into the membrane [Chang et al., 2002; Trussell et al., 2006; Judd, 2005]. Although MBR processes have been applied successfully in municipal and

industrial wastewater treatment, membrane fouling, which is responsible for high operational and maintenance costs, is still the major obstacle for broader use of this technology [Le-Clech et al., 2006; Chang et al., 2007; Li and Wang, 2006]

2.1.3.1 Particle transport behavior and anatomy of membrane fouling

According to the International Union of Pure and Applied Chemistry (IUPAC) [Koros et al., 1996], membrane fouling is defined as "the process resulting in the loss of performance of a membrane due to the deposition of suspended or dissolved substances on its external surface, at its pore openings, or within the pores". In order to understand the mechanism of fouling, the core issue is to focus on the movement behavior of particles. In the MBR filtration process particles in the vicinity of the membrane surface are subjected to a flux induced pulling force to the membrane surface, shear force induced diffusion and Brownian diffusion. The collective effects of various dynamic factors are schematically represented in Fig. 2.4:

(1) Particle concentration gradient or polarity close to the membrane surface;

(2) Formation of a layer of cake on the membrane surface;

(3) Some of the membrane pores are completely or partially blocked.

Each of the above factors directly contributes to the membrane fouling, therefore, the total fouling resistance R_T is sum of all of resistances [Evenblij, 2006; Ravazzini, 2008; Judd, 2006], i.e.

$$R_T = R_m + R_{pb} + R_{ck} + R_{cg} \qquad (2\text{-}6)$$

Where:

R_m = intact membrane resistance

R_{pb} = pore blocking resistance

R_{ck} = resistance caused by the cake layer

R_{cg} = concentration gradient resistance

It should be noted that magnitude of each resistance component is dependent on the membrane material and configuration, fluid characteristics and operating conditions.

Concentration gradient resistance R_{cg}

Cake resistance R_{ck}

Clean membrane resistance   Pore blocking resistance R_{pb}
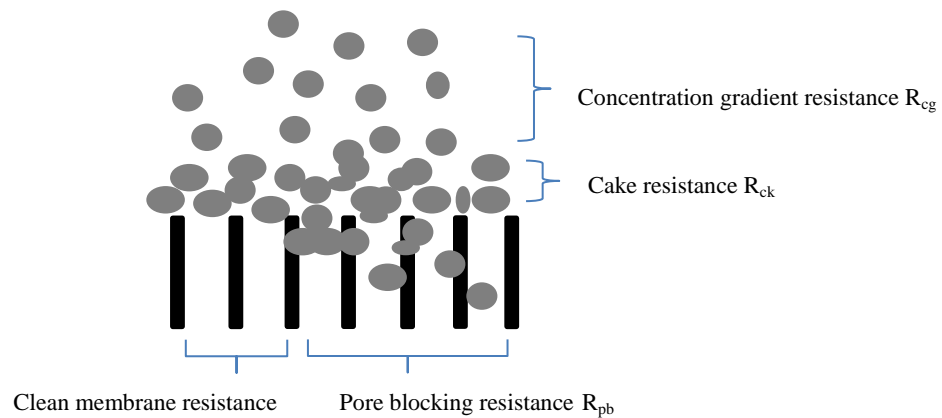
Fig. 2.4 Schematic of interaction of particles and membrane fouling

2.1.3.2 Membrane fouling factors

Membrane fouling has been a prevalent research topic in the past three decades since MBRs became an attractive wastewater treatment alternative. Various factors affecting membrane fouling have been investigated by academics and application engineers [Lojkine et al., 1992; Chang et al., 2002; Le Clech et al., 2006; Evenblij, 2006]. In general, membrane fouling in MBR systems is attributed to three classes of factors, i.e, membrane characteristics, feed / biomass characteristics and MBR operating conditions, as shown schematically in Fig. 2.5 [Le-Clech et al., 2006, Judd, 2006]. Recently, the osmotic pressure in the cake layer of a microfiltration

membrane was identified as a main contributor to filtration resistance through mathematical

modelling [Zhang et al., 2014]. The mathematical model was developed based on chemical

potential difference between cake layer and effluent in a submerged membrane bioreactor, and

experimental data verified validity of the model.

In fact, some of the factors are interacted each, for example, the operating conditions greatly

affect the feed / biomass characteristics and a certain biomass requires certain optimal operating

conditions to ensure the MBR process to proceed successfully. The influencing mechanism of

each parameter on fouling is briefly analyzed and discussed in the following sections.
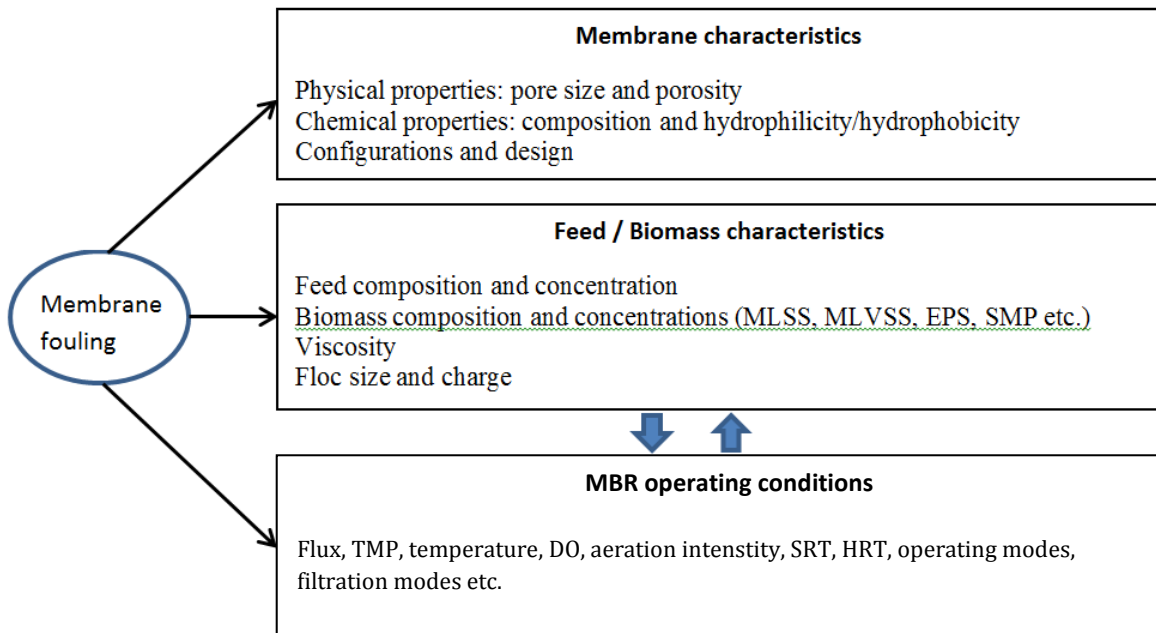
Fig. 2.5 Membrane fouling factors in a MBR system

Membrane fouling can be further subdivided into reversible fouling, irreversible fouling and

irrecoverable fouling. Reversible fouling means it can be removed by physical means such as

backflush or scouring, and irreversible fouling means that it can be removed by chemical

cleaning, whereas irrecoverable fouling cannot be mitigated by any physical or chemical

approaches and therefore the permeability is lost permanently. The extent and rate of the irrecoverable fouling decides the lifetime of a membrane module [Judd, 2006; Meng et al., 2009]. Reversible, irreversible and irrecoverable fouling occurs sequentially and on distinct time scales during MBR operation. Specifically, the fouling after short time of operation (maybe as short as minutes) is caused by pore clogging and cake formation on the membrane surface. This type of fouling can largely be removed by mechanical cleaning measures such as relaxation or back flushing and thus is considered reversible fouling. After weeks or even months of operation, the fouling cannot be removed by the physical approaches and then chemical cleaning is needed to resume most of the permeability, and this type of fouling is called irreversible. Finally, after several years (five to seven years, for example) the membrane reaches a state where neither the physical nor chemical means are capable of recovering the membrane to a workable condition; the usability of the membrane function is eventually terminated by irrecoverable fouling [Kraume, 2007].

2.1.3.2.1 Fouling stages

The progress of membrane fouling is not linear, but with three stages of accelerating fouling processes reported by Zhang et al. (2006) and Judd (2006): initial conditioning fouling, steady fouling and TMP jump. In the stage of initial conditioning fouling, small particles or colloids in the fluid are adsorbed or sucked into the membrane pores. Flux or shear forces were proven to be unrelated to conditioning fouling [Ognier et al., 2002]. The extent and initial conditioning fouling rate are associated with the membrane characteristics such as pore size and chemical polarity etc. and concentration of EPS or SMP.

The steady fouling starts when the filtration cake layer is formed on the membrane surface. Generally growth of the cake layer is a dynamic process and requires a certain time to reach to the maximum cake thickness. During this period of time membrane fouling increase steadily. Finally, when the biocake covers the entire membrane surface and the local flux is higher than the critical flux, the fouling suddenly aggregates and causes a TMP jump, which necessitates membrane fouling.

2.1.3.2.2 Influence of membrane characteristics on fouling

The physical properties (e.g. pore size, porosity and configuration) and chemical composition of the membrane module have a significant impact on fouling in the MBR process [Judd, 2006]. It has been reported that polyvinylidene fluoride (PVDF) membranes are more immune to irreversible fouling than polyethylene (PE) membranes [Yamato et al., 2006]. As for the effect of pore size on fouling, smaller pore size tends to reject entry of the floc particle into the membrane and thus reduce pore blocking. On the contrary, large pore size membranes are more prone to pore blocking.

Hydrophilic membranes are generally considered to be more resistant to fouling due to the charge repelling effect between the membrane and the negatively charged particles or colloids in the biomass [Madaeni et al., 1999; Yu et al., 2005; Le-Clech et al., 2006].

2.1.3.2.3 Influence of feed-biomass characteristics on fouling

Characteristics of the feed including the chemical composition and solid content affect the biological growth kinetics of biomass or the biomass characteristics, thus impacting the membrane fouling propensity. For example, synthetic wastewater with higher concentrations of COD and TN was found to accelerate membrane fouling [Le-Clech et al., 2003; Wei et al., 2012].

The physical properties of the biomass such as floc size distribution, TSS, VSS, temperature and viscosity are generally considered to be the direct factors affecting fouling.
Judd (2006) mentioned that the floc size and distribution are the leading contributing factors for fouling. Small enough constituents freely pass the membrane pore together with permeate and have no contribution to the fouling process. On the other hand, large particles are most likely to be prevented from reaching the membrane surface due to the fluid back-transport actions, suggesting that only the particles with sizes within a certain range really cause fouling. This may be especially true when the nominal pore size is close to the membrane pore size [Evenblij, 2005] though the weight of fouling contribution varies based on the observations by different authors [Itonaga et al., 2004; Wisniewski et al., 1998], probably due to the difference in methodologies.

Intuitively, higher TSS and VSS should exacerbate membrane fouling as more particles are to be deposited on the membrane surface. Though this conclusion has been experimentally supported by some investigators [Defrance et al., 1999; Brookes et al., 2006], contradictory results were also reported by the other authors, e.g. the impact was found insignificant [Le-Clech et al., 2003; Lesjean et al., 2005] or even negative [Cicek et al., 1999; Chang et al, 2005; Meng et al., 2006].

Apart from difference in the experimental methodologies, interaction complexity of the suspended solids with the membrane surface is probably the major cause for the confusing outcomes. Therefore, MLSS or MLVSS alone seems to be a poor parametric indicator for predicting membrane fouling propensity.

It is generally agreed that high biomass viscosity causes more serious membrane fouling [Mulder, 2000; Watanabe et al., 2006] as more viscous biomass tends to strongly attach to the membrane surface. At low temperature, the viscosity of water increases, therefore, the resistance to filtration increases. For example, Jiang et al. (2005) reported worsening membrane fouling at 13-14 ^{o}C compared to 17-18 ^{o}C.

Low temperature also affects the physical properties of biomass as well as the bacterial physiology [Judd, 2006; Wei et al., 2012]:

(1) Low temperature induces de-flocculation of the biomass;

(2) Release of SMP and reduced biological activity produce more membrane foulants at low temperatures;

(3) Low temperatures reduce the particle back transport velocity in the vicinity of the membrane surface

All of the above factors are responsible for aggregation of membrane fouling. Influence of low temperature on membrane fouling will be addressed in further detail in later sections.

Generally, presence of the filamentous bacteria indicates high viscosity and elevated concentration of EPS [Meng et al., 2009] and increased fouling tendency has been reported by some research groups [Chae et al., 2006; Meng et al., 2007; Sun et al., 2007]

EPS are the polymeric compounds including carbohydrates, proteins, nucleic acids present on or outside the cellular surface and in the microbial aggregates such as biofilms, flocs and sludge. It is vital for the survival of microorganisms because it enables cell attachment and protects them from external invasion [Flemming et al., 2001]. EPS are rich in negatively charged groups such as carboxyl, phenolic, alcoholic, hydroxyl, phosphoric and sulfhydryl as well as nonpolar radicals such as aromatics and aliphatics, carbohydrate chains etc. The duality of hydrophilic and hydrophobic structures make EPS capable of wetting and cross-linking both hydrophilic and hydrophobic surfaces [Chang and Lee, 1999; Rosenberger et al., 2002]. A great number of studies have been conducted to correlate EPS concentration and membrane fouling in MBRs [Nagaoka et al., 1996; Nagaoka et al., 1998; Cho and Fane, 2002; Meng et al., 2006; Kent et al., 2011; Jamal et al., 2014]. It is widely agreed that EPS concentration positively affects membrane fouling in the following ways:

(1) EPS as a highly hydrated gel covers the membrane surface and prevents water from permeating membrane. Polysaccharide-like foulants are neutral in terms of the electric charge, Interaction between EPS molecules and membranes include dipole-dipole attraction and hydrogen bonding etc. [Stec et. al., 1995; Chang et al., 1998].

(2) Higher EPS cause quicker formation of biocake on the membrane surface. EPS bind the microbes together and are embedded in the deep layers of biocake, which not only contribute to formation and growth of the biocake, but also assist in strengthening the mechanical stability of biocake [Nagaoka et al., 1998; Nagaoka et al., 1999; Laspidou et al. 2002].

According to the matrix distinguishable by the common extraction methods, EPS are divided into two categories: bound EPS (e.g. capsular polymers, condensed gels, loosely bound polymer and attached organic materials) and soluble EPS (soluble macromolecules, colloids, and slimes etc.) [Neilsen et al., 1999]. Bound EPS are released directly from microorganisms and present tightly around the live cells, whereas soluble EPS are usually produced from cellular lysis and then diffuse into the bulk solution. Soluble EPS is also called soluble microbial products (SMP) [Rosenberger et al., 2002] and can also come from components of the wastewater influent. Fig. 2.6 schematically displays the spatial environment and formation of both bound and soluble EPS.
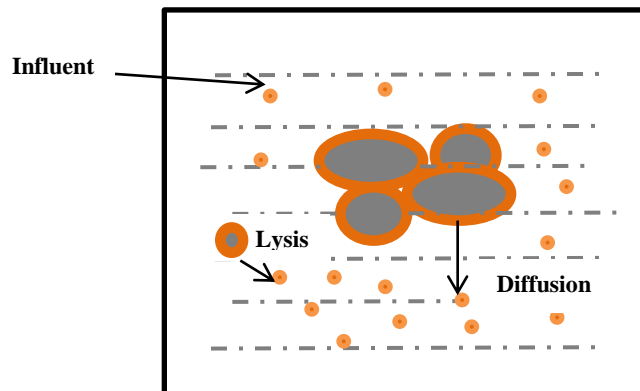
Fig. 2.6   Schematic illustration of source and surroundings of the bound EPS and soluble EPS

The composition of EPS depends on the influent matrix, dissolved oxygen or aeration intensity, HRT, MLSS, temperature and STR, etc. Conclusions of some investigations are summarized in Table 2.3. Conflicting results are reported from different investigations, due to the variation in

experimental conditions and lack of standard sample preparation and test methods for EPS. For

example, the ion exchange resin method [Frølund et al., 1996; Gorner et al., 2003; Jang et al.,

2005] may produce significantly different results in comparison with the other popular protocols

such as heating extraction [Morgan et al., 1990] or formaldehyde separation [Zhang et al., 1999].

Table 2.3 Impacting factors of EPSs in MBR process

Parameters	Impact on EPS concentration in the biomass	Sources
SRT	Shorter SRT increases EPSs Longer SRT increases EPSs but reduces biodegradable EPSs	Cho et al., 2005; Ng et al., 2006; Ahmed et al., 2007 Patsios et al., 2011 Brookes et al., 2003
Temperature	EPSs increase at lower temperatures	Al-Halbouni et al., 2008; Wang et al., 2010
HRT	Shorter HRT increases EPSs Longer HRT increases EPSs	Fallah et al., 2010 Baek et al., 2010
MLSS	Higher MLSS decreases EPSs Higher MLSS increases EPSs	Dizge et al., 2013 Chabalina et al., 2012
DO	Higher EPSs at lower DO	Kim et al., 2006
Feed	Higher biodegradable COD causes higher EPSs	Peng et al., 2011

2.1.3.2.4 Influence of operating conditions on fouling

Flux

Intuitively, high flux accelerates membrane fouling, which has also been experimentally and mathematically proven in the previous studies [Le-Clech et al., 2003; Gugliemi et al., 2007]. Therefore, flux has been a primary operational parameter since the onset of MBR technology. About two decades ago, Field et al. [1995] first proposed the concept of "critical flux", meaning a flux threshold "below which a decline of flux with time does not occur; above it fouling is observed." Though critical flux is practically impossible to obtain because even at a zero flux, membrane pore blocking by static adsorption of the inorganic and organic constituents in the mixed liquor or attached microbial growth on the membrane surface still fouls the membrane [Brookes et al., 2004; Ognier et al., 2001; Wen et al., 2004]. Nevertheless, the critical flux concept opened up an interesting perspective on MBRs, directly leading to a proposition of the more practical concept of sustainable flux [Bacchin et al., 2006; Fan et al., 2006]. Sustainable flux depends on the particular operating conditions such as temperature, hydrodynamics, feed conditions, TSS and SRT, and above a certain flux threshold, the rate of fouling is not sustainable or acceptable to achieve the designed process efficiency.

Air scouring intensity

Air bubbles from aeration close to the membrane surface create shear force and turbulence which prevent deposition of large particle on the membrane surface due to increased back transport. Therefore air scouring is the most common and effective fouling reduction strategy currently used in the MBRs for municipal wastewater treatment [Ueda et al., 1997; Sofia et al., 2004; Le-

Clech et al., 2006; Fang and Zhou, 2007; Nywening and Zhou, 2009]. However, excessive aeration intensity may in fact cause negative influence on fouling [Park et al., 2005; Ji et al., 2006], and there may be two mechanisms associated with it [Wisniewski et al., 1998; Tardieu et al., 1999]:

(1) Less aeration sensitive fine particles with lower shear diffusion ability and lateral migration velocity may accelerate blocking of the membrane pores;

(2) Higher aeration tends to break down the flocs and thus causes fouling deterioration.

2.1.3.3 Microscopic observation of membrane fouling through NMR or MRI technologies

The magnetic resonance imaging (MRI) is a revolutionary medical imaging technique developed in early1970s based on the proton nuclear magnetic resonance (1H NMR), a spectroscopic method for in-depth analysis of molecular structure. It produces high quality images of the inside of the human body for disease diagnosis [Callaghan, 1994]. In MRI, the targeted imaging area is exposed to a strong magnetic field oscillating at appropriate resonance frequency. The magnetically susceptible hydrogen atoms contained in water molecules produce position encoding signals that distinguish the different parts of tissues due to variations in water molecule content. Therefore, MRI is truly an in situ non-destructive imaging technology. In the recent years, researchers started to extend application of NMR and MRI to membrane fouling investigation. Von der Schulenburg et al. [2008] first applied NMR to study the temporal and spatial biofouling evolution of a spiral wound reverse osmosis (RO) membrane, including the velocity field and change of membrane porosity, from which the effective membrane surface area is measured. As a result the RO membrane biofouling was able to be quantitatively described and its influence on hydrodynamics and mass transport was identified. Using MRI

technology, Vrouwenvelder et al. [2009] focused on the biofilm accumulation based fouling characteristics of feed and spacer in RO filtration. Direct observations of fouling layer formation on the feed channel spacer demonstrated the effect on the velocity profiles and hydrodynamics of feed composition and spacer configurations. Furthermore, the same group [Vrouwenvelder et al., 2010] applied a mathematical model to simulate the dynamic biofouling progress on the spiral wound RO membrane modules. The MRI observational results confirmed with the numerically predicted fouling features on the feed spacers, and it was concluded that biomass growth on the feed spacer contributes more than membrane fouling itself to the RO flux declining.

2.1.3.4 Membrane fouling control technologies

As membrane fouling has always been the bottleneck in MBR operation, over the past two decades tremendous efforts have been made to develop various fouling prevention and alleviation technologies, mainly focused on four areas [Park et al., 2005; Chen et al., 2012; Ivanovic et al., 2008], i.e.

(1) Membrane material and surface modification [Liu et al., 2012; Bruening et al., 2008; Boributh et al., 2009];

(2) Influent pretreatment [Du et al., 2009; Citulski et al., 2008; Zhang et al., 2014];

(3) Modification of the physical and chemical characteristics of biomass [Tsai et al., 2004; Hu et al., 2014; Pramanik et al., 2014];

(4) Membrane cleaning [Zhou et al., 2007; Zhang et al., 2008; Kimura et al., 2014]

In the following sections the focus will be on modification of the biomass characteristics through strategies such as fouling control through P removal, quorum quenching, coagulation and utilizing the electrokinetic technology as a promising new alternative. Lastly, nanocomposite and graphene oxide modified membrane and membrane cleaning will also be briefly reviewed as they represent an important direction in the future research on MBR develoipment.

2.1.3.4.1 Nanocomposite and graphene oxide modified membrane

Nanocomposite materials and technologies have been and continue to be hot research topics in material science, and are recently finding application in membrane filtration process. The most common nanocomposite modified membranes can be divided into four categories [Jun and Deng, 2015]: the conventional nanocomposite, thin-film nanocomposite, thin-film composite with nanocomposite substrate and surface located nanocomposite. The prominent advantage of the nanocomposite-modified membranes is the possibility of achieving special functionalities such as antibacterial, photocatalytic or adsorptive capabilities through manipulating the membrane's structure and relevant physicochemical properties including hydrophilicity, porosity, charge density, and thermal/mechanical stability. Ajmania et al. [2012] added layered carbon nanotubes (CNTs) of different physiochemical properties onto low pressure membranes and studied the antifouling effect with natural surface water. It was found that membranes modified with the largest diameter pristine multi-walled CNTs (MWCNTs) had the best fouling reduction performance. A membrane with a CNT loading of 22 g/m^2 extended the cleaning cycle interval by three-fold. Destruction of foulant, especially the larger organic macromolecules, is considered to the main cause of decreased filtration resistance.

Recently graphene oxide (GO)-assisted membranes such as freestanding GO membranes, GO-surface modified membranes and casted GO-incorporated membranes are emerging as a novel fouling combating technology, especially in the field of desalination [Hegaba et al., 2015]. GO contains abundant hydrophilic groups such as epoxide, carboxyl and hydroxyl which can serves functional reactive sites. Zhao et al. [2014] developed a GO modified polyvinylidene fluoride (PVDF) nanosheet membrane and determined its surface properties using multiple techniques including scanning electron microscopy (SEM), contact angle measurements, and X-ray photoelectron spectroscopy. The GO modified PVDF membrane was then tested in a submerged membrane bioreactor system. The results showed higher critical flux, sustained filterability, less EPS deposition on the membrane surface, looser and thinner biocake layer and cleaning intervals of three times longer in comparison with the regular PVDF membrane. Lee et al. (2014) discovered that adding about 1 wt% of graphene oxide into the membrane materials dramatically increased the membrane's antifouling capability, evidenced by 5 times longer intervals between chemical cleanings.

2.1.3.4.2 Fouling control through P removal

In the water environment, the biologically assimilated forms of phosphorus are ortho-phosphate, monobasic phosphate and dibasic phosphate, which are converted from inorganic polyphosphates and dissolved organic phosphorous through hydrolysis or lysis [Holtan et al., 1988; Maher and Woo, 1998]. In microorganisms, the molar ratio and mass ratio for carbon (C), nitrogen (N) and phosphorous (P) are 100:20:1.7 and 100:23:4.3, respectively [Tchobanoglous et al., 2003]. Compared to carbon, though the demand for P is relatively low, as an essential

element for microbial cells, P deficiency restricts the microbial growth. Phosphorous as a limiting factor has been extensively reported for drinking water (Miettinen et al., 1997; Kasahara et al., 2004; Torvinen et al., 2007), surface water (Mohamed et al., 1998; Mohamed et al., 2003) and wastewater (Alphenaar et al., 1993). In recent years, it was found that biofouling was completely inhibited at low phosphate concentrations [Vrouwenvelder et al., 2000; Vrouwenvelder et al., 2010] and controlling phosphate concentration has been proposed as an alternative approach for membrane fouling reduction [Van der Kooij et al., 2007; Galjaard et al., 2008].

2.1.3.4.3 Quorum quenching

One of the major challenges in membrane fouling control is to inhibit the microbial growth on the membrane surface. Though application of antibiotics or antimicrobial compounds in MBRs such as such as nitrofurazone, chlorhexidine, silver salts, polymerized quaternary ammonium surfactants, anionic nanoporous hydrogels and antibacterial peptides is an effective method [Ponnusamy et al., 2009; Lade et al., 2014], the drawback is that most of the antibiotics indiscriminately kill non-target microorganisms and their residues pollute the aquatic environment. In addition, the biofilm producing microbes may develop physiological protection mechanism against further application of antimicrobial compounds to compromise their antifouling effect [Davies et al., 2003]. About a decade ago, a new strategy based on the quorum quenching mechanism was adopted for membrane fouling inhibition [Dobretsov et al., 2009], exhibiting a promising potential for a novel environment-friendly antifouling approach. The intercellular communications of microbes rely on a process called quorum sensing (QS). QS plays a critical role in generation of EPS, motility, swarming and biofilm formation through

sensing small signal molecules called auto-inducers (AIs) [Dong et al., 2007; Lowery et al., 2010; Dobretsov et al., 2011]. The previous investigations have reported three types of AIs, i.e. oligopeptides and N-acylhomoserine lactones (AHL) as messengers for Gram+ and Gram- bacteria respectively, and autoinducer-2 (AI-2) which coordinates the communications for both. A few natural substances have been found to be effective in quorum quenching process, including: curcumin, vanillin, flavonoids, furanones and some enzymes etc. [Rudrappa et al., 2008; Choudhary et al., 2010; Truchado et al., 2012; Oh et al., 2012]. Quorum quenching is capable of controlling membrane fouling by disturbing the bacteria's AIs-mediated quorum sensing activities, rather than using bactericides to inactivate microbes. In spite of high interest in the MBR research community, there is still a long way to go for practical application of QS in membrane filtration of water and wastewater treatment process [Paul et al., 2009; Kim et al., 2013].

2.1.3.4.4 Membrane cleaning

In MBR, membrane fouling is inevitable, so sustainable MBR operation requires periodical cleaning to recover the membrane module's effective filterability. Cleaning scheduling can be based on a certain time interval of stable MBR operation or the preset upper TMP limit typically recommended by the manufacturers.

Membrane cleaning can be divided into in-situ and ex-situ cleaning depending on whether the cleaning process occurs inside or outside the MBR reactor, or it be distinguished by the foulant removing mechanism: physical, chemical or biological cleaning [Wang et al., 2014].

In-situ and ex-situ cleaning

In-situ cleaning, also called online cleaning, is conducted inside the MBR reactor itself and therefore doesn't require additional cleaning vessels. Typical in-situ cleaning methods include ultrasonication, backflush, intermittent filtration or relaxation, suspended carrier scouring, biological cleaning and maintenance cleaning in place (CIP) [Brepols et al., 2008]. Ex-situ cleaning requires extra cleaning tank and combined physical and chemical cleaning processes may be involved. In-situ cleaning is practiced much more frequently, typically from once in a few minutes to a few months; most of them (except intermittent filtration or relaxation) are carried out in parallel with membrane filtration, so flux production is not disturbed. In contrary, ex-situ cleaning is considered only after in-situ cleaning fails to stop the fouling status and is the last cleaning effort exerted to recover membrane's performance and may be practiced once from 6 months to three years [Ayala et al., 2011].

Physical, chemical and biological cleaning

Physical cleaning typically includes ultrasonication, backflush, vibration, intermittent filtration or relaxation, suspended carrier scouring. As mentioned previously, those cleaning methods are usually integrated as an in-situ cleaning processes to control reversible fouling and require no chemicals. They are indispensable to reduce the frequency of chemical cleaning and extend the life time of membrane module in the practical MBR process. In chemical cleaning, foulants adsorbed or attached to the membrane are removed by oxidation or dissolution using chemical

reagents such as citric acid, oxalic acid, hydrochloric acid, hypochlorite and hydrogen peroxide etc. Generally chemical cleaning is able to remove the substances causing irreversible fouling, and thus it is another indispensable step in MBR operation, though the acids, alkalines or oxidants used may do damage to the membrane materials. Biological cleaning is a novel class of cleaning technology emerging in recent years [Kim et al., 2013], including enzymatic cleaning, energy uncoupling, and quorum quenching. Compared to the matured and widely applied physical and chemical cleaning methods, biological cleaning is still under development and it may be still years away before it becomes practical application in MBR. The types of fouling with specific regard to cleaning methods are briefly presented in Table 2.4

Table 2.4   Membrane fouling features and cleaning approaches

Features	Fouling development time	Appropriate cleaning approaches
Physically reversible fouling	Minutes	relaxation, backflush, ultrasonication, vibration, biological cleaning
Chemical reversible fouling	Weeks to months	Chemical cleaning
Irreversible fouling	5 – 7 years	Nothing can do about it

2.1.4 Removal of endocrine disrupting compounds (EDCs) in MBR

EDCs are natural or synthetic organic compounds that may interfere with the normal functions of the endocrine system such as synthesis, transportation and action of natural hormones in the body [Crisp et al., 1998]. Due to human activities, EDCs have extensively existed in the surface waters and the negative impacts on reproductive function, neuro system development and

immune function have been extensively reported [Auriol et al., 2006]. Among the large number of EDCs, natural (E1, β-E2, estriol [E3]) and synthetic ethinylestradiol (EE2) hormones are considered to be the main contributors to the estrogenic activities observed in municipal wastewater and the receiving water [Auriol et al., 2006]. In the last two decades, wastewater treatment has been extended from the conventional solid and nutrient removal to destruction of emerging compounds including EDCs [Snyder et al., 2001]. As a synthetic estrogen for producing contraceptive medication EE2 is the most potent EDC in municipal wastewater (Johnson et al. 2001) due to its structural resistance to biodegradation [Kidd et al., 2007]. As a result, EE2 at parts per trillion (PPT) levels was identified to affect the reproducibility of aquatic species [Desbrow et al., 1998, Esperanza et al., 2004; Kidd et al., 2007].

Measurement of EDCs in wastewater is very complicated and lab intensive due to their low content, complex matrices, lengthy sample preparation and easy sample contamination. The most common analytical techniques are GC-MS-MS and biological assay. GC-MS-MS is capable of separating and determining the concentrations of individual EDCs, yet the biological assay represented by the yeast estrogen-screening (YES) assay developed and refined in the last two decades [Villalobos et al., 1995; Routledge et al., 1996], is more favourable because it determines the overall estrogenic activity (EA), i.e. the total estrogenic effect on an organism. EA is a more accurate measurement than the concentrations of individual EDCs because the corresponding relationships between estrogenic impact and concentration are poorly quantified. In addition, the estrogenic influences of both parent compounds and subsequent intermediates or derivatives are collectively accountable. EA is typically measured against a basic EDC standard 17β-estradiol or E2 and expressed by E2-Eq concentration in ng/L (Yang et al., 2008).

The concentrations of EE2 in municipal wastewater are highly variable, ranging from not detectable to a few hundred ng/L depending on the influent characteristics and determination methods [Birkett et al., 2003; Pauwels et al., 2008]. Removal of EE2 in the wastewater treatment process is mainly through biodegradation and sludge adsorption, and the efficiency is dependent on the operating conditions such as SRT, HRT, TSS and temperature etc. Generally longer SRT, higher HRT, higher temperature and more TSS are favourable for EE2 elimination [Price et al., 2004; Koh et al., 2009]. Therefore, MBR characterised by longer SRT and higher TSS is advantageous for EE2 removal [Cicek et al., 1999; Cicek 2002]. In addition to the enhanced biological destruction, the membrane material together with the dense biocake layer on membrane surface serve as physical barrier for size exclusion of EE2 to effluent [Urase et al., 2005; Melin et al., 2006]. Therefore, generally 70% - 80% of EE2 removal rates (higher than those of the conventional ASP), were reported [Lee et al., 2008; Cirja et al., 2008; Yang et al., 2008; Yang et al., 2009].

2.2 Electrocoagulation (EC) and Application in the Wastewater Treatment

EC was first reported for electrolytically treating sewage in London in 1889 and patented in the United States in 1909 [Vik et al., 1984]. During 1940's and 1950's this technology was used to purify surface water [Matteson et al., 1995]. EC as one of the electrokinetic technologies has gained increasing interests in water and wastewater treatment in the last two decades. In EC, sacrificial anodes typically made of aluminum or iron generate coagulants (aluminum hydroxide or ferric hydroxide) in situ to aggregate flocs or directly decompose the contaminant in the

wastewater. The coagulated and flocculated particles are subsequently removed from the treatment stream and separated through sedimentation or filtration. In the following sections, EC reactor configurations, electrochemical mechanisms, electrode materials, critical factors affecting EC kinetics and removal efficiency, advantages of EC in comparison with conventional chemical coagulation as well as applications in the industrial and wastewater treatment are briefly summarized. The role and effect of EC on membrane filtration in MBRs will be discussed in detail in a later section.

2.2.1 EC reactor configuration

Like a standard electrolytic cell, the basic EC reactor consists of one anode, one cathode, electrolytic fluid (wastewater to be treated) and a power supply unit, as schematically represented in (a) of Fig. 2.7. The anode (Al or Fe) metal dissolves into cations with valance of +2 (Fe) or +3 (Al) that enter bulky solution and are further hydrolyzed into monomeric and polymeric hydrated ions [Mollah et al., 2004], e.g. $Al(OH)^{2+}$, $Al(OH)_2^+$, $Al_2(OH)_2^{4+}$, $Al(OH)_4^-$, $Al_6(OH)_{15}^{3+}$, $Al_7(OH)_{17}^{4+}$, $Al_8(OH)_{20}^{4+}$ for Al electrode and $Fe(H_2O)_6^{3+}$, $Fe(H_2O)_5(OH)^{2+}$, $Fe(H_2O)_4(OH)^{2+}$, $Fe_2(H_2O)_8(OH)^{24+}$ and $Fe_2(H_2O)_6(OH)^{44+}$. Hydrogen gas as the inevitable by-product releases from the surface of cathode.
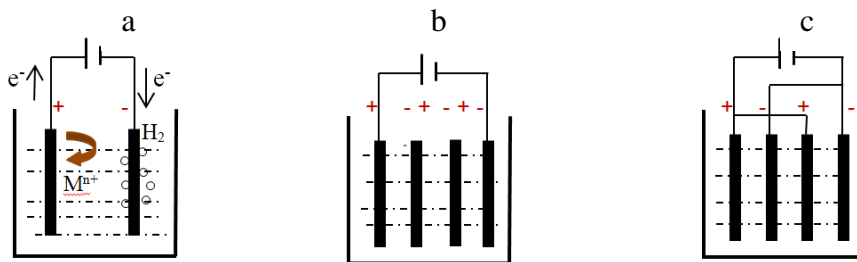
Fig. 2.7 Schematic representation of EC reactor configuration

(a). Basic EC unit, (b). Bipolar electrode EC, (c). Monopolar electrode EC

69

In practical application, the singe anode-cathode electrode pair configuration usually falls short of the required treatment efficiency due to limited electrode surface area. Consequently, over the years two other popular configurations have been developed, i.e. monopolar and bipolar electrode modes as shown in (b) and (c) of Fig. 2.7, respectively. In the bipolar arrangement, a number of conductive metal plates are placed between the anode and cathode without any electrical connection, whereas in the monopolar electrode EC configuration, multiple pairs of anode / cathode are interleaved through regulation of specific electric devices. Both monopolar and bipolar electrode modes provide higher cation release rates as the anode surface area is multiplied.

Pollutant removal efficiency and operating cost are the two major indicators in selecting a treatment process. Studies on several monopolar and bipolar EC configurations [Bayramoglu et al., 2007; Golder et al., 2007; Asselin et al., 2008; Ghosh et al., 2008; Wang et al., 2009] revealed that monopolar configuration is superior to the bipolar arrangement in terms of operating cost but bipolar electrodes are more effective in removing some contaminants.

As for the power supply, since the invention of this technology, direct current (DC) has been used in EC systems. However, in recent years application of alternating current (AC) has been investigated in a few studies [Wang et al., 2007; Eyvaz et al, 2009; Vasudevan et al., 2011]. Compared to the DC powered EC, AC has the advantage of suppressing electrode passivation and lower energy consumption [Vasudevan et al., 2011].

2.2.2 Chemical/electrochemical reactions in EC process

The chemical reactions for this process are as following:

At anode: $Fe^0(S) \longrightarrow Fe^{2+} + 2e^-$ (2-7)

            $Al^0(S) \longrightarrow Al^{3+} + 3e^-$ (2-8)

At cathode: $2H_2O + 2e^- \longrightarrow 2OH^- + H_2(g)$ (2-9)
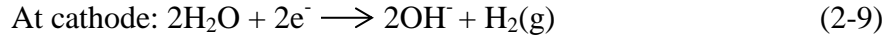
In bulk solution,

(1) For Fe anode:

$3Fe^{2+} + 2PO_4^{3-} \longrightarrow Fe_3(PO_4)_2 \downarrow$ (2-10)

$3Fe^{2+} + O_2 + 2H_2O \longrightarrow 3Fe^{3+} + 4OH^-$ (2-11)

$3Fe^{3+} + 9OH^- \longrightarrow 3Fe(OH)_3 \downarrow$ (2-12)

$Fe^{3+} + PO_4^{3-} \longrightarrow FePO_4 \quad \downarrow$ (2-13)
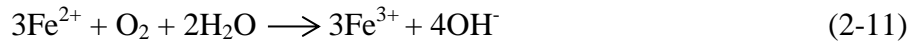
(2) For Al anode:

When Al is used as the anode, the electrochemically generated hydrated aluminum ions are not stable in aqueous solution and tend to form polynuclear hydroxylaluminum aggregates by following a stepwise deprotonation-dehydration mechanism [Rodriguez et al., 2007], i.e.

$Al^{3+} + 6H_2O \longrightarrow Al(H_2O)_6^{3+}$ (2-14)

$2Al(H_2O)_6^{3+} \rightarrow Al_2(OH)_2(H_2O)_8^{4+} + 2H_3O^+$ (2-15)

                $\llcorner\!\!\rightarrow Al_6(OH)_{12}(H_2O)_{12}^{6+}$

                     $\llcorner\!\!\rightarrow Al_{10}(OH)_{22}(H_2O)_{16}^{8+}$

                         $\llcorner\!\!\rightarrow Al_{24}(OH)_{60}(H_2O)_{24}^{12+}$

                              $\llcorner\!\!\rightarrow [Al(OH)_3]_m.(H_2O)_n$

$Al^{3+} + PO_4^{3-} \longrightarrow AlPO_4 \quad \downarrow$ (2-16)
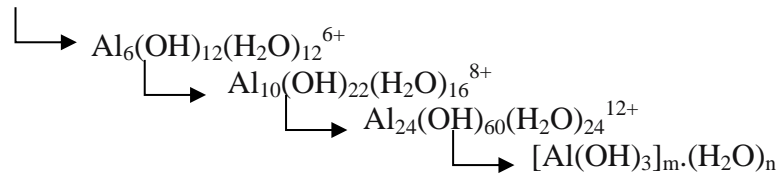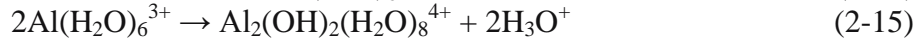
2.2.3 EC mechanisms

It is well known that many contaminants in water and wastewater are contained in fine particles called colloids with one-dimensional sizes ranging from 1 to 10 micron [Cosgrove et al., 2010; Masliyah et al., 1994]. As high as 50 - 70 % of organic substances in municipal wastewater exist in the colloidal form. In surface water color, turbidity, bacteria, viruses, algae and organics are also primarily associated with colloids [Crittenden et al., 2005]. Colloidal particles are typically surface charged through ion adsorption, lattice imperfections or isomorphic replacement as well as ionization of active groups such as carboxyl, amino, hydroxyl, sulfonic etc. Due to electrostatic attraction a surface charged particle tends to affect the ionic distribution in the surrounding solution, i.e. absorb ions of opposite charge and repel those with the same charge. As a result the electrical double layer (EDL) is formed, as shown in Fig. 2.8.
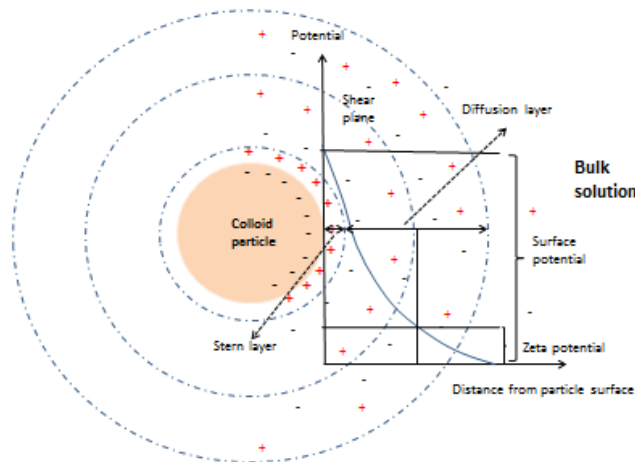
Fig. 2.8 Schematic representation of electric double layer

One of the most important parameters of colloids is zeta potential ξ, i.e. the electric potential difference between the shear plane of a colloidal particle and the bulk solution. The zeta potential is an indirect indicator of the electrical charge of the colloidal particle and can be experimentally

quantified by determining the electrophoretic mobility of a particle in the presence of an electrical field. The typical zeta potential of wastewater colloids ranges from 12 to 40 mv [Crittenden et al., 2005].

$$\xi = \frac{4\pi v}{\varepsilon V x} = \frac{4\pi \mu EM}{\varepsilon}$$ (2-17)

Where: v = particle velocity (m.s^{-1})
ε = dielectric constant
Vx = applied potential per unit length (V.m^{-1})
EM = electrophoretic mobility (m$^2 \cdot$V$^{-1}\cdot$s^{-1})
μ = viscosity of surrounding fluid (Pa·s)

In wastewater treatment, coagulation is the process by which colloidal particles and small solid suspensions are destabilized by high valence metallic ions to form larger agglomerates that are subsequently separated through settling, centrifuging or filtering. According to the Schulze-Hardy rule, the dosage for effective coagulation is logarithmically related to charge. The coagulation potentials of Na^+, Ca^{2+} and Al^{3+} are in the ratio of 1:100:1000. Therefore, salts of aluminum iron or their polymeric compounds are the typical coagulants in water and wastewater treatment. The destabilization mechanisms of coagulation process can be summarized as follows:

1. Compression of the electric double layer

   By adding coagulant the ionic strength of solution increases, consequently thickness of the electric double layer is repressed and reduced. The counter ions are driven closer to the surface and the repulsion force becomes more compromised by Van der Waals forces.

2. Neutralization of colloid charge

   The positively charged counter ions (Fe^{3+}, Al^{3+} or their hydrated forms) are brought closer to the surface of the colloid by electrostatic attraction and negate the primary charge of the colloid, thus reducing the zeta potential.

3. Interparticle bridging

   The metallic salts or polymerized forms may interact and bridge colloidal particles, which facilitates particle agglomeration and eventual flocculation.

4. Colloidal entrapment and enmeshment

   During precipitation the aluminum or iron hydroxides form three-dimensional polymeric structures and capture the colloidal particles.

2.2.4 Critical factors affecting EC kinetics and removal efficiency

EC is a versatile process capable of treating various industrial and municipal wastewater, and the pollutant removal kinetics and efficiency are directly affected by multiple factors such as electrode material and configuration, treatment time, wastewater characteristics, current density, solution chemistry, including pH and the chemical composition, electrode passivation status. Among those parameters electrode material, pH and current density are the most critical factors which are briefly reviewed below.

2.2.4.1 Electrode material

Aluminum, iron or stainless steel are the most common materials used for EC electrodes as these metals have high coagulation powers, are readily available, cost-effective and relatively non-toxic. As afore-mentioned, aluminium anode releases Al(III) ions in a one-step electrochemical reaction whereas generation of ferric ions are produced in two independent mechanisms, i.e. iron atoms are first oxidized into ferrous ions, and the latter is subsequently converted into ferric ions

by oxygen in air or wastewater [Sasson et al., 2009; Cocke et al., 2009; Linares et al., 2009]. Due to high solubility of its hydroxide and lower positive charge density, ferrous ion is not as efficient as ferric ions in EC process [Bagga et al., 2008]. Therefore, presence of sufficient oxygen or an oxidizing environment is essential for successful electrocoagulation with iron electrode. In spite of a few exceptions, most of the EC studies have shown that aluminum has a better pollutant removal efficiency than iron, however, relatively higher Al(III) toxicity, lower concentration tolerance in effluent and the surface water and higher price compared to iron make selection of EC electrodes application specific [Katal et al., 2011]. It should be noted that titanium anode has also been sporadically reported with superior treatment efficiency [Mollah et al., 2004] due to its high positive charge density. Recently, Naje et al. [2015] used titanium electrode to obtain high removal of COD (93.5%), TSS (97%), turbidity (96%), phenols (99%) and phosphate (97%) from the textile wastewater. However, because of its high cost, using titanium as the EC anode is generally not considered in practice.

2.2.4.2 pH

The pH of the solution may directly affect the chemical dissolution of electrodes, both anode and cathode [Refait et al., 1997; Chen et al., 2004]. When aluminum is used as the EC electrodes, as an active metal it may react with H^+ or OH^- , and generate Al^{3+} and AlO_2^- under acidic (pH < 5) and alkaline (pH >9) conditions. Fe may also react with H^+ under acidic (pH < 5) condition and release ferrous ions. Secondly, speciation of hydrated metal hydroxides is dependent on pH of the solution, and the amount of highly charged cations and hydroxides decide the coagulation power for destabilizing colloids. At highly alkaline pH the main species of Al and Fe are

Al(OH)$_4^-$ and Fe(OH)$_4^-$ ions, which have demonstrated poor coagulation performance. In addition, oxidation of Fe(II) to Fe(III) cannot occur if pH is less than 5 [Sasson et al., 2009, Picard et al., 2000]. Generally the optimal coagulation pH is in the range of 5 and 8, and iron outperforms aluminum at pH values outside this range [Mouedhen et al., 2008].

2.2.4.3 Current density

At low or medium current density and near neutral pH, coagulant production can be calculated according to Faraday's electrolysis law. However at high current density, dramatic pH increase in the solution may chemically dissolve the metal cathode [Sasson et al., 2009, Picard et al., 2000]. Overly high current density should be avoided because it not only leaves extra metal ions in the effluent but also produces large amount of explosive hydrogen gas. The optimal current density is typically dependent on the wastewater characteristics.

2.2.5 Advantages of EC in comparison with conventional chemical coagulation

Chemical coagulation using iron and aluminum salts or their polymeric forms have been used to destabilize colloids to precipitate the solids or soluble metals species in the water and wastewater, followed by sedimentation or filtration. These conventional processes require supply of iron or aluminum chemicals and the generated sludge has dramatically different characteristics compared to the EC process. Overall, in comparison with the conventional chemical coagulation, EC is widely recognized for the following advantages:

1. Except for the Al or Fe metal anodes, no corrosive chemicals are required, thus there is no need to deal with the residual chemicals in the effluent and secondary pollution is prevented [Mills et al., 2000; Melhem et al., 2010]. In addition, as there are no inert anions from the chemicals added into the wastewater stream, the total dissolved solids are reduced and the final sludge production is decreased. Finally, avoidance of the chemicals also save capital and operating costs for chemical handling facilities;

2. The EC equipment is easy to install and operate, which is advantageous to automate the treatment process. The electrolytic processes in the EC reactors can be fully controlled electrically and, with no moving parts, the EC facilities require less maintenance;

3. The flocs generated in the EC process tend to be much larger and contain less bound water. They are also proven to be more acid-resistant and stable under shear stress, and therefore, can be readily settled or dewatered;

4. The hydrogen gas bubbles generated in the EC process can be utilized as floatation means to remove the pollutant from the biomass;

5. Without the need for constant supply of chemicals, EC is characterized by easy operation and process control. Therefore, it may be more readily implemented in a developing-country or could be an effective decentralized water and wastewater treatment alternative in remote areas or in the event of emergencies.

2.2.6 Application of EC process in water and wastewater treatment

In the past three decades, EC has been investigated for treatment of wastewater containing heavy metals, oil and grease, dyes from the textile industry, landfill leachate, phenols and heavy metals

[Mohammad et al., 2004]. Table 2.5 presents some of the recent applications of EC in treatment of oil and grease, dye, heavy metals, turbidity and color in industrial wastewater as well as BOD and solids in municipal wastewater. The removal efficiencies of almost all studies were found to be dependent on the electrode material, initial pH, the pollutant concentrations, the applied current density and the electrolysis time. The table shows that excellent removal efficiency (>95%) was achieved in almost all of the studies, though the current density varies over a wide range. More studies on the practical applications are needed since nearly all of the existing investigations are in bench scale. The effect of EC on membrane fouling reduction in MBR will be the focus in Section 2.3.3.

Table 2.5 Recent applications of EC in the industrial and municipal wastewater treatment

Source of water or wastewater	Electrode materials	Current or current density	Treatment efficiency	Reference
Wastewater from the food industry containing oil and grease	Fe and Al-Bipolar	0.2– 0.6 A	95-99% of COD	[Chen et al., 2000]
	Corrugated Al plate	40 - 220 A	95-99% of oil	[Rubach and Saur 1997]
	Flat sheets of steel/stainless steel	60 - 140 A/m^2	85–99% of oil	[Mostefa et al., 2004]
	Al electrodes-Monopolar	100 - 300 A/m^2	80–99% of oil	[Carmona et al., 2006]
Color, dye	Fe and Al plates, and cylindrical graphite	1 - 5 A/m^2	85-99% of dye	[Gurses et al., 2002]
	Al, Fe, and stainless steel-Monopolar	1 - 4.5 A/m^2	95-99.6% of dye	[Kim et al., 2002]
	Al/Al-Monopolar	2.5 - 25 A/m^2	70-92.5% of dye	[Can et al., 2003]
	Carbon steel plates- Bipolar	4A	97-99% of dye	[Mollah et al., 2004b]
	Al_Fe monopolar	45 - 200 A/m^2	85-99% of dye	[Bayramoglu et al., 2004]

	Al/Al - Monopolar	25 - 250 A/m^2	60-95% of dye	[Kobya et al., 2005]
	Mild Steel electrode pair	1 - 30 A/m^2	80-99% of dye	[Golder et al., 2005]
	Al/Al - Monopolar	100 A/m^2	70-80% of dye	[Can et al., 2006]
Heavy metals	Two Fe/stainless steel electrodes	50 - 125 A/m^2	75–95% of Arsenic	[Balasubramanian et al., 2001]
	Al/Al-Monopolar	420 mA	80-90% of Cr	[Park et al., 2002]
	Fe-Fe	100 - 500 A/m^2	65-88% of Cu, Zinc	[Ninova et al., 2003]
	Fe, Al	15 - 22 A/m^2	Max. 99%	[Kumar et al., 2004]
	Fe-Fe	0.8 - 1.2 A/dm^2	80-98% of Arsenic	[Hansen et al., 2005]
	Fe/Fe electrodes-Monopolar	0.1 A	80-97% of Cr	[Gao et al., 2005]
	Fe/Fe electrodes-Monopolar	0 - 3A	75-95% Silica nano- particles	[Den et al., 2005]
	Seven parallel plates of Fe and Carbon steel	4 - 5 A	60-99% of Arsenic	[Parga et al., 2005]
	Al-Fe	2.5 A/m^2	99% of Arsenic	[Kobya et al. 2011]
Turbid industrial wastewater	Fe/Stainless steel	0.2 - 1 A	80-95% of turbidity	[Abuzaid et al., 2002]
	Al/Al Monopolar	0.5 - 2.5 A	60-88% of turbidity	[Sivakumar et al., 2004]
Wastewater containing organic and inorganic pollutants	Fe	22.4 A/m^2	BOD: 96% Cr: 100 % TSS: 96% TKN: 62% TDS: 50%	[Kongjao et al., 2008]
Textile wastewater	Al	80 A/m^2	Turbidity: 90% TS: 50% COD: 70%	[Zodi et al., 2010]
	Fe/Al electrodes-	30 - 80 A/m^2	50-80% COD removal	[Hutnan et al., 2005]

	monopolar				
Municipal wastewater	Fe	20 A/m^2		Calcium 98% Total hardness: 97% Turbidity: n.d.	[Malakootian et al., 2010]
	Stainless steel	30 A/m^2		TSS: 95% Turbidity 93% BOD 99%	[Bukhari et al., 2008]

2.3 Membrane fouling control by electrokinetic technologies

Due to ionization and absorption, most polymeric and ceramic membranes used in the water and wastewater treatment processes are negatively charged, especially under high pH conditions. Considering the electrical charge characteristics of both raw water/wastewater and membrane materials, one promising direction towards hindering cake accumulation on the membrane surface is use of electrokinetic technologies. Hybrid water / wastewater treatment processes combining electric field application and membrane filtration including electrophoresis-based electrofiltration, dielectrophoretic flux enhancement and electrocoagulation (EC) pretreatment have gained interest [Pletcher et al., 1990; Goodridge et al., 1994; Prentice et al., 1991].

Emerging in the 1970s, the electrokinetic technologies have been increasingly investigated as promising membrane fouling control strategies. Electrophoresis and di-electrophoresis function through an electrokinetic mechanism, i.e. relying on uniform or non-uniform electric fields to transport fouling particles away from the membrane surface [Vonzumbusch et al., 1998; Weigert et al., 1999; Lee et al., 2002; Yang et. al., 2002]. In EC, the colloidal particles are aggregated to form larger flocs which subsequently increase the porosity of biocake and thus improve the

membrane filterability. Furthermore, the freshly generated coagulants adsorb the extracellular polymeric substance (EPS), the major membrane foulants in bulk fluid, and affect the growth kinetics and structural characteristics of the biocake on the membrane surface. Compared to various afore-mentioned membrane fouling combating approaches, electrokinetic technologies offer the following technical and economic advantages:

(1) Versatile applicability: applicable to a variety of industrial and municipal wastewater at any capacity;

(2) Configuration simplicity and scalability: the core electrokinetic configuration consists of a DC or AC power supply unit and electrode array, which is simple to design, install and scale up;

(3) Small footprint: the electrokinetic setup is usually compact and sometimes can be placed in the existing reactors;

(4) Performance predictability: the electric field strength can be accurately calculated and generation of the metal cations follows chemometrics, which make the treatment efficiency highly reproducible and predictable;

(5) Amenability to operation automation: the most important operating parameters of an electrokinetic process are current and voltage which are easy to be digitally controlled and can facilitate process operation automation.

(6) Minimum chemical demand and waste production: electrokinetic processes utilize electricity to mitigate membrane fouling through physical mechanism or electrochemical reactions with the chemical constituents in the water/wastewater to be treated, generally requiring no consumption of external chemicals. As a result, the waste stream or sludge is reduced accordingly;

(7) High energy efficiency: electrokinetic processes are normally operated at ambient temperature, which is energy efficient;

(8) Lower capital and operating costs: the construction of electrolytic cells and peripheral equipment are generally simple and inexpensive, and process automation further cuts operation costs.

It should be noted that membrane fouling control using electrokinetic technologies has mostly been studied in lab scale for water or industrial wastewater treatment and integration of these technologies into municipal wastewater MBR remains a challenge due to issues such as availability of sustainable electrode materials and frequent electrode cleaning. In this thesis the three electro technologies of electrophoresis, di-electrophoresis and EC are briefly reviewed in terms of the underlying principles, individual pros and cons and future application perspectives, which may serve as general guidelines for their integration into a membrane filtration system to control membrane fouling.

2.3.1 Electrofiltration

2.3.1.1 Background

Electrophoresis is the migration of charged particles in a fluid in the presence of a uniform electric field. This physical phenomenon was first discovered in 1807 by Reuss [1809] who observed that a homogeneous electric field might induce the movement of clay particles suspended in water. Electrophoresis found its first application in filtration enhancement by Beechold in 1926 [Beechold, 1926], but the theoretical foundation was laid in the 1960s [Moulik et. al, 1971; Bier et al., 1967; Moulik et al., 1967] and 1970s [Moulik, 1976].

In electrofiltration, a direct current field is applied in the direction of the filtration flow. The negatively charged colloidal particles are subjected to the electrophoretic force and have a tendency to overrun the hydrodynamic resistance force and move against the fluid flow or away from the membrane surface. As a result, formation of the membrane surface cake can be eliminated or significantly mitigated under sufficient electrical field strength. The filtration resistance is thus decreased and permeation flux is increased accordingly. The movement dynamics of a colloidal particle in the electro-filtration media can be illustrated in Fig. 2.9.
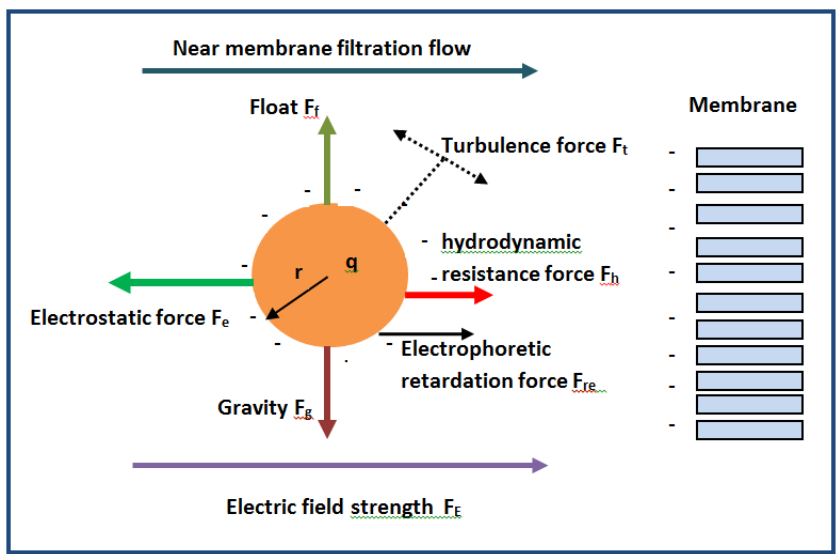
Fig. 2.9 Dynamics of a colloidal particle in an electro-filtration system

Due to various intricate diffusion mechanisms such as Brownian diffusion, shear induced diffusion, and concentration gradient diffusion, migration of a particle in the filtration medium is the combined effect of multiple driving forces, namely, its gravity F_g, buoyancy F_f, electrophoretic retardation force F_{re}, turbulence force F_t, electrostatic force F_e as well as the hydrodynamic resistance force F_h. Among these forces the turbulence force may be exerted in

any direction. If there exists no turbulence caused by mechanical mixing or aeration, the trajectory of the particle is mainly dependent on the relative magnitude of the electrostatic force and the hydrodynamic resistance force. For simplicity, the other forces are not taken into account in the following calculations when the Reynolds number is very small ($< 10^{-3}$).

In Fig. 2.9 q is the particle surface charge and it can be calculated based on the zeta potential of the colloidal solution [Huisman et al., 1998]:

$$q = 6\pi r \varepsilon_d \xi \qquad (2\text{-}21)$$
$$F_e = qE = 6\pi r \varepsilon_d \xi E \text{ (Coulomb's law)} \qquad (2\text{-}22)$$
$$F_g = \pi r^3/6(\rho_f - \rho_t)g \qquad (2\text{-}23)$$
$$F_h = 6\pi r \eta v_e \text{ (Stokes' law) [Agana et al., 2011]} \qquad (2\text{-}24)$$
$$F_f = 0.761(\tau_w^{1.5} r^3 \rho_t/\eta) \text{ [Stamatakis et al., 1993]} \qquad (2\text{-}25)$$

where: r is the particle's hydrodynamic radius (m)
   ε_d is the dielectric permittivity of water (S/m)
   ξ is the zeta potential (V)
   E is the external electric field strength (V/m)
   η is the viscosity of the colloidal solution (Pa·s)
   v_e is the colloidal particle's electrophoretic velocity (m/s)
   ρ_t is the density of the influent at 20 ^{0}C (998.2 kgm^{-3})
   ρ_f is the density of the particle at 20 ^{0}C (kg/m^3)
   F_e is the electrostatic force (N)
   F_g is the gravity (N)
   F_h is the hydrodynamic resistance force (N)
   F_f is the float (N)

In an electrofiltration system, two types of electrodes are usually utilized: flat plate or concentric cylinder electrodes and their electric field strengths can be calculated as following:

For the flat plate electrode, $E = \dfrac{\emptyset}{d}$ (2-26)

Where: $\emptyset$ is the electric potential of flat plate electrode (V)

   D is the distance between the electrode plates (m)

For the concentric cylinder electrode, $E = \dfrac{(\emptyset o - \emptyset i)}{r ln(\frac{ro}{ri})}$ [Huotari et al., 1999]   (2-27)

$\emptyset_o$ is the electric potential at the outer electrode (V)
$\emptyset_i$ is the electric potential at the inner electrode (V)
r_o is the radius of the outer electrode (m)
r_i is the radius of the inner electrode (m)
r is the radial coordinate (m)

The electrophoretic mobility of a charged particle (u_e) is defined as: $u_e = v_e / E$ (2-28), and V_e is

the particle's migration velocity (m/s). When $F_e < F_h$, the colloidal particle would migrate

towards the membrane and a cake layer would form on the outer surface; When $F_e > F_h$, the

colloidal particle would be driven away from the membrane and therefore no cake layer would

be accumulated, and the existing cake layer could even be eroded. However, when $F_e = F_h$, i.e.

the electrical force and the hydrodynamic force are balanced, there would be no net particle

migration towards the membrane and the electric field is referred to as the critical electric field

which can be calculated using the following equation:

$$E_{crit} = J_{max} / u_e \qquad\qquad\qquad (2\text{-}29)$$

where J_{max} is the maximum solvent flux at a given TMP, equal to the flux through clean

membrane. From Equation (2-22) and (2-24) it is derived that, at the equilibrium state, the

particle's migration velocity is:

$$V_e = \varepsilon_d \xi E / \eta \qquad\qquad\qquad (2\text{-}30)$$

2.3.1.2 Configuration

In electrofiltration the ultimate purpose is to use the external electric field to divert the colloidal

particles away from the membrane surface and subsequently reduce fouling. Though a number of

studies have been reported in the last four decades, basically only two configurations have been

proposed [Kyllönen et al., 2005]: one is like a "sandwich" setup where an electric field is applied

across the membrane with one electrode on either side of the membrane (Fig. 2.10), and the other is that an electric field is applied between membrane and another electrode, with the membrane or membrane support used as the cathode (Fig. 2.11). In the latter case, the membrane or membrane support must be made of conductive materials such as metal, carbon or special ceramics etc. As the membrane itself acts as the cathode, there is a net electric voltage across the membrane pores, resulting in electro-osmosis, which further enhances the fluid permeation in addition to the electrophoresis effect.
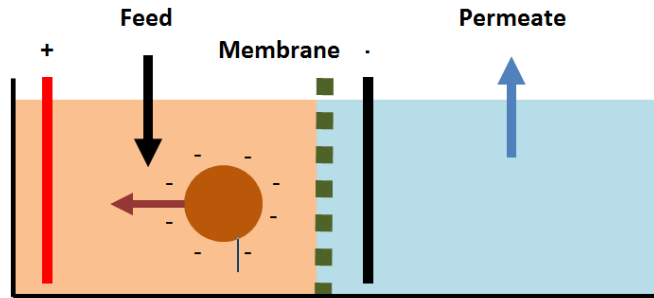
Fig. 2.10 Typical configuration of electro-filtration using flat sheet membrane
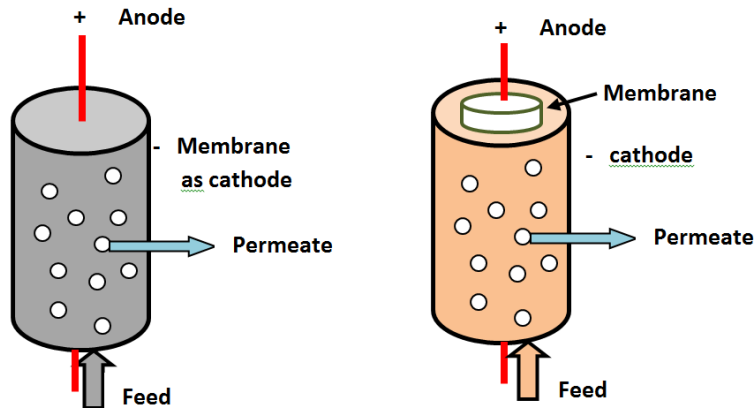
Fig. 2.11 Configuration of electro-filtration using tubular membrane

One of the major challenges in the commercialization of electro-filtration is the lack of inexpensive and electrochemically stable or corrosion-resistant electrode materials. As electron

gaining reactions occur at the cathode, stability of the cathode material is not critical, and usually stainless steel is a good choice. However, at the anode the electrochemically active metal will lose electrons and erode due to generation of metal ions. Therefore, ideally the anode should be made of inert graphite or titanium coated with a noble metal such as platinum or its oxide.

2.3.1.3 Applications

Electrophoresis-based permeation flux enhancement and membrane fouling reduction have been investigated for decades in the water and wastewater treatment industries [Huotari et al., 1999; Zumbusch et al., 1998; Lentsch et al., 1993; Brisson et al., 2007]. Electrophoresis may be driven either by constant or pulsed electric field [Iritani et al., 2000]. A parametric study on cross-flow electromembrane system was conducted for separating a solid/liquid suspension containing 50 g/L of silicium oxide particles [Lazarova et al., 2002]. Extensive operating conditions were examined: applied voltage (0–200 V), feed concentration (1 - 5 wt.%), temperature (15 - 50 ^{0}C), TMP (1–3 bar) and filtration linear velocity (0.1–0.34 m/sec). The results indicated that the filtration flux was improved as much as 366% under an applied electric field strength of E = 133V/cm. Akamatsu et al. [2010] applied an electric field intermittently to a crossflow membrane filtration system for activated sludge and successfully suppressed membrane fouling. An electric field strength of 6 V/cm with an on/off operating mode every 90 seconds effectively diverted the activated sludge flocs away from the membrane surface and thus improved the average permeate flux.

The pulsed electric field was evaluated in dead end microfiltration of a titanium suspension [Ahmad et al., 2000]. Pulse variables such as the interval, duration and strength were extensively investigated. 10 seconds of pulse duration at shorter pulse interval and 100 V applied voltage offered the best efficiency of biocake removal. With the electric pulse the flux was found to have significantly improved through electrophoretic dislodging of particles away from the membrane surface and electroosmostic enhancement in the filter cake. The effect of a pulsed square wave on flux enhancement in electrodialysis was investigated by Lee et al. [2002, 2004]. The optimal frequency to mitigate fouling potential was found to be 50Hz. It was suggested that pulsing electric field could be used as a cleaning-in-place method for improving the ED performance. Recently, impact of a high voltage impulse (HVI) (electric field strength ranged from 4 to20 kV/cm, with the pulse duration between 20 to 70 µs) on membrane fouling in a MBR was studied [Lee et al., 2014]. After HVI induction, permeate flux was found to be consistently higher than that of the control. In addition, HVI caused a change of the mixed liquor properties: decrease in sludge or MLSS production and increase in the concentrations of soluble-chemical oxygen demand (SCOD), total nitrogen (TN), total phosphorus (TP), polysaccharide as well as protein in the bulk solution, suggesting HVI dislodged the deposited cake layer on the membrane surface and induced sludge solubilisation.

Weigert et al. [1999] quantitatively studied the influence of both constant and pulsed electric fields on membrane filtration. As high as 10-fold increase in permeate flux was achieved with application of the electric field. It is interesting to note that for mineral suspension, constant field showed greater permeate improvement, whereas for biomass the pulsed field demonstrated better

flux enhancement. Estimation of specific energy consumption indicated the electrofiltration system's significant energy-saving potential.

The effect of electric field on the filtration performance was modelled on a 50-nm ceramic membrane submerged in the CED paint wastewater containing 5% (v/v) suspension [Agana et al., 2012]. At a TMP of 100 kPa, the filtration efficiency increased with various applied voltages. However, there was no positive effect on the membrane filtration performance at high TMPs of 200 and 300 kPa.

The concentration polarization in membrane filtration and electric field assisted flux enhancement effects were modelled by Sarkar et al.[2010]. The numeric simulation results showed that the imposed electric field might induce significant membrane fouling reduction and flux improvement. At a cross-flow velocity of 2.1 m/s and with feed containing 7.5 kg/m^3 of gelatin, the flux increased by 167%, when an electric field of 1300 V/m was applied. The predicted flux increase was verified with experimental data.

Table 2.6 presents some of the work in which the electric field strength and fouling mitigation effect are clearly described. This table shows that membrane fouling can be reduced significantly only if high electric field intensity is used. In addition, most of the electrically enhanced filtration studies were conducted with synthetic wastewater or suspensions in bench scale; full scale application in real wastewater treatment process has not been reported.

Table 2.6 Some applications of electrophoresis in membrane fouling control

Pilot scale or bench scale	Filtration medium	Electric filed strength	Antifouling Effect	Ref.
Bench scale pretreatment	Real sewage	0 – 10,000 V/cm	Coagulation dose saved by 75% for 95% turbidity removal	[Kim et al., 2007]
Bench scale	Oil emulsion	150 V/cm	Flux increased from 35 to 70 L/(m^2.h)	[Cornelissen, 1997]
Bench scale	Water soluble polymer	1,670 V/cm	10-fold increase in the flux	[Akay et al., 1997]
Bench scale	Oil emulsion	24 V/cm	Flux increased from 75 to 350 L/(m^2.h)	**[Huotari et al., 1999]**
Bench scale	Gelatin	24 V/cm	Flux increased from 4 to 12 L/(m^2.h)	[Rios et al., 1988]
Bench scale	Kaolin suspension	0.01A /cm^2 of the electrode area	Filtration time reduced by 50% when current applied only 37% of the process time	[Larue et al., 2003]
Bench scale	TiO$_2$ suspension	100 V	Water recovery increased from 77% to 96%	[Ahmad et al., 2001]
Bench scale	Real sewage	20 V/cm	Flux increased from 35.67 to 36.73 L/(m^2.h)	[Chen et al., 2007]
Pilot scale	SiO$_2$ suspension	0 -125 V/cm	Flux increased from 34 to 102 L/(m^2.h)	[Lee et al., 2007]
Bench scale	Synthetic wastewater	6 V/cm	Flux increased 3.5 times compared to 0 electric field	[Akamatsu et al., 2010]
Bench scale	Synthetic CED paint wastewater	20, 40 and 60 V	Flux was directly proportional to the applied voltage at TMP of 100 kPa, but showed no improvement at 200 and 300 kPa of TMP	[Agana et al., 2012]
Pilot scale	Mineral suspension and biomass	Constant field: 0 - 350 V/cm Pulsed field: 150 V/cm	Flux increased by nearly 10-fold	[Weigert et al., 1999]
Bench scale	Activated sludge	Pulsed field: 4 to 20 kV/cm Duration: 20 to 70 μs	Flux increased by nearly 11% - 30%	[Lee et al., 2014]
Bench scale	Synthetic juice	0 -1600V/m	3.3 fold increase in permeate flux	[Sarkar et al., 2010]
Bench scale	SiO2 suspension	133V/cm	Permeate flux increased by 366%	[Lazarova et al., 2002]

According to Equation 2-22 the electrophoretic force relies on not only on the electric filed intensity but also the magnitude of the colloidal particle's surface charge. Contrary to the afore-mentioned electrophoretic strategies requiring an external electric field across the filtration membrane, Lee et al. [2007] simply employed an electrostatic device to change the surface charge of feed solutes to reduce membrane fouling. A high voltage electrostatic device (30 kV) was used to modify the surfaces of TiO_2 and SiO_2 nanoparticles from positively charged to negatively charged, and the zeta-potentials were shifted by apprioximately -40 mV. Though no additional electric field was applied, the increased electrostatic repulsion among the colloidal particles and with the membrane, affected the accumulation characteristics of the filtration cake on the membrane surface. Consequently this led to membrane fouling retardation and filterability improvement.

Wang et al. [2011] developed a novel bio-electrochemical membrane reactor with the aim of combining MBR and microbial fuel cells (MFC) to treat wastewater while recovering bioenergy. In the integrated MBR and MFC system, a stainless steel mesh was used as cathode and the biofilm attached on it served as the filtration medium. In addition to flux enhancement, a maximum power density of 4.35 W/m^3 or a current density of 18.32 A/m^3 were harvested under the experimental conditions (HRT = 150 min. and external resister = 100 Ω), which demonstrated the promising potential for wastewater treatment, MBR filtration mitigation and energy recovery. The same group designed and operated another flux enhancing electrofiltration system in which bioanode-generated electricity with maximum power output of 1.43 W/m^3 or 18.49 A/m^3 was utilized to mitigate the membrane fouling [Wang et al., 2013]. As a result, the cake layer deposited in the membrane surface was substantially reduced, though the oxidative

breakdown of the membrane foulants by electrochemically produced H_2O_2 was also considered a contributing factor.

2.3.2 Dielectrophoretic flux enhancement

2.3.2.1 Background

DEP phenomena was first reported in the 1950s [Pohl, 1951; Pohl, 1958] and has been revived due to its application for manipulation and separation of colloidal particles in the last two decades [Green et al., 1998; Morgan et al., 1999; Dussaud et al., 2000]. The fundamental physical mechanism underlying DEP is the interaction of induced dipoles of colloidal particles with a spatially non-uniform electric field. When subjected to an external electric field E, a neutral suspension particle and the surrounding medium in a colloidal solution tend to be polarized and the colloidal particle therefore becomes a dipole, as shown in Fig. 2.12. In most aqueous colloidal solutions, the suspension particles have significantly smaller dielectric constants than water (< 10 vs. ~ 80), consequently they are less polarized. The particle's surface charges interact with the electric field and generate Coulomb force F which is dependent on the medium and particle's electrical properties as well as the particles' shape and size. In a homogeneous field (Fig. 2.12 a), the net force exerted on the colloidal particle will be zero but in the presence of a non-uniform external electric field (Fig. 2.12 b), the colloidal particles are subjected to a dielectrophoretic force F_{DEP}, which drives the particles to move in the direction of electric field. F_{DEP} can be expressed in the following equation:

$$F_{DEP} = 2\pi r^3 \epsilon_m R_e[K(\epsilon_p^*, \epsilon_m^*)]\Delta(\mathbf{E.E}) \quad (2\text{-}30)$$

Where: r - radius of the suspended particle (m)

E - electric field intensity (N/C)

ϵ_m - complex dielectric constant of the suspended particle

ϵ_p - complex dielectric constant of the suspending medium

$R_e[K(\epsilon_p^*, \epsilon_m^*)]$ - complex Clausius-Mossotti function $(\epsilon_p^* - \epsilon_m^*) / (\epsilon_p^* + 2\epsilon_m^*)$
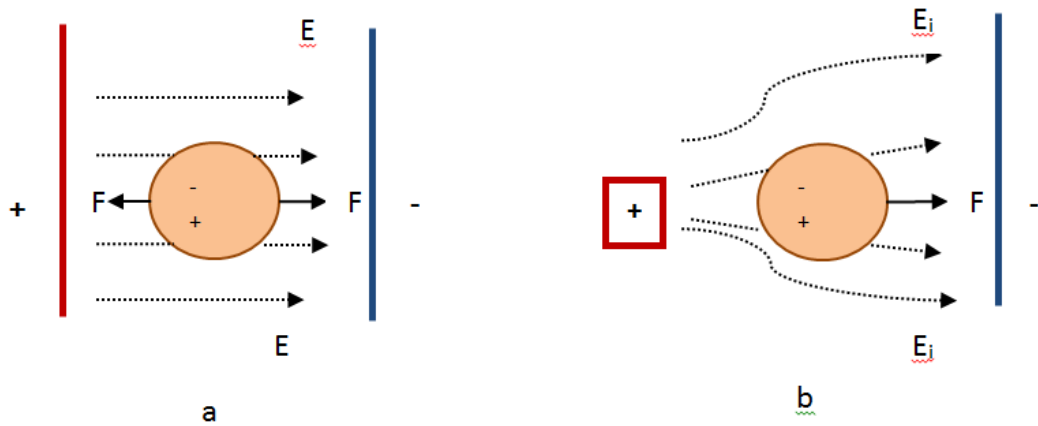
Fig. 2.12 Particle movement in homogeneous or non-homogeneous electric field

2.3.2.2 Application

Application of this technology in membrane filtration processes is mainly attributed to the work by Molla et al. [2005; 2008]. The proposed configuration is to embed an array of parallel microelectrodes on the membrane. Numerical simulations of dielectrophoretic forces and trajectories of colloidal particles were performed for a crossflow membrane filtration process when subjected to nonuniform electric field. It was theoretically demonstrated that membrane fouling can be controlled by applying the repulsive dielectrophoretic forces on the suspended particles in the fluid [Molla et al., 2007; Molla et al., 2008]. In addition, alternating of the flow field near the membrane surface further resists accumulation of particles on the membrane. The simulated results were successfully applied in separation of small amounts of droplets from

water-in-oil emulsions and levitation of the polystyrene latex particles suspended in an aqueous medium on a permeable glass substrate. Another interesting design is a multilayered porous medium alternately inserted with conductive and nonconductive materials [Molla et al., 2005]. By applying AC of appropriate amplitude and frequency, the retention behaviour of particles on the filtration media can be manipulated. Recently, Hawari [2015] conducted a biomass filtration experiment aiming at suppressing fouling with DEP force at electrical field intensities of 6 - 160 V and frequencies of 50 - 1000 Hz. A stronger electrical field generated greater DEP force and thus resulted in better membrane fouling mitigation effect, and higher frequencies were capable of achieving improved permeate flux. However, the side effect of stronger electrical field or higher frequencies was the substantial Joule heating, which caused reduce permeate flux. In spite of being the first attempt of biomass filtration by the DEP technology, the experimental setup is not a MBR system because the biomass was killed by autoclave prior to the filtration tests. Therefore, this study cannot be regarded as a practical application of DEP technology in MBR.

2.3.3 Electrocoagulation

2.3.3.1 Electrocoagulation as a pretreatment process in MBR or membrane filtration

As described in Section 2.2, in EC high valence cations such as aluminum or ferric ions are generated in situ by electrochemically dissolving the aluminum or iron anode. The freshly produced aluminum or ferric ions are highly efficient coagulants and are hydrolyzed into aluminum hydroxide or ferric hydroxide. These iron or aluminum hydroxides are capable of destabilizing the colloids and subsequently accelerating the separation of sludge from biomass. In addition, the aluminum hydroxide or ferric hydroxides may strongly adsorb EPSs from the mixed liquor. According to Section 2.1.3, in MBRs the two critical fouling factors are TSS and

94

EPS concentrations. Both are major contributors of biocake on the membrane surface. In the past two decades, sporadic researches have been conducted to integrate EC and MBR in an attempt to mitigate membrane fouling.

Pouet and Grasmick [1994] integrated EC into the pretreatment step for crossflow microfiltration of municipal wastewater, and reported that the permeation flux for a 0.1 μm microporous membrane increased from 0.02 m^3/m^2h to 0.35 m^3/m^2h due to electrochemical conversion of the colloidal fraction into larger particulates. Al-Malack et al. [2006] studied the fouling mechanism of a woven fabric membrane used to filter kaolin suspension with continuous addition of electrochemically produced ferric coagulant at different kaolin concentrations and crossflow velocities (CFV). They concluded that with EC membrane fouling followed the classical cake filtration model, in contrast to the dominant pore blocking mechanism in the absence of EC. EC-assisted membrane process was also evaluated with ceramic membranes for removing selenium from industrial wastewater [Mavrov et al., 2006]. The microfiltration showed very stable operation and the filtration cake could be easily removed by back-pulsed air. In addition, compared to the conventional ferric coagulation/filtration process, the yield of solid waste was reduced by 40%. Ashima Bagga etc. [2008] explored the influence of EC on microfiltration when iron was used as anode and concluded that membrane fouling was not mitigated under the various experimental conditions because highly soluble ferrous ions rather than ferric ions were produced at the anode during the EC process. Aluminum was therefore recommended as the anode material. Mariam et al. [2010] developed an EC-nanofiltration system for treating leachate and proved that EC outperformed chemical coagulation in terms of organic removal and fouling reduction.

EC was used as a pretreatment process for a bench-scale seawater ultrafiltration system [Timmes et al., 2009]. The performance evaluation parameters include TMP, UF filtration resistances and post-cleaning flux recovery under sub- and super-critical flux conditions. It was found that in-line EC reduced the UF membrane filtration resistance under all coagulation and flux conditions. In addition, EC offered superior membrane fouling mitigation efficiency than chemical coagulant ferric chloride of the equivalent dosage. Sasson et al., [2009] pretreated a synthetic wastewater containing chemical mechanical polishing particles with EC prior to electroflocculation and found that the filtration energy consumption was reduced by over 90% due to membrane fouling mitigation. The sweep-coagulation mechanism was indirectly explained through scanning electron micrographs of the fouled membrane surface: the amorphous iron-hydroxide particles accumulated on the membrane surface and served as a secondary filtration medium, which not only hindered the colloids from entering into and plugging the pores but also decreased the hydraulic resistance of the cake due to EC enhanced particle aggregation. In a similar electrocoagulation/electrofiltration (EC/EF) treatment experiment with chemical mechanical polishing wastewater [Yang et al., 2006], the final filtration rate was found to increase by approximately 10-fold when the applied electric field intensity reached 60V/cm. Tanneru et al. [2012] took advantage of the thick cake formed on the surface of the microfilter through electrocoagulation with aluminum to enhance removal of viruses from the surface water. In most of these studies EC was used as a pretreatment step in the lab-scale, and no full-scale application has been reported for municipal wastewater treatment. Recently, Nguyen et al. [2014] investigated the effect of EC as a post-treatment means in a pilot scale hybrid treatment system which integrated rotating hanging media bioreactor (RHMBR) and submerged membrane

bioreactor (SMBR). Nearly 100% of NH_4^+-N and T-P were removed and very low TSS, COD, BOD and coliform bacteria concentrations were observed in the effluent.

2.3.3.2 Electrokinetically enhanced MBR

In the past few years, a new type of hybrid MBR called Submerged Membrane Electro-bioreactor (SMEBR) was developed and extensively studied [Bani-Melhem et al., 2010; Bani-Melhem et al., 2011; Ibeid et al., 2013; Hasan et al., 2012; Ibeid et al., 2013; Hasan et al., 2014]. In SMEBR the membrane module is encircled by a pair of cylindrical meshed electrodes. Consequently, various physical, chemical and biological processes occur simultaneously in the reactor: the main physical phenomenon is electrokinetic migration of the biomass flocs away from the membrane surface, the chemical processes include in situ release of metal ions as an efficient coagulant precipitating phosphate. At the core, SMEBR is still an activated sludge reactor with biological nitrification process. Bani-Melhem et al. [2010, 2011] first developed and validated the SMEBR system in multiple phases, while the design constraints and criteria of the SMEBR were also proposed. With intermittent application of direct current (15 min ON/45 min OFF), the membrane fouling rate was reduced by 16.3% and the specific resistance to filtration (SRF) decreased by as much as 40%. Hasan et al. [2012] studied the influence of sludge properties in a pilot SMEBR on membrane fouling. Statistical analysis showed that the mean particle size diameter is inversely correlated to the TMP in SMEBR whereas MLSS is positively corelated to the membrane filtration resistance, which are both opposite to the observations in a control MBR. This contrary trend was also observed for the impact of soluble EPS on membrane fouling, which suggests that membrane fouling reduction in SMEBR is mainly attributed to the

97

electrokinetic effect rather than changes in the chemical compositions or particle size differences. Influence of direct current (DC) field on the activated sludge was also investigated in bench-scale. The normal range of MLSS (5 – 15 g/L) was tested at various current densities ranging from 5 to 50 A/m^2 [Ibeid et al., 2013]. The sludge filterability was improved by over 200 times between 15 and 35 A/m^2, along with 4.8-fold decrease in the specific resistance to filtration. Protein, polysaccharides and organic colloids in the sludge supernatant were removed by 43%, 73% and 91%, respectively. Relationship between the feed protein content and membrane fouling rate was also studied in SMEBR [Ibeid et al., 2013]. The membrane fouling rate was found to be reduced by more than 5-fold when the protein concentration was over 80 mg/L. The following pilot SMEBR with real municipal wastewater showed an advantage of a third of the membrane fouling rate. Recently a pilot system was operated to investigate the start-up period performance of SMEBR [Hasan et al., 2014]. TMP increased very slowly at 0.02 kPa/d and time to filter 100 ml of sludge was shortened by 78%, demonstrating significant membrane fouling abatement.

The author designed and implemented a novel electrically enhanced membrane bioreactor (EMBR) as an alternative decentralized wastewater treatment system with improved nutrient removal and reduced membrane fouling at low temperature[Wei et al., 2012]. It was found that TMP increased significantly slower in the EMBR and the interval between the cleaning cycles of the EMBR increased at least twice, demonstrating the application potential of the electrokinetically assisted MBR in cold regions. Effects of membrane fouling reduction in electrokinetically enhanced MBRs are presented in Table 2.7.

Table 2.7 Examples of membrane fouling reduction in electrokinetically enhanced MBRs

Filtration medium and membrane	Anode material	Electric filed strength	Antifouling Effect	Reference
Synthetic wastewater, MF	Al	0.4 A	Flux recovery efficiency > 90%	[Sasson et al., 2009]
Synthetic wastewater, UF	Iron	0.28 - 1.14 V/cm	Specific resistance to filtration (SRF) reduced by 40%, and membrane fouling rate dropped by 16.3%	[Bani-Melhem et al., 2010; 2011]
Synthetic wastewater, UF	Al	1.2 V/cm, intermittently	Interval between membrane cleaning cycle increase twice	[Wei et al., 2012]
Real municipal wastewater, UF	Al	12 A/m^2, intermittently	The time to filter 100 mL of the sludge decreased by 78%	Hasan et al., [2012, 2014]
Activated sludge	Al	5 - 50 A/m^2, intermittently	The specific resistance to filtration (SRF) was reduced by 80%	[Ibeid et al., 2013]
Synthetic wastewater, UF	Al	15 A/m^2, intermittently	Membrane fouling rate 5.1 times to 5.8 times	[Ibeid et al., 2013]

2.3.3.3 Challenges in the EC-enhanced MBR

Though significant membrane fouling reduction and advantages over chemical coagulation in the

EC pretreatment or hybrid MBR systems have been reported, the potential negative impact was

also addressed in a couple of studies and cannot be neglected. Timmes et al. [2010] compared the

performance of UF filtration setup after feed pretreatment by a pilot-scale EC or ferric chloride

coagulation reactor. The TMP with EC increased slightly faster than that under chemical

coagulation though subcritical flux was operated for both scenarios. It might be attributed to the

presence of soluble Fe(II) which is detrimental to membrane filtration [Bagga et al., 2008]. It

should be noted that such a problem would not come up if aluminum was used as the anode. Yu et al. [2013] studied the influence of alum and $FeCl_3$ on ultrafiltration (UF) membrane fouling, $FeCl_3$–UF exhibited significantly higher membrane fouling rate than the alum–UF system, and the observed smaller primary particles, denser and thicker cake layer, which was considered to be responsible for the inferior membrane performance with the ferric salt.

Another drawback of the EC technology is electrode fouling: the EC electrodes were coated with precipitates of metal hydroxides which result from the reaction of newly produced ferric or aluminum ions with hydroxyl ions or phosphate present in the vicinity of electrodes. Solutions to prevent precipitate accumulation on electrodes may include:

1 Suppression by low-frequency sonication [Kovatcheva et al., 1999] or electromagnetic Field [Ni'am et al., 2006];

2 Deliberate design of the electrode configuration and the influent flow channel [Mills et al., 2000];

3 EC units are operated under short hydraulic retention times or high enough linear flow velocity;

4 Higher current density is applied so that the generated hydrogen gas (at cathode) can dislodge the precipitates on the electrode surface;

5 The electrode polarities are progressively reversed toward longer cycling times, that ensures that the precipitates on both cathode and anode are equally removed during the experimental period [Timmes et al., 2010];

6 Periodic manual or mechanical abrasion.

2.3.4 Abiotic ammonification in the electrokinetic technologies

In the last two decades more electrokinetic technologies have been studied or applied in wastewater treatment process, including elecrofiltration [Hofmann et al., 2006; Agana et al., 2011], electrochemical oxidation/reduction [Sunderland et al., 1997; Shen et al., 2003], electrocoagulation/ electroflotation [Mollah et al., 2004; Emamjomeh et al., 2009], electro-dewatering [Chu et al., 2004; Esmaeily et al., 2006] and hybrid processes such as submerged membrane electro-bioreactor [Bani-Melhem et al., 2011; Hasan et al., 2014] or electrically enhanced membrane bioreactor [Wei et al., 2012]. However, the side effects of electric application are usually neglected or overlooked, e.g. reversal of nitrification or electrochemical reduction of nitrate into ammonium.

Electrochemical treatment of nitrate has been applied to industrial wastewater such as low-level nuclear wastes [Prasad et al., 1995; Katsounaros et al., 2009; Steimke et al., 2011] and effluent from regeneration of the ion exchangers [Paidar et al., 2004; Dortsiou et al., 2009] where the environment is too hostile for biological processes. Electrochemical denitrification has also been investigated to remove nitrate from groundwater [Dash et al., 2005]. Commonly used electrode materials are aluminium, iron, titanium and catalytic alloys such as Pt, Pd, Zn or Cu [Polatides, 2005] and boron doped diamond [Lévy-Clément et al., 2003; Matsushima et al. 2009]. Nitrogen gas is the desirable end product, however, selective reduction of nitrate to nitrogen is difficult to achieve due to the chemical valence complexity of elemental nitrogen.

Though electrokinetic technologies and electrochemical nitrate removal processes have co-existed for a number of years, they were studied or operated independently with different

objectives and consequently, electrochemical generation of ammonium from nitrate was largely

ignored in the electrokinetic processes such as electrofiltration, electroosmosis and electro-

dewatering. As shown in Table 2.8, both aluminium and iron have been tested at various pHs and

electric current densities and over 90% of nitrate was removed. Alkaline pH range favoured the

process and the optimum pH was typically found to be 9. In spite of significant nitrate removal

efficiency, the nitrate destiny was mostly overlooked [Tchamango et al., 2010; Ricordel et al.,

2010; Malakootian et al., 2011; El-Shazly, 2011; 2013; Pak, 2015]. Ammonium, the usually

dominant side product was particularly rarely reported [Emamjomeh and Sivakumar, 2005;

Lacasa et al., 2011; Symonds et al., 2015].

Table 2.8 Examples of nitrate removal in the electrocoagulation process

Electrode	Current density (mA/cm^2)	pH range	Nitrate (NO_3^-) removal	Ammonium (NH_4^+) observation	Reference
Iron	0.125 – 0.5	5 - 11	Over 95%	No	[Koparal at al., 2002]
Iron	N.A.	9 -11	Over 90%	NH_4 increased while NO_3^- decreased	[Sivakumar., 2005]
Al, Fe	0.1 - 0.2	5 – 9, Optimum pH 7.34	89.7%, iron was more effective in NO_3^- removal	No	[Malakootian et al., 2011]
Al, Fe	1, 3, 5	6 – 9, not controlled	Over 95%	Reported, but not explained	[Lacasa et al., 2011]
Al	10	3 – 12 Higher pHs favour NO_3^- removal	Up to 90%	No	[El-Shazly, 2011]
Al	0.78 to 2.34	3 – 9 Higher pHs favour NO_3^- removal	84% - 90%	No	[El-Shazly, 2013]
Al	4.9 – 44.1	3.8 -10.1, initial pH independent	40.6% - 61.1%	Yes, 53.4 – 59.1% 10% – 20% of NH_4^+ adsorbed	[Yehya et al., 2014]

				on solids	
Al, Fe	6 - 14	7 – 11, optimum pH 9	77.67% to 91%	No	[Pak et al., 2015]
Al	10.2 – 18.1	Not controlled	89.7%	Over 60% NH_4^+ increase	[Symonds et al., 2015]
Al, Fe	25	7 ± 0.1	92% for Al - Fe pair; 80% for Fe - Fe pair	NH_4^+ increased 10% to 20%	[Govindan et al. 2015]

2.4 Bacterial viability under electric fields in the wastewater treatment

Biological processes in wastewater treatment facilities rely on the mixed microorganism communities to remove organic matter and nutrients (N and P) from raw wastewater. Therefore, the influence of electric current on bacterial activity or viability has been one of the major concerns when applying electro-technologies.

Under the stress of electric current, a bacterial cell's metabolism, physiology, shape and movement may be impacted [Jackman et al., 1999; Satoshi et al., 1997; She et al., 2006; Thrash and Coates et al., 2008]. Sakakibara and Kuroda [1993] reported that there was a linear relationship between the decrease of denitrification rate and the increase of the electric current applied. Alshawabkeh et al. [2004] investigated the effect of electro-stimulation on an aerobic culture and found that a small window of DC fields (between 0.57 and 1.14 V/cm) resulted in improvement in the biological removal of chemical oxygen demand (COD). Liu et al. [1997] explored the bactericidal mechanisms of low amperage (10 - 100 mA) electric current (DC) on *Staphylococcus epidermidis* and *Staphylococcus aureus* and demonstrated that an electric current as low as 10 mA introduced the antibacterial substances of H_2O_2 and chlorine, at the cathode and anode, respectively. Many changes can be observed in the cell's physiology and structure in

response to these compounds. Ultimately, if concentrations of these substances are too high, the cell may lose its viability altogether, which has been used as a bactericidal approach. Luo et al. [2005] studied cell surface properties of phenol-degrading bacteria in the presence of low, moderate and high currents. They concluded that at low current (< 20 mA), there were no significant changes in cell surface properties such as surface hydrophobicity, electrostatic charge and cell shape. Exposure to a DC of more than 20 mA (up to 40 mA) did produce significant changes and caused an increase in surface hydrophobicity and flattening of the cells. Loghavi et al. [2007] applied moderate electric field across microbial growth media of Lactobacillus acidophilus and observed that stress caused by the electric field induced an increase in the bacteriocin (proteinaceous toxinsproduced by bacteria) production and an increase in transmembrane conductivity and diffusive permeability of nutrients, surfactants, bacteriocin and autoinducers. Li et al. [2001] demonstrated that the metabolism of nitrifying bacteria was inhibited when electric current was above 2.5 A/m^2 (in an activated sludge process) or 5 A/m^2 (in biofilms) and the nitrification rate in a biofilm was reduced by 20%. *Thiobacillus* ferrooxidans and *Acidiphilium* SJH was found by Jackman et al. [1999] to be inactivated with current intensity of 20 A/m^2, but the sulphur-oxidizing bacteria activity at high cell densities could be recovered after the electricity was turned off. Tokuda and Nakanishi [1995] reported that direct electric current might sterilize the suspensions of some bacterial cells such as *Escherichia coli* IFO 3301 and *Pseudomonas aeruginosa* IFO 2689 and that their death rate was proportional to the current intensity. The high voltage impulse technique (electric field of 20–80 kV/cm) was used to inactivate microorganisms [Grahl et al., 1996; Hülsheger et al., 1983] due to electroporation and generation of highly oxidative species such as the hydroxyl radical (•OH) which is capable of efficiently degrading organics [Sugirato et al., 2003; Johnson et al., 2006]. Dong et al. [2015]

challenged the survivability of *E. coli* and *B. subtilis* under the harsh battery cycle conditions and found their viability not affected at current intensity of 0.18-0.80 mA cm^{-2} and 1.4-2.1 V. Recently Delaire et al. [2015] investigated attenuation of *Escherichia coli* (*E. coli*) *by* Fe-EC. Inactivation of *E. coli* is also considered to be attributable to the oxidative stress of ferrous ions by which the generated strong oxidants such as Fe(IV) and free radical OH**.** act as strong bactericides.

2.5 Summary and conclusion

Application of membrane filtration for water and wastewater treatment has increased dramatically over the past two decades due to increasingly tightening legislation, water scarcity and economic feasibility. Membrane separation technology relies on porous membranes as a physical barrier to filter out the particulates in a suspension through size exclusion. Membrane separation was originally used for water purification such as seawater desalination. It has been extended to wastewater treatment first as an alternative to secondary clarification and then directly integrated into the conventional activated sludge tank, called submerged MBR. Compared to a typical ASP, MBRs offer advantages such as smaller footprint, reduced sludge production, operating flexibility or automation and most importantly, consistent and superior effluent quality including higher removal efficiency for emerging chemicals such as EDCs. However, membrane fouling, an inevitable phenomenon compromising MBR's performance, remains a major obstacle for widening application of this technology in the wastewater treatment industry. Membrane fouling rate is dependent on membrane characteristics (pore size and porosity, composition and hydrophilicity/hydrophobicity, configurations and design), Feed and

biomass characteristics (composition and concentrations, e.g. MLSS, MLVSS, EPS, SMP etc., viscosity, floc size and charge) as well as operating conditions (flux, TMP, temperature, viscosity, DO, aeration intensity, SRT, HRT, operating modes; filtration modes etc.). The content of EPS determines the characteristics of biomass such as hydrophobicity, adhesion, flocculation and settleability and EPS play a key role in the biocake formation on membrane surfaces and have been widely recognized as major foulants [Cosenza et al., 2013].

In the past two decades, the afore-mentioned fouling factors have been exhaustively investigated and various mitigation measures have been adopted in MBR design and operation, such as membrane material modification, MBR configuration optimization, feed pretreatment, control of MBR operating conditions including HRT, SRT, air scouring intensity, coagulation addition into the biomass, the application of ozone, electric field and ultrasound. However, fouling control in MBR remains a major challenge. The electrokinetically enhanced MBR (EMBR) technology developed in recent years provides a new pathway for combating membrane fouling. As a promising antifouling approach, EMBR combines the advantages of electrokinetic mechanism with biological process and membrane filtration and has demonstrated significant success in retardation of TMP jump. However, some fundamentals remains to be investigated, such as fouling reduction mechanisms, systematic exploration about the heterotrophic bacteria's viability under electric field in biological wastewater treatment, electrochemical reduction of nitrate into ammonium and prevention, electrokinetic effect on EDC destruction or attenuation. With respect to application, no work has been reported on nutrient removal including denitrification, and especially MBR performance at low temperatures, which is a typical challenge for a conventional MBRs due to accelerating membrane fouling.

CHAPTER 3 MATERIALS AND METHODS

Preceded by the DC power supply and membrane description, the materials and multidisciplinary methods are presented sequentially based on the the research topics, as shown in Fig. 3.1.
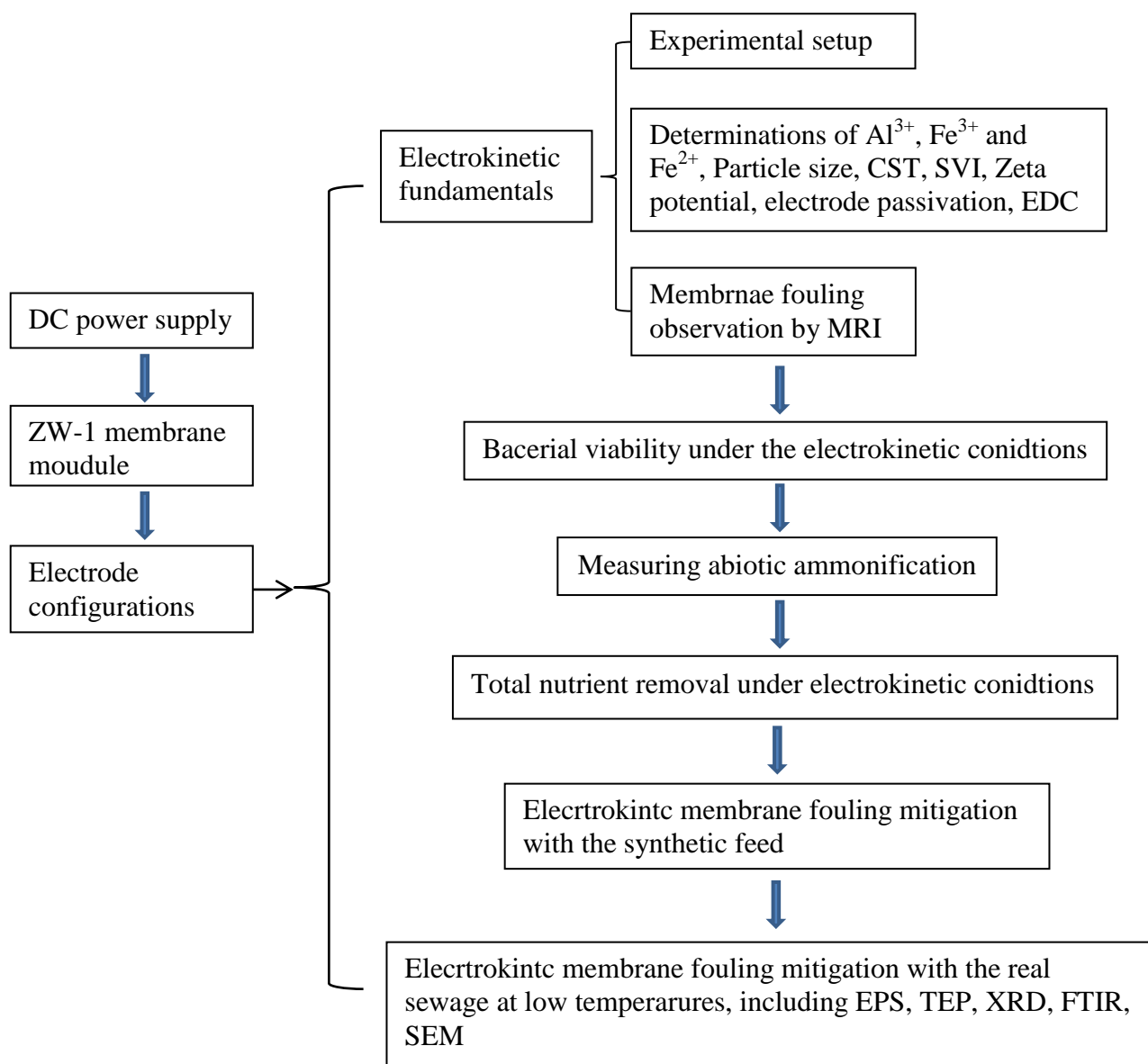
Fig. 3.1 Material and methods by research topics

3.1 DC electric supply unit

A Kepco BOP 100-2D unit (KEPCO, Inc., USA) was used to supply the DC power for the entire research project. With two bipolar control channels, this unit is able to operate in a constant voltage or current mode. The positive and negative current or voltage limits can be manually set or remotely programmed, as shown in Fig. 3.2.

Fig. 3.2 Kepco BOP 100-2D DC unit (KEPCO, Inc., USA)

3.2 Membrane module

The hollow fiber ZW-1 membrane module (GE Water & Process Technologies, Lifecycle Services) was used for batch tests and continuous MBR operations in this research. ZW-1 is one of the most popular membrane modules for lab scale MBR research. As shown in Fig. 3.3, the effective membrane body is 8 cm long and 3-3.5 cm in diameter. The module consists of an aeration tube surrounded by hollow fiber bundles. Air is diffused through the orifices at the foot of the aeration tube. Permeate is sucked out through the hole in top of the header. The

specifications and operating conditions are presented in Table 3.1. A Masterflex L/S pump (Cole Parmer, USA) was used for permeate withdrawal. The transmembrane pressure (TMP) was monitored by a liquid pressure gauge (Cole Parmer, USA) (-60 kPa to 0 kPa) in the suction line. The aeration flow rate was fixed at 1.2 L/min. Prior to MBR operation, the preservative glycerin were removed by continuously running the permeate suction pump until the TOC concentrations between the influent (DI water) and effluent was less than 3 mg/L.
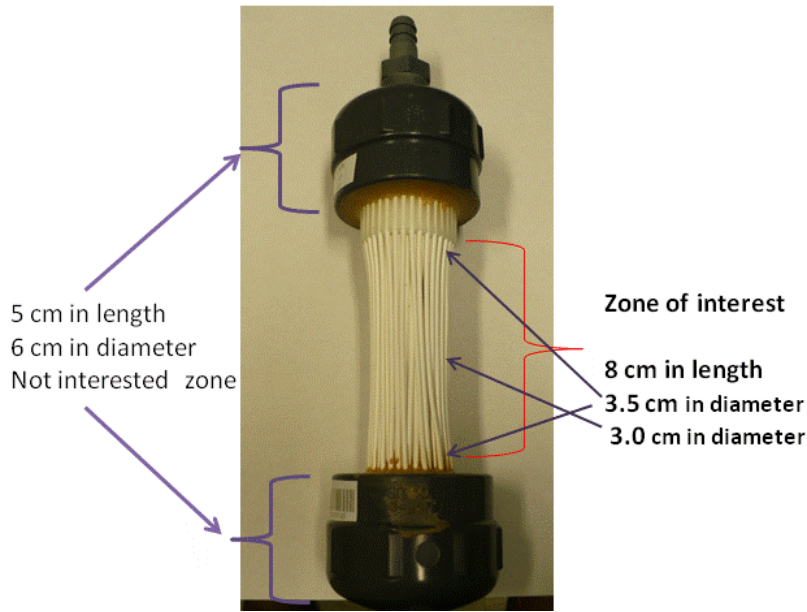
Fig. 3.3 ZW-1 membrane module

Table 3.1 Specifications and operating conditions of ZW-1 membrane module

Model	ZW-1, Submersible Module
Configuration	Outside/In Hollow Fiber
Effective Membrane Surface Area	$0.047\ m^2$
Nominal Pore Diameter	0.04 µm
Permeate (Fiber Side) Hold-up Volume	10 mL
Maximum Transmembrane Pressure	62 kPa (0.62 bar)

Permeate Flow Range	5 – 25 mL/min
Typical Operating TMP	10-50 kPa (0.1 to 0.5 bar)
Maximum Operating Temperature	40 °C (104 °F)
Operating pH range	5-9
Maximum Cleaning Temperature	40°C (104 °F)
Maximum TMP Back Wash Pressure	55 kPa (0.55 bar)
Maximum Aeration Flow per Module	$1.8 \text{ m}^3/\text{h}$
Cleaning pH Range	2-10.5
Maximum OCl- Exposure (ppm-hours)	1000000
Maximum OCl- Concentration (ppm)	1000
Maximum Feed Suspended Solids (mg/L)	25000

3.3 Configurations of electrodes

The EC efficiency is dependent on the production rate of cationic ions which is in turn proportional to the surface area of electrodes. Over the past decades, a few electrode configurations were developed with the aim of maximizing the ratio of electrode surface area to volume to be treated [Belhouta et al., 2010; Mollah et al., 2001 and Modirshahla et al., 2008]. Increasing the number of electrodes was found to be the most efficient approach. Generally there are three ways to achieve the goal, parallel monopolar electrodes, serial monopolar electrodes and bipolar electrodes, as shown in Fig. 3.4. At the beginning of this research, parallel monopolar electrodes, serial monopolar electrodes and bipolar electrodes were all tested for the

optimum nutrient removal and membrane fouling reduction efficiencies. However, it was found

that these multiple electrode configurations introduced severe accumulation of precipitates on the

electrode surface and significantly increased the electric resistance. Therefore, a normal anode-

cathode electrode pair was used for the subsequent experiments.
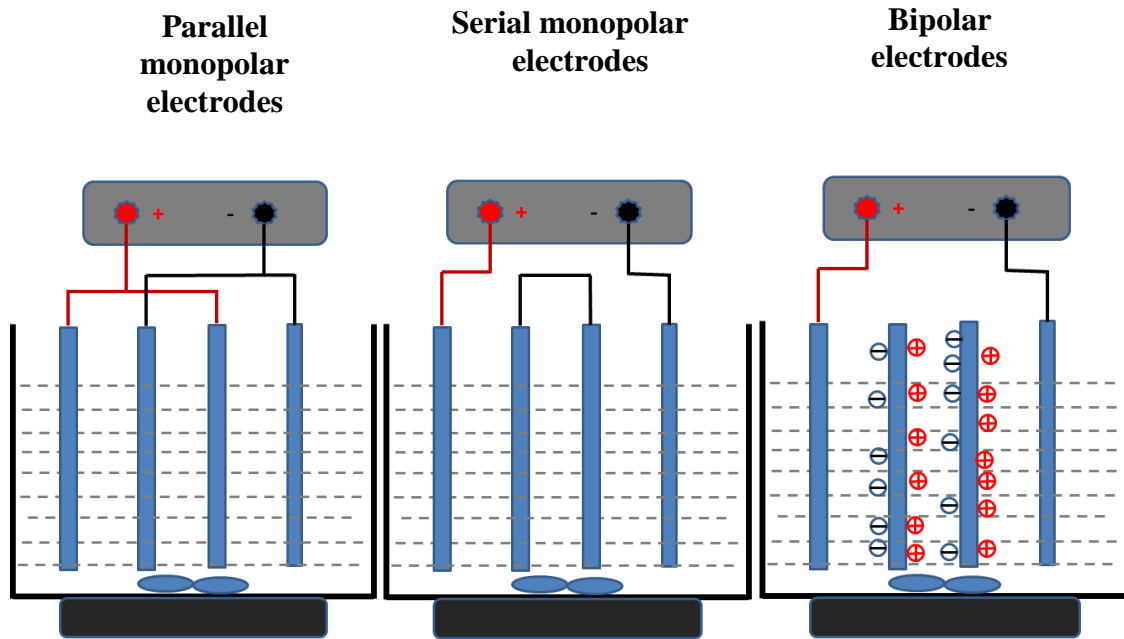
Fig. 3.4 Configurations of multiple electrode arrays [after Chen, 2004]

3.4 Electrochemical fundamentals of Fe and Al electrodes in electrokinetic technologies

3.4.1 Experimental setup

Anode-cathode: Al-Al and Fe-Fe [Wei et al., 2012] were used in a 1 L acrylic batch reactor filled

with 800 mL of synthetic groundwater or activated sludge (AS) mixed liquor process from the

local North End Water Pollution Control Center in Winnipeg, MB. The reactor was covered to

minimize the impact of oxygen in the air during the electrolytic process. The metal coverage of

meshed aluminum and iron electrodes were 79.8% and 62.8%, and the dimensions are 9 cm x 9 cm for aluminum electrodes and 10.2 cm x 10.2 cm for iron electrodes respectively, the effective surface area of both electrodes was 65 cm^2 and the distance between the electrodes was 5 cm. Firstly, all electrodes were rinsed with acetone to remove oil/grease film on the surface and then dipped into 12% HCl solution for 2 min. to remove the oxides. The direct current (DC) field was supplied by a Kepco BOP 100-2D unit (KEPCO, Inc., USA). The experiments were run for three hours and 6 mL of sample was taken out every 5 minutes for the first 15 min. and once in every 15 min. for determination of nitrate, nitrite and ammonium using QuickChem QC8500 (HACH, USA). Values of pH and oxidation reduction potential (ORP) were measured using Accumet XL50 Dual Channel meter (Thermo Fisher Scientific Inc.). Dissolved oxygen (DO) was monitored by Orion Star and Star Plus Meter (Thermo Fisher Scientific Inc DO of 0 mg/L was achieved by purging the electrolytic fluid with nitrogen gas and aeration was supplied to maintain the fluid at various DO levels by the MIQ/TC 2020 XT controller (Germany) as required. The experimental setup is illustrated in Fig. 3.5.
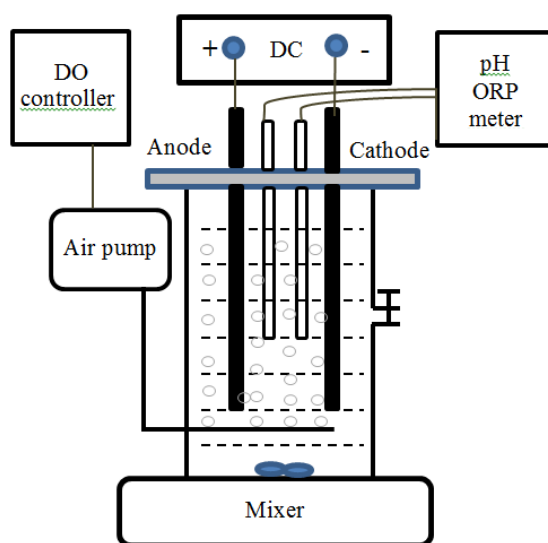
Fig. 3.5 Setup for the electrochemical fundamentals

For change of pH in the electrolytic fluid Section 4.1.1, the electrolytic solution consisted of 60 mg/L of chloride solution and conductivity was adjusted to 1000 μs/m with sodium sulphate, initially the fluid's pH was adjusted to 7.0 with 15 N sodium hydroxide solution and the current intensity = 10 A/m^2. For pH variations in separate electrolytic cells, the two cells are connected by a slat bridge containing 1 M sodium sulphate solution, as shown in Fig. 3.6. All chemicals were purchased from Sigma-Aldrich Corporation (USA). The standard method [APAH et al., 2005] was followed in all sample preparation and determination. All experiments were conducted in duplicate.
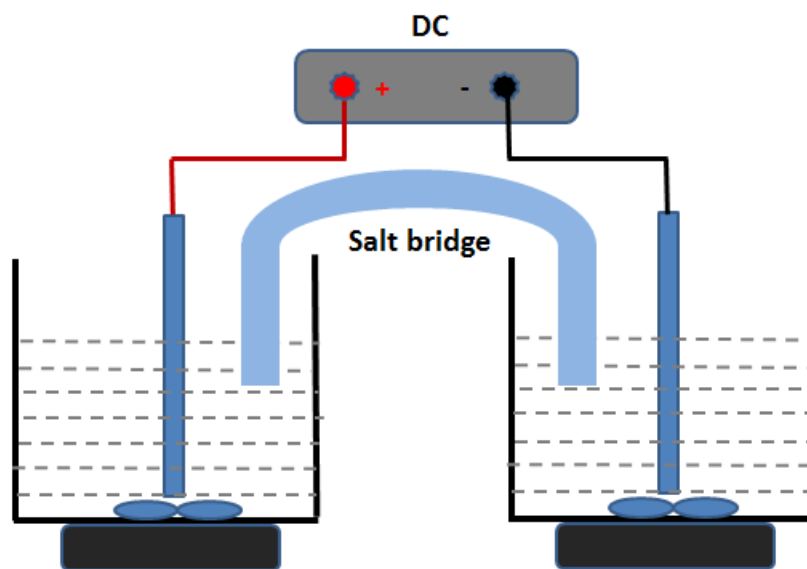
Fig. 3.6 Setup for the electrochemical fundamentals (separate electrolytic cells for Section 4.1.1)

3.4.2 Determination of Al^{3+}, Fe^{2+} and Fe^{3+}

Al^{3+}, Fe^{2+} and Fe^{3+} were determined by HACH DR 2800 spectrophotometer based on Method 8012 Powder Pillows (Al^{3+}), Method 8008 FerroVer® Powder Pillows (total iron) and Method 8146 Powder Pillows (Fe^{2+}). Being a measurable species, Fe^{2+} reacts with ferrozine and form a

ferrous ferrozine complex (Fe(II)FZ3) of which absorbance is spectrophotometrically quantified at the wavelength of 562 nm. In order to measure ferric ions, they must be first reduced to ferrous ions by ascorbic acid and combined with the already existing ferrous ions to be determined as the total iron. Then, ferric iron concentration was calculated by subtracting the ferrous iron concentration from the total iron concentration. To prepare a sample for the cationic analysis, 5 mL of sample was taken and acidified to pH < 2 wiht 10 N HCl and filtered by 0.45 μm syringe filter. The sample was diluted appropriately to meet the determination range.

3.4.3 Methods for floc size, CST, SVI, zeta potential and electrode passivation studies

Standard chemical coagulation procedures are followed: 30 s of fast coagulant mixing at 120 rpm with the biomass and then half of an hour slow stirring for floc aggregation. The two coagulant doses were equivalent to the theoretical electrocoagulation doses for one hour (27 mg/L of Al^{3+}) and two hours (54 mg/L of Al^{3+}), the reactor volume was 8.5 L, Al-Al electrodes were used and the experimental setup is presented in Fig. 3.7. The setup remains the same for CST, SVI, zeta potential and electrode passivation studies.

Particle size analysis was performed with laser diffraction using a Malvern Mastersizer 2000 particle size analyzer (UK). Type 319 Multi-CST and 7x9 cm CST papers (Triton Electronics, UK) were used for CST measurement. Zeta potential was determined with Zeta Meter 4.0 (Zeta-Meter Inc., USA). As the solid concentration of sludge sample was too high for direct zeta potential analysis, 50 ml of sludge sample was centrifuged at 5000 rpm for 5 min. The sample was prepared by mixing the supernatant with a few drops of the activated sludge and

immediately put inside the electrophoretic cell for measurement of the flocs' zeta potential. At least 10 measurements were performed and the mean value was reported as the final result. The values of SVI and capillary suction time (CST) were tested according to APHA 21st Edition [2005].
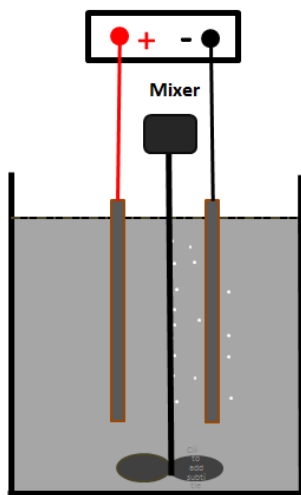
Fig. 3.7 Setup for electrokinetic impact on floc size

3.4.4 Non-invasive observation of electrokinetic membrane fouling reduction by MRI

The setup for electrokinetic membrane fouling reduction by MRI is schematically displayed in Fig. 3.8. At the specified time points after current and filtration application, the membrane module was taken out from the reactor, special care was taken to avoid lose water inside the membrane pores and in its vicinity. As illustrated in Fig. 3.9, a surface coil of 4 cm in i.d. was placed in the middle of the membrane module and then fixed in a holder. The membrane module together with the surface coil were wrapped with plastic film and put into the vertical bore of a 3 T (128 MHz for protons) Bruker MRI system (Germany). ^{1}H signal was recorded predominately

from the water content of membrane module. 2D structural images were acquired using a Rapid

Acquisition Relaxation Enhancement (RARE) pulse sequence.
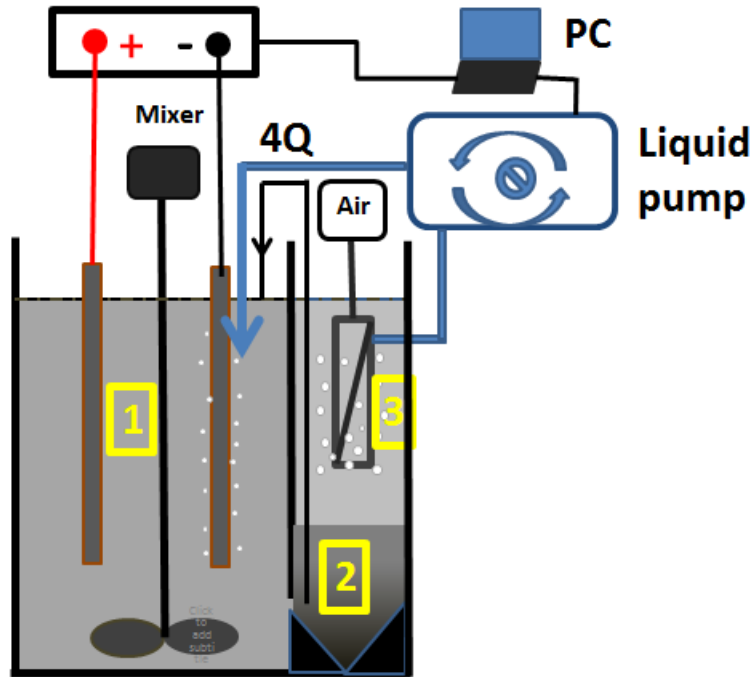
Fig. 3.8 Setup for electrokinetic membrane fouling reduction by MRI
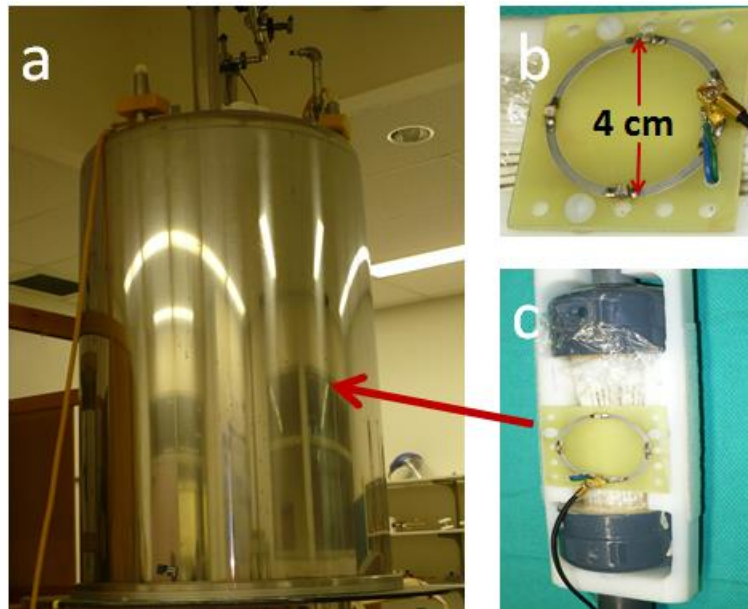
Fig. 3.9 Surface coil, membrane module and MRI scanner

3.4.5 EDC dosing and analysis

With relative activity to EE2 ranging from 1.2 [Yang et al., 2009] to 1.5 [Nishihara et al., 2000], E2 is usually used as the calibration standard in EDC related researche [Routledge et al., 1996; Yang et al., 2009]. E2 and EE2 were purchased as powder from Sgima Aldrich Canada. First 100 mg of E2 and EE2 was dissolved in 1 L ethanol solutions, then 1 mL sample was taken and diluted into a 1 L aqueous solution respectively. The obtained 100 µg/L of E2 and EE2 stock solutions were stored in a -4 ^{0}C fridge. The concentrations of E2 working standards were 50, 100, 300, 500, 750, 1000 ng/L. The concentrations of EE2 in real wastewater is very low (typically ≤20 ng/L), which is close to the lower detection limit of typical chemical or bioassay methods [Briciu et al., 2009]. In this research 500 ng/L of EE2 was spiked into the ASP biomass for treatment experiments. Due to lack of the more sensitive EDC analytical instrument such as HPLC-MS-MS, this concentration was chosen based on the limit of the YES bioassay method previously studied by Yang et al. [2009] and other investigators [Vader et al., 2000; Holbrook et al., 2004; Cirja et al., 2007].

Sample preparation: cyclohexane was used as the extraction solvent to concentrate the feed, the sludge filtrate and filtration cake and the effluent. 10 mL cyclohexane was added into 10 mL sample and extraction was conducted on a shaker at 100 rpm for four hours. The cyclohexane phase was dried under nitrogen and reconstituted in 1 mL ethanol. These samples were then placed on a 96-well optical plate. Blank ethanol and E2 standards were also placed on the plate and allowed to dry. The plates were then filled with the estrogen-sensitive yeast and allowed to incubate for 72 hours. The yeast releases an enzyme in proportion to the amount of estrogen

present. The yellow solution turns into pink, red, or purple, depending on the concentration of estrogen. The colour changes were determined using a BioTek Microplate Reader with KC Juniour Software and the obtained EE2 concentration was related to the standard E2 concentrations as E2-eq.

3.5 Bacterial viability of biomass subjected to the electrokinetic technology

The heterotrophic bacterial mass was taken from a membrane bioreactor (MBR) which contained about 6 g/L of total suspended solids (TSS). 900 mL of MBR biomass was placed in a 1 L beaker, a pair of aluminum electrodes were inserted into the biomass. The effective electrode area was 9cm x9 cm, the distance between the electrodes was 5 cm and the direct current electricity was supplied by a Kepco BOP 100-2D unit. 30 mL of biomass was taken out for various analyses. pH was measured using Accumet XL50 Dual Channel meter (Fisher Scientific), dissolved COD and TOC were determined by HACH Spectrophotometer DR/2500 and Tekmar Dohrmann Phoenix 8000, respectively. Viability of bacteria was measured using the LIVE/DEAD® BacLight™ Bacterial Viability kits (P/N L13152) supplied by Molecular Probes, Inc. (Eugene, Oregon, USA), and Bio-Tek PowerWave XS was used for the microplate reading of viability tests. The specific oxygen uptake rate (SOUR) was measured following Standard Methods for the Examination of Water & Wastewater (21st edition) and dissolved oxygen (DO) was monitored by Orion Star and Star Plus Meter (Thermo Scientific). All trials were performed in triplicates.

The LIVE/DEAD *Bac*Light bacterial viability kit from Molecular Probes was reported for successfully determining the fraction of active cells [Boulos et al., 1999; Bunthof et al., 2001]

and employed to test the bacterial viability in presence of electric current in this research. The *Bac*Light stain package contains two nucleic acid-binding stains with different spectral characteristics and cell penetration capacity: one is SYTO 9 green-fluorescent nucleic acid, and the other one is red-fluorescent nucleic acid, propidium iodine. SYTO 9 penetrates all bacterial membranes (both live and dead) freely and stains the cells green, while highly charged propidium iodide only penetrates damaged cell membranes and stains the cells red, consequently the SYTO stain fluorescence intensity is decreased. Simultaneous application of both stains thus enables measurement of the relative ratio of viable cells with an intact membrane and dead cells with a compromised membrane. Calibration was performed following the supplier's protocol, except the suggested *E. coli* suspensions was replaced by the MBR biomass. A standard curve was prepared for each microplate and a typical one is shown in Fig. 3.10.
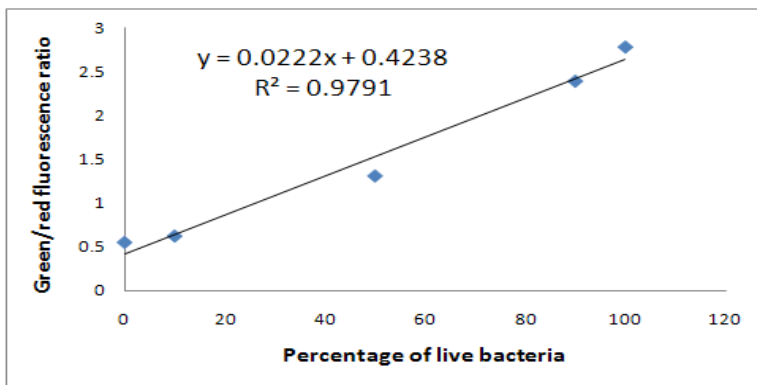
Fig. 3.10 Typical standard calibration curve for bacterial viability test

3.6 Prevention of abiotic ammonification in the electrokinetic technology

The experimental setup is the same as Fig. 3.5. All chemicals were purchased from Sigma-Aldrich Corporation (USA). The standard method [APAH et al., 2005] was followed in all sample preparation and determination. In order to investigate the electrokinetic behaviour of

nitrate reduction and explore the strategies for supressing the ammonification process, batch tests were performed under varied conditions as presented in Table 3.2. All experiments were conducted in duplicate. Though there are eight possible intermediates or end products from electrochemical reduction of nitrate, only ammonium and nitrite yields were tracked due to instability or analytical difficulties for the other substances.

Table 3.2 Experimental parameters for electrochemical fundamentals

Electrodes	(1). Al-Al (9 cm x 9 cm meshed sheets)
	(2). Fe-Fe (10.2 cm x 10.2 cm meshed sheets)
Electrolytic fluid	(1). Sodium nitrate solution containing 40 mg/L of NO_3^--N, electric conductivity was adjusted to 1400 µs/cm by adding sodium sulphate
	(2). AS mixed liquor (TSS 1800 mg/L to 2100 mg/L) and the nitrate concentration was adjusted to 40 mg/L
Current intensity	1 mA/cm^2, 5 mA/cm^2, 10 mA/cm^2
DO	0, 0.5 mg/L, 2.0 mg/L
Initial pH	7.0 ± 0.5
Temperature	Ambient ($20 \pm 1 \, ^0$C)

3.7 Total nutrient removal in an electrically enhanced MBR

3.7.1 Feed composition

Synthetic wastewater was used in this research. Its composition is presented in Table 3.3. All chemicals were purchased from Sigma Aldrich.

120

Table 3.3 Feed wastewater composition

Chemical	Concentration (mg/L)
Glucose	240.00
Yeast extract	160.00
$MnSO_4.H_2O$	4.58
$FeSO_4.7H_2O$	3.40
KCl	10.50
K_2HPO_4	60.00
$NaHCO_3$	550.00
$CaCl_2$	5.50
NH_4Cl	125.00
$MgSO_4.7H2O$	75.00

3.7.2 Experimental setup

Two identical submerged membranes were used for the experiment, one was placed in a control reactor, and the other was placed in a reactor with a pair of cylindrical meshed aluminum electrodes placed around the membrane module (Elektorowicz et al., 2008). Dimensions of the electrodes are: inner cylinder (8 cm i.d. x 13.5 cm high, 24.6 cm in perimeter); outer cylinder (11 cm i.d. x 13.5 cm high, 34.6 cm in perimeter). Each reactor consists of aerobic zone (3.72 L) and anoxic zone (2.50 L) which were separated by a baffle but connected through the gap at the bottom (Fig. 3.11). The membrane used is a proprietary ZW-1 hollow fiber module from GE Water and Process Technologies, with nominal pore size of 0.04 μm and nominal membrane

surface area of 0.047 m^2. Meshed aluminum electrodes (containing 0.2% Cu, 0.6% Si, 0.7% Fe, 1-1.5% Mn, 0.1% Zn, 96.9% - 97.4% Al) at the distance of 1.1 cm were applied. DC power was supplied by a Kepco 100-4D power unit, the electrode operating mode was constant voltage of 1.82 V DC/cm. Such a voltage generated a current of approximately 0.05 A between the electrodes, which did not exhibit adverse influence on the growth of microorganisms in the biomass, based on the preliminary study and literature (Drees et al., 2006; Liu et al., 1997; Loghavi et al., 2007). Using Labview 8.2, a power control program was developed, the electrode polarities were switched every two minutes for passivation reduction and equal consumption of two electrodes. Masterflex L/S pumps were used for aeration, membrane scouring, and permeate withdrawal.
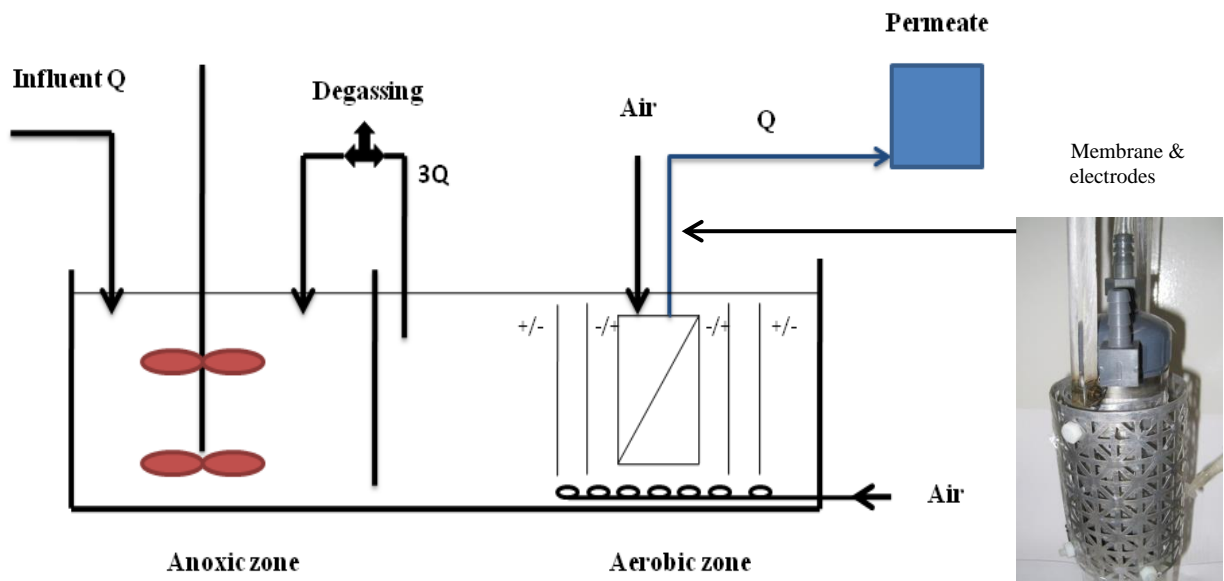
Fig. 3.11 Schematic of experimental set-up

The synthetic feed was introduced into the reactors by gravity, using float valves. The reactors were seeded with waste activated sludge (WAS) from the Winnipeg North-End WWTP prior to the experimental start-up.

3.7.3 Operating conditions

The HRT was maintained at 13.8 hours and the SRT at 21 days. DO in the aerobic zone was controlled at 5.0 – 5.5 mg/L, and DO in the anoxic zone was less than 0.1 mg/L (mostly undetectable). The values of pH in both MBRs were 7.2 – 7.7, within the optimum pH range of denitrification, phosphorus precipitation and floc formation (6 – 8), thus no adjustment was necessary. The membrane modules were back-flushed with permeate for 30 s every 10 min. and chemically cleaned with 200 mg/L of NaOCl solution for 5 hours every three weeks, during which there was no significant flux decline. The biomass was first cultivated in an aerobic MBR (6.6 L) to TSS concentration of 10 g/L over a three month period. Then, it was split into two equal portions for the two reactors. Two membrane modules were run in parallel for 21 days (one SRT) without electrical current, to demonstrate their similar filtration characteristics (e.g. initial TMP and dTMP/dt). Then, electrodes were inserted in one reactor (EMBR) to test the performance of the new design.

3.7.4 Analytical methods

DO concentration was measured by a DO meter (HACH sensION 378, USA). Particle size analysis was performed using Spectrex PC2200 (USA), total nitrogen and COD tests were conducted on HACH DR2500, ammonia, nitrite, nitrate and phosphate were determined by LACHAT QuickChem 8500, TOC was analyzed by Tekmar Dohrmann Phoenix 8000 and mixed liquor suspended solids (MLSS) were tested according to APHA [2005].

3.8 Membrane fouling mitigation in an electrically enhanced MBR system fed with synthetic wastewater

3.8.1 Experimental setup

Following the initial batch tests, EMBR was constructed by directly placing meshed aluminum electrodes in a MBR where a baffle was placed between the electrodes (11 cm x 14 cm) and membrane module. The membrane zone had a conic bottom and was not additionally aerated except the necessary membrane air scouring. Due to filtration, the biomass concentration in this zone is polarized and the settled biomass is accumulated at the conic bottom where it is pumped back to the electrode zone at 4 times of the feed flow rate (Fig. 3.12). Another membrane bioreactor was also built as a control; it had the same configuration as the EMBR but without electrodes. The working volume of both reactors was 8.5 L. The membrane used was a proprietary ZW-1 hollow fiber module from GE Water and Process Technologies, with nominal pore size of 0.04 μm and nominal membrane surface area of 0.047 m^2.
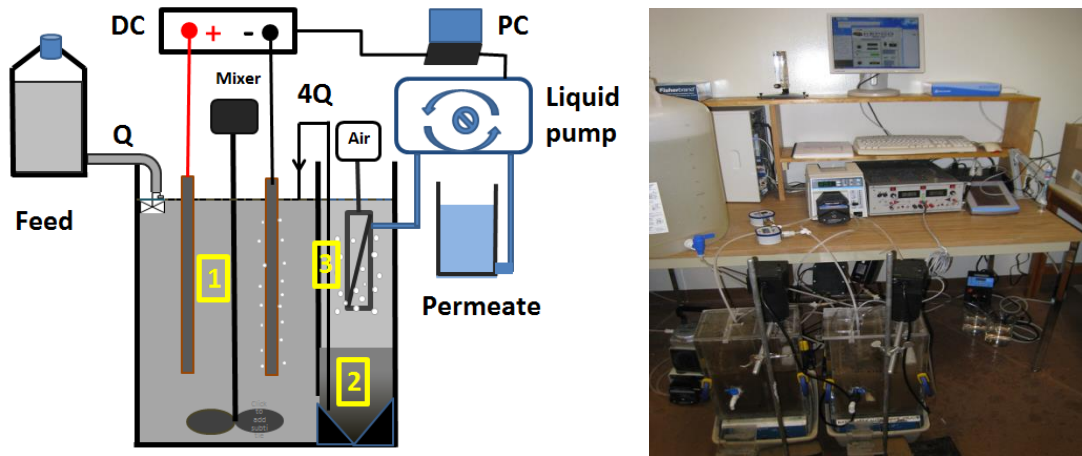
Fig. 3.12 Schematic and actual experimental set-ups

DC power was supplied by a Kepco 100-4D power unit, the electrode operating mode was constant voltage of 1.2 V DC/cm, 10 min. on and 30 min. off alternatively. Such a voltage generated a current of approximately 0.05 A between the electrodes, which did not exhibit adverse influence on the growth of microorganisms in the biomass, based on preliminary study and literature [Drees et al., 2006; Liu et al., 1997, Loghavi et al., 2007; Wei et al., 2011]. Masterflex L/S pumps were used for aeration, membrane scouring, and permeate withdrawal.

The synthetic feed [Wei et al., 2009] was introduced into the reactors by gravity, using float valves. The reactors were seeded with waste activated sludge (WAS) from the Winnipeg North-End WWTP prior to the experimental start-up.

3.8.2 Operating conditions

HRT = 15 hours, SRT = 15 days; DO in both MBRs was controlled at 4.0 − 4.5 mg/L. The values of pH in both MBRs were 6.8 − 7.4, within the optimum pH range of denitrification, phosphorus precipitation and floc formation (6 − 8), thus no adjustment was necessary. The membrane modules were back-flushed with the permeate for 30 s every 10 min. and chemically cleaned up with 200 mg/L of NaOCl solution for 5 hours whenever TMP reached the limit of 6 psi. The biomass was first cultivated in the two reactors over a two month period to reach a steady TSS concentration of 6 g/L. Two membrane modules were run in parallel for 15 days (one SRT) without electrical current, to demonstrate their similar filtration characteristics, e.g. initial TMP and dTMP/dt, then, electrodes were inserted in one reactor (EMBR) to test the performance of the new design.

3.8.3 Analytical methods

DO concentration was measured by a DO meter (HACH sensION 378, USA). Particle size analysis was performed using Mastersizer 2000 (UK), total nitrogen and COD tests were conducted on HACH DR2500, ammonia, nitrite, nitrate were determined by LACHAT QuickChem 8500, TOC was analyzed by Tekmar Dohrmann Phoenix 8000 and mixed liquor suspended solids (MLSS) were tested according to APHA (2005). Soluble extracellular polymeric substances (EPS) were measured as the sum of carbohydrate and protein in the supernatant of biomass after centrifuge at 10,000g for 15 min. Carbohydrate was determined according to Dubois et al. [1956], D-glucose-monohydrate was used for calibration (2 - 100 mg/L) and the absorbance was quantified at 490nm by a spectrophotometer (Ultraspec 2100 Pro, Fisher Scientific, USA), the carbohydrate results are represented as glucose equivalents. The modified Lowry's method [Lowry et al., 1951] was followed for the protein tests. Cambridge Stereoscan 120 *S*canning electron microscope fitted with a Kevex 7000 EDS spectrometer were used for element mapping and cell image collection.

3.9 Membrane fouling retardation in an EMBR system with real municipal wastewater at low temperatures

3.9.1 Experimental setup and operating conditions

Two membrane bioreactors were used, with one as EMBR and another as the control MBR working side by side. Working volume (8.5L) of both reactors consisted of two zones (hereafter

called reaction zone and membrane zone, with approximate volume ratio of 3:2) separated by a baffle with a 1 cm of gap above the reactor bottom. ZW-1 hollow fiber membrane modules (nominal pore size of 0.04 μm and nominal surface area of 0.047 m^2) from GE Water and Process Technologies were applied for all experiments. As the membrane modules were fabricated manually, there existed slight differences in filtration resistance characteristics due to inconsistent hollow fiber layouts evidently demonstrated by three-dimensional magnetic resonance imaging. Therefore, prior to MBR operation, a number of new ZW-1 modules were tested, only those with the similar intrinsic membrane resistance and transmembrane pressure increasing rate were screened for and applied in this study. In the EMBR, a pair of meshed iron electrodes (11 x 14 cm, 2 cm apart) was placed in the reaction zone and electricity was supplied by a Kepco 100-4D DC power unit. The electrode operating mode was 10 min on and 30 min off alternatively at the constant current intensity of 5.2 A DC/m^2. Such a current intensity did not exhibit an adverse influence on the growth of microorganisms, based on previous study [Wei et al., 2012]. Precipitation of phosphate by the electrically generated ferrous ions and accumulation of the negatively charged flocs driven by the electrophoretic force form a layer of inorganic and organic barrier on the anode surface, which is usually referred as electrode passivation, was observed. Anode passivation prevents further Faradaic coagulant dissolution and must be eliminated or minimized for successful implementation of this technology. In this work, an electric polarity switch strategy was adapted, i.e. a wavelet program was developed to reverse the electric polarities every 12 hours with duration of 20 min. The hydrogen gas produced at the cathode expels and dislodges the precipitates on the electrode efficiently. In addition, the anodic iron plate was taken out twice a week during the power off cycle for manually removing precipitated deposits. The electrode surface was washed and brushed, then, it was rinsed with

acetone to remove oil/grease film on the surface and then dipped into 12% HCl solution for 2 minutes. Masterflex L/S pumps were used for aeration, membrane scouring, and permeate withdrawal. The membrane zone had a conic bottom, which was not additionally aerated. The biomass in this zone was concentrated, settled and accumulated in the conic bottom. Then, it was pumped back to the zone between electrodes at four times the feed flow rate (Figure 3.12).

The reactors were seeded with waste activated sludge (WAS) and fed with the primary effluent from the Winnipeg North- End WWTP prior to the experimental start-up. The biomass was first cultivated in the two reactors over a 2-month period to reach a steady TSS concentration of approximately 6 g/L. Two membrane reactors were run in parallel for 15 days without electrical current, to demonstrate their similar filtration characteristics, e.g. initial TMP (transmembrane pressure) and dTMP/dt. Then, electrodes were inserted into one reactor (EMBR) for testing the performance of a new design. The two reactors were operated at solids retention time (SRT) of 15 days and hydraulic retention time (HRT) of 15h in constant flux mode of 12 L/h.m^2 under 20 ^{0}C, 15 ^{0}C, 10 ^{0}C, 5 ^{0}C respectively in an environmental chamber.

Dissolved oxygen (DO) in both MBR and EMBRs was controlled at 4.0–4.5 mg/L. The values of pH in both MBRs were 6.8–7.4, within the optimum pH range of denitrification, phosphorus precipitation and floc formation [Wei et al., 2012], thus no adjustment was necessary. The membrane modules were back-flushed with permeate for 30 s every 10 min and chemically cleaned up with 200 mg/L of NaOCl solution for 5 h whenever transmembrane pressure (TMP) reached the limit of 50 kPa.

3.9.2 Determination of EPS

EPS comprise a variety of organic substances such as polysaccharides, proteins, lipids and humic substances that come from either the metabolic activities of microorganisms or raw wastewater. They include bound EPS (condensed gels or polymers closely bound to cells) and soluble EPS or SMP (dissolved in the surrounding solution). Soluble EPS or SMP (soluble microbial products) and bound EPS were assessed using the thermal extraction method [Drews et al., 2005]. In brief, 50 mL of fresh MBR biomass was dewatered by centrifugation at 5000 rpm for 5 min, then, the supernatant was filtered by 0.45 µm glass fiber filter (Whatman, USA) and the filtrate was tested as SMP. The sludge pellet was resuspended in a mixture of 15 mL of 0.05% NaCl solution and 35 mL deionized water and agitated by vortex mixer for 1 min. The sludge suspension was then placed in 80 ^{0}C water bath for 10 min before centrifuging again at 8000 rpm for 5 min. The supernatant was used to measure the bound EPS. As EPS (both bound or SMP) is predominantly composed of proteins and polysaccharides, the proteins and polysaccharides were quantified separately using the modified Lowry method [Lowry et al., 1951] and phenol–sulfuric acid colorimetric method [Flemming et al., 2001], respectively. Bovine serum albumin and glucose were used as calibration standards for proteins and polysaccharides, respectively. All analyses were performed in duplicate and the mean values were reported.

3.9.3 Other physical and chemical parameters

DO concentration was measured by a DO meter (HACH sensION 378, USA). Particle size analysis was performed using Mastersizer 2000 (UK). Total nitrogen, total phosphorus and

chemical oxygen demand (COD) tests were conducted on a HACH DR2500 spectrophotometer. Ammonia, nitrites, nitrates and phosphates were determined by LACHAT QuickChem 8500, Total organic carbon (TOC) was analyzed by Tekmar Dohrmann Phoenix 8000, while mixed liquor suspended solids (MLSS), volatile suspended solids (MLVSS), SVI, and capillary suction time (CST) were tested according to APHA 21st Edition [2005].

Zeta potential was determined with Zeta Meter 4.0 (Zeta-Meter Inc., USA). As the solid concentration of sludge sample was too high for direct zeta potential analysis, 50 ml of sludge sample was centrifuged at 5000 rpm for 5 min. The sample was prepared by mixing the supernatant with a few drops of the activated sludge and immediately put inside the electrophoretic cell for measurement of the flocs' zeta potential. At least 10 measurements were performed and the mean value was reported as the final result.

3.9.4 Determination of TEP

The method for TEP analysis is based on the protocol developed by De la Torre et al. [2008]. In brief, in a 25 mL volumetric flask, 5mL of pre-filtered sample with 0.5 mL of 0.055% (m/v) alcian blue solution and 4.5 mL of 0.2 M acetate buffer solution (pH 4) were mixed and stirred for 1 min. TEP in the sample reacts with alcian blue and produces a precipitate which was separated by centrifuge at 15,300 rpm for 10 min. Finally the residual alcian blue is determined by spectrophotometer at 602 nm. Xanthan gum is used as the calibration standard and the measured TEP concentration is expressed as xanthan gum equivalent (mg/L). A typical calibration standard curve is presented in Fig. 3.13.
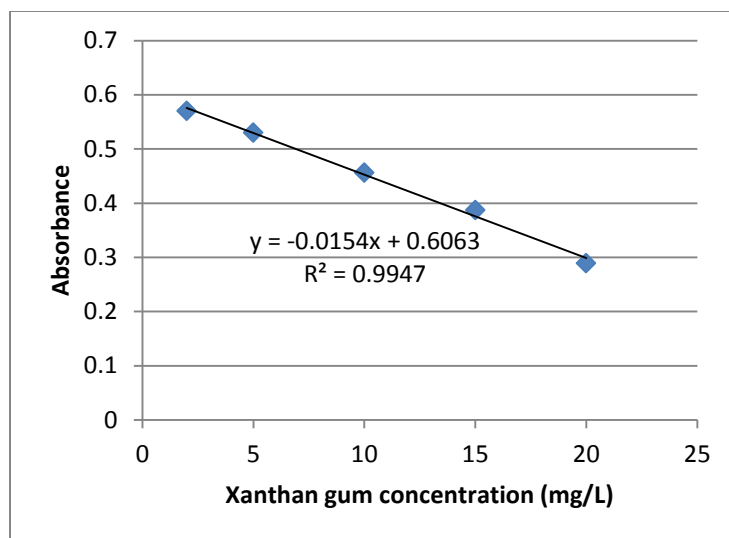
Fig. 3.13 Representative TEP calibration standard curve

3.9.5 Determination of FTIR and XRD

Samples were prepared using stock KBr that was stored in a warming oven at 100 ^{0}C. Approximately 4.5 mg of sample was mixed with approx. 150 mg of KBr and pressed into a 13mm IR pellet. FTIR was acquired with Bruker Tensor 27 (Germany). A background spectra was collected prior to each sample spectra. Both background and sample spectra used scanning times of 100 scans. Spectral range was 4000 cm^{-1} to 400 cm^{-1}. One spectrum was collected for each sample immediately following pellet preparation. The pellets were placed in the warming oven over the weekend to drive off any absorbed water and a second spectrum was then collected for each sample. All results were baseline corrected.

XRD images were acquired with a Siemens (Bruker) D5000 powder diffractometer. The D5000 system uses a K710H 2.7kW sealed-tube type X-Ray generator with the vertical goniometer housed in a fully-enclosed radiation cabinet. The goniometer is in Bragg-Brentano (θ-2θ)

geometry and uses Cu radiation. The system is equipped with computer-controlled divergence and receiving slits, a rotating sample holder, diffracted beam graphite monochromator and a scintillation detector. Data was collected using Bruker's DIFFRACplus software and processed with MDI Jade+ software.

CHAPTER 4 RESULTS AND DISCUSSIONS

4.1 Electrochemical fundamentals of Fe and Al electrodes in electrokinetic technologies

In EC and the other electrokinetic technologies [Elektorowicz et al., 2012; Bani-Melhem et al., 2011], Al and Fe are usually used as electrodes, metal ions are electrochemically generated and subsequently subject to hydrolytic reactions by following the equations (Equations 4-1 - 4-7) below:

Oxidation reactions at the anode (aluminum or iron):
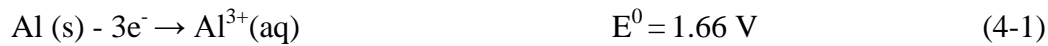
$$Al\ (s)\ -\ 3e^- \rightarrow Al^{3+}(aq) \qquad\qquad E^0 = 1.66\ V \qquad\qquad (4\text{-}1)$$

$$Fe\ (s)\ -\ 2e^- \rightarrow Fe^{2+}(aq) \qquad\qquad E^0 = 0.44\ V \qquad\qquad (4\text{-}2)$$

Where E^0 is the standard oxidation or oxidation potential depending on the actual electrochemical reactions

Ferrous ions may be further oxidized into ferric ions in the presence of oxygen:

$$Fe^{2+}(aq)\ \textbf{-}\ e^- \rightarrow Fe^{3+}(aq) \qquad\qquad\qquad (4\text{-}3)$$

$$4Fe^{2+}(aq) + O_2 + 10H_2O(l) \rightarrow 4Fe(OH)_3(s) + 8H^+ \qquad\qquad (4\text{-}4)$$
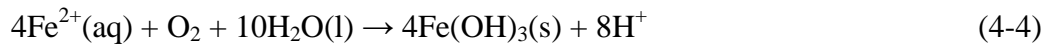
The ferric and aluminum ions are in stable redox states but hydrolyzed instantly:

$$Fe^{3+}(aq) + 3H_2O(l) = Fe(OH)_3 + H_3O^+(aq) \qquad\qquad (4\text{-}5)$$

$$Al^{3+}(aq) + 3H_2O(l) = Al(OH)_4^- + 4H_3O^+(aq) \qquad\qquad (4\text{-}6)$$
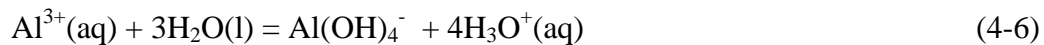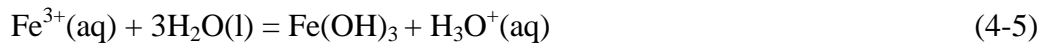
The anodic reaction $6H_2O(l)\ -\ 4\ e^- \rightarrow O_2(g) + 4\ H_3O^+(aq)$ $E^0 = -1.229\ V$ does not occur because the system is thermodynamically unfavourable (Gibbs free energy $\Delta G^0 = -nFE^0 > 0$).

At cathode, the dominant electrochemical reactions can be described by Equations (4-7) [Paidar et al., 1999; Fanning et al., 2000]:

$$2H_2O(l) + 2e^- \rightarrow H_2(g) + 2OH^-(aq) \qquad\qquad E^0 = -0.8277 \ V \qquad (4\text{-}7)$$
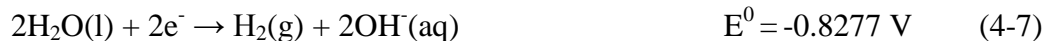
The other side electrochemical reactions under specific conditions are described in the following sections. Aluminum, iron or stainless steel are the most common materials for EC electrodes as these metals have high coagulation powers, readily available, cost-effective and relatively non-toxic. Titanium anode has also been sporadically reported in a few researches with superior EC treatment efficiency [Mollah et al., 2004] due to its high positive charge density, e.g. recently Naje et al. [2015] used titanium electrode to obtain high removal of COD (93.5%), TSS (97%), turbidity (96%), phenols (99%) and phosphate (97%) from the textile wastewater. However, because of its high cost using titanium as the EC anode is generally prohibitive in practice. Therefore, in this thesis only Fe and Al are utilized for various parametric experiments and compared for some specific effects. The other factors affecting the electrocoagulation include pH, current density, electrolysis time and composition of the supporting electrolyte etc., which are addressed in detail below based on experimental results.

4.1.1 Change of pH in the electrolytic fluid

pH of the electrolytic solution may directly affect the chemical dissolution of electrodes, both the anode and cathode [Refait et al., 1997; Chen et al., 2004]. E.g. When aluminum is used as the EC electrodes, as an active metal it may react with H^+ or OH^-, generating Al^{3+} and AlO_2^- under acidic (pH < 5) and alkaline (pH >9) conditions, respectively. In this experiment the electrolytic solution consisted of 60 mg/L of chloride solution and conductivity was adjusted to 1000 µs/m with sodium sulphate. Initially the fluid's pH was adjusted to 7.0 with 15 N sodium hydroxide solution and the current intensity = 10 A/m^2. In the one tank experiment, pH changes over the 2

hours of electrolysis time are presented in Fig. 4-1. Over two hours of electrolysis, pH of the electrolytic fluid went up about 2 units for both Al-Al and Fe-Fe electrodes as no buffering reagents existed in the electrolytic medium. This was due to release of hydroxyl ions OH⁻ by Equation (4-7), which is in agreement with the previous observation [Bani-Melhem et al., 2010; Bani-Melhem et al., 2011; Ibeid et al., 2013; Hasan et al., 2012; Ibeid et al., 2013].
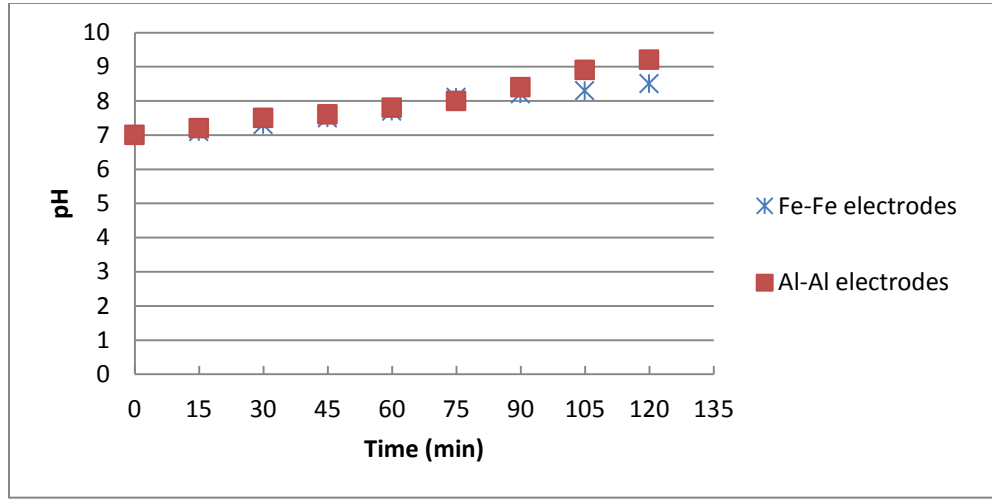
Fig. 4-1 pH changes over time in one electrolytic cell

Fig. 4-2 and Fig. 4-3 display the pH variations in separate electrolytic cells for both Al-Al and Fe-Fe electrodes, it is interesting to note that pH in the Al cathode tank increased by nearly 3 units, whereas pH in the Al anode tank decreased slightly by 0.6 units. Similarly, pH in the Fe cathode tank increased by nearly 2 units, whereas pH in the Al anode tank decreased slightly by 0.4 units. The electrochemical and hydrolytic reactions at the cathode and anode can explain the different pH trends. Equation (4-7) is obviously responsible for the pH upward changes in both Fe and Al cathode tanks, based on hydrolytic Equations (4-5) and (4-6), the newly generated ferric and aluminum ions are subject to hydrolysis. Just like chemical coagulation, the ferric and aluminum ions hydrolyze into their respective hydroxides and generate hydrogen ions. Aluminum is a more active metal than iron, as a result, its redox reaction and electrolysis in

aqueous solution are more intensive than the latter, which explains the difference in pH variations. Compared to strong cathodic electro reduction, hydrolysis of cations is a less intensive process. Overall in an usually one-tank electrochemical configuration the net effect on pH is increase in alkalinity, which is favourable in EMBR where nitrification and electrokinetic process is integrated in one tank because nitrification consumes alkalinity whereas the afore-mentioned electrokinetic process makes up the alkalinity loss. Together with the buffering capacity of biomass, the electrokinetic technology automatically maintain relatively neutral acid-base environment in the mixed liquor and favours the microbial growth without pH adjustment with extra acidic or basic solution.
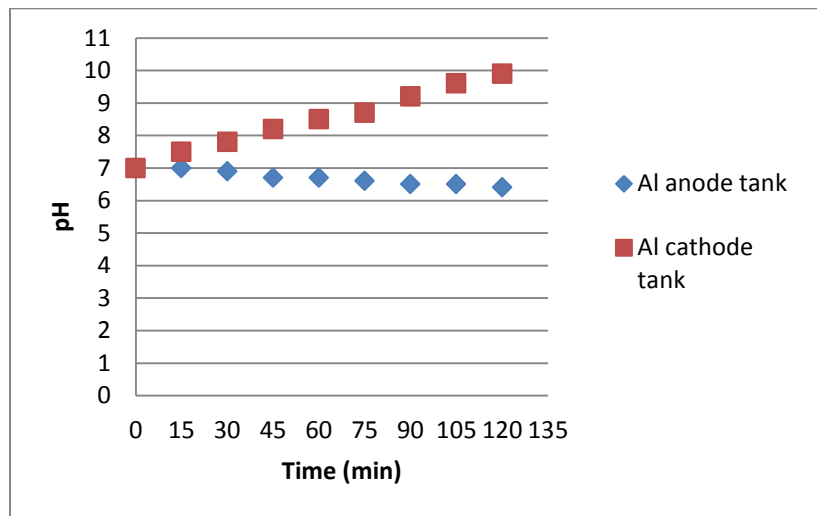
Fig. 4-2 pH changes over time in separate electrolytic cells (Al-Al electrodes)
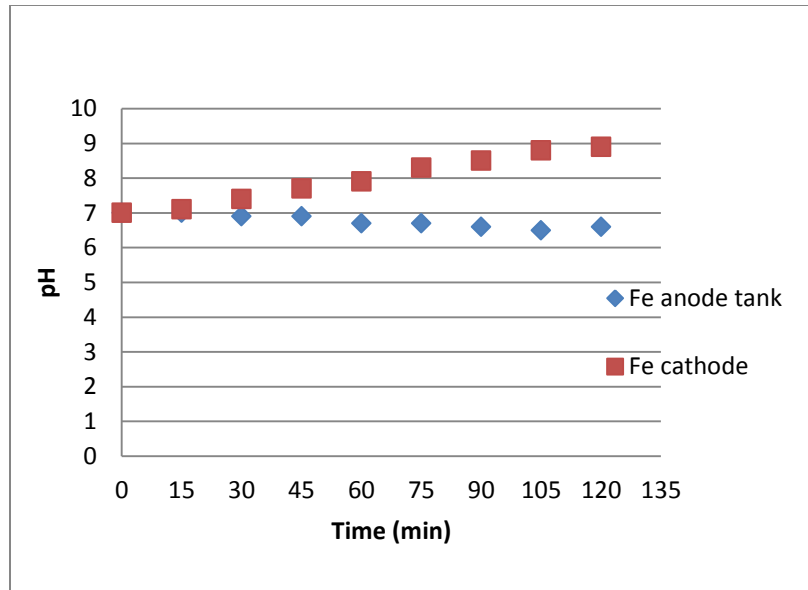
Fig. 4-3 pH changes over time in separate electrolytic cells (Fe-Fe electrodes)

Fe may also react with H^+ under acidic (pH < 5) conditions and release ferrous ions. Secondly, speciation of hydrated metal hydroxides is dependent on pH of the solution, and the amount of highly charged cations and hydroxides decide the coagulation power for destabilizing colloids. At highly alkaline pH the main species of Al and Fe are $Al(OH)4^-$ and $Fe(OH)4^-$ ions, which have been demonstrated to have poor coagulation performance. In addition, oxidation of Fe(II) to Fe(III) cannot occur if pH is less than 5 [Sasson et al., 2009, Picard et al., 2000]. Generally the optimal coagulation pH is in the range between 5 and 8, and iron outperforms aluminum at higher and lower pH values [Mouedhen et al., 2008].

4.1.2 Current efficiency in electrokinetic technology

The current efficiency can be calculated based on the theoretical yield of metal ions based on Faraday's law and the determined mass of total metal cations in the liquid and solid phases:

137

$$\text{Current efficiency} = (\frac{I * t * M}{n * F * V}) / [M^{3+}] * 100\% \qquad (4\text{-}8)$$

Where:

$[M^{3+}]$ is molar concentration of electrochemically generated metal cation (g/L),

I is the current (A),

t is the electrolytic time (s),

M is the molecular mass of the metal (g mol/L),

n is the number of lost electrons per metal atom,

F is Faraday's constant (96,485 C/mol).
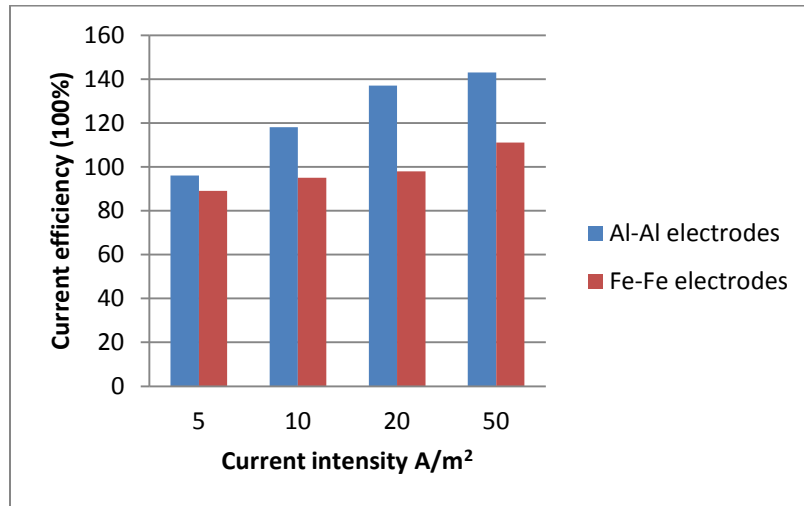
Fig. 4-4 Current efficiency vs. current intensity

From Fig. 4-4, for Fe-Fe electrodes, the current efficiency is close to 100% unless at high current intensity of 50 A/m^2. Whereas for Al-Ale electrodes, the current efficiency is significantly higher than unity; for exemple, at high current intensity of 50 A/m2, the current efficieny was observed to be from 118% to 143%. Several studies have reported that the cation yields of Al anode are significantly higher than 100%, ranging from 105% and 190% of the theoretical value [Picard et

al., 2000; Kongjao et al., 2008; Terrazas et al., 2010; Şengil et al., 2009; Kobya et al., 2011; Mouedhen et al., 2008; Yetilmezsoy et al., 2009], while the yield of ferrous ions is generally in agreement with the chemometric prediction [Picard et al., 2000]. The extra yield of aluminum ions is attributed to cathodic Al dissolution and pitting corrosion, especially when concentration of chlorine ions in the sample is high [Chen et al., 2004]. Analysis of the electrochemical behavior of all involving substances attributes the excess high current intensity to the following factors:

(1). The previous section demonstrates that pH of the electrolytic fluid goes up dramatically to medium and strong alkaline (>9) as the current intensity increases, in the alkaline solution aluminum ions are not only generated through electrochemical dissolution, but also through chemical reaction [Sasson et al., 2009, Picard et al., 2000]:

$$2Al + 2OH^- + 6\,H_2O \rightarrow 2[Al(OH)_4]^- + 3H_2 \qquad\qquad (4\text{-}9)$$
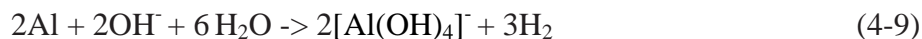
Chemical dissolution can occur on the metals both at anode and cathode. It should be noted that chemical reactions between iron and OH^- is slow and the thus the contribution to ferric is very limited.

(2). At high current intensity, the high current efficiencies can also be attributed to the temperature increase due to joule heating of the electrolytic solution. Temperature of the solution was found to increase by 3.5 degree after half hour at the current intensity of 50 A/m^2. Higher temperature might accelerate chemical dissolution of aluminum [Davis, 1999; Valenzuela et al., 2002; Mouedhen et al., 2008].

(3). The last reason for increased current efficiencies can be the presence of chloride ions in solution, which is reported to cause pitting of aluminum electrodes [Bockris et al., 2000;

Mouedhen et al., 2008; Li et al., 2009; Huang et al., 2013; Hossini and Rezaee, 2014] based on the following (4-10 to 4-11) equations [Wang et al., 2009]:

$$2Cl^-(aq) - 2e^- \rightarrow Cl_2 (g) \qquad (4\text{-}10)$$

$$Cl_2(g) + 2H_2O(l) \rightarrow HClO(aq) + H_3O^+(aq) + Cl^-(aq) \qquad (4\text{-}11)$$
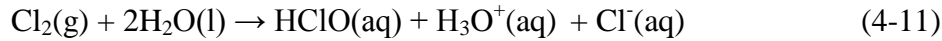
HClO is a strong oxidant, under the acidic environment it may react with aluminum and produce aluminum ions. The strong oxidizing capacity of chloride ions has also been extensively reported for degradation of COD from wastewater [Wang et al., 2009; Hossini and Rezaee, 2014; Li et al., 2009].
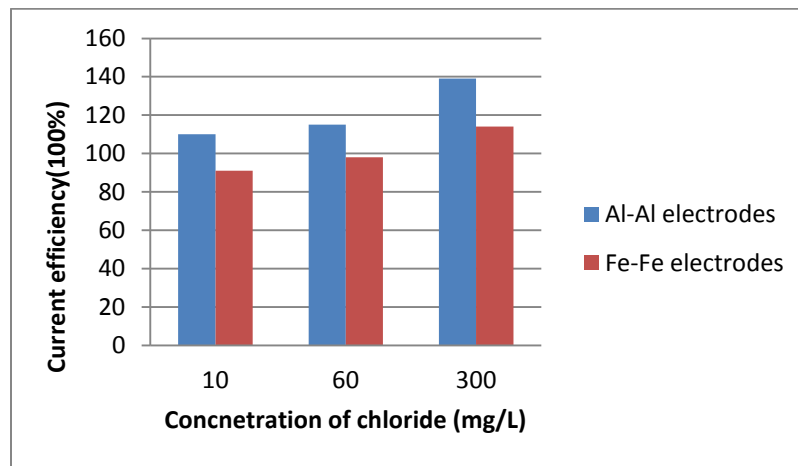
Fig. 4-5 Current efficiency vs. chloride concentration

Overly high current density should be avoided because it not only leaves extra metal ions in the effluent but also produces large amount of explosive hydrogen gas. The optimal current density is typically dependent on the wastewater characteristics.

4.1.3 Species of iron and dynamics of ferric ions in the electrolytic solution

As afore-mentioned, aluminium anode releases Al(III) ions in a one-step electrochemical reaction whereas generation of ferric ions are produced in two independent mechanisms, i.e. iron atoms are first oxidized into ferrous ions, and the latter is subsequently converted into ferric ions by oxygen in air or wastewater [Sasson et al., 2009; Cocke et al., 2009; Linares-Hernández et al., 2009]. It was reported that oxidation of ferrous into ferric ions by DO (> 3.5 mg/L) in a nearly neutral solution follows a pseudo first-order kinetics with a rate constant = 0.5 hour^{-1} [Stumm and Lee, 1961; Pham and Waite, 2008].

In this research, first nitrogen gas constantly purged the electrolytic fluid to DO = 0, and then DO was controlled at four levels (0, 0.5, 1, and 3 mg/L) during a half hour of electrolysis, at the end samples were taken immediately for ferrous/ferric analyses under nitrogen blanket. As shown in Fig. 4-6, at DO = 0 mg/L nearly all of dissolved iron was in the form of ferrous, and when DO = 1 mg/L, dissolved iron existed almost entirely as ferric ion.
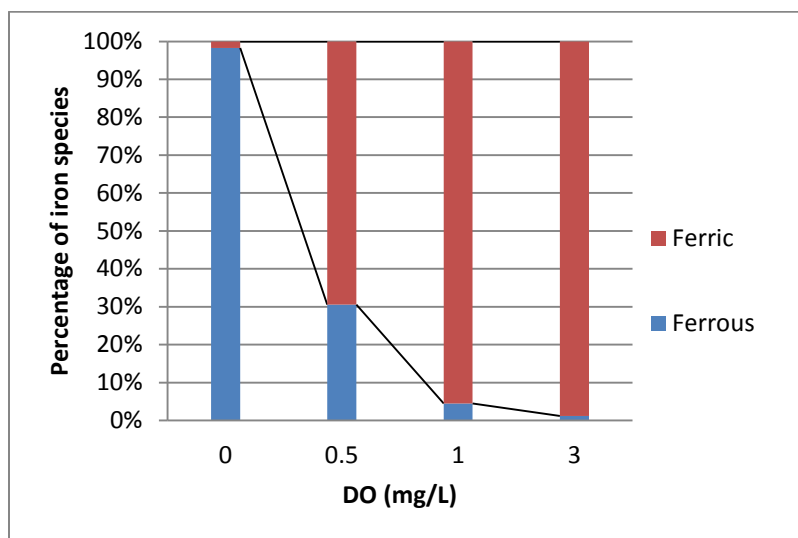
Fig. 4-6 Species of iron at various DO level

Generation and distribution of the ferric ions are dynamically demonstrated in Fig. 4-7. The red color represents existence of ferric ions and its intensity suggests the concentrations of ferric ions

generated. The mechanisms are as follows: the ferrous ions anodically produced from Equation (4-2) are oxidized to ferric ions by DO; the freshly formed ferric ions react immediately with thiocyanate ions to produce red complex ferric thiocyanate:

$$Fe^{2+} + O_2 + 2H_2O \rightarrow Fe^{3+} + 4OH^- \tag{4-12}$$

$$Fe^{3+} + nSCN^- \rightarrow Fe(SCN)n^{3-n} \text{ (red)} \tag{4-13}$$
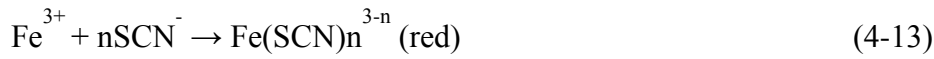
After 0.5 min. of electric application, form of the ferric ions is visible in vicinity of the anode, more and more ferric ions are generated as electrolysis proceeds between 2 and 5 min. During the same time, driven by electrophoretic force, the ferric ions traveled towards the cathode along the direction of the electric field. At 5 min. ferric ions reached the surface of cathode and filled in most of the space between anode and cathode. Right after aeration, the ferric ions distributed homogeneously in the entire electrolytic cell and therefore the localized red zone disappeared immediately. However, as soon as the aeration stopped, the red zone reappeared and the developing patterns are the same as initially. This experiment pictorially shows the real-time generation dynamics of the ferric ions and impact of shear forces or turbulence on the spatial distribution of ferric ions in the electrolytic cell.

a: 0.5 min
b: 2 min
c: 5 min
d: applying aeration,
e: 2 min. after aeration stopped)
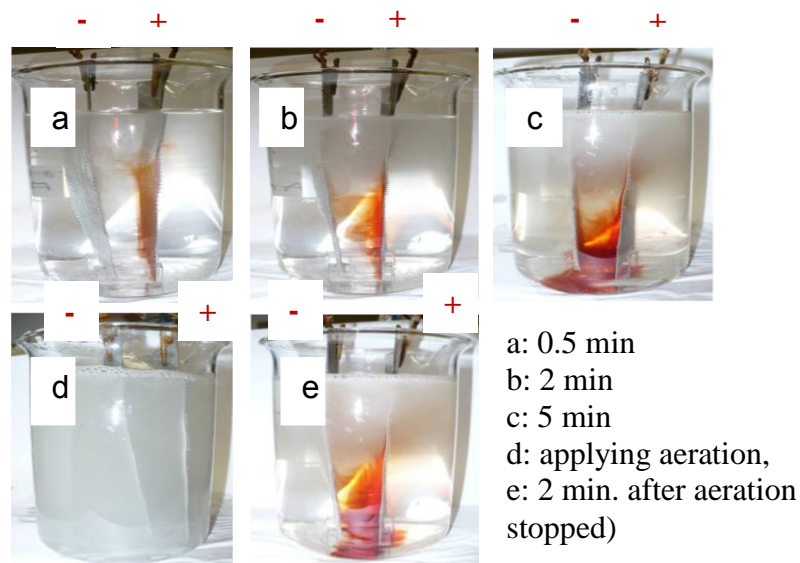
Fig. 4-7 Dynamic generation and distribution of ferric ions in the electrolytic cell

Due to high solubility of its hydroxide and lower positive charge density, ferrous ions are not as efficient as ferric ions in the EC process [Bagga et al., 2008]. Therefore, presence of sufficient oxygen or an oxidizing environment is essential for successful electrocoagulation with iron electrodes.

In spite of a few exceptions, most of the EC studies have shown that aluminum has a better pollutant removal efficiency than iron, however, relatively higher Al(III) toxicity, lower concentration tolerance in effluent and the surface water and higher price compared to iron make selection of EC materials case specific [Katal et al., 2011].

4.2 Flocs size distribution in the electrokinetic technologies

4.2.1 Formation of floc size in the coagulation process

The mixed liquor of ASP process in the wastewater treatment is typically classified into three constituents, i.e. the suspended solids ($> 1 \mu m$), colloids (0.1 to 1 μm) and soluble ($< 0.1 \mu m$) (Metcalf & Eddy, 2003). For more than half a century the chemical coagulation has been applied to destabilize and aggregate the suspended solids and enhance their separation from water through sedimentation or filtration. Alum, ferrous / ferric salts or their polymers are usually used as the coagulants. In addition to effective removal of the solids, removal of soluble organics and some inorganic metal ions are also improved due to chemical coagulation. Charge neutralization and pollutant enmeshment are the two primary mechanisms of chemical coagulation [Amirtharajah and Mills, 1982; Letterman et al., 1999]. Efficiency of the charge neutralisation is

143

characterized by the low repulsion forces between biomass particles. Enmeshment and bridging

of particles are the major holding forces for flocs, this type of binding strength has been reported

to be one to two orders of magnitude stronger than van der Waals attractive forces created by

charge neutralisation [Bache et al., 1997; Xu et al., 2011].

In chemical coagulation, typically two-stage mixing is practiced, i.e. 30 s of fast mixing at 120

rpm followed by half hour of slow stirring at 30 rpm. During the fast mixing period Al or ferric

cations of the coagulant first undergo rapid hydrolysis within 1 to 7 seconds [Amirtharajah and

Mills, 1982] followed by enmeshment of colloids trapped by the amorphous solid-phase

hydroxide.

The biomass floc coagulation rate and the final steady-state size are the results of dynamic

equilibrium between breakage and aggregation of flocs at the specific shear force intensity which

can be expressed by the following model [Jarvisa et al., 2005; Mikkelsen et al., 2002]:

$$R_f = kR_g - R_b \qquad (4\text{-}14)$$

Where:

R_f = the net floc size growth rate
k = particle collision factor
R_g = floc size growth rate due to collision
R_b = floc size breakage rate
R_g and R_b are dependent on the applied shear rate which is usually quantified by the average
velocity gradient [Yukselen et al., 2002]:
$$G = \sqrt{\varepsilon/v} \qquad (4\text{-}15)$$
$$\varepsilon = (P_0 N^3 D^5) / V \qquad (4\text{-}16)$$
Where:
G = the average velocity gradient (s^{-1})
v = the kinematic viscosity (m s^{-1})
ε = the energy dissipation rate per unit mass of fluid (Nms^{-1} kg^{-1})
P_0 = the power number of the mixing blade
N = the mixing blade speed (rps)

D = the mixing blade diameter (m)
V = volume of the coagulation tank (m^3)

When $kR_g = R_b$ or $R_f = 0$, the steady-state floc size is obtained. The particle collision factor k

varies depending on the shear intensity and the particle size at any time point. kR_g decreases as

the floc size increase due to declining number of particles, on the contrary, R_b increases as more

and more larger flocs exist in the system, and therefore, the coagulation equilibrium will

eventually be reached with characteristic floc sizes though irreversible breakage phenomenon

was reported by some researchers [Brakalov, 1987; Francois, 1987; Spicer et al., 1998; Gregory

and Dupont, 2001] .

An empirical equation for the steady state floc size can be expressed as the following [Jarvisa et

al., 2005; Kim et al., 2007]:

$$d = CG^{-\gamma} \qquad\qquad\qquad (4\text{-}17)$$

Where:

d = the floc diameter (m)

γ = the steady state floc size exponent
C = the floc strength co-efficient
The logarithmic form of the exponential Equation (4-17) is:
$$\text{Log}d = \text{log}C - \gamma \text{log}G \qquad\qquad (4\text{-}18)$$

Coefficients γ and C can be obtained through regression of Equation (4-18) with a series of

experimentally observed values for d and G.

The steady-state floc size of a coagulation process is virtually an indirect measurement for the

average floc strength at specific shear intensity. The average floc strength can be experimentally

determined with external particle breakage technologies which are capable of supplying uniform,

accurate and controllable energy onto a floc suspension. The commonly used energy dissipation

technologies include mechanical mixing, ultrasound, vibrating or the sensitive

micromanipulators developed in the recent years [Mikkelsen et al., 2002; Yukselen et al., 2002; Kim et al., 2007].

Floc strength coefficient (FSC) = d_2/d_1 (4-19)

where d_1 and d_2 are the average floc size before and after the breakage experiment.

4.2.2 Impact of chemical coagulation and electrocoagulation in floc size in batch tests

Fig. 4.8 shows the floc size distribution of ASP biomass after chemical coagulation. In this experiment standard chemical coagulation procedures were followed, i.e. a 30 s of fast coagulant mixing at 120 rpm with the biomass and then half of an hour slow stirring for floc aggregation. The two coagulant doses are equivalent to the theoretical electrocoagulation doses for one hour and two hours, respectively. As expected, the average floc sizes increased by 36.4% and 66.5% at doses of 27 mg/L and 54 mg/L of Al^{3+} [Verma et al., 2012]. However, the particle size of biomass in the electrocoagulation tanks tended to decrease. Table 4.1 and Fig. 4.10 indicate the flocs size decreased by 18.9% over two hours of coagulation. Fig. 4.9 is the overlay images of original particle size acquisition of 4 trials. Fig. 4.11 and Fig. 12 and Table 4.2 are the results of different biomass from another source, again the average floc size dropped by 28.03% over 2 hours of coagulation period. A similar floc size reduction tendency was also overserved in the continuously operating MBR and EMBR, which is contrary to the observations by most of the other researchers [Larue et al., 2003; Harif et al., 2012; Lakshmanan et al., 2009; Larue et al., 2003]. The unexpected floc size change can be attributed to the following reasons:

146

(1). As stated previously, the steady state floc size is the dynamically equilibrated result of floc aggregation and breakage, which is dependent on the prevailing shear conditions. In chemical coagulation, normally a half hour of slow mixing allows the flocs to attach together, whereas in this research, aeration is constantly supplied due to the need for membrane scouring. Therefore, the shear stress generated by the aeration in the combined aerobic and electrode tank prevents the flocs from attaching and merging, it may even break some of the flocs with less strength.

(2). Although chemical coagulation and electrocoagulation resemble each other in the surface charge neutralization mechanism, flocs aggregation or disintegration follow different mechanisms, as proposed by Harif et al. [2012]. Reaction Limited Cluster Aggregation (RLCA) is mainly responsible for particle growth in chemical coagulation, whereas in EC Diffusion Limited Cluster Aggregation (DCLA) is dominant. Consequently, EC generated flocs are more fragile, contain less bound water and are prone to restructuring and compaction;

(3). As stated in the later sections and early reports in literature, EC is efficient in removing EPS including TEP from the mixed liquor, EPS or TEP play a crucial role in floc aggregation through the hydrophobic interactions between microbial cells. In addition, the VSS/TSS ratio decreases significantly [Wei et al., 2012] and the flocs become less viscous, therefore, reduction of the EPS concentration may cause floc disintegration or breakage. When the aeration intensity exceeds the shear energy required to break individual flocs or those in a suspension, particle breakage becomes irreversible and floc re-growth or secondary aggregation cannot occur.

Lastly, it is necessary to address some issues and challenges in the existing particle size measuring technologies. Floc size is an important parameter for biomass characterization and over the last decades a few quantitative floc size measurement techniques have been developed. The most popular ones are light scattering and transmission, microscopy and photography, and today all of the techniques include image software for accurate and fast data analysis. Due to the fragile nature of flocs, non-destructiveness or non-disturbance is crucial to any successful particle size determination approach and so far none of the above methods is perfect. Microscopy and photography require very diluted and small amount of sample for sufficient light transmission and that usually changes the matrix environment of flocs and representativeness of the sample. As a result, large number of repeated measurements are needed to ensure reliability of the determined results. The popular light scattering particle size measurement technique relies on constantly pumping the suspension through a laser beam window; however, the particle size is usually alternated due to damage made by the pumping device. Three types of suspension delivery techniques (peristaltic pump, a syringe pump and a hand pipette) were compared by Spicer et al. (1998) and a peristaltic pump on the return side of the measuring cell was reported as the most favourable delivery method. One common drawback of all particle size techniques is that they are based on optical measurements. Optical measurements are more appropriate for solid spheres made of the same substance. As the biomass flocs are in highly irregular shape, the measurement based on light scattering patterns is liable to deviation.
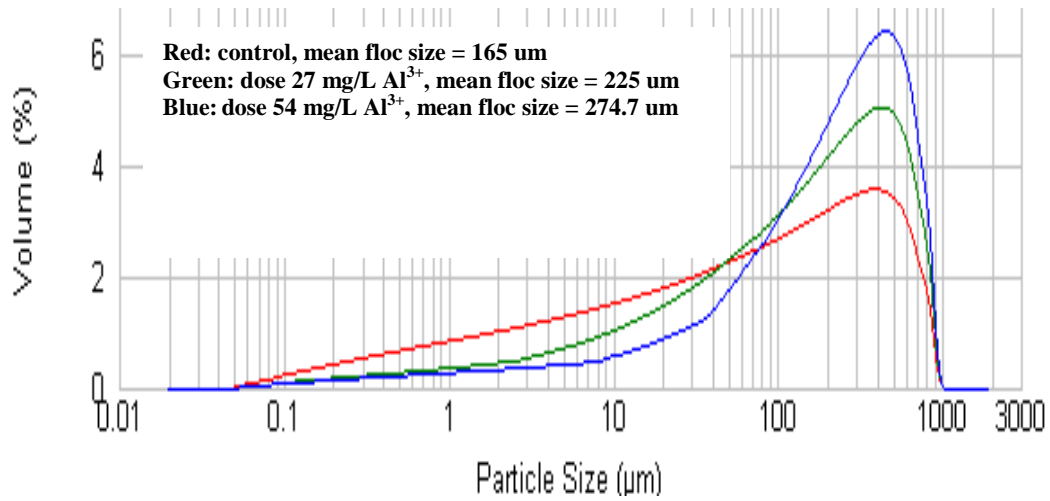
Fig. 4.8 Particle size distribution of ASP biomass after chemical coagulation
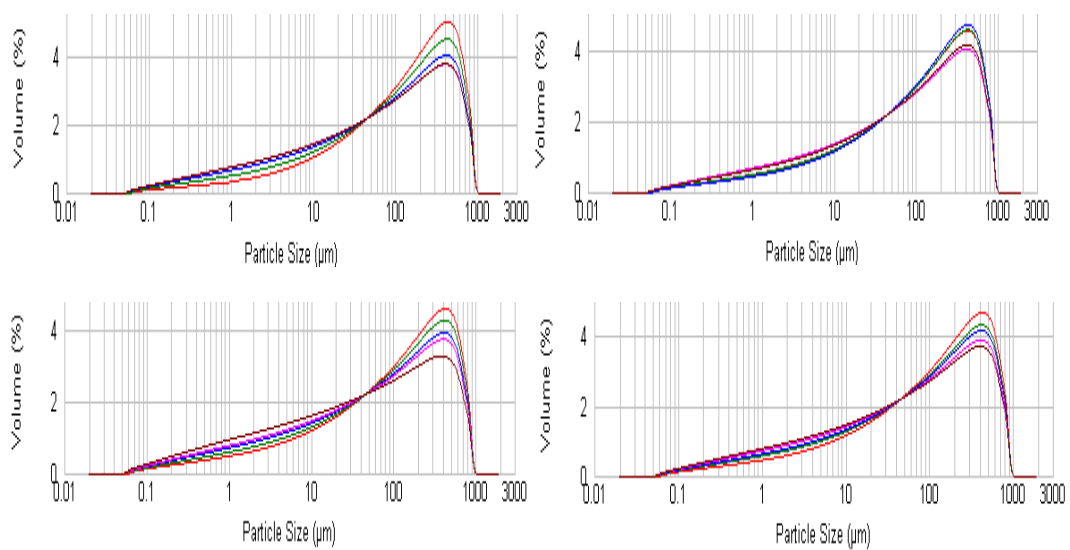
Fig. 4.9 Particle size distribution of ASP biomass after electrocoagulation (2 hour)

Table 4.1 Particle size distribution of ASP biomass after electrocoagulation

T(min)	$D_{0.1}$(µm)	$D_{0.5}$ (µm)	$D_{0.9}$ (µm)	Mean (µm)	σ(µm)
0	4.6	131.5	561.9	213.2	9.1
30	3.1	114.6	548.2	201.2	6.2

149

60	2.6	102.9	536.7	192.6	14.3
90	1.7	83.7	517.4	178.3	5.4
120	1.6	77.8	508.2	172.9	14.9
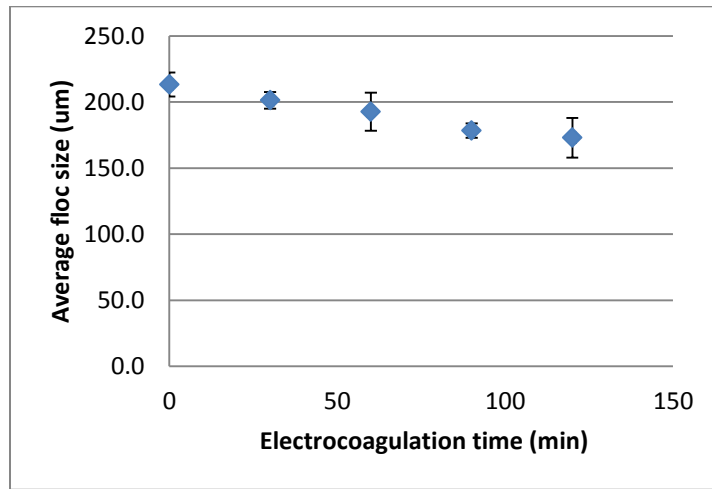
Fig. 4.10 Average floc size of ASP biomass after electrocoagulation (2 hour)
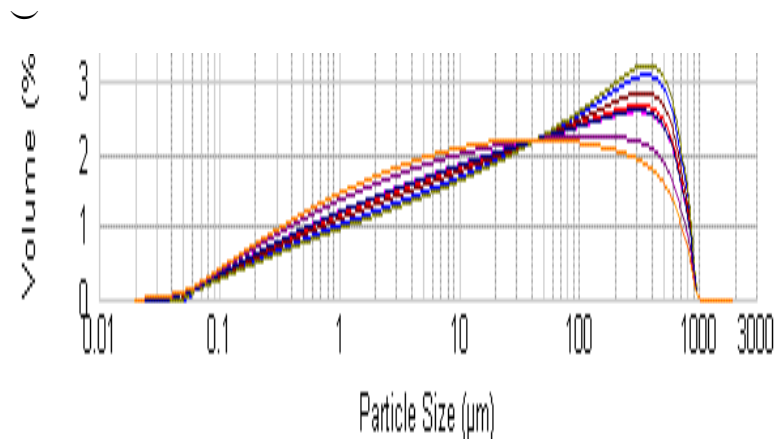
Fig. 4.11 Particle size distribution of another ASP biomass after electrocoagulation (2 hour)

150
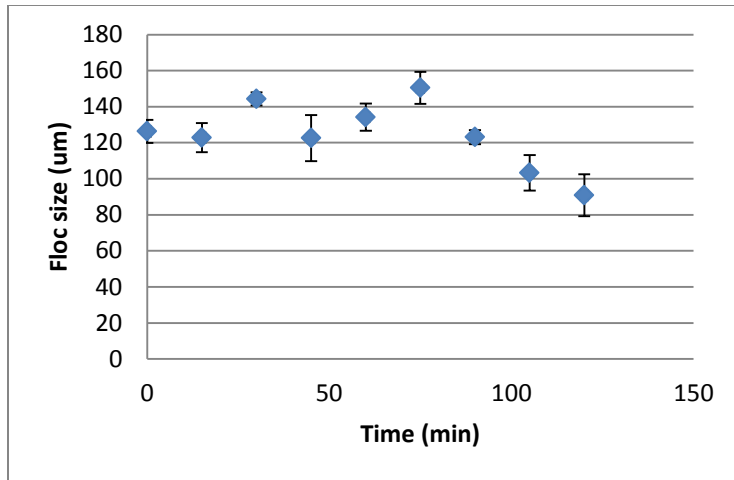
Fig. 4.12 Average floc size of another ASP biomass after electrocoagulation (2 hour)

Table 4.2 Average floc size of another ASP biomass after electrocoagulation

T (min)	Mean (μm)	σ (μm)
0	126.3	6.4
15	122.8	8.1
30	144.3	3.6
45	122.6	12.8
60	134.2	7.6
75	150.5	8.9
90	123.1	3.9
105	103.3	9.8
120	90.9	11.6
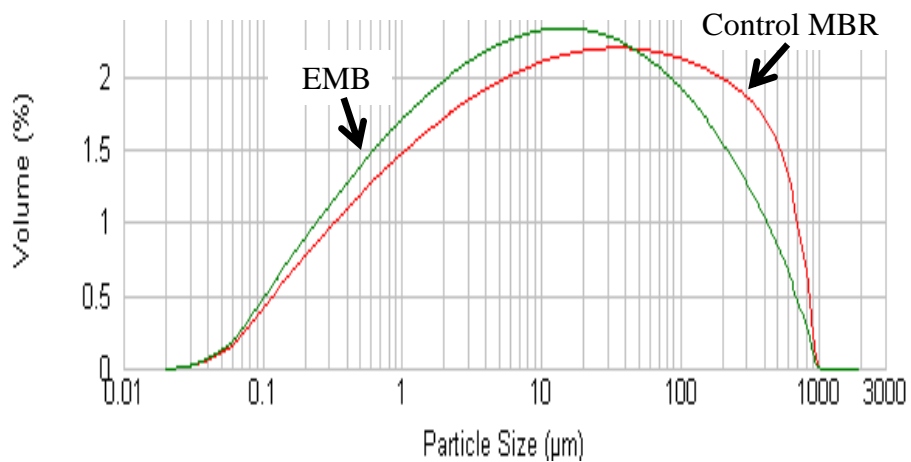
Fig. 4.13 Flocs size distribution of EMBR and control biomass at 10 ^{0}C.

151

4.3 CST and SVI of electrokinetically treated sludge

CST is a common indicator of sludge dewaterability or filterability. It is dependent on the temperature and sludge characteristics such as TSS content, flocs size and EPS concentration and composition [Dentel and Abu-Orf, 1995]. As presented in Fig. 4-14, the sludge treated by both Fe-Fe and Al-Al electrodes display a general trend of CST decrease as the current application time increases (Fe: 5.6% - 26.1% , Al: 6.8% - 23.5%), suggesting electrocoagulation improves sludge filterability due to reduced soluble EPS concentration in the sludge as presented in the following sections.
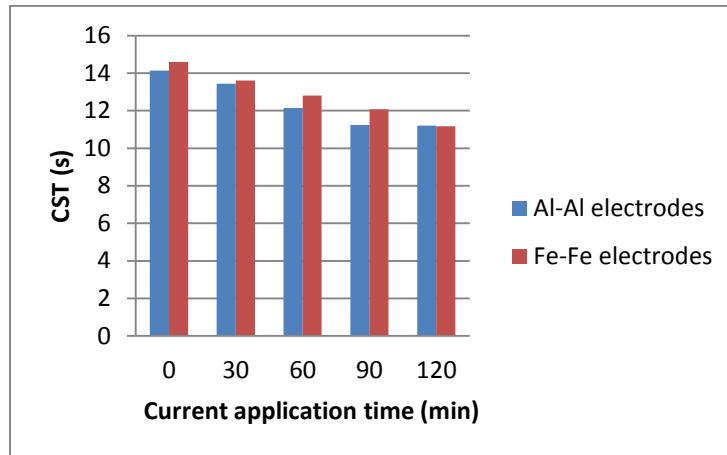
Fig. 4.14 CST vs. current application time

Sludge volume index (SVI) is the most widely used parameter to quantify MLSS settleability in routine wastewater treatment operations [Daigger et al., 1985]. Fig. 4-15 indicates that Both Fe-Fe and Al-Al electrodes reduces SVI significantly, with 5.5% - 21.4% by Al electrode and 7.8% - 30.2% by Fe electrode, respectively, demonstrating significant improvement in sludge setteability by electrocoagulation. Fe electrode is slightly more efficient than Al electrode which is in agreement with the observations by Zodi et al. [2009].
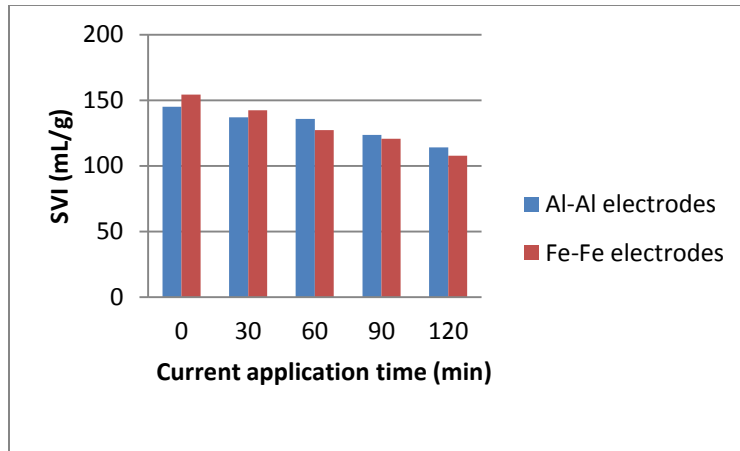
Fig. 4.15 SVI vs. current application time

4.4 Zeta potential change of biomass treated with the electrokinetic technology

Zeta Potential measures the electrical charge of the colloidal particles in the mixed liquor and can be directly calculated from electrophoretic mobility of flocs. Most colloidal particles in wastewater are negatively charged due to: 1) ionizable anion groups such as amino or hydroxyl groups etc. 2) adsorption of anions on the surface of colloids and 3) lattice imperfections. In EMBR, the electrochemically generated aluminum or ferric ions neutralize the colloid charge and destabilize the colloidal suspension, which can be demonstrated by the upward zeta potential shift from -22.8 to 4.2 mv for Al-Al electrode (Fig. 4.16) and from -24.8 to 2.2 mv for Fe-Fe electrode (Fig. 4.17), suggesting the superior electrocoagulation effect. The results indicate that Al-Al electrode is slightly more efficient in charge neutralization of activated sludge.
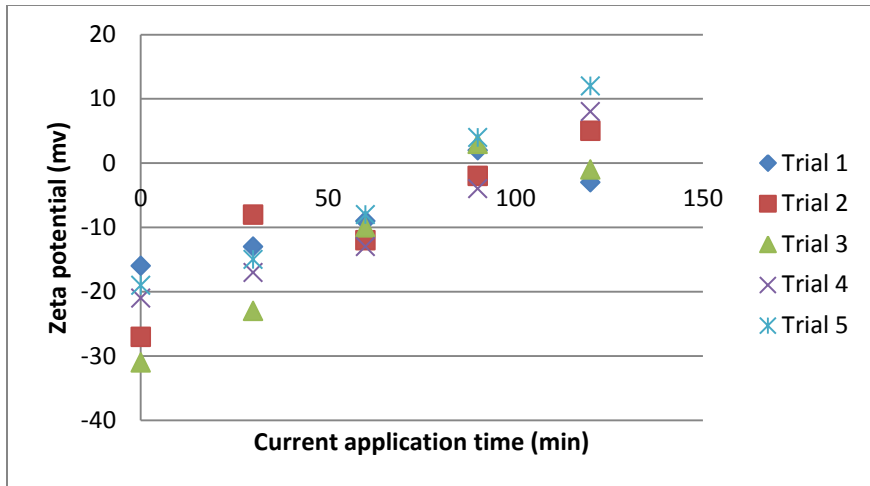
Fig. 4.16 Zeta potential vs. current application time (Al-Al electrode)
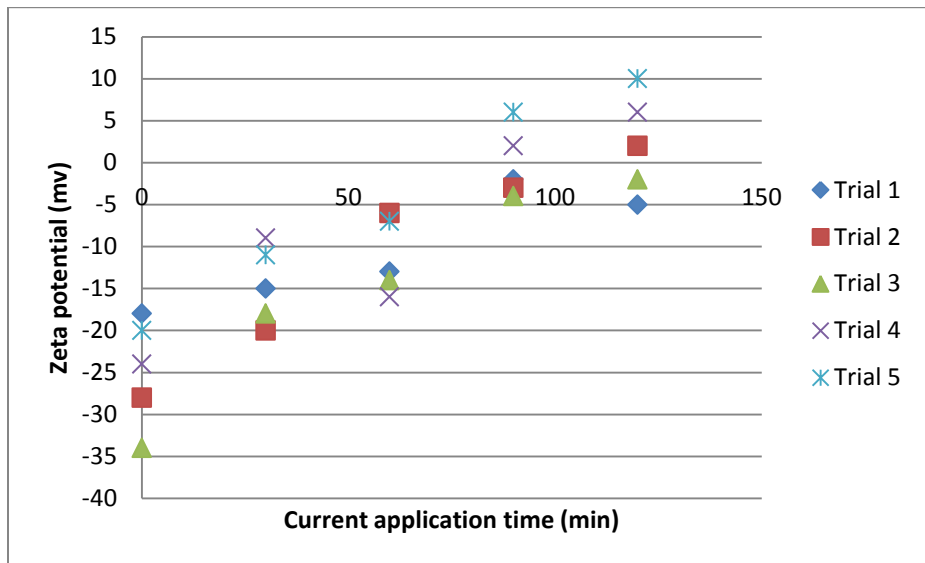
Fig. 4.17 Zeta potential vs. current application time (Fe-Fe electrode)

4.5 Electrode passivation and mitigation strategies

Precipitation on the electrode surface and the resulting electrode passivation is the major

challenge for broader application of electrokinetic technologies such as EC [Vik et al., 1984;

Mollah et al., 2004; Wang et al., 2007]. The negative impacts of electrode passivation on the

154

electrokinetic processes include declining of the anodic release of metal cations, decreased conductivity of the electrodes, reduced wastewater treatment efficiencies and waste of energy. Therefore, minimization of electrode passivation is crucial for successful application of electrokinetic technologies. Mechanistically the precipitates on the electrode surface have the following sources:

(1). Chemical reaction: The electrochemically generated metal ions react with the hydroxyl group and phosphate to produce precipitates of metal hydroxide and phosphate salt, as shown in Equation 4-20 - Equations 4-23 and Fig. 4.18

$$Al^{3+} + 3OH^- \rightarrow Al(OH)_3 \downarrow \qquad\qquad (4\text{-}20)$$

$$Al^{3+} + PO_4^{3-} \rightarrow AlPO_4 \downarrow \qquad\qquad (4\text{-}21)$$

$$Fe^{3+} + 3OH^- \rightarrow Fe(OH)_3 \downarrow \qquad\qquad (4\text{-}22)$$

$$Fe^{3+} + PO_4^{3-} \rightarrow Fe\,PO_4 \downarrow \qquad\qquad (4\text{-}23)$$
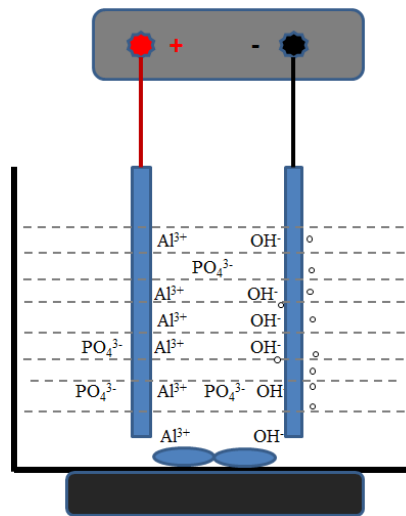
Fig. 4.18 Schematic illustration of precipitating ions in EC with Al-Al electrodes

(2). Electric charge attraction effect: the negatively charges particles or flocs in the fluid are attracted to the positively charged anodic surface.

Though presence of chloride in industrial and municipal wastewater may alleviate the passive

film on the anode surface to some extend [Szklarska-Smialowska, 1986], the most common

approaches to deal with the precipitates are:

(1) Use turbulent shear to drive the metal ions away and prevent their accumulation on the

electrode surface;

(2) Periodical reversal of the electric polarity. This method makes use of the catholically

generated hydrogen gas which is capable of pushing the precipitated scale off the electrode

surface (Equation 4-7).

(3) Remove precipitates mechanically or manually at a certain interval.

As the preventative measures for precipitate formation, in addition to turbulent mixing,

periodical reversal of the electric polarity is another common strategy. The production rate of

hydrogen gas can be calculated by the following equation:

$$r_{H_2} = \frac{I * 22.4}{2 * F} * 1000 \quad (\text{ml/s}) \qquad\qquad (4\text{-}24)$$

For the experimented current intensities of 0.05 A, 0.1 A, 0.2 A, 0.5 A and 1 A, r_{H_2} are listed in

Table 4.3

Table 4.3 Production rates of hydrogen gas at various experimented current intensities

Current intensity (A)	0.05	0.1	0.2	0.5	1
H_2 producing rate (ml/s)	0.005	0.01	0.02	0.05	0.1

It was found that when current intensity ≤ 0.2 A, polarity reversal had minimal impact on electrode passivation reduction. However, if current intensity was above 0.2 A, frequent polarity reversal (< 5 min per cycle) was detrimental to electrode passivation. This is because aluminium ions react with hydroxyl groups before they are able to diffuse into the bulk solution.

4.6 Non-invasive observation of electrokinetic membrane fouling reduction by MRI

MRI as an in-situ non-invasive imaging tool has been recently applied for membrane fouling studies [Schulenburg et al., 2008; Vrouwenvelder et al., 2009; Vrouwenvelder et al., 2010]. In MRI, the protons in water molecules are excited by radio frequency emitted from the coil placed on the target object, and magnetic field gradient is generated for spatially structural encoding based on ^{1}H signal, which is acquired predominately from the water content in the sample. In MRI contrast of the relaxation time T_2 is presented in the digitized image and allows identification of localized environment details within a sample, such as the polymeric membrane materials and pores filled with free water [Schulenburg et al., 2008].

Fig. 4.19 and Fig. 4.20 (in false color) show the cross-sectional MRI images of ZW-1 membrane after 0, 1 and 2 hours without and with electric current application (Al-Al and Fe-Fe). The regional brightness represents the differentiated content of local water molecules. Therefore, those areas with strong signal intensity suggest more water filled space or less fouling region, whereas the darker places indicate the spaces are occupied by membrane material itself or foulants. Without application of current severe fouling is evident in the control membranes (in F of both Fig. 4.19 and Fig. 4.20) because half of the cross-section images are invisible as the fouling cake on the membrane surface gave little to no MRI signals due to shorter T_2 NMR relaxation time of the small amount of trapped water.
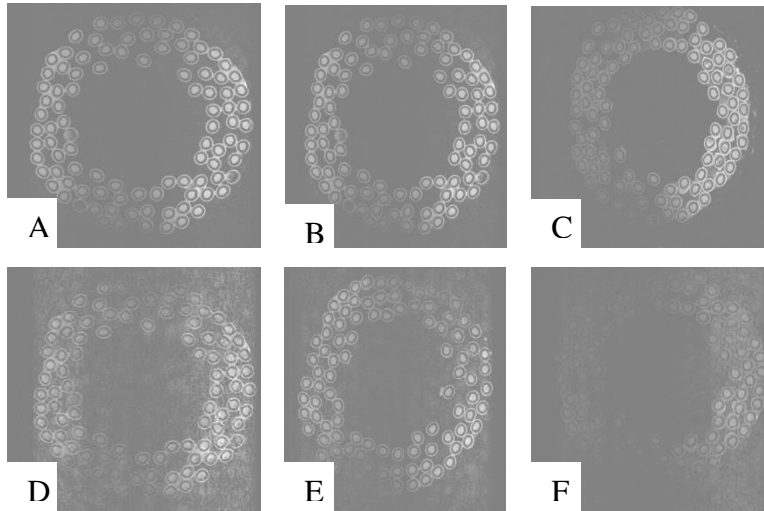
Fig. 4.19 Cross-sectional MRI images of ZW-1 membrane (A, B, C correspond to 0, 1 hour and 2 hours after current application in EC; D, E, F correspond to 0, 1 hour and 2 hours without current application, Al-Al electrodes)
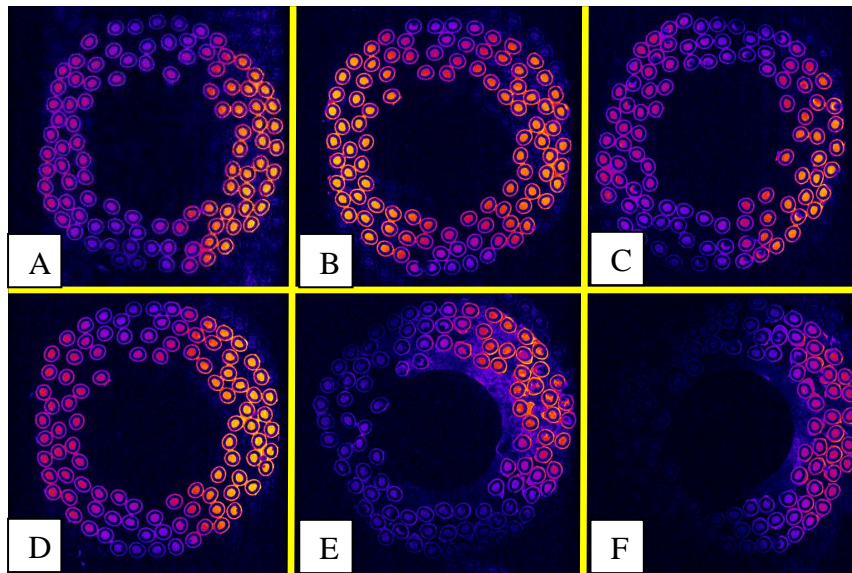
Fig. 4.20 Cross-sectional MRI images of ZW-1 membrane (A, B, C correspond to 0, 1 hour and 2 hours after current application in EC; D, E, F correspond to 0, 1 hour and 2 hours without current application, Fe-Fe electrodes)

4.7 Efficiency of electrokinetic EDC removal

The negative impact of EE2 to aquatic organisms has been of great concern in the past two decades [Clouzot et al., 2010]. EE2 was chosen as the research target for EDC as it is one of the most potent endocrine disrupters. EDC may be removed through three mechanisms, i.e. adsorption by the sludge, biodegradation, and oxidation by the electrochemically generated oxidants such as ozone and chlorine [Andersen et al., 2005]. As Henry's law constant for EE2 is $7.94 * 10^{-12}$ atm.m³/mol [de Mes et al., 2005], its vapor pressure at room temperature is fairly low [Clara et al., 2005b; Cirja et al., 2008], and this loss of EE2 by evaporation can be negligible. EE2 molecule is hydrophobic and its solubility in water is very low. Therefore, in a CAS system EE2 is primarily removed by adsorption [Andersen et al., 2005] and biodegradation through co-metabolism by ammonium monooxygenase, the nitrification enzyme [Yi and Harper, 2007]. As shown in Fig. 21, after 15 hours of electrocoagulation, the E2-equivalent estrogenic activities were reduced by 57.9% and 49.2% with Fe and Al electrodes, respectively. Electrocoagulation with Al-Al electrodes is slightly more efficient than that with Fe-Fe electrodes for EE2 removal.
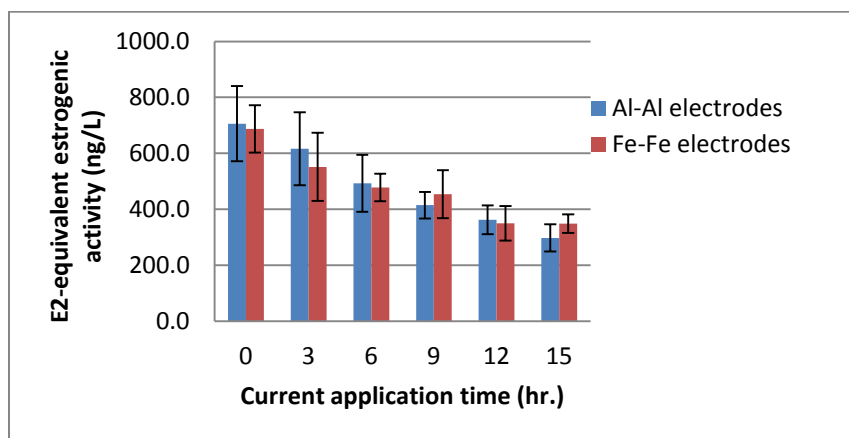
Fig. 4.21 Removal of EE2 by electrocoagulation

159

4.8 Bacterial viability of biomass subjected to the electrokinetic technology

When the AC or DC current is applied to a pair of electrodes placed in a microbial suspension, an electric field is generated, which act on the microbes between electrodes. If the electric field is beyond a certain threshold, it may significantly change the cell's shape, surface hydrophobicity and net surface charge. The electric field may also affect the orientation of membrane components such as lipids. All of these effects can potentially result in irreversible permeabilization of the cell membrane and subsequent leakage of essential cytoplasmic constituents and decreasing respiratory rate [Chen et al., 2002]. Along with the action of electric field on microbial cells, electrochemical redox reactions occur simultaneously on the electrode surfaces [Thrash and Coates, 2008]:

At anode:

$$2\ H_2O - 4e^- \rightarrow O_2(g) + 4H^+ \qquad (4\text{-}25)$$
$E^0 = 1.23$ V (vs. NHE) if nonreactive material such as platinum is used

$$2Cl^- - 2e^- \rightarrow Cl_2(g) \qquad (4\text{-}26)$$
$E^0 = 1.358$ V (vs. NHE) if there is considerable amount of chloride ions

$$Al\ (s) - 3e^- \rightarrow Al^{3+}\ (aq) \qquad (4\text{-}27)$$
$E^0 = 1.66$ V (vs. NHE) if active material (e.g. Al) is used.

At cathode:

$$2\ H_2O + 2e^- \rightarrow H_2(g) + 2OH^- \qquad (4\text{-}28)$$
$E^0 = 0.828$ V (vs. NHE)

$$O_2(g) + 2H^+ + 2e^- \rightarrow H_2O_2 \qquad (4\text{-}29)$$
$E^0 = 0.695$ V (vs. NHE) if the fluid is acidic
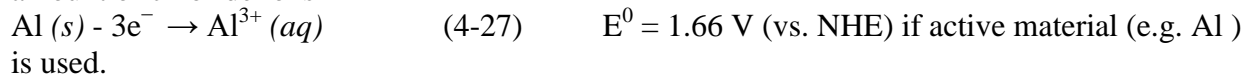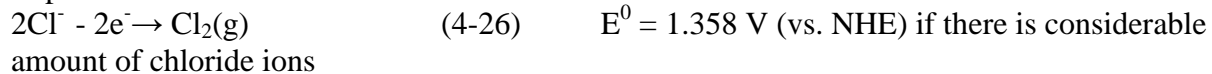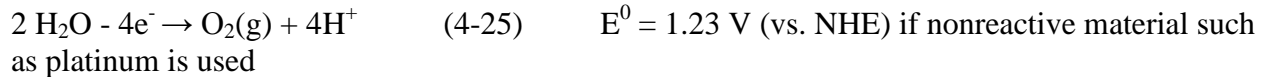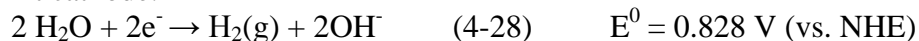
The above electrochemical reactions suggest potentially dramatic pH change in the localized vicinity of the electrodes in a non-buffered stationary system and production of toxic hydrogen peroxide and chlorine or subsequent hypochlorous acid. These may penetrate into the interior of the cells via the pores and accelerate the inactivation process.

In this study the cell viability in presence of aeration (3.4 L/min) and electric currents of various intensities were investigated for duration of 4 hours and the results are presented in Fig. 4.22.

When the applied electric density is less than 6.2 A/m^2, there was no significant (<10%) live cell percentage reduction compared to the initial biomass or the control sample. However, the live cell percentage dropped 15% and 29% at the current density of 12.3 A/m^2 and 24.7 A/m2, respectively. This suggests that under the studied conditions 6.2 A/m^2 is the current density the bacteria could tolerate and above that range, detrimental effects can be expected to the cell. Fig. 4.23 shows that after 8 hours of electric application at current density of 6.2 A/ m^2, dissolved COD and TOC were removed by 78.1% and 75.8% respectively. The mechanisms of COD and TOC removal may include [Moreno-Casillas et al., 2007]: (1) direct electrochemical oxidation of organic substances into carbon dioxide; (2) adsorption or encapsulation into the mesh-like precipitate of aluminum hydroxyl and (3) oxidation of the organics by electrochemically generated oxidants such as perchloride or hydrogen peroxide etc.
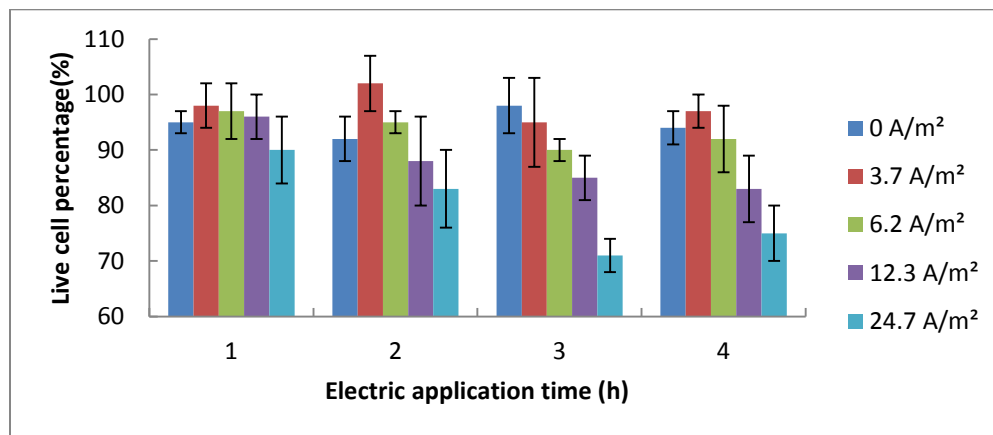
Fig. 4.22 Effect of current intensity and duration on the relative live cell percentage
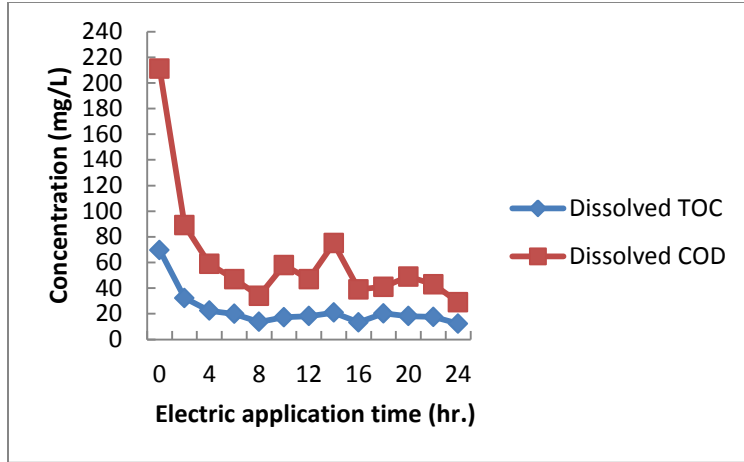
Fig. 4.23 Effect of current duration on dissolved TOC and COD (current density 6.2 A/m^2)

In this research active metal aluminum is used as the anode material, so its dissolution reaction Al (s) - 3e$^-$ → Al^{3+} (aq) is electrochemically preferred to 2 H$_2$O - 4e$^-$ → O$_2$(g) + 4H$^+$ due to higher standard oxidation potential. In an electrochemical reactor the applied electric voltage U can be calculated based on the following equation [Drees et al., 2003]:

U = E$_{eq}$ + d*j/κ + anode overpotential + cathode overpotential   (4-30)

Where E$_{eq}$ = equilibrium potential difference between the anode and the cathode (V)

κ = fluid conductivity (mho/m)

d = distance between electrodes (m),

j = current density (A/m^2)

When U is large enough (8 V in this study), it may overcome the equilibrium potential difference, electrode overpotentials and ohmic potential drop, and induce the electrochemical reactions in Equations (4-25) – (4-29). In addition, as shown in Fig. 4.24 the pH of the biomass increased significantly to a level hostile for the bacteria when current densities reached or exceeded 12.3A/m^2. Fig. 4.25 demonstrated that the biomass's SOUR dropped by 42% after 4 hours of electric application at current density of 24.7 A/m^2.

162
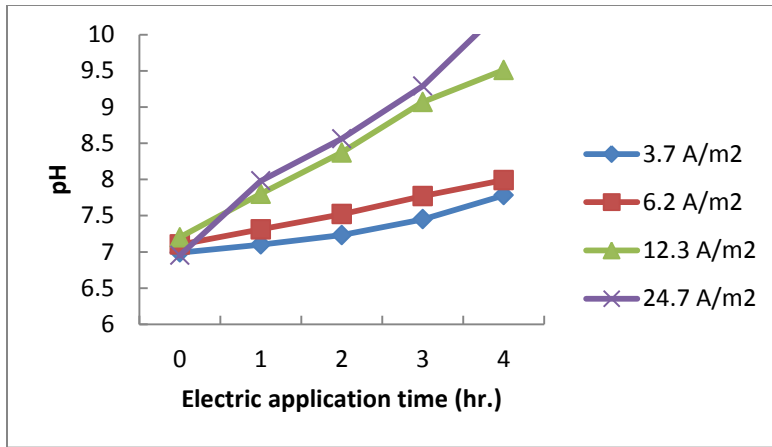
Fig. 4.24 Effect of current intensity and duration on pH
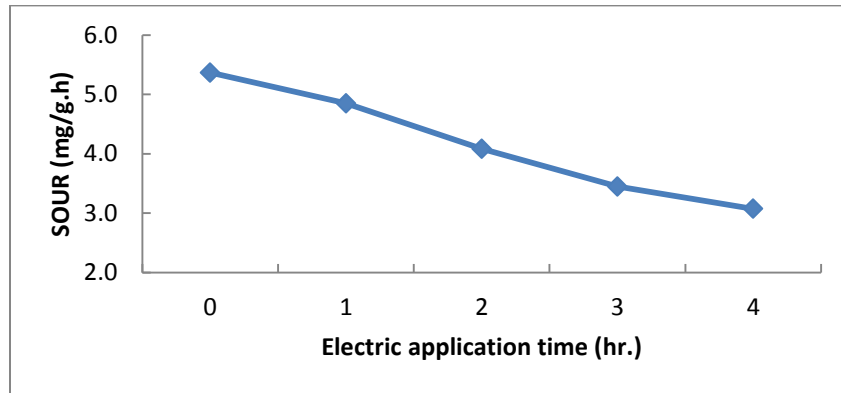
Fig. 4.25 SOUR of biomass vs. current duration (current density 24.7 A/m^2)

The temperature changes observed during application of electric current at room temperature were displayed in Fig. 4.26. The maximum change at all current densities during 4 hours was less than 2°C. Therefore, the temperature changes monitored should not have caused bacterial inactivation.
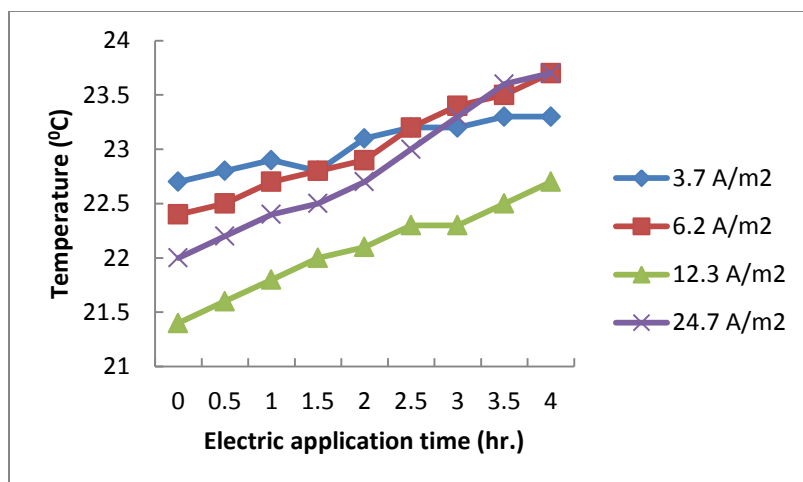
Fig. 4.26 Effect of current intensity and duration on the biomass temperature

Bacteria experience different micro-environments in an electrochemical reactor, especially when the reactor is not stirred or there is little mixing. As shown in Fig. 4.27, bacterial cells on the cathode surface were directly subjected to significantly elevated pH and action of electric field, consequently exhibiting highest death rate, whereas bacteria outside the space between electrodes had the highest viability because they were beyond influence of the electric field and are least affected by the toxicity of electrochemical by-products. Therefore, for a wastewater treatment process in which an electro technology is incorporated, strong mixing is desirable to enhance dispersion and diffusion of microorganisms and prevent localized cell inactivation.

Direct currents may also be used to stimulate bacterial activity and metabolism in a process called electro-stimulation. Several studies have been conducted on the stimulatory effects of low level direct currents on microbial growth. Nakanishi et al. [1998] reported that electro-stimulation of cells induces changes in DNA and protein synthesis, membrane permeability and cell growth and revealed that at low current level, bacterial activity and metabolism which were

measured in terms of alcohol production were enhanced, though the mechanism of these changes is still not well understood. In research reported here, no electro-stimulation effect was observed.
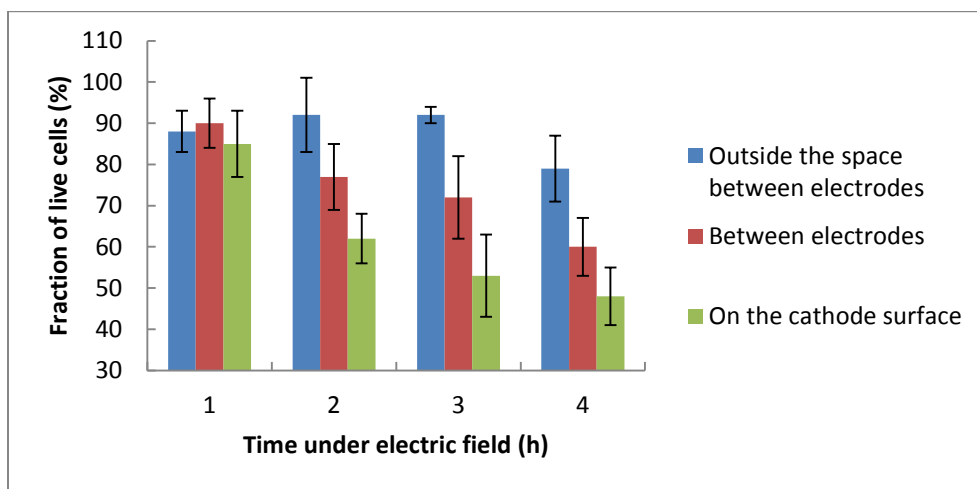
Fig. 4.27 Bacterial viability in the different zones relative to electrodes when no mixing was applied in reactor (current density = 12.3 A/m^2)

4.9 Prevention of abiotic ammonification in the electrokinetic technology

The electrochemical reduction of nitrate is a very complicated process, primarily due to the multiple valences of nitrogen. As shown in Table 4.4, in acidic or alkaline solutions nitrate may be reduced into a variety of derivatives successively or in parallel. In addition, autocatalytic reactions are also involved over time, leading to a large number of intermediates and final products [Prasad et al., 1995; Katsounaros et al., 2009].

Table 4.4 Reduction potentials of nitrogen species under acidic and basic solutions

Condition	Reduction								
	$\leftarrow$								
	-3	-2	-1	0	+1	+2	+3	+4	+5

Acidic	NH_4^+	$N_2H_5^+$	NH_3OH^+	N_2	N_2O	NO	HNO_2	N_2O_4	NO_3^-
Reduction potential	1.275	1.41	-1.87	1.77	1.59	0.99	1.07	0.803	
Basic	NH_4OH	N_2H_4	NH_2OH	N_2	N_2O	NO	NO_2^-	N_2O_4	NO_3^-
Reduction potential	0.1	0.73	-3.04	0.94	0.76	0.46	0.867	-0.86	

When aluminum or iron is used as the anode in the electrochemical process with nitrate containing fluid as the electrolytic media, the following oxidation-reduction reactions (4-31, 4-32) occur:

At the anode (Al or Fe):

$$Al\ (s) - 3e^- \rightarrow Al^{3+}(aq) \qquad\qquad E^0 = 1.66\ V \qquad\qquad (4\text{-}31)$$

$$Fe\ (s) - 2e^- \rightarrow Fe^{2+}(aq) \qquad\qquad E^0 = 0.44\ V \qquad\qquad (4\text{-}32)$$

where E^0 is the standard oxidation or oxidation potential depending on the actual electrochemical reactions. The single-step reaction $Fe(s) - 3e^- \rightarrow Fe^{3+}$ ($E^0 = 0.037\ V$) has been disproved [Lakshmanan et al., 2009].

The aluminum ion is an electrochemically stable species and it undergoes hydrolysis:

$$Al^{3+}(aq) + 3H_2O\ (l) = Al(OH)_4^- + 4H_3O^+\ (aq) \qquad\qquad (4\text{-}33)$$
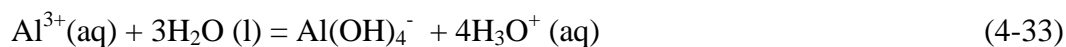
Whereas ferrous ions may be further oxidized into ferric ions or ferric hydroxide in presence of oxygen:

$$Fe^{2+}(aq) - e^- \rightarrow Fe^{3+}(aq) \qquad\qquad E^0 = -0.771 \text{ V} \qquad\qquad (4\text{-}34)$$

$$4Fe^{2+}(aq) + O_2 + 10H_2O~(l) \rightarrow 4Fe(OH)_3(s) + 8H^+ \qquad\qquad (4\text{-}35)$$
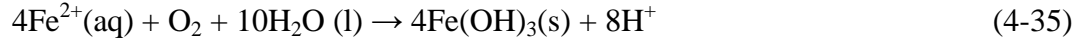
Unless under high electric density the anodic reaction $6H_2O(l) - 4~e^- \rightarrow O_2(g) + 4~H_3O^+(aq)$ $E^0 =$ -1.229 V doesn't occur because it is thermodynamically unfavourable (Gibbs free energy $\Delta G^0 = -nFE^0 > 0$).

At the cathode, the dominant electrochemical reactions can be described by Equations (4-36) - (4-39) [Paidar et al., 1999; Fanning et al., 2000]:

$$2H_2O~(l) + 2e^- \rightarrow H_2(g) + 2OH^-(aq) \qquad\qquad E^0 = -0.8277 \text{ V} \qquad\qquad (4\text{-}36)$$

$$NO_3^-(aq) + H_2O~(l) + 2e^- \rightarrow NO_2^-(aq) + 2OH^-(aq) \quad E^0 = 0.01 \text{ V} \qquad\qquad (4\text{-}37)$$

$$NO_2^-(aq) + 2H_2O(l) + 3e^- \rightarrow \tfrac{1}{2}N_2(g) + 4OH^-(aq) \quad E^0 = 0.406 \text{ V} \qquad\qquad (4\text{-}38)$$

$$NO_2^-(aq) + 5H_2O(l) + 6e^- \rightarrow NH_3(g) + 7OH^-(aq) \quad E^0 = -0.165 \text{ V} \qquad\qquad (4\text{-}39)$$

4.9.1 The electrochemical reduction behavior of nitrate and influences by the electrode materials and electric intensity

To isolate the effect of electrochemical reduction of nitrate, at first a nitrate-containing electrolytic fluid was tested with Al and Fe electrodes at various current intensities. Nitrate is a stable and readily soluble nitrogen species with low tendency for being co-precipitated or adsorbed [Yehya et al., 2014]. As shown in Fig. 28 and Fig. 4.29, the concentrations of nitrate decreased substantially. For Al-Al electrodes, nitrate was removed from 85.5% at 1 mA/cm^2 to

99% at 10 mA/cm^2, which is significantly higher than 60.5% to 81.5% for Fe-Fe electrodes at the same current intensities. On the other hand, ammonium concentrations greatly increased in the reactors, from 0 to 31.3 mg/L - 38.1 mg/L for Al-Al electrodes or 21.9 mg/L - 30.4 mg/L for Fe-Fe electrodes over three hours of experimental runs. In all cases, small amount of nitrite was identified during the first one and a half hour though it disappeared at the end. Sum of nitrate, nitrite and ammonium concentrations at any time point for both Al and Fe electrodes account for over 88.75% of the total nitrogen of 40 mg/L originally contained in nitrate, suggesting that under the experimental conditions in this study, nitrate was almost chemometrically converted into ammonium with negligible amount of other nitrogen species.
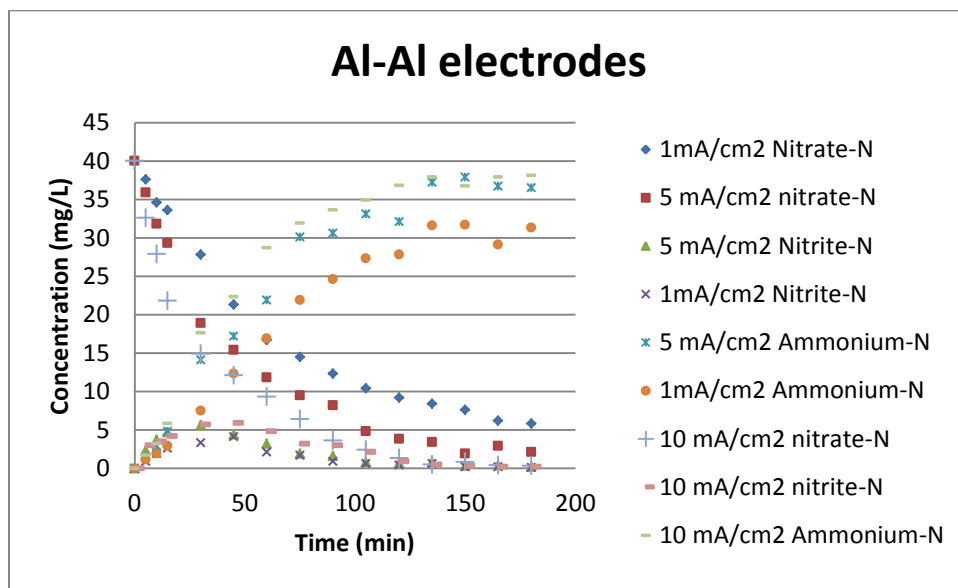
Fig. 4.28 Concentration profiles of nitrate, nitrite and ammonium for Al-Al electrodes
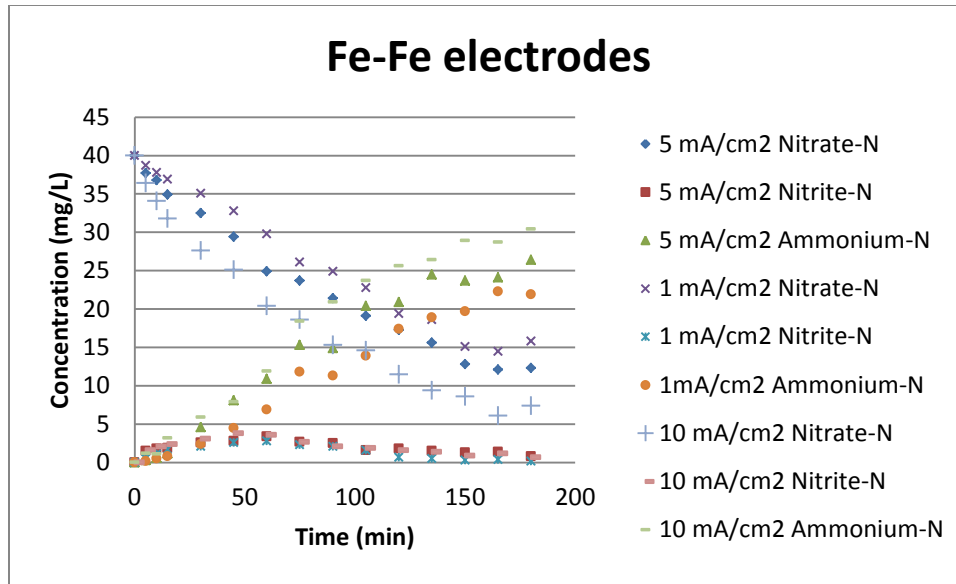
Fig. 4.29 Concentration profiles of nitrate, nitrite and ammonium for Fe-Fe electrodes

Fig. 4.30 displays the effect of electrode materials and electric current density on ammonium yield. It is noted that at any current intensity, Al electrode generated more ammonium from nitrate than Fe electrode, ranging from 19.25% to 23.5%. This is because thermodynamically aluminium is more active than iron and thus it is a stronger reductant, as indicated by their standard reduction potentials of 1.66 V vs. 0.44 V. This result is in agreement with the previous work on water turbidity removal by electrocoagulation [Rahmani et al., 2008], but in contradiction to the conclusion drawn by Malakootian et al. [2011] who stated that iron electrodes are more efficient in nitrate removal than aluminum electrodes due to high density of iron hydroxide ions. The observational inconsistency may be attributed to differences in experimental conditions, especially in the initial DOs, since the surface oxides on both metals were removed from the electrodes prior to use by acidic dissolution, eliminating the difference in the electron releasing efficiency due to oxide barriers. Fig. 4.30 also shows that greater current intensity leads to higher ammonium yield for both aluminium and iron electrodes, which agrees

169

with a previous study [Polatides et al., 2005]. Similar electrochemical reduction profiles of nitrate have also been reported on other electrode materials such as Fe [Scott, 1985; Katsounaros et al., 2006], Pb [Bockris et al., 1997], and Cu [Bouzek et al, 2001; Polatides et al., 2005].
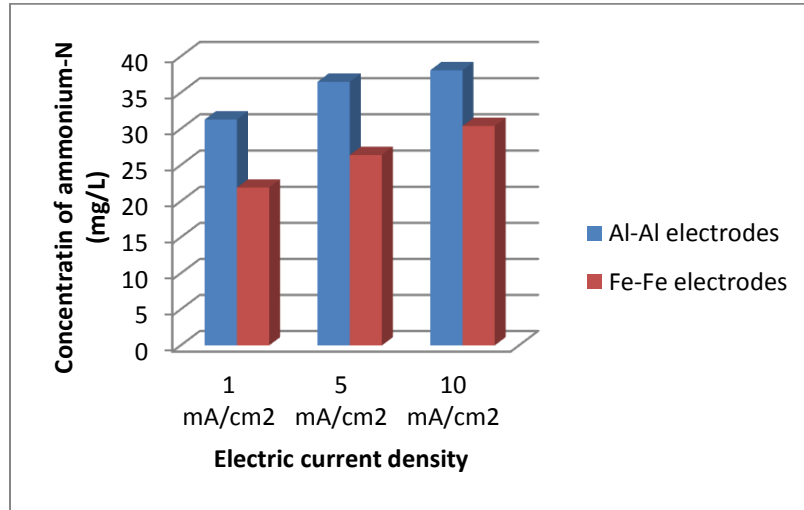
Fig. 4.30 Effect of electrode materials and electric current density on ammonium yield

Previous studies [Wei et al., 2012; Hasan et al., 2014] have shown that pH will increase in the vicinity of cathode and decrease in the vicinity of anode as hydroxyl ions are released according to Equation (4-36) and hydrogen ions are hydrolytically generated based on Equations (4-37 – 4-39) in synthetic wastewater without buffering capacity. As shown in Fig. 4.31, the net effect of pH variation in bulk solution is 1- 3 units upward, whereas pH in the AS mixed liquor ranged from 7.3 to 7.9, mostly centred around 7.5.
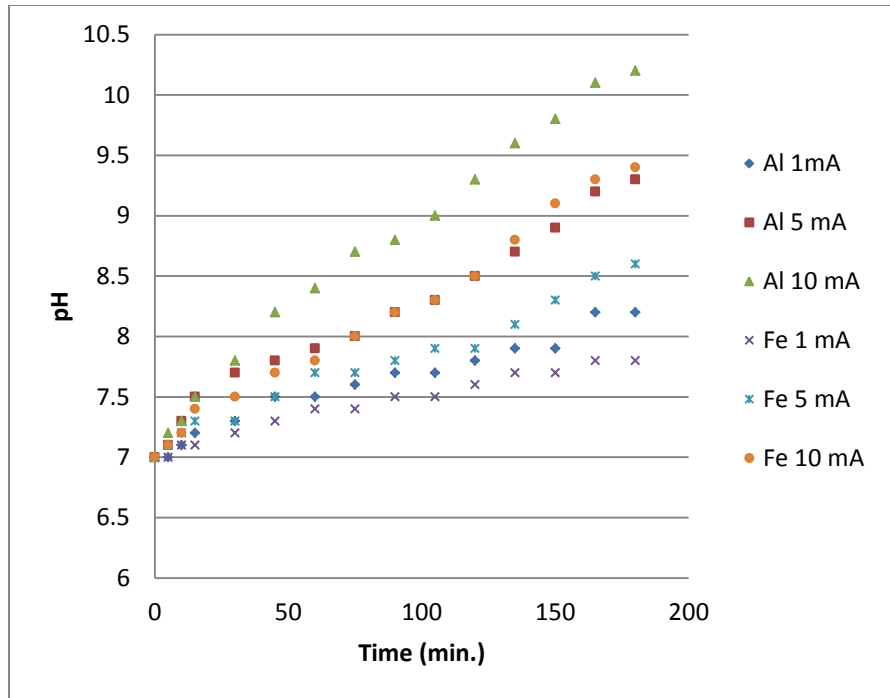
Fig. 4.31 pH changes over time at various current densities

When AS mixed liquor was subjected to a fixed current density of 5 mA/cm^2, the concentration variations of nitrate, nitrite and ammonium are presented in Fig. 4.32. For both aluminum and iron electrodes the rates of nitrate declining and ammonium increasing are significantly lower than those in the synthetic wastewater. At the end of experimental runs ammonium concentrations are only 38.9% (Al-Al electrodes) and 42.8% (Fe-Fe electrodes) of those of the synthetic wastewater at the same current density. The factors contributing to lower ammonium yield in the AS mixed liquor may include:
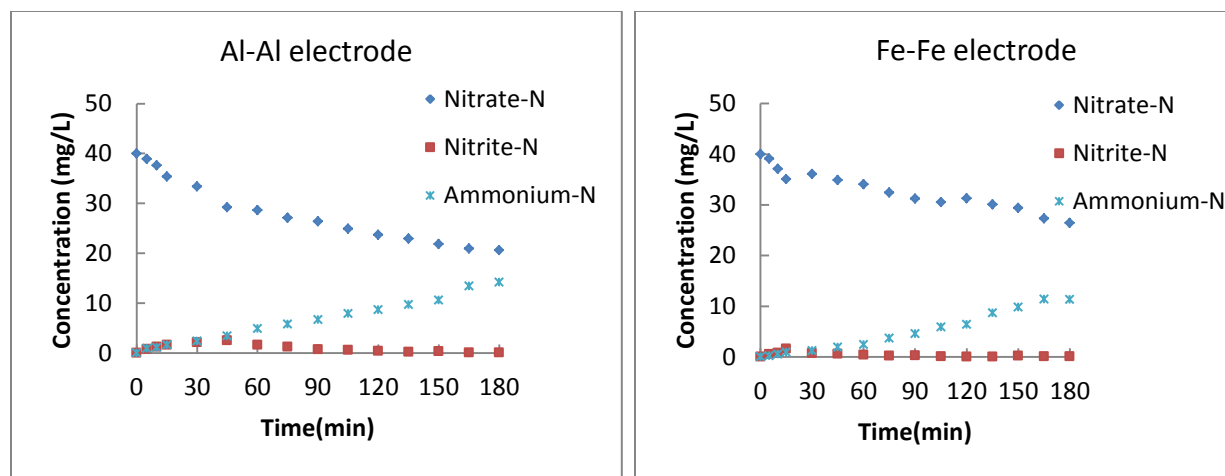
Fig. 4.32 Concentration profiles of nitrate, nitrite and ammonium

in the AS mixed liquor (current density: 5 mA/cm^2)

(A) Lower mass transport and electron transfer efficiency. Mass transport and electron transfer are critical steps in defining the electrochemical reaction rate. According to the Frumkin's theory of slow discharge [Frumkin, 1933], as a Group II anion, nitrate is reduced by receiving one electron from cathode and one proton from donors such as H_2O or H_3O^+. In electrochemical reactions, nitrate ions must travel toward the cathode surface from the bulk solution and the generated ammonium ions need to leave the cathode to the bulk by diffusion. TSS in the AS mixed liquor tends to lower the diffusion efficiencies of nitrate and ammonium toward and away from the cathode. Similarly, the electron jump between the metal cathode and liquid phase is also affected, resulting in reduced electron transfer efficiency.

(B) Influence of Cl$^-$. It has been reported that Cl$^-$ assists in removal of nitrate and ammonium following Equations (4.40 - 4.43) [Li et al., 2009; Huang et al., 2013 and Hossini et al., 2014]:

$$2Cl^-(aq) - 2e^- \rightarrow Cl_2 (g) \tag{4.40}$$

$$Cl_2(g) + 2H_2O(l) \rightarrow HClO (aq) + H_3O^+(aq) + Cl^-(aq) \tag{4.41}$$

172

$$2HClO \text{ (aq)} + 2NH_3(aq) \rightarrow N_2(g) + 2HCl(aq) + 2H_2O(l) \qquad (4.42)$$

$$NH_3(aq) + 4HClO \text{ (aq)} \rightarrow NO_3^- \text{ (aq)} + 5H^+(aq) + 4Cl^-(aq) + H_2O(l) \qquad (4.43)$$
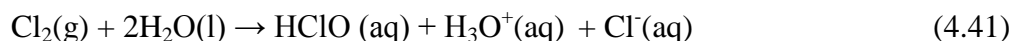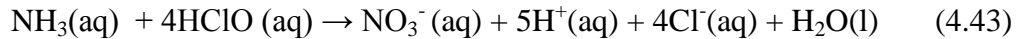
Cl^- is reduced to chlorine which is then converted into a strong oxidant hypochlorite; the latter may further react with ammonium and generate nitrogen gas or nitrate. In the AS mixed liquor the concentration of Cl^- was determined to be 57 mg/L, though it is significantly lower than the dosed 607 mg Cl^-/L [Hossini et al., 2014] or 304 mg Cl^-/L [Li et al., 2009], the ammonium breakdown effect is still expected.

The effect of electrochemical reduction of nitrate is usually ignored, especially in studies aiming at isolated parameters such as electric stimulation on bacterial activity, electrocoagulation and electrofiltration enhancement etc. For example, in an electric stimulation study by Zaveri et al. [2002], a moderate current of 300 mA was applied, as DO in the reactor was below 1 mg/L and no aeration was supplied for the entire experimental run. The ammonia in the reactor was found higher than in the influent, which was simply caused by electrochemical reduction, as shown in this study. It was then inappropriately concluded that the electro stimulation of nitrification activity was minimal. In fact, nitrate in the feed should be excluded to eliminate generation of ammonia due to the afore-mentioned electric ammonification effect.

4.9.2 The kinetics of ammonium and nitrite production in electrolytic fluids of synthetic water and activated sludge

Equation 4.44 represents the possible cathodic reduction reactions of nitrate. Previous experimental results [Emamjomeh et al., 2005; El-Shazly, 2011; Yehya et al., 2014] and this study have revealed that the yield of nitrogen gas is negligible when aluminium and iron are used as the electrode materials. Therefore, under the electrocoagulation conditions the kinetics of nitrate reduction can be described as a two-step successive process with nitrite being the intermediate and ammonia being the final product:

$$NO_3 \xrightarrow{k_1} NO_2 \xrightarrow{k_2} NH_4^+ \quad\quad (4.44)$$
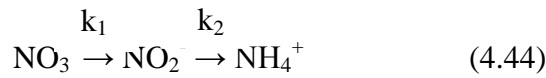
The reaction rates of nitrate, nitrite and ammonium in the system can be presented as the following:

$$\frac{d[NO_3^-]}{dt} = -k_1 [NO_3^-] \quad\quad\quad (4.45)$$

$$\frac{d[NO_2^-]}{dt} = k_1 [NO_3^-] - k_2[NO_2^-] \quad\quad\quad (4.46)$$

$$\frac{d[NH_4^+]}{dt} = k_2 [NO_2^-] \quad\quad\quad (4.47)$$

The solutions to the above equations using Laplace transform are [Katsounaros et al., 2006]:

$$[NO_3^-] = [NO_3^-]_0 * e^{-k1 *t} \quad\quad\quad (4.48)$$

$$[NO_2^-] = k_1*[NO_3^-]_0 * \frac{e^{-k_2 t}-e^{-k1 t}}{k_1-k_2} \quad\quad\quad (4.49)$$

$$[NH_4^+] = [NO_3^-]_0 *[1 + \frac{k_1 e^{-k_2 t}-k_2 e^{-k1 t}}{k_2+k_1}] \quad\quad\quad (4.50)$$
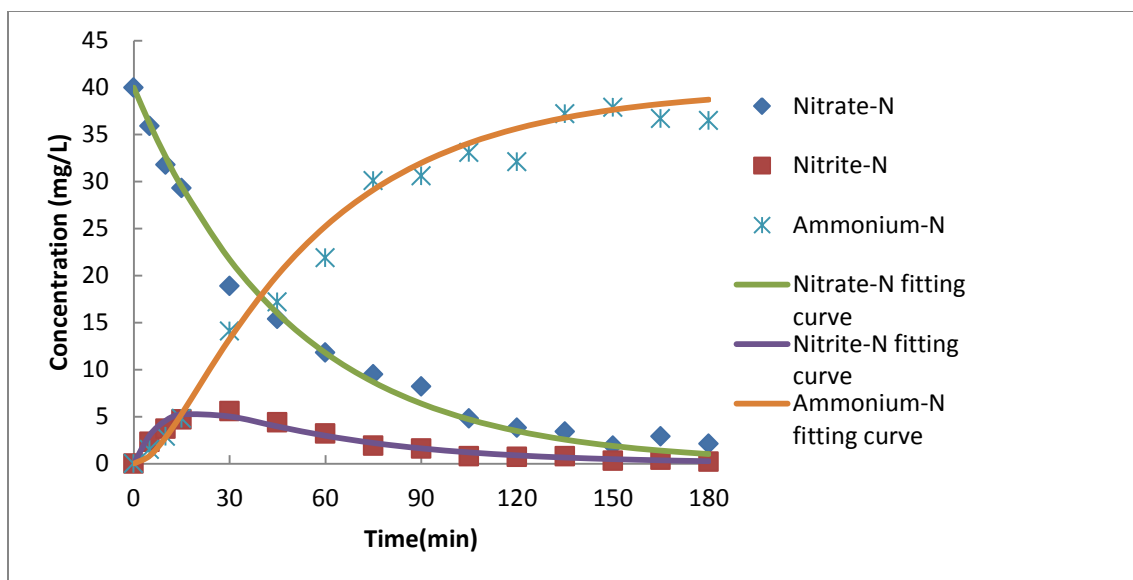
Fig. 4.33 First-order kinetics of nitrate reduction on Al cathode
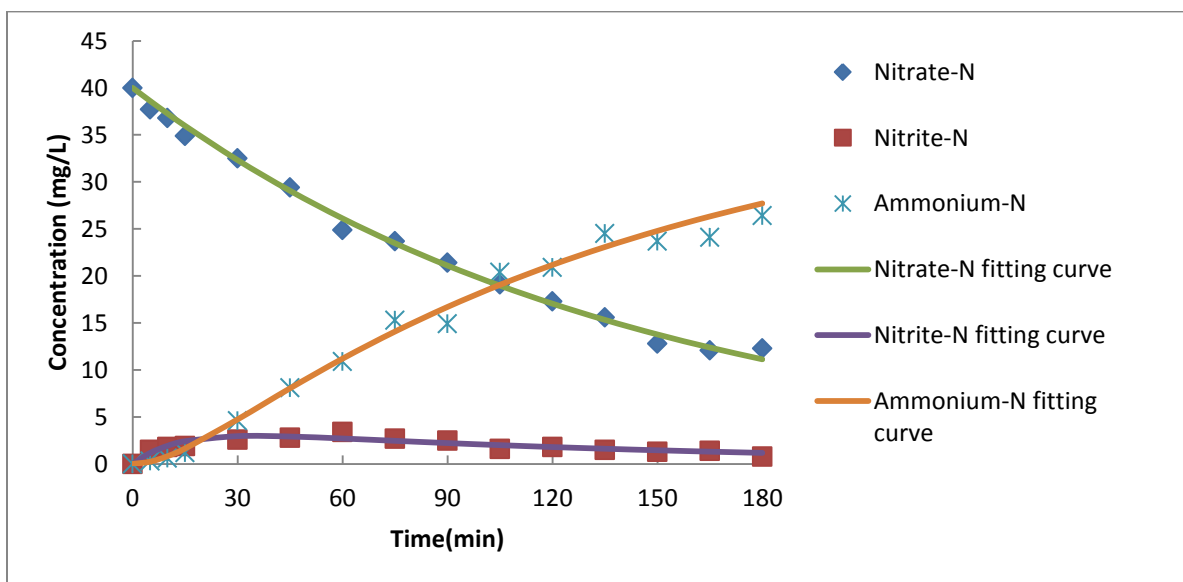
Fig. 4.34 First-order kinetics of nitrate reduction on Fe cathode

Table 4.5 First-order kinetic constants of nitrate reduction

Electrodes		Current intensity (mA/ cm^2)	K_1 (min$^{-1)}$)	K_2 (min$^{-1)}$)	Reference
Anode	Cathode				
Ti/IrO$_2$–Pt	Fe	20	1.7×10^{-2}	0.637	[Li et al. 2010]

175

Platinized Pt foil	Sn85Cu15	(2.0 V)	2.94×10^{-2}	1.05×10^{-3}	[Polatides et al., 2005]
Boron-doped diamond	Boron-doped diamond	40	4.62×10^{-3}	2.1	[Pérez et al., 2012]
Al	Al	(10 – 50 mA)	3.75×10^{-4} - 1.63×10^{-3}	1.83×10^{-3} - 5.15×10^{-3}	[Desai, 2010]
Platinized Pt foil	Tin	(2.5 V)	0.059	0.089	[Katsounaros et al., 2006]
Al	Al	5	0.02038	0.1006	This study
Fe	Fe	5	0.00711	0.07472	

The rate constants in Formula (14) are obtained by fitting the experimental data to Equations (18) – (20) using MATLAB:

For Al cathode: k_1 = 0.02038 with 95% confidence bounds (0.01906, 0.02171),

k_2 = 0.1006 with 95% confidence bounds (0.09073, 0.1104)

For Fe cathode:

k1 = 0.00711 with 95% confidence bounds (0.006871, 0.007349)

k2 = 0.07472 with 95% confidence bounds (0.06752, 0.08193)

As the key intermediate, nitrite is highly unstable and can be either oxidized to oxidation states +4 (NO_2^-) and +5 (NO_3^-) or reduced to oxidation states as low as -3 (NH_4^+). In the widely accepted two-step nitrate reduction mechanism [Scott, 1985; Katsounaros et al., 2006], the kinetic constant k_2 of Stage Two was found to be 5 (Al cathode) or 10 times (Fe cathode) of the kinetic constant k_1 of Stage One, suggesting nitrate reduction to nitrite is the rate limiting step. This is in agreement with the observations by some other researchers [Hansen et al., 1996; Li et al. 2010 and Pérez et al. 2012]. That explains why the amount of NO_2^- present is usually low.

However, the magnitudes of k_1 and k_2 is highly dependent on a number of electrolytic conditions, which are reflected by the difference of a few orders of magnitudes in the determined k_1 and k_2 values, as presented in Table 4.5, in which the ratios of k_2 to k_1 range from 0.4 [Polatides et al., 2005] to 455[Pérez et al., 2012]. Apart from the direct electro reduction mechanism, the other physiochemical interaction may also be involved in the kinetic process. For example, recently adsorption of ammonium by aluminum hydroxide was proven to follow the initial electro-reduction of nitrate into ammonium in the abiotic denitrification mechanism using a simple isothermal adsorption model [Yehya et al., 2014].

4.9.3 Inhibition of ammonification from electrochemical reduction of nitrate

Electrokinetic technologies including electrocoagulation are increasingly applied in wastewater treatment. However, as presented in the prior work and this investigation, toxic ammonia is usually the dominant by-product, which requires secondary treatment by physical or chemical means such as air stripping and chemical oxidation [Meyer et al., 2005]. The yield of ammonium is greatly affected by electrode material, current intensity, pH, chloride and temperature [Reyter et al., 2006; Li et al., 2009; Pérez et al., 2012].

The final part of this research is to seek a simple but efficient approach to suppress or prevent the abiotic ammonification by controlling the oxidation-reduction environment in the electrolytic fluid by DO management.

Oxidation-reduction potential (ORP) is a measure of an aqueous system's ability to gain electrons (being reduced) or donate electrons (being oxidized) [Okey et al., 1961; Kishida et al.,

2003]. ORP of a solution is dependent upon its oxidation and reduction agents. For a particular

oxidation reduction reaction, it can be expressed as the following formula [Lie et al., 1994]:

$$ORP = E^0 + \frac{RT}{nF}\log(\frac{A_{ox}}{A_{re}})$$
(4.51)

Where

E^0 = standard potential of a specific oxidation reduction reaction

R = gas constant

T = absolute temperature

n = number of electrons involving in a oxidation reduction reaction

F = Faraday constant

A_{ox} = activity of the oxidizing agent

A_{re} = activity of the reducing agent

In a complicated electrolytic system with multiple oxidizing and reducing agents, the above ORP

is a collective indicator for the electrochemical environment. Positive ORP suggests the tendency

to accept electrons and thus an oxidative environment, whereas negative ORP implies the ability

to donate electrons or a reductive environment. All of the important biological processes such as

nitrification, denitrification and cBOD and biological phosphorus removal involved in

wastewater treatment are oxidation-reduction reactions [Koch et al. 1985; Ghusain et al., 1995;

Fuerhacker et al., 2000]. Therefore, ORP has been chosen as a parameter for monitoring and

controlling various nutrient removal processes [Kjaergaard et al., 1977; Charpentier et al., 1987;

Lo et al., 1994; Li et al., 2001]. ORP is known to be positively associated to DO concentration in

aqueous solution [Okey et al., 1961; Lo et al., 1994; Li et al., 2001] when DO is above 0.1

mg/L[Myers et al., 2006]. Thus in biological nutrient removal systems ORP is typically

controlled by adjusting DO concentration through manipulating aeration intensity. Fig. 4.35 shows the correlation between ORP and DO in synthetic wastewater and AS mixed liquor during electrolysis with Al or Fe electrodes. It should be noted that: (1) as DO in the electrolytic fluid increased from 0 to 2, ORP correspondingly went up from -220 mV to 265 mV (Al electrode) or from -175 mV to 342 mV (Fe electrode) for the synthetic wastewater, and from -124 mV to 332 mV (Al electrode) or from -76 mV to 425 mV (Al electrode) for the AS mixed liquor, respectively; (2) at the same DO level, ORP in the synthetic wastewater is lower than that in the AS mixed liquor, which may be attributed to the presence of some other oxidizing species in the latter; (3). at the same DO level, ORP with Al electrode is slightly lower than that with Fe electrode, which is the result of two conflicting ORP influencing factors: the reducing environment generated by the more active Al element outperformed that created by conversion from ferrous into ferric ions, which was observed recently [Ciblak et al., 2012].
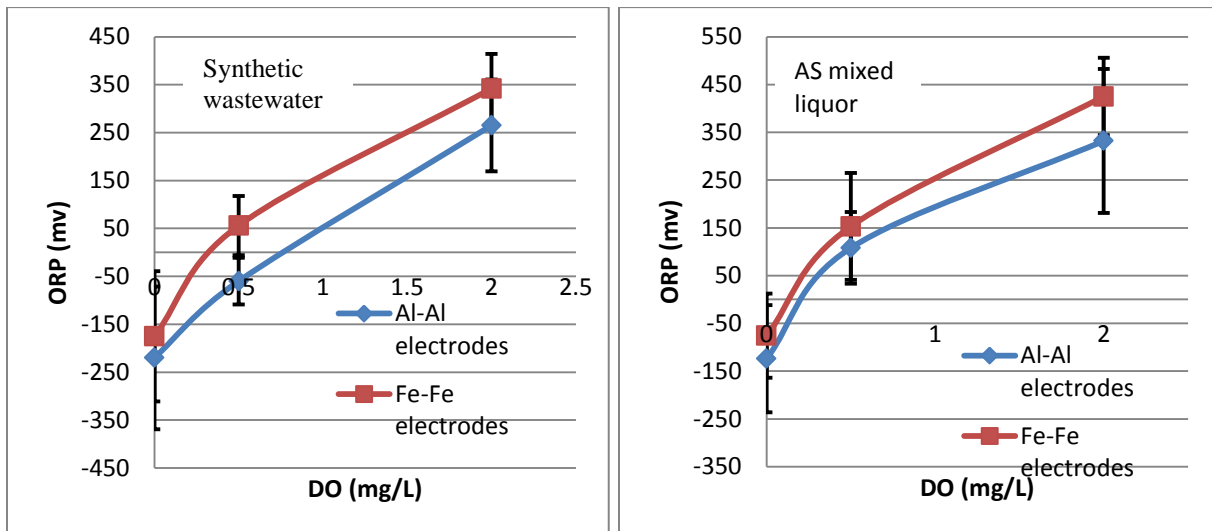
Fig. 4.35 DO and ORP in the electrolytic fluids

Figures 4.36 - 4.39 display the concentrations of nitrate, nitrite and ammonium in the synthetic wastewater and AS mixed liquor with Al and Fe electrodes at the current density of 5 mA/cm^2.

The concentrations of nitrate and ammonium at the end of experimental runs are presented in Table 4.6. Compared to nearly complete reduction from nitrate to ammonium when DO = 0 mg/L, the ammonium yields decreased substantially with 0.5 mg/L of DO, ranging from 7.25% to 24.5% of the initial nitrate-N. With 2 mg/L of DO, for both Al and Fe electrodes the amount of ammonium produced is negligible and nitrate remained unchanged in the aqueous media. The equivalent minimum ORP to completely suppress ammonium generation is 265 mV, which is generally in agreement with the favourable ORP range of 220 mV to -375 mV for denitrification and nitrate reduction [Hossini et al., 2014]. Biological denitrification requires a reducing aqueous environment and occurs at ORP in the range of -100 mV (Zehnder and Stumm, 1988) to + 100 mV [Zhao et al., 1999; Dabkowski et al., 2008]. Dissolved oxygen supercedes nitrate as an electron acceptor until ORP drops to around +100 mV when nitrate becomes the preferred electron acceptor. As a result, DO adversely impacts biological denitrification, for example, a DO concentration as low as 0.2 mg/L may reduce denitrification rates by 50-90% [Metcalf and Eddy, 2003].

Table 4.6 Concentrations of nitrate and ammonium after three hours of electric application

DO (mg/L)	Electrode	Synthetic wastewater		AS mixed liquor	
		NO_3^-(mg/L)	NH_4^+(mg/L)	NO_3^-(mg/L)	NH_4^+(mg/L)
0.5	Al	28.2	9.8	35.6	3.9
	Fe	31.8	7.1	37.5	2.9
2.0	Al	38.9	0.4	39.1	0.2
	Fe	39.8	0.3	39.6	0.1
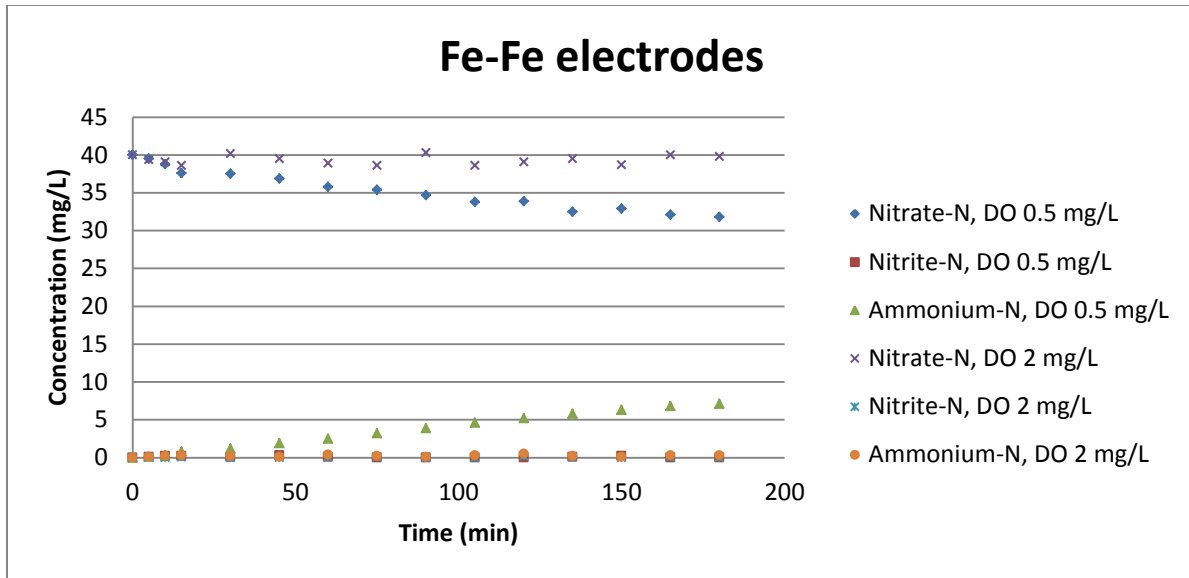
Fig. 4.36 Concentration profiles of nitrate, nitrite and ammonium in the synthetic wastewater

(Fe-Fe electrode, current density: 5 mA/cm^2)
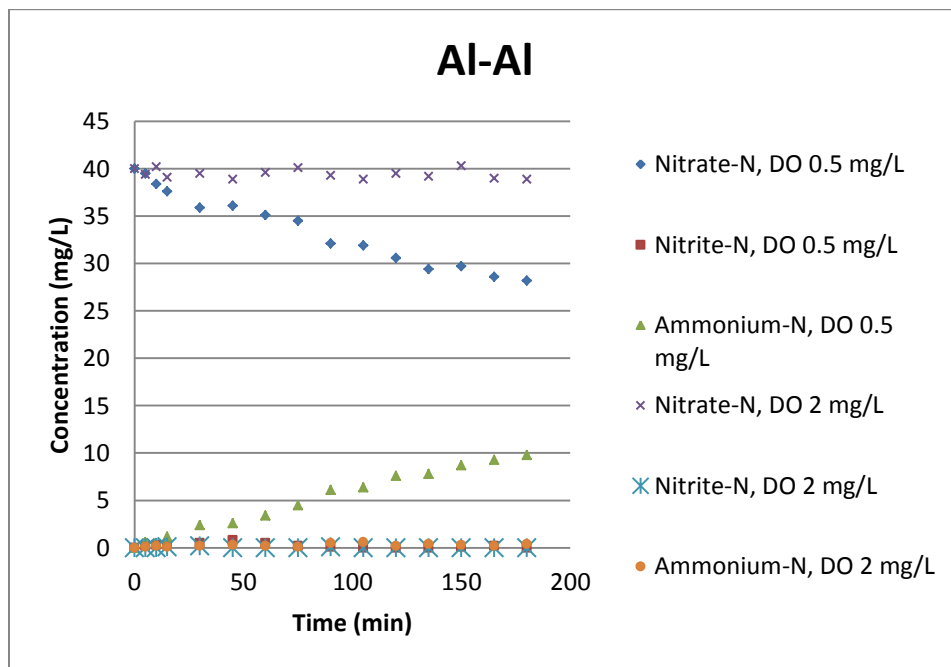
Fig. 4.37 Concentration profiles of nitrate, nitrite and ammonium in the synthetic wastewater

(Al-Al electrode, current density: 5 mA/cm^2)
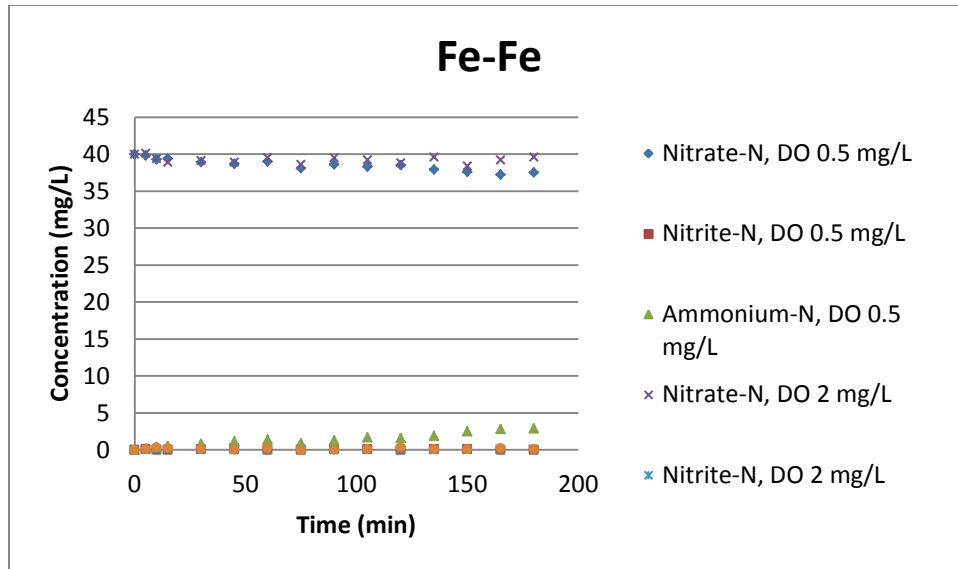
Fig. 4.38 Concentration profiles of nitrate, nitrite and ammonium in the AS mixed liquor

(Fe-Fe electrode, current density: 5 mA/cm^2)
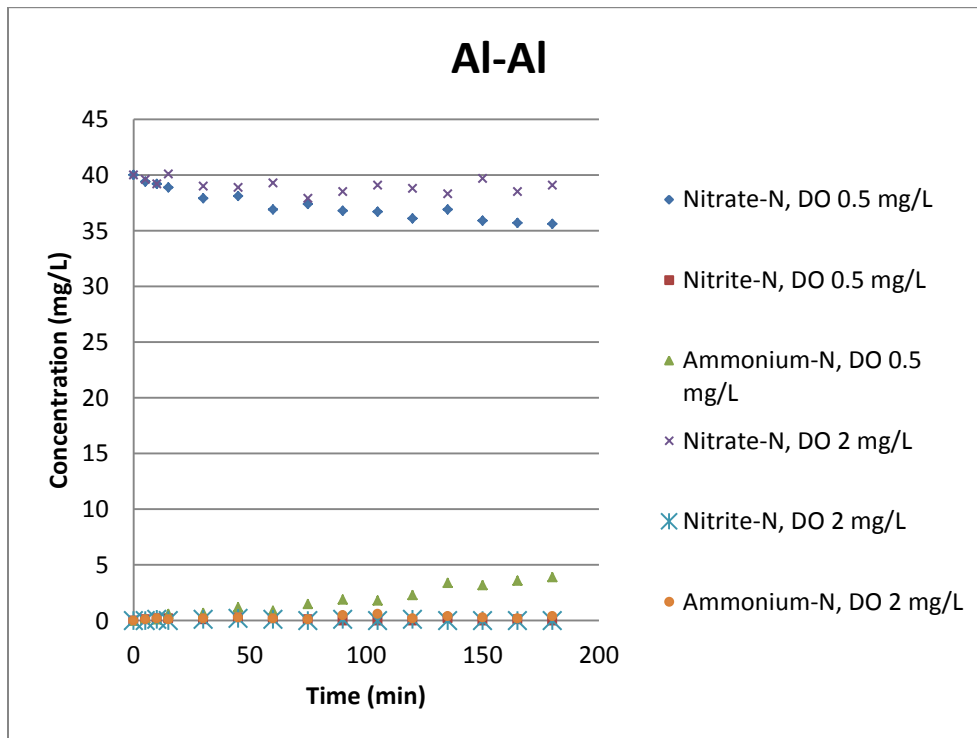
Fig. 4.39 Concentration profiles of nitrate, nitrite and ammonium in the AS mixed liquor

(Al-Al electrode, current density: 5 mA/cm^2)

That oxygen supersedes nitrate in electron capturing ability can be explained by their thermodynamics:

$$\tfrac{1}{2}O_2 + 2H^+ + 2e^- \rightarrow H_2O \qquad\qquad E^0 = 0.816 \text{ V} \qquad (4.51)$$

$$NO_3^- + 10H^+ + 8e^- \rightarrow NH_4^+ + 3H_2O \qquad E^0 = 0.36 \text{ V} \qquad (4.52)$$
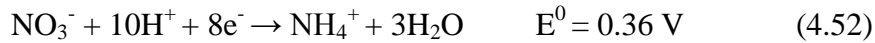
O_2 is a stronger oxidant than nitrate and is more readily reduced than nitrate. In other words, nitrate reduction can only occur after O_2 is depleted, which directly leads to inhibition of biological or abiotic denitrification under aerobic conditions. Therefore, maintaining DO at a certain level in the aqueous media treated by electrokinetic technologies such as electrocoagulation can be used as a simple but efficient approach to prevent electrochemical reduction of nitrate into more detrimental ammonium.

If DO in the electrolytic reactors is not controlled, as indicated in Fig. 4.40, DO in both synthetic wastewater and AS mixed liquor will be depleted within an hour. Rapid electrochemical DO consumption or depletion was also observed previously by Tchamango et al. [2008] and Ricordel et al. [2010], who treated dairy wastewater and surface water using EC, respectively. It is noted that DO with the Fe-Fe electrode decreased faster than that of Al-Al electrode, which can be explained by the fact that oxidation of ferrous ions into ferric ions consumes more oxygen according to Equation (2.21). Accordingly, ORP dropped from about 350 mV to -250 mV, resulting in a favourable environment for electroreduction of nitrate into ammonium [Sorensen, 1978; An et al., 2009; Wei et al., 2012]. Ghernaout et al. [2008] and Linares-Hernandez et al. [2009] proved such an electrochemical reaction by excluding biological denitrification.
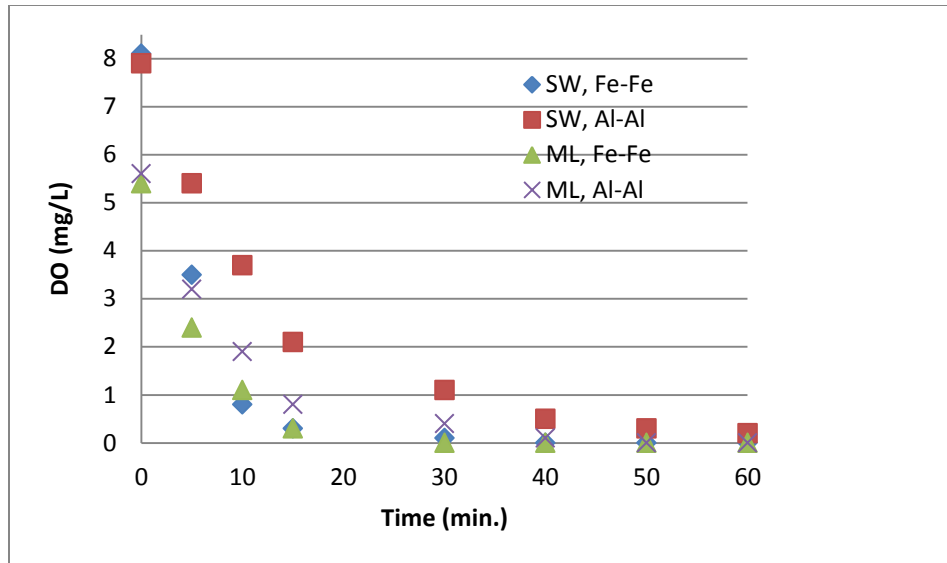
Fig. 4.40 DO depletion profile in the electrolytic reactor (current intensity = 5 mA/cm^2)

4.10 Total COD and nutrient removal in an electrically enhanced MBR

4.10.1 COD removal

Fig. 4.41 shows the COD concentration profiles of the influent, control and EMBR over the experimental period. Both reactors achieved excellent COD removal efficiencies (93.8% for control MBR and 94.3% for EMBR, respectively). Good carbon degradation capabilities of both reactors are documented by the low TOC concentrations in the effluent (10.2 mg/L for control MBR vs. 7.5 mg/L for EMBR, Fig. 4.42). The lower TOC concentration in the EMBR effluent points to the positive effect of electrokinetic enhancement on organics removal.
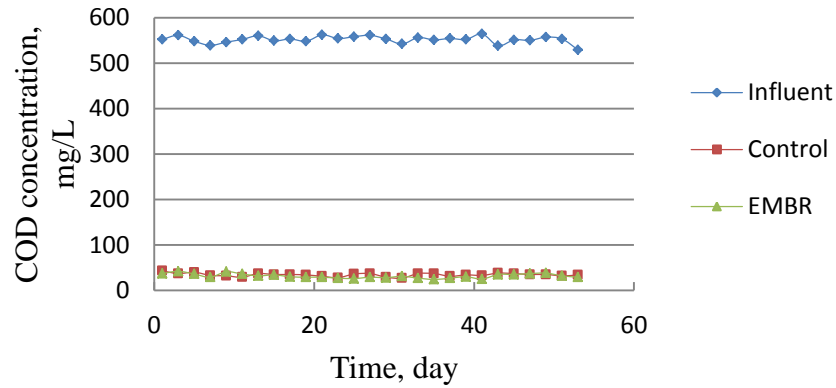
Fig. 4.41 COD concentrations in the influent and effluents of the

control MBR and EMBR
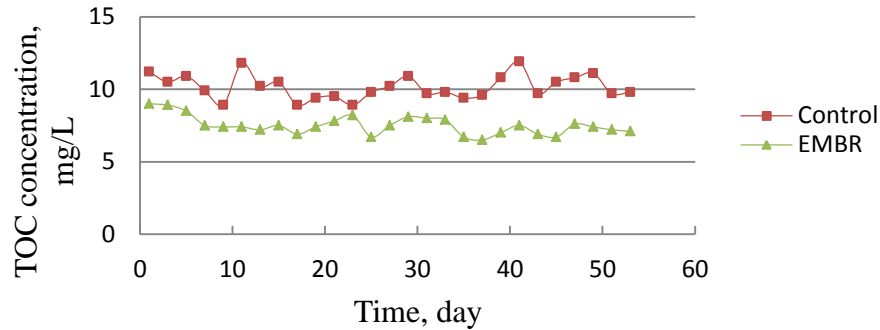
Fig. 4.42 TOC concentrations in the effluents of the control MBR and EMBR

4.10.2 Nitrogen removal

Fig. 4.43 shows almost 100% of ammonium-N removal in both reactors. However, due to foaming, the control MBR experienced some problems between day 39 and 45. Without adding extra carbon source in the denitrification zone, total nitrogen removals were found to be 76.7% and 77% prior to foaming in the control and EMBR (Fig. 4.43). This indicates that the direct current at the tested voltage gradient had no influence on nitrogen removal. Fig. 4.43 and Fig.

4.44 also suggests that the foaming in the control reactor affects both nitrification and denitrification processes. Filamentous bacteria cause sludge bulking in the ASP process and foaming in the MBR system [Meng et al., 2007]. Applications of selectors, coagulants, high DO conditions and alkalinity adjustment are the most common strategies to suppress filamentous bacteria [Pan et al., 2010; Liu et al., 2006]. In EMBR the effect of electrocoagulation and electrochemical supplement of alkalinity are attributed to a foaming-free operation.
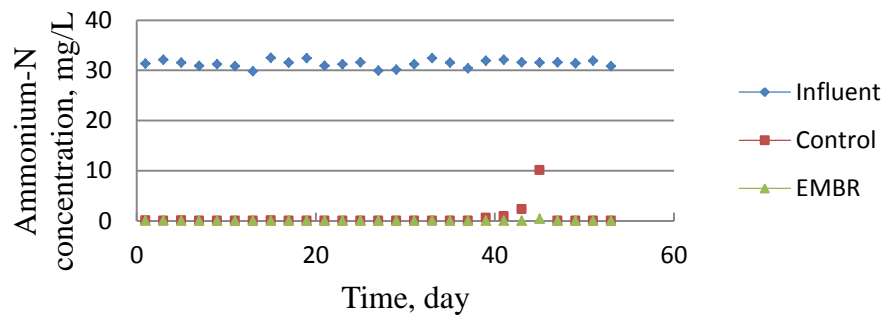
Fig. 4.43 Ammonium-N concentrations in the influent and

effluents of the control MBR and EMBR
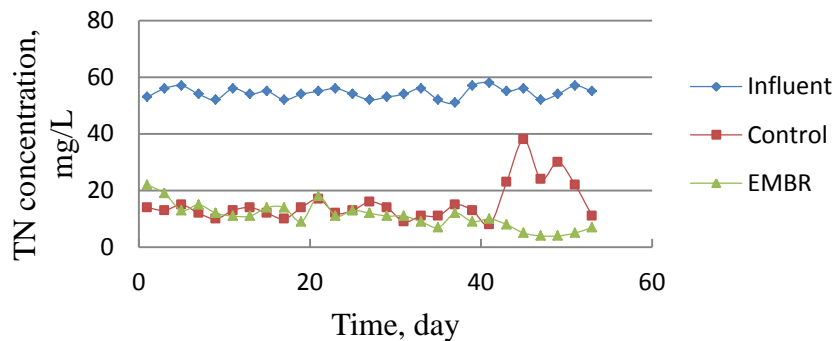
Fig. 4.44 Total nitrogen concentrations in the influent and effluents of

MBR (control) and EMBR

4.10.3 Phosphorus removal

As shown in Fig. 4.45, when the two reactors run in parallel as MBRs, similar Ortho-P removal efficiencies were observed (20.8% and 18.9% respectively). After DC current was applied to the EMBR, immediate drop of Ortho-P concentration in the effluent was seen. The overall Ortho-P removal increased to 86.6%, implying the advantage of EMBR for phosphorus reduction.
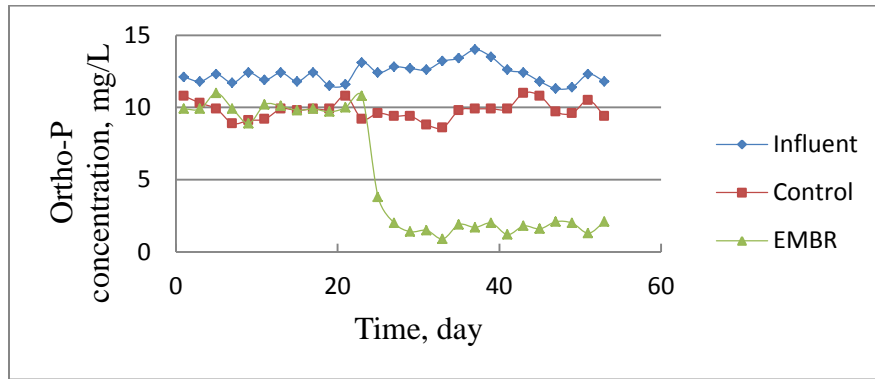
Fig. 4.45 Ortho-P concentrations in the influent and effluents of the control MBR and EMBR (the current was turned on after day 21)

In this experimental set-up, the biomass was forced to pass the electrodes before reaching the membrane surface. At the anode, $Al \rightarrow Al^{3+} + 3e^-$ (eq.1), the freshly generated aluminum ions then entered into the biomass solution where the following reactions occurred:

$$3Al^{3+} + 2PO_4^{3-} + 3H_2O \rightarrow (AlOH)_3(PO_4)_2 + 3H^+ \qquad (4.53)$$

$$Al^{3+} + PO_4^{3-} \rightarrow AlPO_4 \qquad (4.54)$$

$$Al^{3+} + 3H_2O \rightarrow Al(OH)_3 + 3H^+ \qquad (4.55)$$
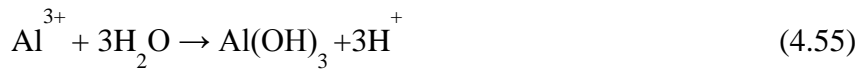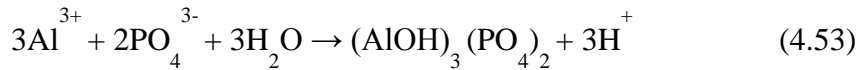
Therefore, PO_4^{3-} was either precipitated into $(AlOH)_3(PO_4)_2$ and $AlPO_4$ or adsorbed by $Al(OH)_3$, a strong adsorption agent produced during the process. At the cathode, the reaction was most

likely $6H_2O + 6e^- \rightarrow 3H_2(g) + 6OH^-$, together with the denitrification process, this assisted in recovering the alkalinity consumed during nitrification.

In EC, chemical reaction and electric charge attraction cause unfavorable precipitates on the electrode surfaces which hinder further electrochemical reactions of the inner metal and increase electric impedance. Though turbulent mixing and periodical reversal of the electric polarity were applied to minimize precipitation, precipitates still accumulated on the electrode surface over time as shown in Fig. 4.45, therefore, in this study the electrodes were manually cleaned daily.
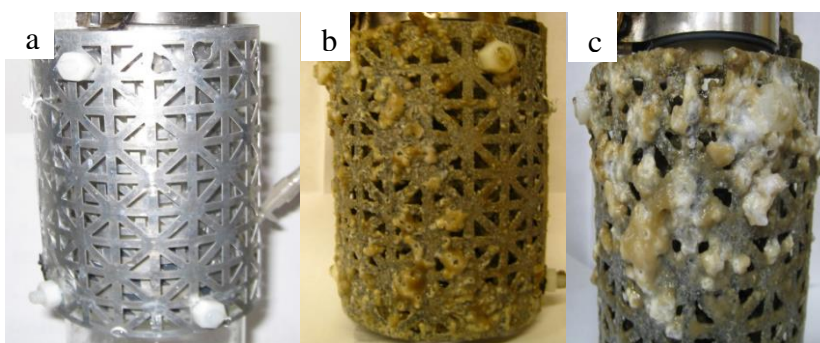
Fig. 4.46 Accumulation of precipitates on the anode (a: new electrode, b and c: precipitates on the anode after 3 days and one week without manual cleaning, respectively)

Direct current plays complex electrochemical roles in an EMBR and may induce simultaneous chemical/biological oxidation and reduction, ionization, hydrolysis, coagulation as well as flotation etc., which remain to be explored in depth. In this research, the current was found to be capable of achieving excellent phosphorus removal, even at power consumption as low as 0.22 kWh/m^3 with synthetic feed. The effect of current on membrane fouling needs to be further investigated. During the experimental period, the trans-membrane pressure (TMP) of EMBR was found to be smaller than that of the control during a one week trial but showed slightly greater increasing rate. This was contrary to expectations and could be attributed to the following

factors: (1) the membrane in EMBR was surrounded by the electrodes, which may reduce the turbulence or shear force close to the membrane surface; (2) the electro-coagulated flocs are denser than those in the regular MBR biomass and more shear resistant; (3) the agglomerated particles may be disaggregated by the peristaltic pump used for mixed liquor continuous recycling from the aerobic zone to anoxic zone and (4) in the EMBR, the ratio of VSS to TSS decreased from 90% initially to 63% at the end, this elevated mineral content might negatively affect membrane fouling. As membrane fouling is affected by, among others, the biomass characteristics and the hydrodynamic conditions, optimization of the biological process and the hydraulic design are necessary to better control membrane fouling in the EMBR.

4.11 Membrane fouling mitigation in an electrically enhanced MBR system fed with synthetic wastewater

In this research, biomass from the control MBR reactor was subject to a direct electric intensity of 0.05 A for 24 hours in a batch test and the electron micrographs of biomass are shown in Fig. 4.46. The images under the SEM show a mixture of microorganisms and protozoa with diverse shapes and structures. When no current was applied to the sample, their structures ranged from normal round cells to long rods and filamentous spirochetes. When a current of 0.05A was applied to the sample over a period of 24 hours, the majority of the bacteria was the same shape and had similar structures to those cells that didn't receive the electrical treatment. Thus, after comparing the micrographs of the cells that didn't receive the treatment to those that did over 4, 8, 21 and 24 hours respectively, one can conclude that at this particular current (0.05A), no definitive change in cell shape and structure was observed [Wei et al., 2012].
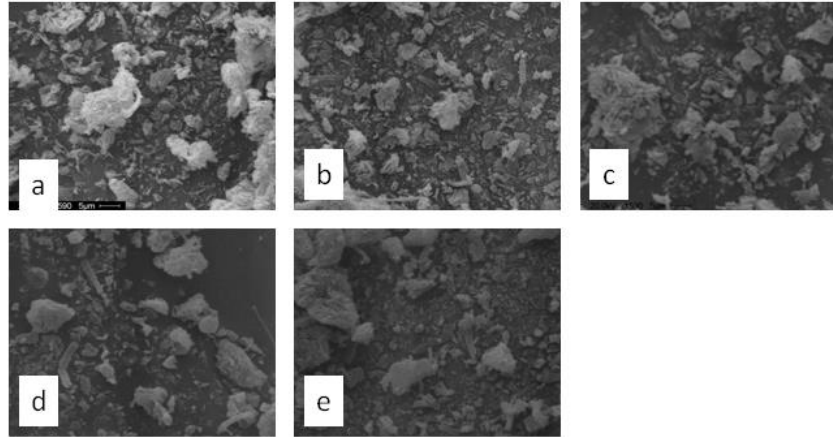
Fig. 4.47 Electron micrographs of biomass subjected to 0.05 A direct electric current

after 0 hour (a), 4 hours (b), 8 hours (c), 21 hours (d) and 24 hours (e).

In this research, the current was found to be capable of achieving significant membrane fouling

reduction. Fig. 4.48 shows that the TMP of EMBR increased considerably more slowly than that

of the control. After the third cleaning cycle, the membrane module in EMBR was kept in

operation until its TMP exceeded the limit of 6 psi. The interval between EMBR's cleaning

cycles was more than twice that of the control, indicating improved filterability of the membrane

in the EMBR system. For the control MBR the TMP profile shows an abrupt jump, but this

phenomenon was not observed in the EMBR system, where the TMP increased steadily to the

limit. The dissolved COD or TOC in the EMBR biomass was reduced from 30% to 51%,

correspondingly, concentrations of the extracellular polymeric substances (EPS), the major

suspected membrane foulant, decreased by 26% to 46% in EMBR. This suggests that speculation

that the memberane fouling was mainly caused by EPS. EPS excreted by microorganisms act as

adhesive to attach the bacterial cells to the membrane surface and provide the nutritional

condition to promote additional microbial growth. In addition, EPS also compromise the fluid

shear forces detaching the biofilm from the membrane [Al-Ahmad et al., 2000], all leading to

membrane fouling [Miyoshi et al., 2009]. In EMBR, the electrochemically generated reactive

190

oxygen species including hydrogen peroxide, ozone, chlorine, and hydroxyl radials are capable

of degrading some of the membrane foulant EPS, and thus hinder formation of the biocake on

the membrane surface [Fu et al., 2010; Modin and Fukushi, 2012; Wang et al., 2013]. This can

be seen seen by Fig. 4.49, showing that the biofilm on the EMBR membrane surface was

significantly suppressed.
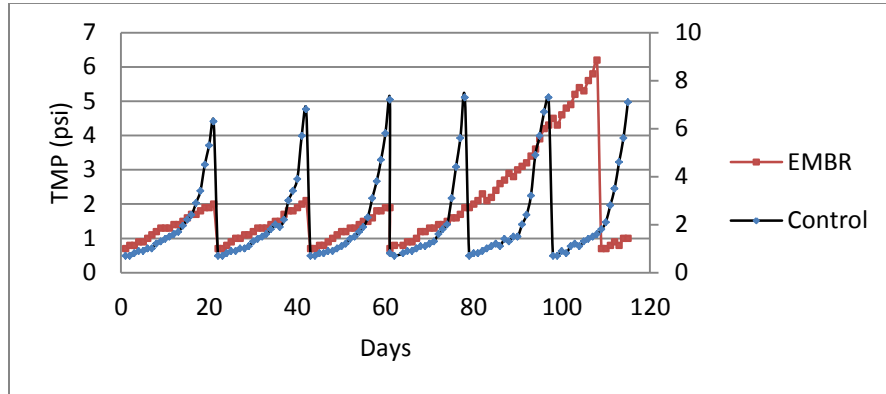
Fig. 4.48 TMP profile (MBR vs. EMBR) with synthetic feed.
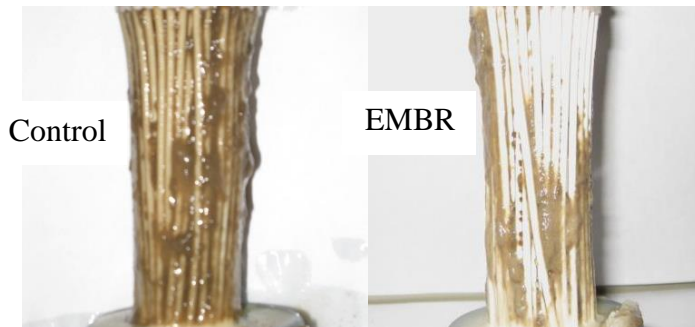
Fig. 4.49 Control and EMBR membranes before chemical cleaning (on Day 61)

Due to precipitation on the surface, the aluminum anode requires daily mechanical cleaning to

eliminate the electric resistance of deposited scale and allow the constantly produced aluminum

ions to disperse into the bulky fluid for electrocoagulation. Fig. 4.50 is the SEM micrograph and

elemental mapping of precipitates on the anode surface on Day 43 and shows the precipitate

contains 38.86% (w/w) of aluminum, 9.63% (w/w) of phosphorus and 35.6% (w/w) of sulphur,

suggesting a substantial portion of the precipitate is aluminum phosphate and a significant

amount of sulphate, the anion with the highest concentration in the fluid, is absorbed into the precipitate. From Fig. 4.51, it is interesting to note that in the accumulated precipitates, the content of elemental aluminum increased from 38.86% (Day 43) to 74.51% (Day 115) but the mass percentage of phosphorus dropped from 9.63% to 0.14% (Day 115). Though Al and Fe electrodes were both used in electrocoagulation, Al is the recommended for better efficiency and produces more stable sludge as ferric ion (III) in $FePO_4$ can be reduced to ferrous ion (II) under low DO conditions in the anoxic or anaerobic process [Bratby et al., 2006; Bagga et al., 2008].
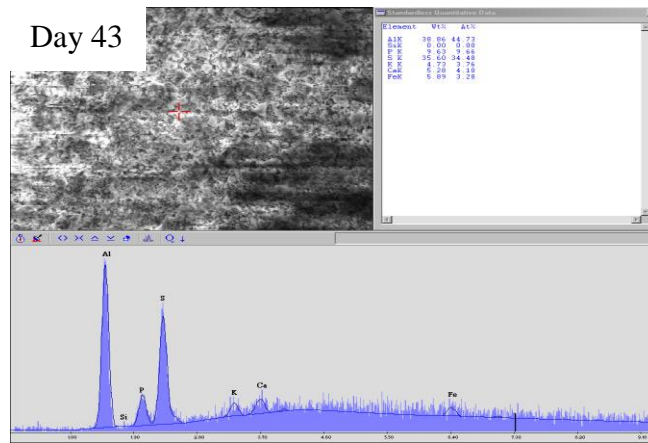
Fig.4.50 SEM micrograph and elemental mapping of precipitates on the anode surface
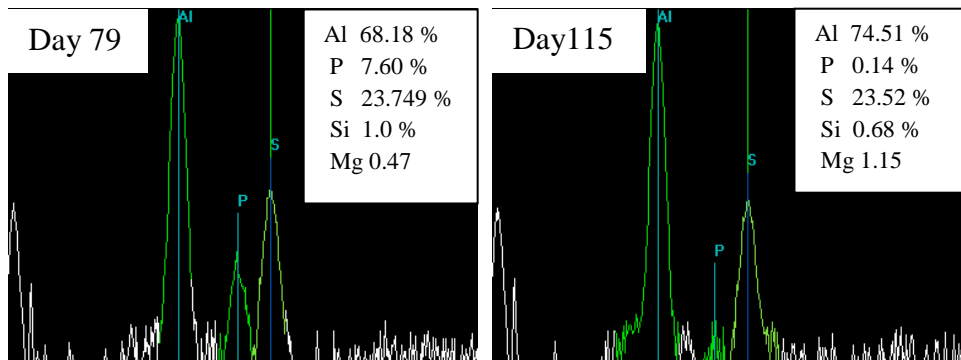
Fig.4.51 SEM micrograph and elemental mapping of precipitates on the anode surface

(Left: Day 79, Right: Day 115)

192

4.12 Membrane fouling retardation in an EMBR system with real municipal wastewater at low temperatures

4.12.1 Quantification of membrane filtration resistances

Membrane fouling can be represented by increasing filtration resistance which causes declining permeate flux under constant pressure mode or rising TMP under constant flux mode. Despite the existence of many filtration models, the resistance-in-series model is selected to evaluate the degree of membrane fouling for its simplicity and suitability for this work. Specifically,

$$R_t = \frac{TMP}{J\mu} \qquad (4.56)$$

$$R_t = R_m + R_p + R_c \qquad (4.57)$$

Where: J - the membrane permeate flux ($m^3/m^2.s$)

TMP - the trans-membrane pressure (Pa),

μ_T - the viscosity of permeate (Pa.s),

R_t - the total filtration resistance (m^{-1}),

R_m - the intrinsic membrane resistance (m^{-1})

R_p - the inner membrane pore blockage resistance (/m) and

R_c - the membrane surface cake layer resistance

The resistance measurement was based on the methodology proposed by Meng et al. (2007) as following:

(1) Rm was determined according to Equation (4.56) based on the flux of reactors and TMP when the new membrane was used to filter deionized water.

(2) R_t was calculated according to Equation (4.56) based on the flux and TMP prior to cleaning.

As the experiments were conducted under four different temperatures, the viscosity of water was

corrected (relative to that at 20 ^{0}C) according to Equation (4.56) :

$$\mu_T = \mu_{20} \cdot e^{-0.0239(T-20)} \qquad (4.58)$$

where T stands for temperature in Celsius.

(3) Whenever the TMP of any membrane module exceeded 50 kPa, both membranes were taken

out of the reactors, the biocake on the membrane surfaces were carefully removed, then the

membranes were thoroughly rinsed with tap water followed by deionized water. The resistance

derived from Equation (4.56) is then considered to be ($R_m + R_p$), therefore, R_c is obtained by

subtracting ($R_m + R_p$) according to Equation (4.57) and finally

(4). R_p is thus the difference between ($R_m + R_p$) and R_m.

To better account for the temperature effect on the MBR flux, a new membrane operating

parameter - specific fouling rate (SFR) was proposed:

$$SFR = dRt/dt = \frac{dTMP}{dt} * \frac{1}{(J*\mu T)} \qquad (4.59)$$

SFR is more accurate for describing the fouling propensity at low temperatures when flux and

viscosity change are taken into account.

4.12.2 Influence of electrokinetics on physical characteristics of mix liquor in EMBR

In electro-technologies, the electric field and electrochemical reactions significantly affect the

sludge characteristics such as dewaterability, settleability and filterability. Sludge volume index

(SVI) is the most widely used parameter to quantify MLSS settleability in the routine wastewater

treatment operations. Daigger et al. (1985) proposed a regression SVI model in which MLSS concentration and temperature are taken in to account:

$$SVI \ (ml/g) = \alpha + \frac{\beta}{MLSS} + \frac{\gamma}{T} + \varepsilon \qquad (4.60)$$

where α, β and γ are regression constants, T is temperature and ε is the random error

Equation (4.60) shows a complex relationship among SVI, MLSS and temperature. In this research, SVIs of MBR (Fig. 4.52) was found higher than that of the conventional ASP system [Chang et al., 1998] with good sludge settleability (SVI ≤ 100 ml/g). SVI displayed a general propensity of increasing as the temperature drops, which is in agreement with previously reported relationship between sludge settleability and temperature [Henry and Salenieks, 1980; Lyko et al., 2008]. However, the EMBR consistently showed superior suspended solid settleability with SVIs around 100 ml/g at all temperatures.
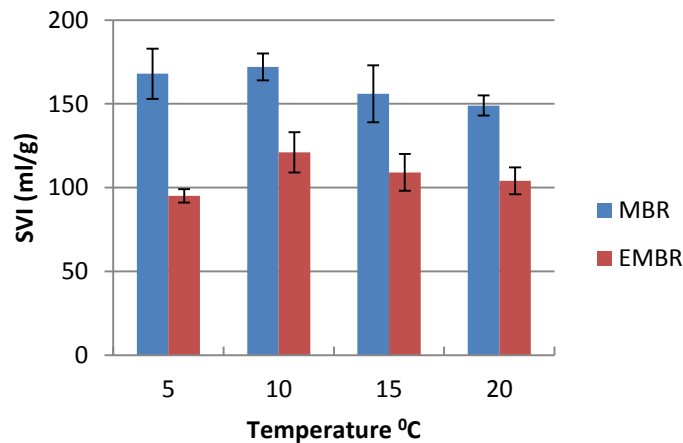
Fig. 4.52 SVI of sludge around membrane at different temperatures
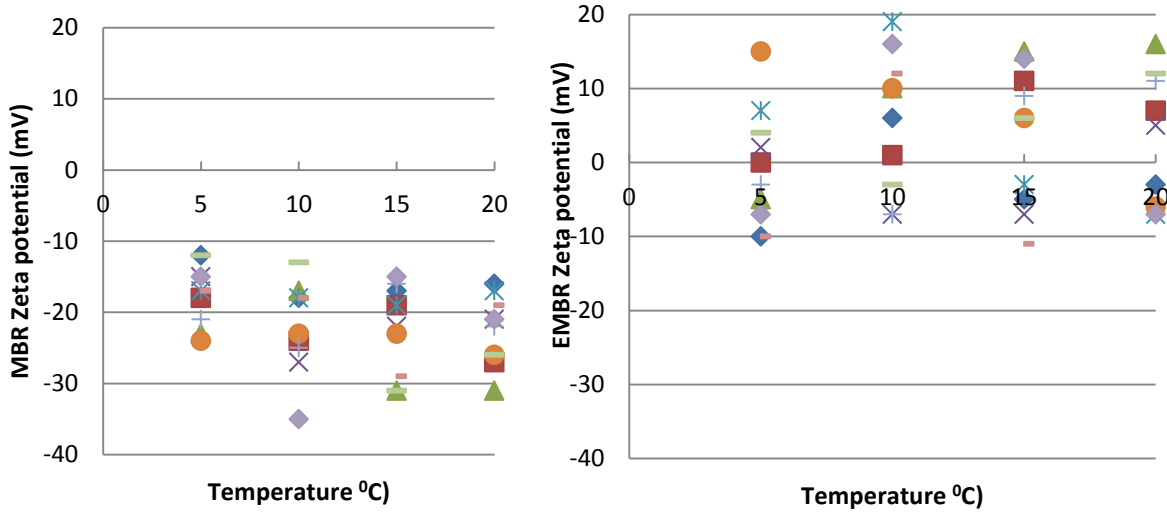
Fig. 4.53 Zeta Potentials in MBR (left) and EMBR (right) at different temperatures

Zeta Potential measures the electrical charge of the colloidal particles in the mixed liquor and can be directly calculated from electrophoretic mobility of flocs. In EMBR, the electrochemically generated ferric ions neutralized the colloid charge and destabilized the colloidal suspension, which can be seen by the upward zeta potential shift from -35 to +20 mV in EMBR, while in MBR to a maximum -12 mV (Fig. 4.53), suggesting the significant charge neutralization effect in EMBR. The electric charge neutralization effect of colloid particles in EMBR is also evidently demonstrated from the electrophoretic mobility of flocs in MBR and EMBR (Fig. 4.54).
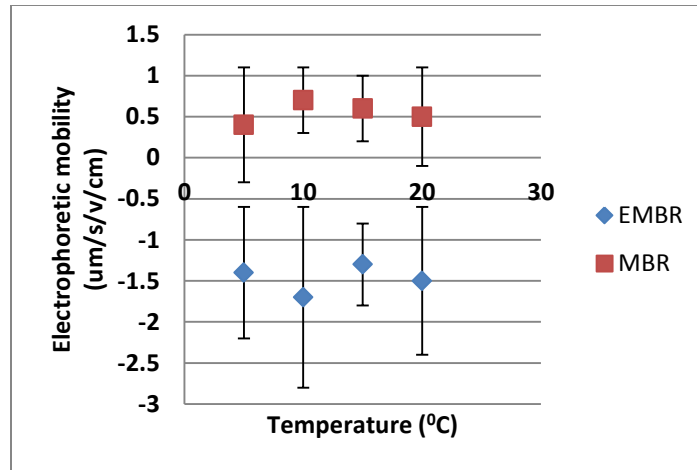
Fig. 4.54 Electrophoretic mobility of flocs in MBR and EMBR at different temperatures

4.12.3 EPS and TEP concentrations in MBR and EMBR

EPS can also assist in microbial adhesion by altering the physicochemical characteristics of the colonized surface and thus enhance cell adhesion, which has been proven to be evident by the biocake formation and accumulation of on the membrane surface in water and wastewater treatment, the interaction of EPS concentration and membrane biofouling layer in dependent on the EPS characteristics, surface charge and morphology of membrane as well as the shear force near the membrane surface [Nguyen et al., 2012]. Tsuneda et al. [2003] reported that the electrostatic interaction dominates attachment of microbes to solid surface at low EPS concentration, however, when EPS level is high it is the polymeric interaction which promotes cell adhesion. Overall, EPS hinder the shear turbulence in vicinity of the membrane surface and enhance concentration polarization, leading to accelerated microbial growth and biofouling. The soluble EPS in the biomass filtrate or soluble microbial products (SMPs) are generally considered as the major foulants, various efforts were undertaken in the recent years to mitigate fouling through reducing SMPs, e.g. adsorption by powdered activated carbon or chemical

197

coagulants. In this study SMP and bound EPS were found to increase in both reactor as the temperature decreased, which are in agreement with the findings of previous lab scale [Barker et al., 1998], pilot scale [Drews et al., 2007] and full scale [Fawehinmi et al., 2004] operations. Fig. 4.55, Fig. 4.56 and Table 4.7 display SMP & bound EPS reduction results for EMBR vs. MBR. In the mixed liquor of EMBR, carbohydrate reduction in SMP was 28.6% to 75% and protein reduction ranged from 58.6% to 70%, however, reduction of bound EPS in EMBR was much lower than SMP, with total EPS decreasing from 1.9% to 22.3%, which can be explained by the complex mechanisms of electrochemical oxidation and physical adsorption by coagulants. Beside the main electrochemical reactions mentioned previously, the following side reactions may also take place simultaneously:
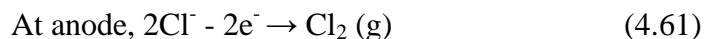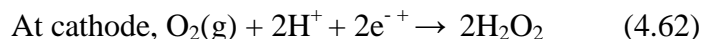
At anode, $2Cl^- - 2e^- \rightarrow Cl_2$ (g) $\qquad$ (4.61)

$E^0 = 1.358$ V (vs. NHE) if there is considerable amount of chloride ions.

At cathode, $O_2(g) + 2H^+ + 2e^{-+} \rightarrow 2H_2O_2$ $\qquad$ (4.62)

$E^0 = 0.695$ V (vs. NHE) if the fluid is acidic.

The above electrochemical reactions suggest potential production of strong oxidants hydrogen peroxide and chlorine or subsequent hypochlorous acid. Furthermore, highly oxidative species such as the hydroxyl radical •OH or free chlorine •Cl may also be generated, which may break down the EPS. As the definition implies, the bound EPS are entrapped in the flocs and much less accessible by the highly oxidative molecules or radicals, therefore, their destruction efficiency might be limited.
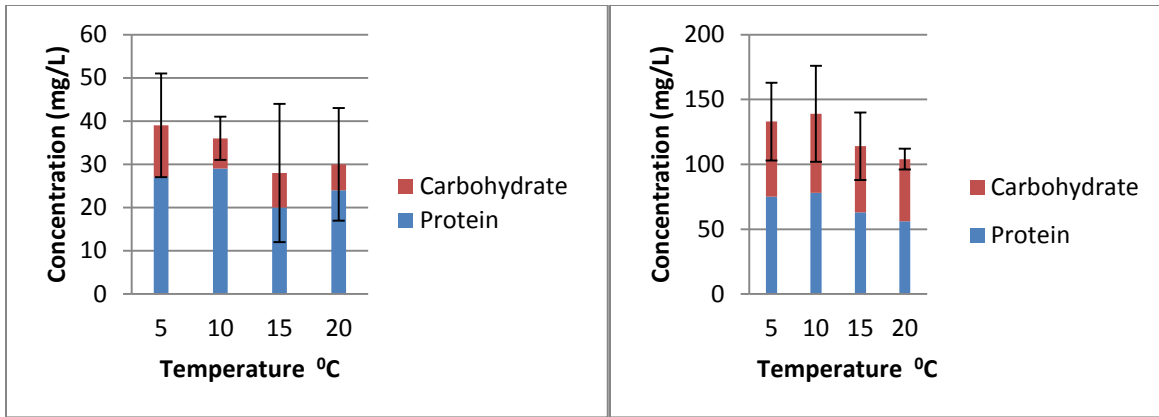
Fig. 4.55 Concentration of SMP (left) and bound EPS (right) in MBR at different temperatures
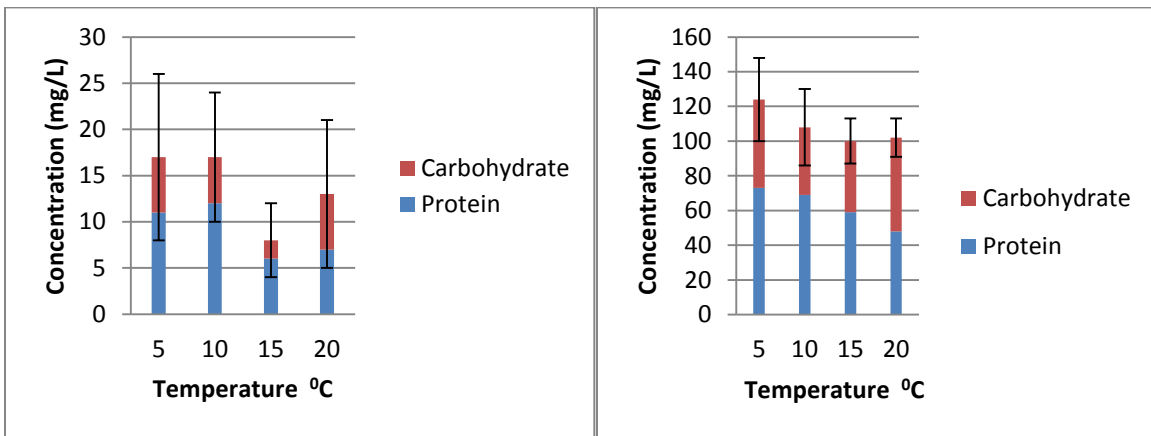
Figure 4.56 Concentration of SMP (left) and bound EPS (right)
in EMBR at different temperatures

Table 4.7 EPS reduction in EMBR comparing to the control MBR

Temperature ^{0}C)	SMP reduction (%)			Bound EPS reduction (%)		
	Protein	Carbohydrate	Total	Protein	Carbohydrate	Total
5	59.3	50.0	56.41	2.7	12.1	6.8
10	58.6	28.6	52.78	11.5	36.1	22.3
15	70.0	75.0	71.43	6.3	19.6	12.3

20	70.8	16.7	60.00	14.3	-12.5	1.9
Average	64.7	42.6	60.15	8.7	13.8	10.8

Though positive relationship between EPS and membrane fouling has been consoistently shown, distinguishing the discrete functions of various components in membrane fouling may assist in developing more effective antifouling strategies. Transparent exopolymer particles (TEP) are originally found in sea water and have been extensively studied in marine ecology (Alldredge et al., 1993; de la Torre et al., 2010; Bar-Zeev et al., 2015). As components of EPS, TEP are a class of acidic sticky particulate polysaccharides which play important roles in a healthy aquatic eco-system. In the last decade, TEP's significant presence in wastewater has been confirmed and as a result increased attention has been focused on their role in membrane fouling [Berman and Holenberg, 2005; De la Torre et al., 2008; de la Torre et al., 2010; Bar-Zeev et al., 2012].

Due to their unique physiochemical properties, TEP can easily attach onto to solid surfaces including membranes. In addition, they are a good source of nutrients for microorganism and can also be colonized by bacteria in membrane filtration or MBR system [Passow, 2002]. Consequently, TEP may in fact initiate membrane biofouling and enhance formation of the subsequent hydrogel layer. Investigations on TEP-related membrane biofouling have been conducted for membrane filtration or MBR of water and wastewater treatment [de la Torre et al., 2010; Bar-Zeev et al., 2015]. Berman et al. [2011] reported a positive relationship between the TEP level in feed water and membrane fouling rate. TEP concentrations were also demonstrated to affect the capillary suction time, membrane fouling rate and critical flux [de la Torre et al., 2008]. Significant amount of TEP were found on the surfaces of fouled RO membranes through autopsy [Villacorte et al., 2009a]. De la Torre et al. [2008] developed a simple and quick TEP

analytical method without use of concentrated sulfuric acid, which makes the quantification of TEP more efficient for future studies on correlation between TEP and biofouling [De la Torre et al., 2008]. As shown in Fig. 4.57, at various temperatures the concentrations of TEP in EMBR was significantly lower than those in MBR, ranging from 22.2% to 47.6%, which is consistent with the SMP reduction as stated previously.
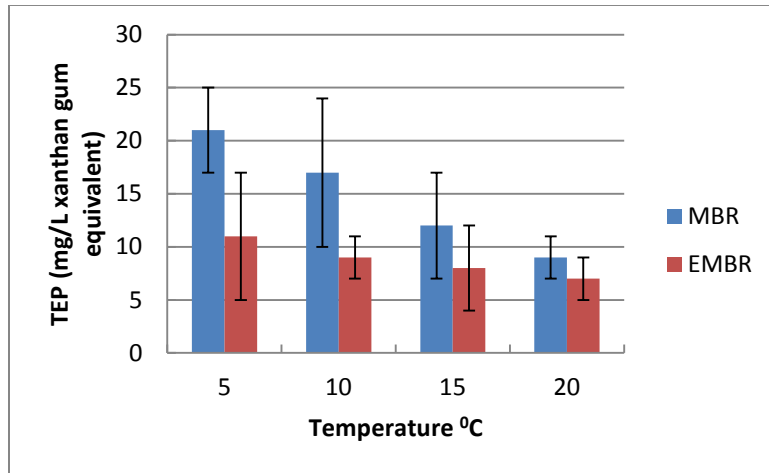
Fig. 4.57 TEP in the biomass filtrates of MBR and EMBR

4.12.4 MBR and EMBR filtration resistance and specific fouling rate (SFR)

For the entire operating period of 5 months, the filtration resistance of EMBR was less than that of MBR. This difference was observed starting after one week of operation (Fig. 4.58). At the end, the filtration resistance of EMBR prior to membrane cleaning was around 3-fold lower than that of the MBR. Furthermore SFRs in EMBR increased at a lower rate than in the control MBR for all temperatures (Figs. 4.59 to 4.62). There were no significant changes in the intrinsic membrane resistance (Rm ranging $0.82 - 1.15 \times 10^{12}\, m^{-1}$) for both control MBR and EMBR between 5 ^{0}C and 20 ^{0}C. Fig. 4.63 illustrates the relative biocake resistance vs. pore blocking resistance, as the temperature drops, the biocake resistance increases while the pore blocking

resistance decreases. It can be postulated that the elevated SMP concentrations at lower temperatures enhanced the formation and growth of a biocake on membrane surface, and a thicker biocake, as secondary filtration membrane, hindered further pore blocking at the latter stage of MBR operation.

With greater binding capacity for organic matter than bound EPS [Kim et al., 2006], SMPs are capable of penetrating into MF and UF membrane pores, then partially accumulating in the pores due to their sticky properties, which contributes to pore clogging and rising TMP in MBR. In this work, as UF membrane modules were applied and the pore clogging was very rapid in comparison to formation of the biofilm. The calculated results indicate that there was no significant difference in clogging resistance between MBR and EMBR, although SMP in the latter was 52.78% to 71.43% lower.
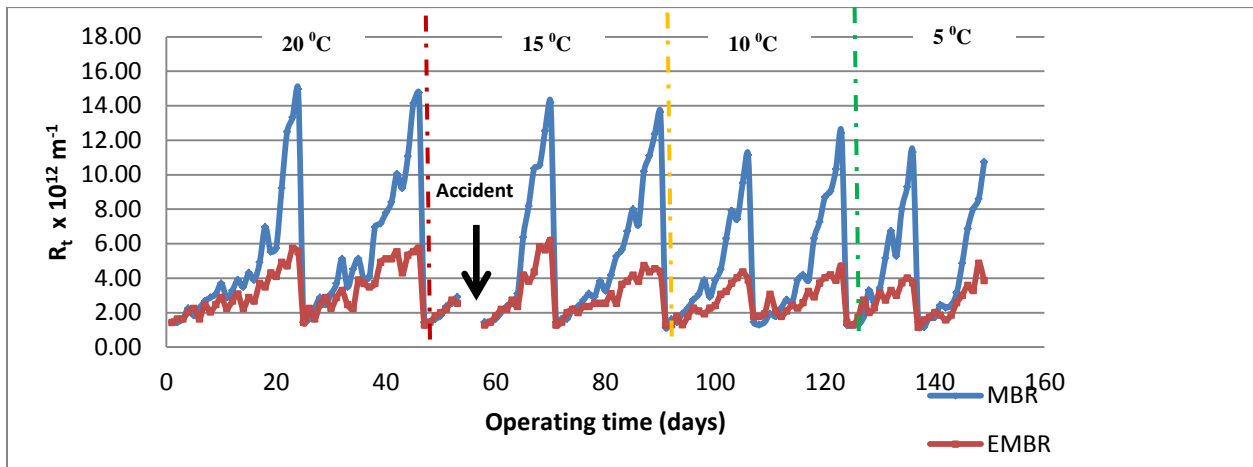
Fig. 4.58 MBR and EMBR resistance profile
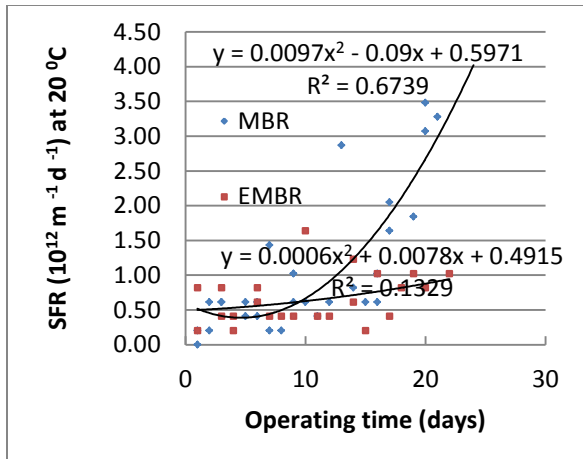
Fig. 4.59 SFR at 20 ^{0}C
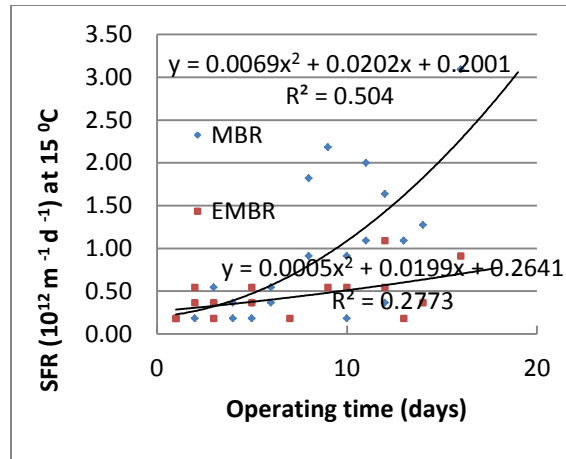
Fig. 4.60 SFR at 15 ^{0}C
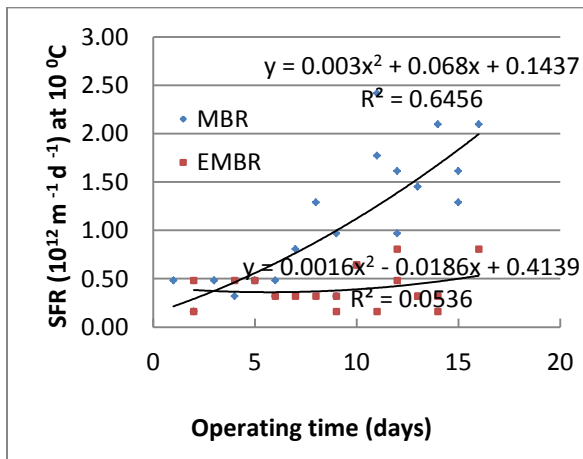
Fig.4.61 SFR at 10 ^{0}C
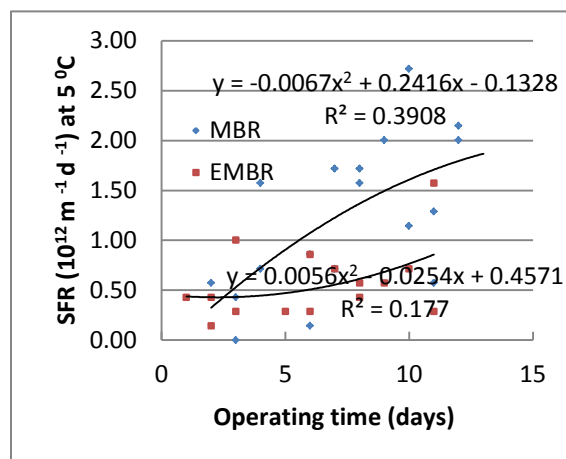
Fig. 4.62 SFR at 5 ^{0}C

Due to multiple polar (e.g. hydroxyl, carboxyl, phenolic, phosphoric etc.) and non-polar (e.g. aromatic, aliphatic and hydrophobic segments in proteins and carbohydrates) functional groups, EPS have strong affinities to both hydrophilic and hydrophobic membrane surface sites and therefore are hydrodynamically and thermodynamically anchored, forming a cross-linking gel matrix. The initial microbial attachment is followed by cell growth, metabolism, multiplication and biofilm development with substrates in the feed water or adsorbed organics on the membrane surface. The biofilm growth is limited by fluid shear forces and finally reaches a steady state

fouling resistance. The kinetics of biocake accumulation can be expressed by the following equation [Horn et al., 2014]:

$$dm/dt = k*(C_b - C_e)^n \qquad (4.63)$$

Where:

    m - mass of VSS of biocake (per unit surface area), kg/m^2

    t - time, s

    C_b - concentration of the EPS in the bulk solution, kg/m^3

    C_e - equilibrium concentration of the EPS at the interface, kg/m^3

    n - order of reaction for the overall deposition process, respectively, dimensionless

    k - kinetic rate constants for the overall deposition reaction, with the dimension of m/s

    (when n = 1).

Fig. 4.64 shows that the biocake mass per unit of membrane surface (measured in VSS) increased as the temperature decreased (by 43% at 5 ^{0}C compared to 20 ^{0}C). As the biocake plays a crucial role in membrane fouling [Chiemchaisri and Yamamoto, 1994], EMBR fouling mitigation is mainly due to reduced SMP concentration by electrokinetic processes.
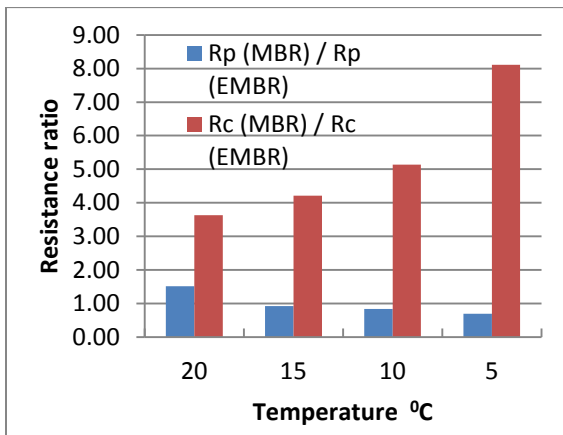
Fig. 4.63 Ratios of R_p and R_c Fig. 4.64 VSS in the biocake on membrane surface of EMBR
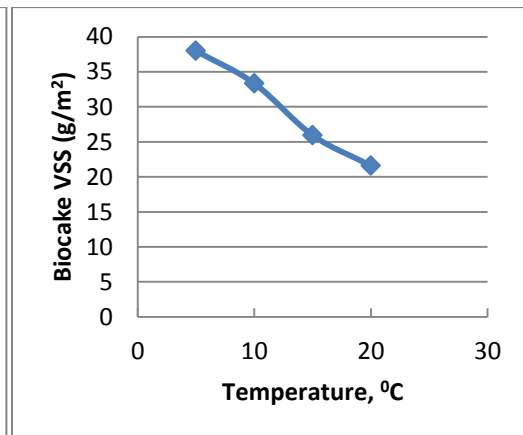
Fig. 4.65 and Fig. 4.66 display the average turbidity and color of MBR and EMBR effluents. Both reactors show very low turbidity, close or lower than the detection limits of the HACH Absorptometric Method 8237, which calibration is based on the formazin turbidity standards and readings are in terms of Formazin Attenuation Units (FAU). That is why at all temperatures the measured turbidity showed very high variability, and there is no difference in turbidity between MBR and EMBR. However, at 5 ^{0}C and 10 ^{0}C the color readings of MBR effluent were significant higher than those of the EMBR effluent, as demonstrated in Fig. 4.67. This is due to the superior decolourisation capability of electrocoagulation at lower temperatures [Sridhar et al., 2011; Khansorthong et al., 2009; Kobya et al., 2010; Ghosh et al., 2008].
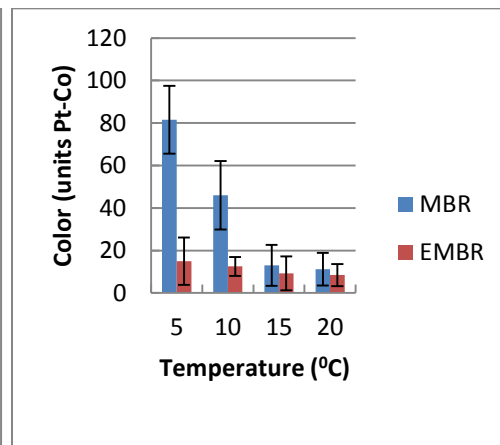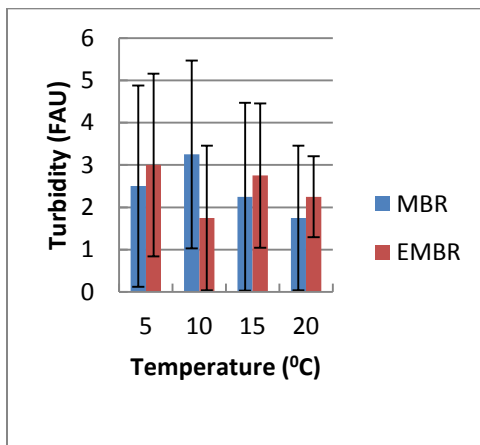
Fig. 4.65 Turbidity of the MBR and
EMBR effluents

Fig. 4.66 Color of the MBR and
EMBR effluents
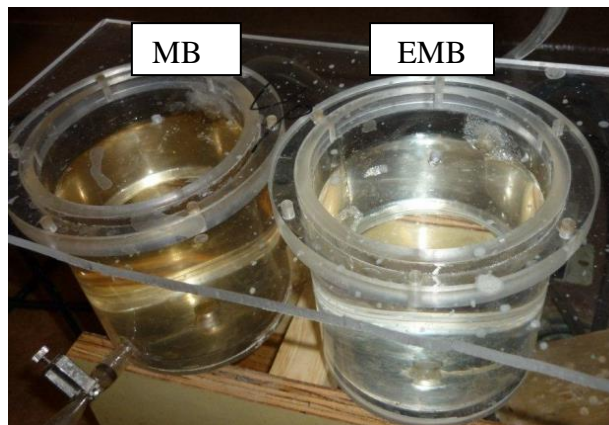
Fig. 4.67 Final effluents of MBR (left) and EMBR (right) after 5 months of operation

4.12.5 Nutrient removal efficiencies and characterization of precipitates on the electrode surface

In spite of the depressed biological activities at low temperatures, both the control MBR and EMBR exhibited successful nitrification at all temperatures, with ammonium-nitrogen removal of over 99%. Although EPS in the biomass was elevated at lower temperature, COD reduction exceeded 90% for both reactors. This could be attributed to the denser biocake on the membrane surface, which excluded most of the COD compositional molecules. In MBR, ortho-P removal ranged from 39 - 56%, whereas in EMBR, ortho-P was removed by 93% - 98% through precipitation and adsorption as discussed previously, which may be another contributing factor for significant membrane fouling reduction in EMBR. Phosphorus is an essential element for the living organisms, in biomass the mass ratio for carbon (C), nitrogen (N) and phosphorous (P) is 100:23:4.3 [Metcalf & Eddy, 2003]. Vrouwenvelder et al. [2010] reported that if phosphate in the feed wastewater containing high carbon substrate concentration is removed during pretreatment, biomass growth can be inhibited due to phosphate deficiency. Therefore, controlling biomass growth through phosphate limitation was proposed as an alternative means of abating biofouling [Vrouwenvelder et al., 2010; Characklis et al., 1990]. Phosphate in EMBR is removed through precipitation and adsorption by the electrochemically generated ferric ions [Rittmann and McCarty, 2001; Rittmann et al. 2011; Wang et al., 2014]. P concentrations at all temperatures ranged between 0.04 – 0.1 mg/L, far below the appropriate phosphate concentration for healthy biofilm growth, thus it can be assured that the formation of biocake was suppressed. Filterability improvement through binding of phosphorus by addition of iron or aluminium salts

into feed or the mixed liquor was observed by several other investigators [Wu et al., 2006; Fan et al., 2007; Koseoglu et al., 2008; Song et al., 2008; Mishima and Nakajima, 2009].

One drawback of the EMBR technology is accumulation of the precipitates on the anode surface. In this research, strong shear force and electric polarity reversal were adopted to minimize the electrode fouling or passivation. However, manual cleanup was still necessary to maintain the electric efficiency. The precipitate was a mix of ferric phosphate, ferric hydroxide and other organic compounds and inorganic salts co-precipitated or adsorbed. The FTIR spectrums in Fig. 4.68 show presence of proteins and hydrocarbons in the precipitates and Fig. 4.69 proved their amorphous structures, suggesting there were no crystallization conditions during formation of precipitates.
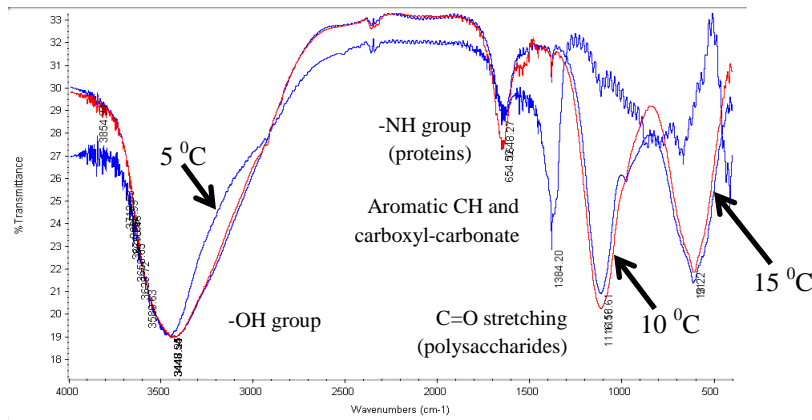
Fig. 4.68 FTIR of the electrode precipitates
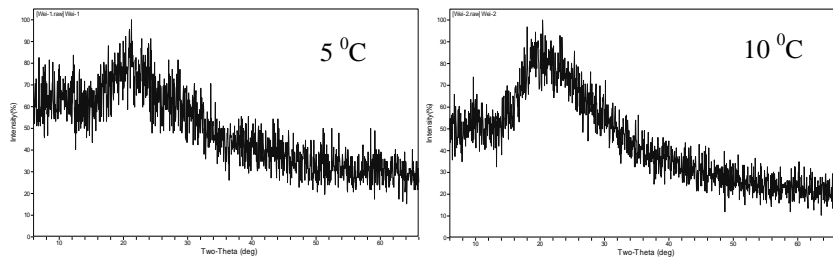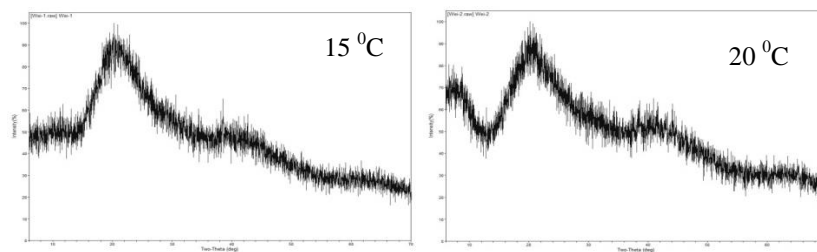
Fig. 4.69 XRD images of the electrode precipitates

CHAPTER 5 ENGINEERING SIGNIFICANCE

This research was carried out in an attempt to facilitate the practical application of electrokinetic technologies in MBR and the findings offer the following engineering significance:

- Developed an EMBR system to mitigate membrane fouling in MBRs - this was demonstrated to work with synthetic and real municipal wastewater;

- Determined the regime for EMBR operation that would not be detrimental to bacterial growth and at the same time ensured successful nutrient removal and membrane filtration with improved MBR performance;

- Demonstrated low temperature operation with long cleaning intervals – this will facilitate future applications in remote northern regions;

- Identified the problem of abiotic ammonia generation and found a method of combatting it;

- Defined electrode passivation as the key problem in EMBR and proposed methods of alleviation.

Engineering economics is a key consideration for application of a new technology. Accurate calculations and comparisons of the operating costs for the electrokinetic process are difficult due to unavailability of a number of variables such as capital and operating costs of the control devices, electrochemical vessels, sludge treatment/disposal systems, electrode cleaning equipment and price differences of electricity and electrodes in different countries and regions. In addition, those costs fluctuate over the course of time; therefore, operating costs can only be obtained through rough estimation on the basis of semi-quantitative analysis. According to the

literature involving EC cost data over the last three decades, generally only costs of electrode materials and power consumption are taken into account as follows:

$$OC = a * \frac{U*I}{V} + b * MC \qquad (5\text{-}1)$$

Where:

OC = Operating cost ($/m^3 of treated wastewater)

a = price of electricity ($/KWH), 0.06175 CAD/kWh in Manitoba according to

http://www.gov.mb.ca/jec/invest/busfacts/utilities/comp_hy_med.html accessed on Sept. 10, 2015.

U = applied electric voltage (V)

I = applied electric current (A)

V = volume of the treated wastewater per hour (m^3/h)

MC = electrode material consumption (hourly metal mass per m^3 of the treated wastewater)

b = price of the electrode material ($ per unit mass of the electrode material), 2.01 CAD/kg of Al and 0.24 CAD/kg of steel as per the London Metal Exchange (LME) on Sept. 10, 2015.

The calculated results show that the OCs for Al and Fe electrodes are 0.16 CAD/ m^3 of the treated wastewater and 0.06 CAD/ m^3 of the treated wastewater, respectively. In fact, the OCs, based on Equation 5-1, are greatly underestimated as electrode passivation, electrode cleanup cost and the waste disposal of electrode materials are not considered. Nevertheless, even with all of these extra operating cost included, it can still be reasonably expected that the OC of the developed EMBR technology is still significantly lower than the electrokinetic costs of some other applications as shown in Table 5.1. The substantial differences in the electrokinetic operating costs for different wastewater sources, targeted pollutants, electrode materials, research needs and study locations are inevitable. The electrokinetic process is still under progress and

some innovations may significantly reduce its cost in the future. New technologies under

development include utilization of the by-product hydrogen gas to compensate the energy

consumption, solar-powered electrokinetic system, recirculation of the electrokinetic sludge

supernatant to reuse as the coagulant, and pretreatment of the wastewater with sonar or magnetic

field technologies prior to electrokinetic process [Espinoza-Quiñones et al., 2009; Kobya et al.,

2010].

Table 5.1 Operating costs of some electrokinetic processes

Source of water or wastewater	Electrode materials	Treatment efficiency	Operating cost	Reference
Electroplating wastewater	Iron	99.4% for cadmium, 99.1% for nickel, 99.7% for cyanide.	$1.05/m^3 for cadmium, $2.45/m^3 for nickel and cyanide	[Kobya et al., 2010]
Remazol Red 3B wastewater	Iron	99% decolorization	3.3 kWh/kg dye at a cost of 0.6 €/m^3	[Kobya et al., 2010]
Fluorescent wastewater from aircraft industry	Al	95% of COD, 99% color, and 99% turbidity	Return of 17 weeks	[Meas et al., 2010]
Oil bilge wastewater	Al and iron electrodes with bipolar (BP) and monopolar (MP) configuration	93% of BOD, 95.6% oil and grease, 99.8% of TSS, and 98.4% turbidity	$0.46/m^3, for energy and electrode consumption, chemicals, and sludge disposal	[Asselin et al., 2008]
Removing iron [Fe(II)] from tap water	Al	Removing a concentration of 15 mg/L Fe(II)	$6.05 USD/m^3	[Ghosh et al., 2008]
Agro-industry wastewater	Mild steel electrodes	82% of COD removal	$0.95 - $4.93 USD/m^3	[Drogui et al., 2008]
Shipping industry wastewater	Al, bipolar electrode arrangements	80% turbidity, 56% of COD, 90% oil and grease, and 89% of BOD	$1.54 - $2.40 CAN/m^3, including energy and electrode consumption and sludge disposal	[Drogui et al., 2009]

211

Pulp and paper mill wastewater	Parallel iron electrodes	97% of color and 77% of COD	US$0.29 /m^3	[Khansorthong et al., 2009]
Paper mill effluent	Aluminum electrode	60% of BOD	$8.34 to $31.74 USD/m^3	[Orori et al., 2010]
Dye polluted wastewater	Parallel-connected Al electrodes	TOC removal varies between 56% and 91% from	US$ 1.3–3.4 per kg TOC	[Eyvaz et al., 2009]
Pulp and paper wastewater	Al	94% of color, 90% of COD and 87% of BOD	US$ 1.52 /m^3 to 1.72 / m^3	[Sridhar et al., 2011]

Apart from demonstrating significant membrane fouling mitigation and nutrient removal capacity and low operating cost, the EMBR system developed in this study has a compact configuration, is easy to operate and maintain and requires no phosphorus precipitating chemicals, suggesting its potential to be an alternative decentralized wastewater treatment system suitable for cold regions.

CHAPTER 6 GENERAL CONCLUSIONS

MBRs have been globally seen as a promising technology for wastewater treatment and reuse. Electrokinetically based EMBRs demonstrated significant advantages in membrane fouling reduction over other conventional antifouling strategies due to the configuration simplicity, operational flexibility and elimination of chemical demand. In this research, after extensive investigation of the technical fundamentals, an EMBR with significantly reduced energy expenditures and chemical consumption was developed. It was demonstrated on real municipal wastewater at various temperatures found in Canadian plants. The main research observations and findings have met the research objectives and could be summarized as follows:

One. The electrochemical and elecrokinetic fundamentals of EMBR were extensively investigated, which paved the way for practical application of this technology as a promising decentrtalized wastewater treatment alternative in the remote northern communities. (1). With separate electrolytic cells the localized pH changes in the vicinities of cathode and anode were proven to be significant and thus sufficient mixing must be provided to avoid inactivation of the microorganisms. (2). Overall, the upward pH trend in a one-tank electrochemical configuration was beneficial to the nitrification process due to increase in alkalinity. For the MBR system studied in this research, no pH adjustment was necessary to maintain a favorable acid-base environment for bacterial growth. (3). Aluminum cathode dissolution and pitting corrosion collectively caused higher cationic aluminum yield than theoretical calculations (ranging from 118% to 143%). The actual Al^{3+} production was dependent on the influent characteristics, including the presence of chlorides which enhances aluminum dissolution. High current density should be avoided because it not only leaves extra toxic Al^{3+} ions in the effluent but also

213

produces large amount of explosive hydrogen gas. (4). When using iron anode, sufficient DO must be present in the electrolytic fluid so that the electrochemically generated ferrous ions can be oxidized to ferric ions which have much lower solubility and higher positive charge density and therefore much higher coagulation efficiency. In addition, the generation and diffusion dynamics of ferric ions in the electrolytic solution was first demonstrated with complexing ferric thiocyanate. (5). It was found that the steady state particle size of biomass was the result of the dynamic equilibrium of floc aggregation and breakage. Due to denser floc mass and lesser amount of bound water contained, biomass in the EMBR showed improved settleability, expressed as SVI which was reduced by 5.5% - 21.4% with Al electrode and 7.8% - 30.2% with Fe electrode. The filterability expressed as capillary suction time (CST) decreased by 5.6% - 26.1% with Fe electrode and 6.8% - 23.5% with Al electrode, respectively. (6). Electrode passivation was found to be a major challenge for broader application of electrokinetic technologies and minimization of electrode passivation was found crucial for successful application of the EMBR. It was found that when current intensity was lower than 0.2 A, polarity reversal had minimal impact on reduction of electrode passivation due to minimum hydrogen yield. With current intensity above 0.2 A, polarity reversal that was too frequent (that is less than 5 min per cycle) was found to be detrimental, as aluminum ions reacted with hydroxyl groups before they were able to diffuse into the bulk liquid. For practical application a mechanical electrode cleaning device must be in place to allow for consistent treatment performance. (7). A new method for *in-situ* non-invasive imaging of membrane fouling in membrane reactors was developed using MRI. The method was demonstrated on conventional MBR and EMBR. (8). It was demonstrated that viability of the microorganisms in an electrically enhanced MBR is dependent on duration of the current application and current density. The bacterial viability was

not significantly (less than 10% of inactivation) affected when the applied current density was less than 6.2 A/m^2. The live cell fraction dropped by 15% and 29% at currents of 12.3 A/m^2 and 24.7 A/m2, respectively. Cells on the cathode surface exhibited the highest death rate, whereas bacteria outside the space between electrodes had the highest viability as they were the least affected by the toxicity of electrochemical byproducts and electric field. It was concluded that sufficient mixing should be provided for an electro technology hybrid wastewater treatment vessel to prevent localized cell inactivation.

Two. Abiotic ammonification was demonstrated with Al and Fe electrodes in a synthetic nitrate wastewater and activated sludge. It was found that: (1). under electrolytic conditions, DO in the treated liquid will be depleted within an hour and thus create an electrochemically reducing environment; (2). under the anaerobic condition in EC nitrate will be nearly chemometrically reduced to ammonium, without generation of nitrogen gas. Intermediate nitrite concentration was very low and was diminished by the biological nitratation process. The anode was the electron donor in this case. (3). Abiotic conversion from nitrate to ammonium followed a two-step first order reaction. For Al cathode: k_1 was 0.02038 with 95% confidence limits, k_2 was 0.1006 with 95% confidence bounds. For Fe cathode: k_1 was equal to 0.00711, with 95% confidence limits, k_2 was 0.07472 with 95% confidence bounds (0.06752, 0.08193). (4). Aluminum was found to have stronger capability than iron for electrochemical nitrate reduction. (5). Aeration was found to be a convenient strategy to suppress the occurrence of electrochemical nitrate reduction. At DO levels larger than 2 mg/L, abiotic ammonification was completely prevented. The finding resolved the problem of abiotic ammonification of nitrate, offering a simple but effective method to prevent it.

Three. With synthetic wastewater, the control MBR and EMBR both removed > 99% of ammonium-N and > 90% of dissolved COD. Through chemical precipitation and physical adsorption, the ortho-P removal in the EMBR was between 93 - 98%, compared with 39 – 56% of ortho-P removal in the MBR, which offers an efficient nutrine control strategy with no chemical consumption and less sludge production.

Four. A new mathematical model was developed for an EMBR, defining the specific fouling rate (SFR) = dRt/dt = d(TMP)/dt x 1/(J*u). (1). The fouling rate was shown to be related to permeate flux and temperature- dependent viscosity. (2). The SFR model was found to more accurately describe the fouling propensity at low temperatures, when flux is taken into account and can be used as a key indicator for evaluating membrane quality. (3). For the first time pore clogging and biocake resistance were quantified with the same membrane module and operating conditions as in a control MBR. Biocake resistance reduction, which resulted from SMP destruction, was found to be a major advantage of electrokinetic technology. (4). Overall comparison of the developed EMBR showed that EMBR offered effective membrane fouling mitigation through eliminating the elevated EPS at low temperatures.

Five. Operation of EMBR at low temperatures has shown that the transmembrane pressure (TMP) increased significantly more slowly in the EMBR and the filtration resistance was about one third of the regular MBR prior to necessitating a chemical cleaning cycle necessary for MBR, suggesting the significant potential for extending the membrane life and MBR operating cost.

Six. The EMBR also exhibited a prominent advantage over conventional MBR in terms of membrane fouling retardation and phosphorus removal at an operating temperature of $10\,^{0}$C and $5\,^{0}$C with real sewage as feed. Despite the membrane fouling suppression advantage, the additional operating costs of EMBR were not significant, with 0.16 CAD/ m^3 of the treated wastewater for Al electrodes and 0.06 CAD/ m^3 of the treated wastewater for Fe electrodes.

REFERENCES

Abuzaid, N.S., Bukhari, A.A., Hamouz, Z.M., (2002). Ground water coagulation using soluble stainless steel electrodes. Adv. Environ. Res. 6 (3), 325-333

Adam, C., Gnirss, R., Lesjean, B., Buisson, H., and Kraume, M. (2002). Enhanced biological phosphorous removal in membrane bioreactors. Water Science and Technology, 46 (4-5), 281-286.

Agana, B.A., Reeve, D., Orbell, J.D. (2012). The influence of an applied electric field during ceramic ultrafiltration of post-electrodeposition rinse wastewater. Water Research 46, 3574-3584

Ahmad, A., Wong, S. S., Teng, T., and Zuhairi, A. (2007). Optimization of coagulation flocculation process for pulp and paper mill effluent by response surface methodological analysis. Journal of Hazardous Materials. 145(1-2): 162-168.

Ajmania, G.S., Goodwin, D., Marsh , K., Fairbrother, D. H., Schwab, K.J., Jacangelo, J.G., Huang, H. (2012). Modification of low pressure membranes with carbon nanotube layers for fouling control. Water Research. 46 (17), 5645–5654.

Akamatsu, K., Lu, W., Sugawara, T., Nakao, S. I. (2010). Development of a novel fouling suppression system in membrane bioreactors using an intermittent electric field. Water Research 44, 825-830

Akbal, F., Camci. M. (2010). Comparison of Electrocoagu- lation and Chemical Coagulation for Heavy Metal Re- moval. Chemical Engineering & Technology, 33(10), 1655-1664.

Al-Ahmad, M., Abd El-Aleem, F.A.; Mutiri, A., Ubaisy, A. (2000). Biofouling in RO membrane systems. Part 1: Fundamentals and control. Desalination, 132, 173–179

Al-Amoudi, A., Williams, P., Mandale, S., and Lovitt, R. W. (2007). Cleaning results of new and fouled nanofiltration membrane characterized by zeta potential and permeability. Separation and Purification Technology. 54(2): 234–240.

Al-Amri, A., Salim, M. R., Aris, A. (2010). The effect of different temperatures and fluxes on the performance of membrane bioreactor treating synthetic-municipal wastewater. Desalination 259, 111-119

Alldredge A. L., Passow U., Logan B. E., (1993). The abundance and significance of a class of large, transparent organic particles in the ocean. Deep-Sea Res Pt I 40(6):1131–1140

Al-Malack, M. H. (2006). Determination of biokinetic coefficients of an immersed membrane bioreactor. Journal of Membrane science, 271, 47-58.

Alphenaar, P.A., Sleyster, R., De Reuver, P., Ligthart, G.-J., Lettinga, G., (1993). Phosphorus requirement in high-rate anaerobic wastewater treatment. Water Research 27, 749 -756

Alshawabkeh, A. N., Shen, Y. P, Maillacheruvu, K. Y. (2004). Effect of DC Electric Fields on COD in Aerobic Mixed Sludge Processes. Environmental Engineering Science. 21(3), 321-329

Amirtharajah, A., Mills, K.M., (1982). Rapid-mix design for mechanisms of alum flocculation. J. Am. Water Works Assoc. 74 (4), 210-216

An, Y., Li, T., Jin, Z., Dong, M., Li, Q., and Wang, S. (2009). Decreasing ammonia generation using hydrogenotrophic bacteria in the process of nitrate reduction by nanoscale zero-valent iron. Science of the Total Environment. 407(21): 5465–5470.

Andersen, H. R., M. Hansen, J. Kjoelholt, F. Stuer-Lauridsen, T. Ternes and B. Halling Soerensen (2005). "Assessment of the importance of sorption for steroid estrogens removal during activated sludge treatment." Chemosphere 61(1): 139-146.

Andersen, H., H. Siegrist, B. Halling-Sorensen and T. A. Ternes. (2003). Fate of Estrogens in a Municipal Sewage Treatment Plant. Environmental Science & Technology 37(18): 4021-4026.

Annaka, Y., Y. Hamamoto, M. Akatsu, K. Maruyama, S. Oota and T. Murakami. (2006). Development of MBR with Reduced Operational and Maintenance Costs. Water Science Technology 53(3): 53-60.

APHA. Standard Methods for the Examination of Water and Wastewater. (2005). 21th edn, American Public Health Association/American Water Works Association/Water Environment Federation, Washington DC, USA.

Aptel, P., Bersillon, J.L., Howell, J.A., Sanchez, V., R.W. Field (Eds.), (1993). Membranes in Bioprocessing: Theory and Applications, Blackie Academic and Professional, London, p. 179.

Arévalo, J., Ruiz, L. M., Pérez, J., Gómez, M. A. (2014). Effect of temperature on membrane bioreactor performance working with high hydraulic and sludge retention time. Biochemical Engineering Journal 88, 42-49

Arruda Fatibello S. H., Henriques Vieira A. A., Fatibello-Filho O. (2004). A rapid spectrophotometric method for the determination of transparent expolymer particles (TEP) in freshwater. Talanta 62, 82-85

Asselin, M, Drogui, P., Benmoussa, H., and Blais J-F. (2008). Effectiveness of electrocoagulation process in removing organic compounds from slaughterhouse wastewater using monopolar and bipolar electrolytic cells. Chemosphere, 72, 1727–1733.

Asselin, M., Drogui, P., Brar, S. K., Benmoussa, H., Blais, J. (2008). Organics removal in oily bilgewater by electrocoagulation process, J. Hazard. Mater. 151, 446-455.

Auriol, M., Y. Filali-Meknassi, R. D. Tyagi, C. D. Adams and R. Y. Surampalli. (2006). Endocrine disrupting compounds removal from wastewater, a new challenge. Process Biochemistry 41(3): 525-539.

Ayala D. F., Ferre, V., Judd, S. J. (2011). Membrane life estimation in full-scale immersed membrane bioreactors, J. Membr. Sci. 378, 95–100.

Bacchin, P., Aimar, P., Field, R. (2006). Critical and sustainable uxes: theory, experiments and Applications. Journal of Membrane Science, Elsevier, 281 (1-2), 42-69.

Bae, T.H., Tak, T.M. (2005). Interpretation of fouling characteristics of ultrafiltration membranes during the filtration of membrane bioreactor mixed liquor. Journal of Membrane Science, 264, pp 151–160.

Bagga, A., Chellam, S., Clifford, D.A. (2008). Evaluation of iron chemical coagulation and electrocoagulation pretreatment for surface water microfiltration, J. Membr. Sci. 309, 82-93.

Bagotsky, V. (2006). Fundementals of Elechtrochemistry. Pennington: John Wiley & Sons, Inc., Hoboken, N.J

Baker, R.W. (2000). Membrane Technology and Applications. McGraw-Hill, New York.

Balasubramanian, N., Madhavan, K., (2001). Arsenic removal from industrial effluent through electrocoagulation. Chem. Eng. Technol. 24 (5), 519-521

Balmer, L. M. and Foulds, A. W. (1986) Separating oil from oil-in-water emulsions by electroflocculation/electroflotation. Filtration and Separation 23 (6), 366-370.

Bani-Melhem K, Elektorowicz M, (2010). Development of a novel submerged membrane electro-bioreactor (SMEBR): performance for fouling reduction, Environ. Sci. Technol., 44, 3298-3304.

Bani-Melhem K, Elektorowicz M., (2011), Performance of the Submerged Membrane Electro-Bioreactor (SMEBR) with iron electrodes for WWT and fouling reduction. J Mem. Sc. 379(1-2), 434-439

Barker, D.J., Stuckey, D.C. (1998). A review of soluble microbial products (SMP) in wastewater treatment systems. Water Research, 33, pp 3063-3082.

Baronti, C., R. Curini, G. D'Ascenzo, A. Di Corcia, A. Gentili and R. Samperi. (2000). Monitoring Natural and Synthetic Estrogens at Activated Sludge Sewage Treatment Plants and in a Receiving River Water." Environmental Science & Technology 34(24): 5059-5066.

Barrabésa, N. and Sá, J. (2011). Catalytic nitrate removal from water, past, present and future perspectives. Applied Catalysis B: Environmental, 104, 1-5

Bar-Zeev E, Berman-Frank I, Girshevitz O, Berman T., (2012). Revised paradigm of aquatic biofilm formation facilitated by microgel transparent exopolymer particles. P Natl Acad Sci USA 109(23):9119–9124

Bate, L. C., & Dyer, F. F. (1968). Particle-size distribution of particles from 10 to 2000 microns by sedimentation analysis. Analytical Chemistry. 40(2), 468-470.

Bayramoglu, M., Can, O.T., Kobya, M., and Sozbir, M. (2004). Operating cost analysis of electrocoagulation of textile dye wastewater. Sep. Purif. Technol., 37, 117–125.

Bayramoglu, M., Eyvaz M., and Kobya, M. (2007). Treatment of the textile wastewater by electrocoagulation: Economical evaluation. Chemical Engineering Journal, 128(2-3), 155-161.

Bayramoglu, M., Kobya, M., Can, O.T., Sozbir, M. (2004). Operating cost analysis of electrocoagulation of textile dye wastewater. Sep. Purif. Technol. 37 (2), 117-125

Bayramoglu, M., Kobya, M., Eyvaz, M., and Senturk, E. (2006). Technical and economic analysis of electrocoagulation for the treatment of poultry slaughterhouse wastewater. Separation and Purification Technology, 51 (3), 404-408.

Bazinet, L. (2004). Electrodialytic phenomena and their applications in the dairy industry: A review. Food Science and Nutrition, 44 (7-8), 525-54.

Bechtel, M. K., Bagdasarian, A., Olson W. P., and Estep T.N. (1988). Virus removal or inactivation in hemoglobin solutions by ultrafiltration or detergent/solvent treatment." Biomaterial. Artificial Cells Artificial Organs, 16,123-128.

Belfroid, A. C., A. Van der Horst, A. D. Vethaak, A. J. Schaefer, G. B. J. Rijs, J. Wegener and W. P. Cofino. (1999). Analysis and occurrence of estrogenic hormones and their glucuronides in surface water and waste water in The Netherlands. The Science of The Total Environment 225(1-2): 101-108.

Belhouta, D., Ghernaouta, D., Djezzar-Douakhb, S., Kellila, A. (2010). Electrocoagulation of a raw water of Ghrib Dam (Algeria) in batch using aluminium and iron electrodes. Desalination Water Treat. 16(1-3), 1-9

Bemberis, I., Hubbard, P.J., Leonard, F.B. (1971). Membrane sewage treatment systems − potential for complete wastewater treatment. American Society of Agricultural Engineers Winter Meeting, 71-878, pp 1-28.

Ben Mansour L., Chalbi S., Kesentini I. (2007). Experimental study of hydrodynamic and bubble size distributions in electroflotation process Indian Journal of Chemical Technology. 14(3): 253-257.

Bensadok, K., Benammar, S., Lapicque, F., & Nezzal, G. (2008). Electrocoagulation of cutting oil emulsions using aluminum plate electrodes. Journal of Hazardous Materials. 152(1): 423-430.

Benschop, M. (2008). Influence of temperature on filtration in membrane bioreactors. MSc thesis, Delft University of Technology, Faculty of Civil Engineering and Geosciences, section Water management.

Berg, G.B. van den, Smolders, C.A. (1990). Flux decline in ultrafiltration processes. Desalination, 77, pp 101-133.

Berman T., Holenberg M. (2005). Don't fall foul of biofilm through high TEP levels. Filtr Separat 42(4):30-32

Bertanza, G. (1997). Simultaneous Nitrification-Denitrification Process in Extended Aeration Plants: Pilot and Real Scale Experiences. Water Science and Technology 35(6): 53-61.

Bhatta, C.P., Matsuda, A., Kawasaki, K., and Omori, D. (2004). Minimization of sludge production and stable operational condition of a submerged membrane activated sludge process. Water Science and Technology, 50(9), 121-128.

Birkett, J. and J. Lester (2003). Endocrine Disrupters in Wastewater and Sludge Treatment Processes. Boca Raton, CRC Press LLC.

Blenkinsopp, S. A., Khoury, A. E., and Costerton, J. W. (1992). Electrical enhancement of biocide efficacy against Pseudomonas aeruginosa biofilms. Appl. Environ. Microbiol. 58:3770-3773.

Bodzek, M., and Krystyna K., (1998). Comparison of various membrane types and module configurations in the treatment of natural water by means of low-pressure membrane methods. Sep. Purf. Tech., 14, 69-78.

Boerlage, S.F.E., Kennedy, M.D., Aniye, M.P., Abogrean, E., Tarawneh, Z.S., Schippers, J.C. (2003). The MFI-UF as a water quality test and monitor. Journal of Membrane Science, 211, pp 1-21.

Boributh, S.; Chanachai, A.; Jiraratananon, R. (2009). Modification of PVDF membrane by chitosan solution for reducing protein fouling. J. Membr. Sci., 342, 97–104.

Bouhabila, E.H., Aim, R. Ben, en Buisson, H. (2001). Fouling characterisation in membrane bioreactors. Separation & Purification Technology, 22-23, pp 123-132.

Boulos, L., M. Prevost, B. Barbeau, J. Coallier, and R. Desjardins. (1999). LIVE/DEAD BacLight: application of a new rapid staining method for direct enumeration of viable and total bacteria in drinking water. J. Microbiol. Methods 37:77-86.

Bratby, J. (2006). Coagulation and Flocculation in Water and Wastewater Treatment. London: IWA Publishing., London, Britain

Brepols, C., Drensla, K., Janot, A., Trimborn, M., Engelhardt, N. (2008). Strategies for chemical cleaning in large scale membrane bioreactors, Water Sci. Technol. 57, 457-463.

Briciu, R. D., Wasik, A. K., and Namiesnik, J. (2009). Analytical Challenges and Recent Advances in the Determination of Estrogens in Water Environments. Journal of Chromatographic Science, 47(2):127-39

Brindle, K., and Stephenson, T. (1996). The application of membrane biological reactors for the treatment of wastewaters. Biotechnology and bioengineering, 49, 601-610.

Brookes, A., Jefferson, B., Guglielmi, G., Judd, S.J. (2006). Sustainable flux fouling in a membrane bioreactor: impact of flux and MLSS. Separation Science & Technology, 41, pp 1279–1291.

Brookes, A., Jefferson, B., Le-Clech, P., Judd, S.J. (2003). Fouling of membrane bioreactors during treatment of produced water. In: Proceedings of the IMSTEC, Sydney, Australia.

Bruening, M.L.; Dotzauer, D.M.; Jain, P.; Ouyang, L.; Baker, G.L. (2008). Creation of functional membranes using polyelectrolyte multilayers and polymer brushes. Langmuir, 24, 7663–7673.

Bruggen, V. D., Vandecasteele, B., Carlo, V., Tim, D. (2003). A review of pressure-driven membrane processes in wastewater treatment and drinking water production." Environmental Progress, 22 (1), 46-56.

Bunthof, C. J., S. van Schalkwijk, W. Meijer, T. Abee, and J. Hugenholtz. (2001). Fluorescent method for monitoring cheese starter permeabilization and lysis. Appl. Environ. Microbiol. 6:4. 264-4271.

Busch, J., Cruse, A., and Marquardt, W. (2006). Modeling submerged hollow-fiber membrane filtration for wastewater treatment. Journal of Membrane Science, 288 (1-2), 94-111.

Cabassud, C., Laborie, S., Durand-Boulier, L., Laine, J.M. (2001). Air sparging in ultrafiltration hollow fibres: relationship between flux enhancement, cake characteristics and hydrodynamic parameters. Journal of Membrane Science, 181, pp 57-69.

Cabassud, C., Masse, A., Espinosa-Bouchot, M., Sperandio, M. (2004). Submerged membrane bioreactors: interactions between membrane filtration and biological activity. In: Proceedings of the Water Environment-Membrane Technology Conference, Seoul, Korea, 2004.

Calderón, K., González-Martínez, K., Montero-Puente, C., Reboleiro-Rivas, P., J.M. Poyatos, B. Juarez-Jiménez, M.V. Martínez-Toledo, Rodelas, B., (2012). Bacterial community structure and enzyme activities in a membrane bioreactor (MBR) using pure oxygen as an aeration source. Bioresour. Technol. 103, 87-94.

Callaghan P. (1994). Principles of Nuclear Magnetic Resonance Microscopy. Oxford University Press. ISBN 0-19-853997-5

Campbell, C. G., S. E. Borglin, F. B. Green, A. Grayson, E. Wozei and W. T. Stringfellow. (2006). Biologically directed environmental monitoring, fate, and transport of estrogenic endocrine disrupting compounds in water: A review. Chemosphere 65(8): 1265-1280.

Can, O. T., Bayramoglu, M., and Kobya, M. (2003). Decolorization of reactive dye solutions by electrocoagulation using aluminum electrodes. Ind. Eng. Chem. Res., 42, 3391-3396.

Canizares, P., Carmona, M., Lobato, J., Martı´nez, F., and Rodrigo, M. A. (2005). Electrodissolution of Aluminum Electrodes in Electrocoagulation Processes. Ind. Eng. Chem. Res. 44(12): 4178-4185.

Canizares, P., Martinez, F., Jimenez, C., Lobato, J., and Rodrigo, M. A. (2006). Coagulation and Electrocoagulation of Wastes Polluted with Dyes. Environmental Science and Technology. 40(20): 6418-6424.

Cargouet, M., D. Perdiz, A. Mouatassim-Souali, S. Tamisier-Karolak and Y. Levi. (2004). Assessment of river contamination by estrogenic compounds in Paris area (France). Science of The Total Environment 324(1-3): 55-66.

Carmona, M., Khemis, M., Leclerc, J.P., Lapicque, F.A. (2006). Simple model to predict the removal of oil suspensions from water using the electrocoagulation technique. Chem. Eng. Sci. 61 (4), 1237-1246

Carter, J. L., and McKinney, R. E. (1973). Effects of iron on activated sludge treatment. J. Env. Eng. Div., 99 EE2, 135–152.

Chae, S. R., Kang, S. T., Watanabe, Y., and Shin, H. S. (2006). Development of an innovative vertical submerged membrane bioreactor (VSMBR) for simultaneous removal of organic matter and nutrients. Water Research, 40, 2161-2167.

Chae, S. R., Shin, H. S. (2007). Characteristics of simultaneous organic and nutrient removal in a pilot scale vertical submerged membrane bioreactor (VSMBR) treating municipal wastewater at various temperatures. Process Biochemistry 42, 193-198

Chae, S.R., Ahn, Y.T., Kang, S.T., Shin, H.S. (2006). Mitigated membrane fouling in a vertical submerged membrane bioreactor (VSMBR). Journal of Membrane Science, 280, pp 572-581.

Chang, I. S., and Kim, S. N. (2005). Wastewater treatment using membrane filtration-effect of biosolids concentration on cake resistance. Process Biochem, 40, 1307-1314.

Chang, I.S., en Lee, C.H. (1998). Membrane filtration characteristics in membrane coupled activated sludge system – the effect of physiological states of activated sludge on membrane fouling. Desalination, 120, 221-233.

Chang, I.S., Gander, M., Jefferson, B., en Judd, S. (2001). Low-cost membranes for use in a submerged MBR. Process Saf. Envir. Prot., 79(3), 183-188.

Chang, I.S., Kim, S.N. (2005). Wastewater treatment using membrane filtration - effect of biosolids concentration on cake resistance. Process Biochemistry, 40, pp 1307–1314.

Chang, I.S., Le Clech, P., Jefferson, B., Judd, S. (2002). Membrane fouling in membrane bioreactors for wastewater treatment. Journal of Environmental Engineering, 1018- 1029.

Chang, I.S., Lee, C.H., Ahn, K.H. (1999). Membrane filtration characteristics in membrane-coupled activated sludge system: the effect of floc structure on membrane fouling. Separation Science & Technology, 34, pp 1743–1758.

Chang, I.S.; Lee, C.H. (1998). Membrane filtration characteristics in membrane-coupled activated sludge system-the effect of physiological states of activated sludge on membrane fouling. Desalination, 120, 221–233.

Chang, W. K., Hu, A. Y. J., Horng, R. Y., and Tzou, W. Y. (2007). Membrane bioreactor with nonwoven fabrics as solid–liquid separation media for wastewater treatment. Desalination, 202(1-3), 122-128.

Characklis, W.G., Marshall, K.C., (1990). Biofilms. John Wiley & Sons, New York

Chen, G. (2004). Electrochemical technologies in wastewater treatment. Separation and Purification Technology, 38, 11-41.

Chen, G., Chen, X., and Yue, P. L. (2000). Electrocoagulation and Electroflotation of Restaurant Wastewater. Journal of Environmental Engineering. 26(9): 858-863.

Chen, J-P., Yang, C-Z., and Zhou, J-H. (2007). The effect of Pulsed direct current field on the on membrane flux of a new style of membrane bioreactor. Chem. Eng. Technol., 30 (9), 1262-1265.

Chen, J-P., Yang, C-Z., Zhou, J-H., and Wang, X-Y. (2007). Study of the influence of the electric field on membrane flux of a new type of membrane bioreactor. Chemical Engineering Journal, 128 (2-3), 177-180.

Chen, V.J.; Ma, P.X. (2002). Nano-fibrous poly(L-Lactic acid) scaffolds with interconnected spherical macropores.. Biomaterials, 25, 2065–2073.

Chen, W.; Liu, J. (2012). The possibility and applicability of coagulation-MBR hybrid system in reclamation of dairy wastewater. Desalination , 285, 226–231.

Chen, X. M., Chen, G. H., Yue, P. L. (2002). Investigation on the electrolysis voltage of electrocoagulation. Chemical Engineering Science. 57(13), 2449-2455

Chen, X., Chen, G., and Yue, P.L. (2000). Separation of pollutants from restaurant wastewater by electrocoagulation. Separation and Purification Technology, 19(1-2), 65-76.

Chen, Z., D. Hu, N. Ren and Z.-P. Zhang. (2008). Simultaneous removal of organic substances and nitrogen in pilot-scale submerged membrane bioreactors treating digested traditional Chinese medicine wastewater. International Biodeterioration & Biodegradation 62(3): 250-256.

Cho, B.D., Fane, A.G. (2002). Fouling transients in nominally sub-critical flux operation of a membrane bioreactor. Journal of .Membrane Science, 209, pp 391–403.

Cho, J., Song, K.G., Ahn, K.H. (2005). The activated sludge and microbial substances influences on membrane fouling in submerged membrane bioreactor: unstirred batch cell test. Desalination, 183, pp 425–429.

Choi, H., Zhang, K., Dionysiou, D.D., Oerther, D.B. and Sorial, G.A. (2005). Influence of crossflow velocity on membrane performance during filtration of biological suspension. Journal of Membrane Science, 248, 189–199.

Choi, H., Zhang, K., Dionysiou, D.D., Oerther, D.B., Sorial, G.A. (2005). Influence of cross-flow velocity on membrane performance during filtration of biological suspension. Journal of Membrane Science, 248, pp 189-199.

Choudhary S, Schmidt-Dannert C. (2010). Applications of quorum sensing in biotechnology. Appl Microbiol Biotechnol. 86:1267-1279

Christensen, B.E., (1989). The role of extracellular polysaccharides in biofilms. Biotechnology 10, 181-202.

Cicek, N. (2002). Membrane Bioreactors in the Treatment of Wastewater Generated from Agricultural Industries and Activities. AIC 2002 Meeting CSAE/SCGR Program. Saskatoon, Saskatchewan, CSAE/SCGR.

Cicek, N. (2003). A Review of membrane bioreactors and their potential application in the treatment of agricultural wastewater. Canadian Biosystems Engineering, 45(6), 37-49.

Cicek, N., Franco, J.P., Suidan, M.T., Urbain, V., Manem, J. (1999). Characterization and comparison of a membrane bioreactor and a conventional activated sludge system in the treatment of wastewater containing high-molecular weight compounds. Water Environment Research, 71, pp 64-70.

Cicek, N., J. Franco, T. Makram, V. Suidan and J. Manem. (1999). Characterization and Comparison of a Membrane Bioreactor and a Conventional Activated-Sludge System in the Treatment of Wastewater Containing High-Molecular Weight Compounds. Water Environment Research 71(1): 64-70.

Cirja, M., P. Ivashechkin, A. Schaeffer and P. Corvini (2008). Factors affecting the removal of organic micropollutants from wastewater in conventional treatment plants (CTP) and membrane bioreactors (MBR). Reviews in Environmental Science and Biotechnology 7(1): 61-78.

Cirja, M., S. Zuehlke, P. Ivashechkin, J. Hollender, A. Sch‰offer and P. F. X. Corvini. (2007). Behavior of two differently radiolabelled 17[alpha]-ethinylestradiols continuously applied to a laboratory-scale membrane bioreactor with adapted industrial activated sludge. Water Research 41(19): 4403-4412.

Clara, M., B. Strenn and N. Kreuzinger. (2004a). Comparison of the behaviour of selected micropollutants in a membrane bioreactor and a conventional wastewater treatment plant. Water Science and Technology 50(5): 29-36.

Clara, M., B. Strenn, E. Saracevic and N. Kreuzinger. (2004b). Adsorption of bisphenol-A, 17[beta]-estradiole and 17[alpha]-ethinylestradiole to sewage sludge. Chemosphere 56(9): 843-851.

Clara, M., B. Strenn, O. Gans, E. Martinez, N. Kreuzinger and H. Kroiss. (2005a). Removal of selected pharmaceuticals, fragrances and endocrine disrupting compounds in a membrane bioreactor and conventional wastewater treatment plants. Water Research 39(19): 4797-4807.

Clara, M., N. Kreuzinger, B. Strenn, O. Gans and H. Kroiss. (2005b). The solids retention time - a suitable design parameter to evaluate the capacity of wastewater treatment plants to remove micropollutants. Water Research 39(1): 97-106.

Clouzot, L., P. Doumenq, N. Roche and B. Marrot. (2010a). Kinetic parameters for 17[alpha]-ethinylestradiol removal by nitrifying activated sludge developed in a membrane bioreactor. Bioresource Technology 101(16): 6425-6431.

Clouzot, L., P. Doumenq, P. Vanloot, N. Roche and B. Marrot. (2010b). Membrane bioreactors for 17[alpha]-ethinylestradiol removal. Journal of Membrane Science 362(1-2): 81-85.

Colborn, T., F. von Saal and A. Soto. (1993). Developmental Effects of Endocrine Disrupting Chemicals in Wildlife and Humans." Environmental Health Perspective 101: 378-384.

Cornel, P., Wagner, M., and Krause, S. (2003). Investigation of oxygen transfer rates in full scale membrane bioreactor. Water Science and Technology, 37(11), 313-319.

Correll, J. (1998). The Role of Phosphorus in the Eutrophication of Receiving Waters. Environmental Quality. 27: 261-266.

Cosenza, A., Bella, G. D., Mannina, G., Torregrossa, M. (2013). The role of EPS in fouling and foaming phenomena for a membrane Bioreactor. Bioresource Technology 147, 184-192

Cosgrove, T. (2010). Colloids Science - Principles, Methods and Applications.: John Wiley and Sons.West Sussex, United Kingdom

Costerton, J. W., B. Ellis, K. Lam, F. Johnson, and A. E. Khoury. (1994). Mechanism of electrical enhancement of efficacy of antibiotics in killing biofilm bacteria. Antimicrob. Agents Chemother. 38:2803-2809.

Cui, C., S. Ji and H. Ren. (2006). Determination of Steroid Estrogens in Wastewater Treatment Plant of A Controceptives Producing Factory. Environmental Monitoring and Assessment 121(1): 407-417.

Daigger G.T and Roper R. E. (1985). The relationship between SVI and activated sludge settling characteristics. J. Water Pollut. Control Fed. 57 (8) 859-866.

Daneshvar, N., Ashassi Sorkhabi, H. and Kasiri, M. B. (2004). Decolorization of dye solution containing Acid Red 14 by electrocoagulation with a comparative investigation of different electrode connections. Journal of Hazardous Materials, 112(1-2), 55-62.

Das, K., Raha, S., and Somasundaran, P. (2009). Effect of polyacrylic acid molecular weight on the floc stability during prolonged settling. Colloids and Surfaces. 351 (1-3): 1-8.

Dash, B. P. and Chaudhari, S. (2005). Electrochemical denitrificaton of simulated ground water. Water Research. 39, 4065–4072

Davies, K. J. P., D. Lloyd and L. Boddy. (1989). The Effect of Oxygen on Denitrification in Paracoccus denitrificans and Pseudomonas aeruginosa. Journal of General Microbiology 135: 2445-2451.

Davis, C. P., N. Wagle, M. D. Anderson, and M. M. Warren. (1991). Bacterial and fungal killing by iontophoresis with long-lived electrodes. Antimicrob. Agents Chemother. 35:2131–2134.

De Freitas, J. M., and Meneghini, R. (2001). Iron and its sensitive balance in the cell. Mutation Res.-Foundam. Mol. Mech. Mutagen., 475, 153-159.

De Gusseme, B., B. Pycke, T. Hennebel, A. Marcoen, S. E. Vlaeminck, H. Noppe, N. Boon and W. Verstraete. (2009). Biological removal of 17[alpha]-ethinylestradiol by a nitrifier enrichment culture in a membrane bioreactor. Water Research 43(9): 2493-2503.

de la Torre T, Iversen V, Meng F, Stüber J, Drews A, Lesjean B, Kraume M. (2010). Searching for a universal fouling indicator for membrane bioreactors. Desalin Water Treat 18(1-3), 264-269

de la Torre T, Lesjean B., Drews A. and Kraume M. (2008). Monitoring of transparent exopolymer particles (TEP) in a membrnae bioreactor (MBR) and correlation with other fouling indicators. Water Science and Technology 58(10): 1903-1909.

de Mes, T., G. Zeeman and G. Lettinga. (2005). Occurrence and Fate of Estrone, 17-estradiol and 17-ethynylestradiol in STPs for Domestic Wastewater. Reviews in Environmental Science and Biotechnology 4(4): 275-311.

Defrance, L., and Jaffrin, M.Y. (1999). Comparison between filtrations at fixed transmembrane pressure and fixed permeate flux: application to a membrane bioreactor used for wastewater treatment. Journal of Membrane science, 152,203–210.

Defrance, L., and Jaffrin, M.Y. (1999). Reversibility of fouling formed in activated sludge filtration. Journal of Membrane science. 157, 73–84.

Defrance, L., Jaffrin, M.Y., Gupta, B. Paullier, P., en Geaugey, V. (2000). Contribution of various constituents of activated sludge to membrane bioreactor fouling. Bioresource Technology, 38, pp 45-53.

Defrance, L., Jaffrin, M.Y., Gupta, B., Paullier, P., and Geaugey, V. (2000). Contribution of various constituents of activated sludge to a membrane bioreactor fouling. Bioresour. Technol., 73, 105–112.

del Pozo, J. L, Rouse, M. S., Mandrekar, J. N., Steckelberg, J. M. and Patel, P. (2009). The Electricidal Effect: Reduction of Staphylococcus and Pseudomonas Biofilms by Prolonged Exposure to Low-Intensity Electrical Current. Antimicrobial Agents and Chemotherapy. 53(1), 41-45

Delaire, C., Van Genuchten C. M., Nelson, K. L., Amrose, S. E., Gadgil, A., J. (2015). E. coli Attenuation by Fe Electrocoagulation in Synthetic Bengal Groundwater: 1 Effect of pH and Natural Organic Matter. Environ Sci Technol. 49(16), 9945-53

Delgado, S., Diaz, F., Vera, L., Diaz, R., and Elmaleh, S. (2004). Modeling hollow-fiber ultrafiltration of biologically treated wastewater with and without gas sparing. Journal of Membrane science, 228, 55–63.

Den, W., and Huang, C. (2006). Electrocoagulation of Silica Nanoparticles in Wafer Polishing Wastewater by a Multichannel Flow Reactor: A Kinetic Study. Journal of Environmental Engineering. 132(12): 1651-1658

Dentel, S.K., and Abu-Orf, M.M. (1995). Laboratory and full-scale studies of liquid stream viscosity and streaming current for characterization and monitoring of dewaterability. Water Research, 29, 2663-2672.

Desbrow, C., E. J. Routledge, G. C. Brighty, J. P. Sumpter and M. Waldock. (1998). Identification of Estrogenic Chemicals in STW Effluent. 1. Chemical Fractionation and in Vitro Biological Screening. Environ. Sci. Technol. 32(11): 1549-1558.

Do, J.-S., and Chen, M.-L. (1994) Decolourization of dye-containing solutions by electrocoagulation. Journal of Applied Electrochemistry 24 (8), 785-790.

Dobretsov S, Teplitski M, Bayer M. (2011). Inhibition of marine biofouling by bacterial quorum sensing inhibitors. Biofouling. 27:893-905

Dobretsov S, Teplitski M, Paul V. (2009). Mini-review: quorum sensing in the marine environment and its relationship to biofouling. Biofouling. 25:413-427

Dolan, M. D., Dave, N. C., Ilyushechkin, A. Y., Morpeth, L. D., and McLennan, K. G. (2006). Review: Composition and operation of hydrogen selective amorphous alloy membranes. Journal of Membrane science, 285,30–55.

Dong Y.H., Wang L.H., Zhang L.H. (2007). Quorum-quenching microbial infections: mechanisms and implications. Philos Trans R Soc Lond B Biol Sci. 362:1201-1211

Drees K. P., Abbaszadegan M,Maier R. M. (2003). Comparative electrochemical inactivation of bacteria and bacteriophage. Water Res., 37 (10), 2291-2300.

Drewes, J. E., J. Hemming, S. Ladenburger, J. Schauer and S. Sonzogni. (2005). An Assessment of Endocrine Disrupting Activity Changes during Wastewater Treatment through the Use of Bioassays and Chemical Measurements. Water Environment Research 77(1): 12-23.

Drews, A., Mante, J., Iversen, V., Vocks, M., Lesjean, B., Kraume, M., (2007). Impact of ambient conditions on SMP elimination and rejection in MBRs. Water Research 41, 3850-3858.

Drews, A., Vocks, M., Iversen, V., Lesjean, B., Kraume, M. (2005). Influence of unsteady membrane bioreactor operation on EPS formation and filtration resistance. In: Proceedings of the International Congress on Membranes and Membrane Processes (ICOM), Seoul, Korea.

Drogui, P., Asselin, M., Brar, S. K., Benmoussa, H., Blais, J. F. (2009). Electrochemical removal of organics and oil from sawmill and ship effluents. Can. J. Civil. Eng. 36, 529-539.

Drogui, P., Asselin, M., Brar, S.K., Benmoussa, H. (2008). Blais J.F. Electrochemical removal of pollutants from agro-industry wastewaters. Sep. Purif. Technol. 61, 301-310.

Droste, R. L. (1997). Theory and practice of water and wastewater treatment. New York : John Wiley & Sons. pp385

Drouiche, N., Ghaffour, N., Lounici, H., Mameri, N., Maallemi, A., and Mahmoudi, H. (2008). Electrochemical treatment of chemical mechanical polising wastewater: removal of fluoride- sludge characteristics- operating cost. Desalination. 223(1-3): 134-142.

Drysdale, G., H. Kasan and F. Bux. (1999). Denitrification by heterotrophic bacteria during activated sludge treatment. Water SA 25(3): 357 - 362.

Du, J.R.; Peldszus, S.; Huck, P.M.; Feng, X. (2009). Modification of poly(vinylidene fluoride) ultrafiltration membranes with poly(vinyl alcohol) for fouling control in drinking water treatment. Water Res., 43, 4559–4568.

Duan, J., and Gregory, J. (2003). Coagulation by hydrolysing metal salts. Advances in Colloid and Interface Science. 100-102: 475-502.

Dubois, M., Gilles, K.A., Hamilton, J.K., Rebers, P.A., Smith, F. (1956). Colorimetric method for determination of sugars and related substances. Analytical Chemistry, 28, pp 350-356.

Durante, F., G. Di Bella, M. torregrossa and G. Viviani. (2006). Particle size distribution and biomass growth in a submerged membrane bioreactor." Desalination 199: 193-495.

Egemen, E., Corpening, J., and Nirmalakhandan, N. (2001). Evaluation of an ozonation system for reduced waste sludge generation. Water science and Technology, 44(2-3), 445-452.

Elektorowicz M, Hasan S, Oleszkiewicz A. J., (2012). A submerged membrane electro bioreactor achieves high removal efficiencyes. Water Environment and Technology, 60-62

Elektorowicz M, Oleszkiewicz J.A. Melhem-Bani K (2008) Submerged Membrane Electro- bioreactor (SMEBR). US Patent Appl. Ser. Number 61/094,266, Sept. 4

El-Gohary, F., Tawfik, A., and Mahmoud, U. (2010). Comparitive study between chemical coagulation/ precipitation (C/P) versus coagulation/dissolved air flotation (C/DAF) for pre- treatment of personal care products (PCPs) wastewater. Desalination. 252(1-3): 106-112.

Esperanza, M., M. T. Suidan, F. Nishimura, Z.-M. Wang, G. A. Sorial, A. Zaffiro, P. McCauley, R. Brenner and G. Sayles. (2004). "Determination of Sex Hormones and Nonylphenol

Ethoxylates in the Aqueous Matrixes of Two Pilot-Scale Municipal Wastewater Treatment Plants." Environmental Science & Technology 38(11): 3028-3035.

Evenblij, H. (2006). Filtration characteristics in membrane bioreactors. PhD thesis, Delft University of Technology, the Netherlands.

Evenblij, H., Geilvoet, S.P., Graaf, J.H.J.M. van der, Roest, H.F. van der (2005). Filtration Characterisation for assessing MBR performance: three cases compared. Desalination, 178, pp 115-124.

Evenblij, H., Graaf, J.H.J.M. van der (2004). Occurrence of EPS in activated sludge from a membrane bioreactor treating municipal wastewater. Water Science & Technology, 50, pp 293–300.

Everett, D. H. (1994). Basic principles of colloid science. The Royal Society of Chemistry, UK.

Eyvaz, M., Kirlaroglu, M., Aktas, T.S., Yuksel, E. (2009). The effects of alternating current electrocoagulation on dye removal from aqueous solutions, Chem. Eng. J. 153, 16–22.

Fan F., Zhou H., and Husain H. (2007). Use of chemical coagulants to control fouling potential for wastewater membrane bioreactor processes. Water Environ Res., 79(9), 952-957.

Fan, F., Zhou, H., Husain, H. (2006). Identification of wastewater sludge characteristics to predict critical flux for membrane bioreactor processes. Water Research, 40, pp 205- 212

Fane, A.G., Fell, C.J.D. (1987). A review of fouling and fouling control in ultrafiltration. Desalination, 62, pp 117-136.

Fane, A.G., Fell, C.J.D., en Nor, M.T. (1981). Ultrafiltration/Activated sludge system - development of a predictive system. Polym. Sci. Technol., 13, 631-658.

Farrell, J., Rose, A.H., (1967). Temperature effects on microorganisms. In: Rose, A.H. (Ed.), Thermobiology. Academic Press, London, 147-218.

Fatone, F., D. Bolzonella, P. Battistoni and F. Cecchi. (2005). Removal of nutrients and micropollutants treating low loaded wastewaters in a membrane bioreactor operating the automatic alternate-cycles process." Desalination 183(1-3): 395-405.

Fatone, F., P. Battistoni, D. Bolzonella, P. Pavan and F. Cecchia. (2008). Long-term experience with an automatic process control for nitrogen removal in membrane bioreactors. Desalination 227(1-3): 72-84.

Fawehinmi, F., Lens, P., Stephenson, T., Rogalla, F., Jefferson, B. (2004). The influence of operating conditions on EPS, SMP and bio-fouling in anaerobic MBR. In: Proceedings of the Water Environment-Membrane Technology Conference, Seoul, Korea.

Fawell, J. K., D. Sheahan, H. A. James, M. Hurst and S. Scott. (2001). Estrogens and estrogenic Activity in Raw and Treated Water in Severn Trent Water. Water Research 35(5): 1240-1244.

Field, R.W., Wu, D., Howell, J.A., en Gupta, B.B. (1995). Critical flux concept for microfiltration fouling. Journal of Membrane Science, 100, 259-272.

Flemming, H. C. (1997). Reverse osmosis membrane biofouling. Exp. Therm. Fluid Sci., 14, 382-391.

Flemming, H.C., Wingender, J. (2001). Relevance of microbial extracellular polymeric substances (EPSs). Part I. Structural and ecological aspects. Water Science & Technology, 43, pp 1–8.

Fonseca, A.C., Summers, R.S., Greenberg, A.R., Hernandez, M.T. (2007). Extracellular polysaccharides, soluble microbial products and natural organic matter impact on nanofiltration membranes flux decline. Environ. Sci. Technol., 41, 2491-2497.

Frølund, B., Griebe, T., Nielsen, P.H., (1995). Enzymatic activity in the activated-sludge floc matrix. Appl. Microbiol. Biotechnol. 43 (4), 755-761.

Frølund, B., Palmgren, R., Keiding, K., Nielsen, P.H. (1996). Extraction of extracellular polymers from activated sludge using a cation exchange resin. Water Research, 30, pp1749–1758.

Fuerhacker, M., H. Bauer, R. Ellinger, U. Spree, H. Schmid, F. Zibuschka and H. Puxbaum. (2000). Approach for a novel control strategy for simultaneous nitrification/denitrification in activated sludge reactors. Water Resources 34(9): 2499-2506.

Futselaar, H., Schonewille, H., Vente, D. de, Broens, L. (2007). NORIT AirLift MBR: sidestream system for municipal wastewater treatment. Desalination, 204, pp 1-7.

Gander, M., Jefferson, B., en Judd, S. (2000). Aerobic MBRs for domestic wastewater treatment: a review with cost considerations. Separation & Purification Technology, 18, 119-130.

Gao, D. W., Wen, Z. D., Li, B., Liang, H. (2013). Membrane fouling related to microbial community and extracellular polymeric substances at different temperatures. Bioresource Technology 143, 172-177

Gao, M., Yang, M., Li, H., Yang, Q., Zhang, Y. (2004). Comparison between a submerged membrane bioreactor and a conventional activated sludge system on treating ammonia-bearing inorganic wastewater. Journal of Biotechnology, 108, pp 265–269.

Gao, P., Chen, X., Shen, F., and Chen, G. (2005). Removal of chromium(VI) from wastewater by combined electrocoagulation–electroflotation without a filter. Separation and Purification Technology. 43(2): 117–123.

Gao, S. Yang, J.X., Tian J.Y., Ma, F., Tu G., Du, M.A. (2010). Electro-coagulation–flotation process for algae removal. J Hazard Mater 177, 336–343.

Gao, W.J., Qu, X., Leung, K. T., Liao, B. Q. (2012). Influence of temperature and temperature shock on sludge properties, cake layer structure, and membrane fouling in a submerged anaerobic membrane bioreactor. Journal of Membrane Science 421, 131-144

Ge, J., Qu, J., Lei, P., and Liu, H. (2004). New bipolar electrocoagulation–electroflotation process for the treatment of laundry wastewater. Separation and Purification Technology. 36(1): 33-39.

Gehlert, G., Abdulkadir, M., Fuhrmann, J., and Hapke, J. (2005). Dynamic modeling of an ultrafiltration module for use in a membrane bioreactor. Journal of Membrane science, 248, 63–71

Geilvoet, S.P., Remy, M., Evenblij, H., Temmink, H., Graaf, J.H.J.M. van der (2006). Tracing membrane foulants in membrane bioreactors by filtration characterisation and fractionation.. Water science and technology: water supply, 6(1), pp 165-172.

Geissler, S., Wintgens, T., Melin, T., Vossenkaul, K., and Kullmann, C. (2005). Modelling approaches for filtration processes with novel submerged capillary modules in membrane bioreactors for wastewater treatment. Desalination, 178 (1–3), 125–134.

Geng Z., Hall E. R. (2007). A comparative study of fouling-related properties of sludge from conventional and membrane enhanced biological phosphorus removal processes. Water Res. 41 (19), 4329-4338.

Geradi, M.H., 1986. Effects of heavy metals upon the biological wastewater treatment process. Public Works, 117, 77–80.

Ghernaout, D., Badis, A., Kellil, A. & Ghernaout, B. (2008). Application of electrocoagulation in Escherichia coli culture and two surface waters. Desalination 219, 118–125.

Ghernaout, D., Ghernaout, B. (2010). From chemical disinfection to electrodisinfection: The obligatory itinerary? Desalin Water Treat 16, 156–175.

Ghosh, D., Medhi, C. R., Purkait, M. K. (2008). Treatment of fluoride containing drinking water by electrocoagulation using monopolar and bipolar electrode connections, Chemosphere 73, 1393-1400.

Ghosh, D., Solanki, H. and Purkait, M.K. (2008) Removal of Fe (II) from tap water by electrocoagulation technique. Journal of Hazardous Materials, 155, 135-143.

Gieseke, A., Tarre, S., Green, M., and Beer, D. (2006). Nitrification in a biofilm at low pH values: Role of in situ microenvironments and acid tolerance. Appl. Environ. Microbiol., 72 (6), 4283-4292.

Gil, J. A., Tu, L., Rueda, A. C., Rodríguez M., Prats M. (2010). Influence of temperature variations on the cake resistance and EPS of MBR mixed liquor fractions. Desalination and Water Treatment 18, 1-11

Golder, A. K., Hridaya, N., Samanta, A.N., Ray, S., (2005). Electrocoagulation of methylene blue and eosin yellowish using mild steel electrodes. J. Hazard. Mater. 127 (1-3), 134-140

Golder, A. K., Samanta, A. N., and Ray, S. (2006). Removal of phosphate from aqueous solutions using calcined metal hydroxides sludge waste generated from electrocoagulation. Separation and Purification Technology. 52(1): 102-109.

Golder, A. K., Samanta, A. N., Ray, S. (2007). Removal of Cr^{3+} by electrocoagulation with multiple electrodes: Bipolar and monopolar configurations, J. Hazard. Mater. 141, 653 - 661.

Gomes, J.A.G., Cocke, D.L., Daida, P., Kesmez, M., Weir, M., Moreno, H., Parga, J.R., Irwin, G., McWhinney, H., Grady, T., and Peterson, E. (2007) Arsenic removal by electrocoagulation using combined Al–Fe electrode system and characterization of products. J. Hazard. Mater. B139 , 220–231.

Gómez-Suárez, C.; Pasma, J.; Van der Borden, A.J.; Wingender, J.; Flemming, H.-C.; Busscher, H.J.; van der Maei, H.C. (2002), Influence of extracellular polymeric substances on deposition and redeposition of Pseudomonas aeruginosa to surfaces. Microbiology, 148, 1161-1169.

Goodridge F. and Scott, K. (1994). Electrochemical Process Engineering, Plenum Press, New York

Gordon C.C. Yang, Chi-Ming Tsai. Performance evaluation of a simultaneous electrocoagulation and electrofiltration module for the treatment of Cu-CMP and oxide-CMP wastewaters. Journal of Membrane Science 286 (2006) 36–44

Gorner, T., Donato, P. de, Ameil, M.H., Montarges-Pelletier, E., Lartiges, B.S. (2003). Activated sludge exopolymers: separation and identification using size exclusion chromatography and infrared micro-spectroscopy. Water Research, 37, pp 2388–2393.

Grahl T, Markl, H. (1996). Killing of microorganism by pulsed electric fields. Appl Micro-biol Biotechnol, 45:148-57.

Grelier, P., Rosenberger, S., and Tazi-Pain, A. (2006). Influence of sludge retention time on membrane bioreactor hydraulic performance. Desalination, 192, 10-17.

Gu, Z., Liao, Z., Schulz, M., Davis, J. R., Baygents, J., and Farrell, J. (2009). Estimating Dosing Rates and Energy Consumption for Electrocoagulation Using Iron and Aluminum Electrodes. Ind. Eng. Chem. Res. 48(6): 3112-3117.

Guglielmi, G., Prakash Saroj, D., Chiarani, D., Andreottola, G. (2007). Sub-critical fouling in a membrane bioreactor for municipal wastewater treatment: experimental investigation and mathematical modelling. Water Research, 41, pp 3903-3914.

Gunder, B., Krauth, K. (1998). Replacement of secondary clarification by membrane separation - results with plate and hollow fibre modules. Water Science & Technology, 38, 383–393.

Gurses, A., Yalcin, M., Dogar, C. (2002). Electrocoagulation of some reactive dyes: a statistical investigation of some electrochemical variables. Waste Manage. 22 (5), 491- 499

Haiyan, R., J. Shulan, N. ud din Ahmad, W. Dao and C. Chengwu. (2007). Degradation characteristics and metabolic pathway of 17[alpha]-ethynylestradiol by Sphingobacterium sp. JCR5. Chemosphere 66(2): 340-346.

Han, M.; Song, J.; Kwon, (2002). A. Preliminary Investigation of Electrocoagulation as a Substitute for Chemical Coagulation. Water Sci. Technol. 2 (5), 73-76.

Han, S.-S., Bae, T.-H., Jang, G.-G., and Tak, T.-M. (2005). Influence of sludge retention time on membrane fouling and bioactivities in membrane bioreactor system. Process Biochemistry. 40(7): 2393-2400.

Han, W.-Q., Wang, L.-J., Sun, X.-Y., and Li, J.-S. (2008). Treatment of bactericide wastewater by combined process chemical coagulation, electrochemical oxidation and membrane bioreactor. Journal of Hazardous Material. 151(2-3): 306- 315.

Hanselman, T., D. Graetz and A. Wilkie. (2003). "Manure-Borne Estrogens as Potential Environmental Contaminants." Environ. Sci. Technol. 37(24): 5471-5478.

Hansen, H., Nu~nez, P., Raboy, D., Schippacasse, I., and Grandon, R. (2007). Electrocoagulation in wastewater containing arsenic: Comparing different process designs. Electrochimica Acta. 52(10): 3464–3470.

Hansen, H.K., Nunez, P., Grandon, R., (2005). Electrocoagulation as a remediation tool for wastewaters containing arsenic. Miner Eng. 19 (5), 521-524

Harif, T., Khai, M., Adin. A., (2012). Electrocoagulation versus chemical coagulation: Coagulation/ flocculation mechanisms and resulting floc characteristics. Water Research 46, 3177-3188

Harms, G., A. C. Layton, H. M. Dionisi, I. R. Gregory, V. M. Garrett, S. A. Hawkins, K. G. Robinson and G. S. Sayler. (2002). Real-Time PCR Quantification of Nitrifying Bacteria in a Municipal Wastewater Treatment Plant. Environmental Science & Technology 37(2): 343-351.

Hasan, S. W., Elektorowicz, M., Oleszkiewicz, J. A. (2014). Start-up period investigation of pilot-scale submerged membrane zelectro-bioreactor (SMEBR) treating raw municipal wastewater. Chemosphere 97, 71-77

Hasar, H., Kinaci, C., and Unlu, A. (2002). Viability of microbial mass in a submerged membrane bioreactor. Desalination, 150, 263-268.

Hashimoto, T. and T. Murakami. (2009). Removal and degradation characteristics of natural and synthetic estrogens by activated sludge in batch experiments. Water Research 43(3): 573-582.

Hawari, A., H. Du, F., Baune, M., Thöming, J. (2015). A fouling suppression system in submerged membrane bioreactors using dielectrophoretic forces. Journal of Environmental Sciences. 29, 139-145

He, S.-b., G. Xue and B.-z. Wang. (2009). Factors affecting simultaneous nitrification and de-nitrification (SND) and its kinetics model in membrane bioreactor. Journal of Hazardous Materials 168(2-3): 704-710.

Hegaba, H.M., Zou, L. Graphene oxide-assisted membranes: Fabrication and potential applications in desalination and water purification. (2015). Journal of Membrane Science. 484(15), 95–106.

Henriques, I. D. S., R. D. Holbrook, R. T. Kelly Ii and N. G. Love. (2005). The impact of floc size on respiration inhibition by soluble toxicants - a comparative investigation. Water Research 39(12): 2559-2568.

Henry, J. G., Salenieks, E. E., (1980). Variation in sludge settleability with temperature. Water Poll. Res. J. Can. 15 (1), 73-82.

Hibiya, K., A. Terada, S. Tsuneda and A. Hirata. (2003). Simultaneous nitrification and denitrification by controlling vertical and horizontal microenvironment in a membrane-aerated biofilm reactor. Journal of Biotechnology 100(1): 23-32.

Hijnen, W.A.M., Biraud, D., Cornelissen, E.R., Van der Kooij, D., (2009). Threshold concentration of easily assimilable organic carbon in feed water for biofouling of spiral-wound membranes. Environmental Science and Technology 43, 4890 - 4895.

Holakoo, L., G. Nakhla, A. S. Bassi and E. K. Yanful. (2007). Long term performance of MBR for biological nitrogen removal from synthetic municipal wastewater. Chemosphere 66(5): 849-857.

Holbrook, R. D., Higgins, M. J., Murthy, S. N., Fonseca, A. D., Fleischer, E.J., Daigger, G.T., Grizzard, T.J., Love, N. G., and Novak, J.T.(2004). Effect of alum addition on the performance of submerged membranes for wastewater treatment." Water Environ. Res., 76 (7), 2699-2702.

Holbrook, R. D., J. T. Novak, T. J. Grizzard and N. G. Love. (2002). Estrogen Receptor Agonist Fate during Wastewater and Biosolids Treatment Processes: A Mass Balance Analysis. Environmental Science & Technology 36(21): 4533-4539.

Holbrook, R. D., N. G. Love and J. T. Novak. (2004). Sorption of 17beta-Estradiol and 17alpha-Ethinylestradiol by Colloidal Organic Carbon Derived from Biological Wastewater Treatment Systems." Environmental Science & Technology 38(12): 3322-3329.

Holman, J. B. and D. G. Wareham. (2005). COD, ammonia and dissolved oxygen time profiles in the simultaneous nitrification/denitrification process. Biochemical Engineering Journal 22(2): 125-133.

Holt, P. H., Barton, G. W., Wark, M., and Mitchell, A. A. (2002). A quantitative comparison between chemical dosing and electrocoagulation. Colloids and Surfaces A: Physicochem. Eng. Aspects, 211,233-248.

Holt, P. K., Barton, G.W. & Mitchell, C. A. (2005). The future for electrocoagulation as a localised water treatment technology. Chemosphere 59, 355–367.

Holtan, H., Kamp-Nielsen, L., Stuanes, A.O., (1988). Phosphorus in soil, water and sediment: an overview. Hydrobiologia 170, 19 - 34.

Hong, S.P., Bae, T.H., Tak, T.M., Hong, S., Randall, A. (2002). Fouling control in activated sludge submerged hollow fiber membrane bioreactors. Desalination, 143, pp 219-228.

Horn, H. and Lackner S. (2014). Modeling of Biofilm Systems: A Review. Adv Biochem Eng Biotechnol 146: 53–76

Horner, G., and Duffey, J.G. (1983). Electrochemical removal of heavy metals from waste water. The American Electroplaters Society Annual Meeting, Denver, CO.

Howland, W. E. (1953). Effect of Temperature on Sewage Treatment Processes, Sewage and Industrial Wastes, 25(2), 161-169

Hu, C.Y., Lo, S.L., Kuan, W.H., (2005). Effects of the molar ratio of hydroxide and fluoride to Al(III) on fluoride removal by coagulation and electrocoagulation. J. Colloid Interf. Sci. 283 (2), 472

Hu, J.; Shang, R.; Deng, H.; Heijman, S.G.J.; Rietveld, L.C. (2014). Effect of PAC dosage in a pilot-scale PAC-MBR treating micro-polluted surface water. Bioresour. Technol., 154, 290–296.

Huang, X., Gui, P., and Qian, Y. (2001). Effect of sludge retention time on microbial behavior in a submerged membrane bioreactor. Process Biochemistry, 36, 1001-1006.

Huisman, I.H., Tragardh, G., Tragardh, C., Pihlajamaki, A., (1998). Determining the zeta-potential of ceramic microfiltration membranes using the electroviscous effect. Journal of Membrane Science 147 (2), 187-194

Hulsheger, H., Potel, J., Niemann, E. G. (1983). Electric field effects on bacteria and yeast cells. Radiat Environ Biophys. 22:149-62.

Hunter, R. J. (1988). Zeta potential in Colloid Science: Principles and Applications. Acadmic Press, UK.

Huyskens, C., Brauns, E., Hoof, E. van, Wever, H. de (2008). A new method for the evaluation of the reversible and irreversible fouling propensity of MBR mixed liquor. Journal of Membrane Science, 1, pp 185-192.

Ibeid, s., Elektorowicz, M., Oleszkiewicz, J. A. (2013). Novel electrokinetic approach reduces membrane fouling. water research 47 (2013) 6358-6366

Irdemez, S., Demircioglu, N., and Yildiz Y. Z. (2006). The effects of pH on phosphate removal from wastewater by electrocoagulation with iron plate electrodes. Journal of Hazardous Materials, 137, 1231–1235.

Irvine, R. L., D. V. S. Murthy, M. L. Arora, J. L. Copeman and J. A. Heidman (1987). Analysis of Full-Scale SBR Operation at Grundy Center, Iowa." Journal (Water Pollution Control Federation) 59(3): 132-138.

Ismail, A. F., and David, L. I. B. (2001). Review: A review on the latest development of carbon membranes for gas separation. Journal of membrane science, 193, 1–18.

Ivanovic, I., Leiknes, T., Ødegaard, H. (2008), Fouling Control by Reduction of Submicron Particles in a BF-MBR with an Integrated Flocculation Zone in the Membrane Reactor. Separation Science and Technology. 43(7), 1871-1883

Jacangelo, J.G., Trussell, R.R., and Watson, M. (1997). Role of membrane technology in drinking water treatment in the United States. Desalination, 113 (2–3), 119–127.

Jackman, S. A., Maini, G., Sharman, A. K., and Knowles, C. J. (1999). The effects of direct electrical current on the viability and metabolism of acidophilic bacteria. Enzyme Microbial. Technology, 24, 316-324.

Jagannadh, S. N., and Muralidhara, H. S. (1996). Electrokinetics methods to control membrane fouling. Ind. Eng. Chem. Res., 35, 1133-1140.

Jain, S., Sharma, A., Basu, B. (2015). Vertical electric field induced bacterial growth inactivation on amorphous carbon electrodes. Carbon, 81, 193-202

Jang, N., Ren, X., Cho, J., and Kim In, S. (2006). Steady-state modeling of bio fouling potentials with respect to the biological kinetics in the submerged membrane bioreactor (SMBR). Journal of membrane science, 284,352-360.

Jang, N., X. Ren, K. Choi and I. Kim (2006). Compariosn of membrane biofouling in nitrification and denitrification for membrane bioreactor (MBR). Water Science Technology 53(6): 43-49.

Jarvisa, P., Jeffersona, B., Gregoryb, J., Parsonsa, S.A. (2005). A review of floc strength and breakage. Water Research 39, 3121-3137

Jass, J., and H. M. Lappin-Scott. (1996). The efficacy of antibiotics enhanced by electrical currents against Pseudomonas aeruginosa biofilms. J. Antimicrob. Chemother. 38:987-1000.

Jass, J., J. W. Costerton, and H. M. Lappin-Scott. (1995). The effect of electrical currents and tobramycin on Pseudomonas aeruginosa biofilms. J. Ind. Microbiol. 15:234–242.

Jenkins, D., M. Richard and G. Daigger (2004). Manual on the causes and control of activated sludge bulking, foaming, and other solids separation problems. London, UK, IWA Publishing.

Jetten, M. S. M., S. Logemann, G. Muyzer, L. A. Robertson, S. de Vries, M. C. M. van Loosdrecht and J. G. Kuenen (1997). Novel principles in the microbial conversion of nitrogen compounds. Antonie van Leeuwenhoek 71(1): 75-93.

Ji, L., Zhou, J. (2006). Influence of aeration on microbial polymers and membrane fouling in submerged membrane bioreactors. Journal of Membrane Science, 276, pp 168-177.

Jiang, J-Q., and Graham, N.J.D. (1998). Pre-polymerized inorganic coagulants and phosphorus removal by coagulation - a review. Water SA., 24 (3), 237–244.

Jiang, T., Kennedy D. M., Guinzobourg, B. F., Vanrolleghem, P.A., and Schippers, J. C. (2005). Optimising the operation of a MBR pilot plant by quantitative analysis of the membrane fouling mechanism. Water Science and Technology, 51 (6-7), 19–25.

Jiang, T., Kennedy, M.D., Meer, W.G.J. van der, Schippers, J.C., Vanrolleghem, P.A. (2003). The role of blocking and cake filtration in MBR fouling. Desalination, 157, pp 335-343.

Jiang, T., Kennedy, M.D., Yoo, C.K., Nopens, I., Meer, W.G.J. van der, Futselaar, H., Schippers, J.C., Vanrolleghem, P.A. (2007). Controlling submicron particle deposition in a side-stream membrane bioreactor: a theoretical hydrodynamic modelling approach incorporating energy consumption. Journal of Membrane Science, 297, pp 141-151.

Jimenez, C., Talavera, B., Saez, C., Canizares, P., and Rodrigo, M. A. (2010). Study of the production of hydrogen bubbles at low current densities for electroflotation process. Journal Chem Technol Biotechnol. 85(10): 1368-1373.

Jin, B., Wilen, B.M. and Lant, P. (2003). A comprehensive insight into floc characteristics and their impact on compressibility and settleability of activated sludge. Chemical Engineering Journal, 95, 221-234.

Jinsong, Z., Chuan, H. C., Jiti, Z., and Fane, A. G. (2006). Effect of sludge retention time on membrane bio-fouling intensity in a submerged membrane bioreactor. Separation science and Technology, 284,352-360.

Johnson, A. C. and J. P. Sumpter. (2001). Removal of Endocrine-Disrupting Chemicals in Activated Sludge Treatment Works. Environ. Sci. Technol. 35(24): 4697-4703.

Johnson, A. C. and R. J. Williams. (2004). A Model To Estimate Influent and Effluent Concentrations of Estradiol, Estrone, and Ethinylestradiol at Sewage Treatment Works. Environmental Science & Technology 38(13): 3649-3658.

Johnson, A. C., A. Belfroid and A. Di Corcia (2000). Estimating steroid oestrogen inputs into activated sludge treatment works and observations on their removal from the effluent. The Science of The Total Environment 256(2-3): 163-173.

Johnson, A. C., H. R. Aerni, A. Gerritsen, M. Gibert, W. Giger, K. Hylland, M. J¸rgens, T. Nakari, A. Pickering, M. J. F. Suter, A. Svenson and F. E. Wettstein (2005). Comparing steroid

estrogen, and nonylphenol content across a range of European sewage plants with different treatment and management practices. Water Research 39(1): 47-58.

Johnson, A. C., R. J. Williams, P. Simpson and R. Kanda. (2007). What difference might sewage treatment performance make to endocrine disruption in rivers? Environmental Pollution 147(1): 194-202.

Johnson, D. C., Dandy, D.S., Shamamian, V.A. (2006). Development of a tubular high-density plasma reactor for water treatment. Water Research. 40(2), 311-22.

Joss, A., H. Andersen, T. Ternes, P. R. Richle and H. Siegrist. (2004). Removal of Estrogens in Municipal Wastewater Treatment under Aerobic and Anaerobic Conditions: Consequences for Plant Optimization. Environmental Science & Technology 38(11): 3047-3055.

Joss, A., S. Zabczynski, A. Gbel, B. Hoffmann, D. Lffler, C. S. McArdell, T. A. Ternes, A. Thomsen and H. Siegrist. (2006). Biological degradation of pharmaceuticals in municipal wastewater treatment: Proposing a classification scheme. Water Research 40(8): 1686-1696.

Judd, S. (2005). Fouling control in submerged membrane bioreactors. Water science and technology, 51 (6-7), 27-34.

Judd, S., (2004). A review of fouling of membrane bioreactors in sewage treatment. Water Science Technology 49, 229–235.

Judd, S.J. (2006). The MBR book: principles and applications of membrane bioreactors in water and wastewater treatment. Elsevier, Oxford.

Jun, Y.N., Deng, B.L. (2015) Polymer-matrix nanocomposite membranes for water treatment. Journal of Membrane Science. 479 (1), 256–275.

Juretschko, S., A. Loy, A. Lehner and M. Wagner. (2002). The Microbial Community Composition of a Nitrifying-Denitrifying Activated Sludge from an Industrial Sewage Treatment Plant Analyzed by the Full-Cycle rRNA Approach. Systematic and Applied Microbiology 25(1): 84-99.

Juretschko, S., G. Timmermann, M. Schmid, K. Schleifer, A. Pommerening-Roeser, H. Koops and M. Wagner (1998). Combined molecular and conventional analyses of nitrifying bacterium diversity in activated sludge: Nitrosococcus mobilis and Nitrospira-Like Bacteria as Dominant Populations. Applied and Environmental Microbiology 64(8): 3042-3051.

Kabdasli, I., Arslan-Alaton, I., Vardar, B., and Tunay, O. (2007). Comparison of electrocoagulation, coagulation, and the Fenton process for the treatment of reactive dyebath effluent. Water Science & Technology. 55(10): 125-134.

Kaleli, H. A., and Islam, M. R. (1997). Effect of temperature on the growth of wastewater bacteria. Toxicol. Environ. Chem., 59 (1-4), 111-123.

Kasahara, S., Maeda, K., Ishikawa, M., (2004). Influence of phosphorus on biofilm accumulation in drinking water distribution systems. Water Science and Technology: Water Supply 4, 389 - 398.

Katal, R., Pahlavanzadeh, H. (2011). Influence of different combinations of aluminum and iron electrode on electrocoagulation efficiency: Application to the treatment of paper mill wastewater, Desalination 265, 199–205.

Katsikaris, K., Boukouvalas, C., and Magoulas, K. (2005). Simulation of ultrafiltration process and application to pilot tests. Desalination, 171 (1), 1-11.

Keefer, C. E. (1962). Temperature and Efficiency of the Activated Sludge Process, Journal of Water Pollution Control Federation, 34 (11), 1186-119

Khan, S. J., Visvanathan, C., Jegatheesan, V. (2012). Effect of powdered activated carbon (PAC) and cationic polymer on biofouling mitigation in hybrid MBRs, Bioresour. Technol. 113, 165-168.

Khanal, S. K., B. Xie, M. L. Thompson, S. Sung, S.-K. Ong and J. van Leeuwen. (2006). Fate, Transport, and Biodegradation of Natural Estrogens in the Environment and Engineered Systems. Environmental Science & Technology 40(21): 6537 - 6546.

Khansorthong, S., Hunsom, M. (2009). Remediation of wastewater from pulp and paper mill industry by the electrochemical technique. Chem. Eng. J., 151, 228-234.

Khongnakorn, W., Mori, M., Vachoud, L., Delalonde, M., Wisniewski, C. (2008). Rheological properties of sMBR sludge under unsteady conditions. Proceedings Toulouse MDIW membranes in drinking and wastewater treatment, 63. Toulouse, France.

Khor, S. L., Sun, D. D., Hay, C. T., and Leckie, J. O. (2006). Comparison of submerged membrane bioreactor in different SRT conditions. Water Practice & Technology, 1(3), 22-28.

Khoufi, S., Feki, F., Sayadi, S. (2007). Detoxification of olive mill wastewater by electrocoagulation and sedimentation processes. Journal of Hazardous Materials. 142(1-2): 58-67.

Khoury, A. E., K. Lam, B. Ellis, and J. W. Costerton. (1992). Prevention and control of bacterial infections associated with medical devices. ASAIO J. 38:M174-M178.

Kidd, K., P. Blanchfield, K. Mills, V. Palace, R. Evans, J. Lazorchak and R. Flick. (2007). Collapse of a fish population aftr exposure to synthetic estrogen. Proceedings from the National Academy of Science 104: 8897-8901.

Kim J. O, Jung, J . T., Tae, I., Aoh, G. H. (2007). Electric fields treatment for the reduction of membrane fouling, the inactivation of bacteria and the enhancement of particle coagulation. Desalination. 202, 31-37

Kim S.R., Oh, H.S., Jo, S.J. (2013). Biofouling control with bead-entrapped quorum quenching bacteria in membrane bioreactors: Physical and biological effects. Environ Sci Technol. 47:836-842

Kim, A.S.; Chen, H.; Yuan, R. (2006). EPS biofouling in membrane filtration: An analytic modelling study. J. Colloid Interface Sci., 303, 243-249.

Kim, E.-H., Dwidar, M., Mitchell, R. J., Kwon, Y.-N. (2013). Assessing the effects of bacterial predation on membrane biofouling, Water Res. 47, 6024–6032

Kim, H.-G., Jang, H.-N., Ka, S.-K., and Lee, D.-S. (2008). Effect of electrocoagulation coupled with MBR on performance of membrane permeability. ICOM 2008 Conference, July 12-18, 2008, Honolulu, Hawaii USA.

Kim, H.Y., Yeon, K.M., Lee, C.H., Lee, S., Swaminathan, T. (2006). Biofilm structure and extracellular polymeric substances in low and high dissolved oxygen MBRs. Separation Science and Technology, 41, 1213–1230.

Kim, S., Park, N., Kim, T., and Park. (2007). Reaggregation of Flocs in Coagulation-Cross-Flow Microfiltration J. Envir. Engrg. 133(5), 507-514

Kimura K., Y. Watanabe. (2005) Baffled membrane bioreactor (BMBR) for advanced wastewater treatment: easy modification of existing MBRs for efficient nutrient removal. Water Sci. Techn., 52 (10-11), 427-434.

Kimura, K., Naruse, T., Watanabe, Y., (2009). Changes in characteristics of soluble microbial products in membrane bioreactors associated with different solid retention times: relation to membrane fouling. Water Research 43, 1033-1039.

Kimura, K.; Tanaka, K.; Watanabe, Y. (2014). Microfiltration of different surface waters with/without coagulation: Clear correlations between membrane fouling and hydrophilic biopolymers. Water Res. 49, 434–443.

Kirk, L., C. Tyler, C. Lye and J. Sumpter. (2002). Changes in Estrogenic and Androgenic Activities at Different Stages of Treatment in Wastewater Treatment Works. Environmental Toxicology and Chemistry 21(5): 972.

Kishino, H., Ishida H., et al.; (1996). Domestic wastewater reuse using a submerged membrane bioreactor. Desalination, 106,115–9.

Knoblock, M. D., Sutton, P. M., Mishra, P. N., Gupta, K., and Janson, A. (1994). Membrane biological reactor system for treatment of oily wastewater. Water Environ Reserach, 66(2), 133–139.

Kobya, M., and Delipinar, S. (2008). Treatment of the baker's yeast wastewater by electrocoagulation. Journal of Hazardous Materials, 154 (1- 3), 1133-1140.

Kobya, M., Can, O.T., and Bayramoglu, M. (2003). Treatment of textile wastewaters by electrocoagulation using iron and aluminum electrodes. Journal of Hazardous Materials, 100 (1-3), 163-178.

Kobya, M., Ciftci, C., Bayramoglu, M., Sensoy, M.T. (2007). Study on the treatment of waste metal cutting fluids using electrocoagulation, Sep. Purif. Technol. 60, 285-291.

Kobya, M., Demirbas, E., Can, O.T., Bayramoglu, M., (2005). Treatment of levafix orange textile dye solution by electrocoagulation. J. Hazard. Mater. 132, 183-188

Kobya, M., Demirbas, E., Parlak, N.U., Yigit, S. (2010). Treatment of cadmium and nickel electroplating rinse water by electrocoagulation. Environ. Technol. 31, 1471-1481.

Kobya, M., Hiz, H., Senturk, E., Aydiner, C., and Demirbas, E. (2006). Treatment of potato chips manufacturing wastewater by electrocoagulation. Desalination. 190(1-3): 201-211.

Kobya, M., Senturk, E., Bayramoglu, M. (2006), Treatment of Poultry Slaughterhouse Wastewaters by Electrocoagulation. J. Hazard. Mater.133 (1), 172-176.

Kobya, M.; Demirbas, E. Sozbir, M. (2010). Industrial wastewaters treated by electrocoagulation. Color Technol., 5, 282-288.

Koerner, W., U. Bolz, W. S¸flmuth, G. Hiller, W. Schuller, V. Hanf and H. Hagenmaier. (2000). Input/output balance of estrogenic active compounds in a major municipal sewage plant in Germany. Chemosphere 40(9-11): 1131-1142.

Koh, Y. K. K., T. Y. Chiu, A. R. Boobis, M. D. Scrimshaw, J. P. Bagnall, A. Soares, S. Pollard, E. Cartmell and J. N. Lester. (2009). Influence of Operating Parameters on the Biodegradation of Steroid Estrogens and Nonylphenolic Compounds during Biological Wastewater Treatment Processes. Environmental Science & Technology 43(17): 6646-6654.

Kongjao, S., Damronglerd, S. and Hunsom, M. (2008). Simul- taneous Removal of Organic and Inorganic Pollutants in Tannery Wastewater Using Electrocoagulation Technique. Korean Journal of Chemical Engineering, 25 (4), 703-709.

Koparal, A. S., and Ogutveren, U. B., (2002). Removal of nitrate from water by electroreduction and electrocoagulation. Journal of hazardous materials, B89, 83–94.

Koros, W.J., Ma, Y.H., Shimidzu, T. (1996). Terminology for membranes and membrane processes; UIPAC recommendations. Journal of Membrane Science, 120, pp 149-159.

Kotoyoshi Nakanishi, Hiroharu Tokuda, Takahiko Soga, Takahiro Yoshinaga and Masahisa Takeda. Effect of Electric Current on Growth and Alcohol Production by Yeast Cells. Journal of Fermentation and Bioengineering 85 (2), 1998. 250-253

Kovatcheva, V., Parlapanski, M. (1999). Sono-electrocoagulation of iron hydroxides, Colloids and Surfaces A: Physicochemical and Engineering Aspects 149, 603.

Krampe, J. and K. Krauth (2003). Oxygen transfer into activated sludge with high MLSS concentrations. Water Science and Technology 47(11): 297-303.

Kraume, M., Wedi, D, Schaller, J., Iversen, V., Drews, A. (2009). Fouling in MBR: what use are lab investigations for full scale operation? Desalination, 236, pp 94-103.

Kreuzinger, N., M. Clara, B. Strenn and H. Kroiss. (2004). Relevance of the sludge retention time (SRT) as design criteria for wastewater treatment plants for the removal of endocrine disruptors and pharmaceuticals from wastewater. Water Science and Technology 150(5): 149-156.

Krzeminski, P., Iglesias-Obelleiro, A., Madebo, G., Garrido, J. M., vander Graaf J. H. J. M., van Lier, J. B. (2012). Impact of temperature on raw wastewater composition and activated sludge filterability in full-scale MBR systems for municipal sewage treatment. Journal of Membrane Science 423, 348-361

Kumar, P.R., Chaudhari, S., Khilar, K.C., Mahajan, S.P., (2004). Removal of arsenic from water by electrocoagulation. Chemosphere 55 (9), 1245-1252

Kurt, U., Talha, G. M., Ilhan, F., and Varinca, K. (2008). Treatment of domestic wastewater by electrocoagulation in a cell with Fe-Fe electrodes. Environmental engineering science, 25(2), 153-161.

Ladan H., Nakhla G., Yanful E.K., Bassi A. S.. (2005). Simultaneous nitrogen and phosphorus removal in a continuously fed and aerated membrane bioreactor. J.Env. Engin. 131 (10), 1469-1472.

Lai, K. M., K. Johnson, M. D. Scrimshaw and J. N. Lester. (2000). Binding of waterborn steroid estrogens to solid phases in river and estuarine systems. Environ. Sci. Technol. 34: 3890-3894.

Lai, K. M., M. D. Scrimshaw and J. N. Lester. (2002b). The Effects of Natural and Synthetic Steroid Estrogens in Relation to their Environmental Occurrence. Critical Reviews in Toxicology 32(2): 113-132.

Laine, J.-M., Vial D., Moulart P., (2000). Status after 10 years of operation overview of UF technology today. Desalination, 131, 17-25.

Lakshmanan, D., Clifford, D.A., Samanta, G., (2009). Ferrous and ferric ion generation during iron electrocoagulation. Environmental Science and Technology 43, 3853-3859.

Larsen, T. A., J. Lienert, A. Joss and H. Siegrist. (2004). How to avoid pharmaceuticals in the aquatic environment. Journal of Biotechnology 113(1-3): 295-304.

Larue, O., Vorobiev, E., (2003). Floc size estimation in iron induced electrocoagulation and coagulation using sedimentation data. Int. J. Miner. Process. 71, 1-15

Larue, O., Vorobiev, E., Vu, C., and Durand, B. (2003). Electrocoagulation and coagulation by iron of latex particles in aqueous suspensions. Separation and Purification Technology, 31(2), 177-192.

Laspidou, C.S., Rittmann, B.E. (2002). A unified theory for extracellular polymeric substances, soluble microbial products, and active and inert biomass. Water Research, 36, pp 2711–2720.

Lawson, W., and Lloyd, R. (1997). Membrane distillation. Journal of Membrane Science. 124 (1), 1-25.

Layton, A. C., B. W. Gregory, J. R. Seward, T. W. Schultz and G. S. Sayler. (2000). Mineralization of Steroidal Hormones by Biosolids in Wastewater Treatment Systems in Tennessee U.S.A." Environmental Science & Technology 34(18): 3925-3931.

Lazarova, Z., Serro, W. (2002). Electromembrane separation of mineral suspensions: Influence of process Parameters. Separation and Purification Technology, 37(3), 515-534

Le-Clech, P., Cao, Z., Wan, P.Y., Wiley, D.E., Fane, A.G. (2008). The application of constant temperature anemometry to membrane processes. Journal of Membrane Science. 284, 416-423

Le-Clech, P., Chen, V., Fane, A.G. (2006). Fouling in membrane bioreactors used in wastewater treatment. Journal of Membrane Science, 284, pp 17-53.

Le-Clech, P., Jefferson, B., and Judd, S. J. (2003). Impact of aeration, solids concentration and membrane characteristics on the hydraulic performance of a membrane bioreactor. Journal of membrane science, 218,117-129.

Le-Clech, P., Jefferson, B., Chang, I.S., Judd, S.J. (2003). Critical flux determination by the flux-step method in a submerged membrane bioreactor. Journal of Membrane Science, vol. 227, pp. 81-93.

Le-Clech, P., Jefferson, B., Judd, S.J. (2005). A comparison of submerged and sidestream tubular membrane bioreactor configurations. Desalination, 2, pp 113-122.

Lee, J. C., Kim, J. S., Kang, I. J., Cho, M. H., Park, P. K., and Lee, C. H. (2001). Potential and limitations of alum or zeolite addition to improve the performance of a submerged membrane bioreactor. Water science and technology, 43 (11), 59-66.

Lee, J., Ahn, W., and Lee, C. (2001). Comparison of the filtration characteristics between attached and suspended growth microorganisms in submerged membrane bioreactor. Water Res., 35(10), 2435–2445.

Lee, J., B. C. Lee, J. S. Ra, J. Cho, I. S. Kim, N. I. Chang, H. K. Kim and S. D. Kim. (2008). Comparison of the removal efficiency of endocrine disrupting compounds in pilot scale sewage treatment processes. Chemosphere 71(8): 1582-1592.

Lee, J., Chae, H. R., Won, Y. J., Lee, K., Lee, C.H., Lee, H. H., Kim, I.C., Lee., J.M. (2013). Graphene oxide nanoplatelets composite membrane with hydrophilic and antifouling properties for wastewater treatment. Journal of Membrane Science. 448, 223–230

Lee, J.S., Chang, I.S. (PRNewswire). (2014). Membrane fouling control and sludge solubilization using highvoltage impulse (HVI) electric fields. Process Biochemistry. 49, 858-862

Lee, S., J.-W. Lee, S. Kim, P.-K. Park, J.-H. Kim and C.-H. Lee. (2009). Removal of 17 [beta]-estradiol by powdered activated carbon--Microfiltraion hybrid process: The effect of PAC deposition on membrane surface. Journal of Membrane Science 326(1): 84-91.

Lee, S.A., Fane, A.G., Amal, R., Waite, T.D. (2003). The effect of floc size and structure on specific cake resistance and compressibility in dead-end microfiltration. Separation Science & Technology, 38, pp 869-887.

Lee, W., S. Kang and H. Shin. (2003). Sludge characteristics and their contribution to microfiltration in submerged membrane bioreactors. Journal of Membrane Science 216(1-2): 217-227.

Lee, Y., and Clark, M.M. (1998). Modeling of flux decline during crossflow ultrafiltration of colloidal suspensions. Journal of Membrane Science, 149, 181–202.

Lehtola, M.J., Miettinen, I.T., Vartiainen, T., Martikainen, P.J., (1999). A new sensitive bioassay for determination of microbially available phosphorus in water. Applied and Environmental Microbiology 65, 2032 - 2034.

Lesjean, B., Rosenberger, S., Laabs, C., Jekel, M., Gnirss, R., Amy, G. (2005). Correlation between membrane fouling and soluble/colloidal organic substances in membrane bioreactors for municipal wastewater treatment. Water Science & Technology, 51, pp 1–8.

Leusch, F. D. L., H. F. Chapman, W. Korner, S. R. Gooneratne and L. A. Tremblay. (2005). Efficacy of an Advanced Sewage Treatment Plant in Southeast Queensland, Australia, to Remove Estrogenic Chemicals. Environmental Science & Technology 39(15): 5781-5786.

Li, B. and S. Irvin. (2007). The comparison of alkalinity and ORP as indicators for nitrification and denitrification in a sequencing batch reactor (SBR). Biochemical Engineering Journal 34(3): 248-255.

Li, H., Yang, M., Zhang, Y., Liu, X., Gao, M., Kamagata, Y. (2005). Comparison of nitrification performance and microbial community between submerged membrane bioreactor and conventional activated sludge system. Water Science Technology, 51, 193–200.

Li, X. G., Cao, H. B., Wu, X. B and Yu, K. T. (2001). Inhibition of the metabolism of nitrifying bacteria by direct electric current. Biotechnology Letters. 23(9), 705-709

Li, X.-a., and Wang, X.-m. (2006). Modeling of membrane fouling in a submerged membrane reactor. Journal of membrane science, 278, 151–161.

Liang, S., Liu, C. and Song, L. (2007). Soluble microbial products in MBR operation: Behaviors, characteristics, and fouling potential, Water Research, 41, 95 – 101.

Liew, M.K.H., Fane. A.G., Rogers, P.L. (1995). Hydraulic resistance and fouling of microfilters by Candidautilis in fermentation broth. Biochemical Engineering and Biotechnology, 48, pp 108-117.

Lim, A.L., and Bai R. (2003). Membrane fouling and cleaning in microfiltration of activated sludge wastewater. Journal of Membrane Science, 216, 279–290.

Lin, C., S.L.Lo, Kuo, C., and C.H.Wu. (2005). Pilot-scale electrocoagulation with bipolar aluminum electrodes for on-site domestic greywater reuse. Journal of Environmental Engineering. 131(3): 491-495.

Lin, H., Wang, F., Ding, L., Hong, H., Chen, J., Lu, X. (2011). Enhanced performance of a submerged membrane bioreactor with powdered activated carbon addition for municipal secondary effluent treatment, J.Hazard. Mater. 192, 1509-1514.

Lin, S.H., and Chen, M.L. (1997). Treatment of textile wastewater by electrochemical methods for reuse. Water Research. 31 (1997), 868 - 876.

Linares, H.I., Barrera, D.C., Roa, M. G., Bilyeu, B., Ureña, M. F. (2009). Influence of the anodic material on electrocoagulation performance. Chem. Eng. J. 148, 97-105.

Liu, H., Zhao, X., & Qu, J. (2010). Electrocoagulation in Water Treatment. In C. C. Chen, Electrochemistry for the Environment. Lausanne: Springer. pp. 245-262.

Liu, L.; Liu, J.; Gao, B.; Yang, F.; Chellam, S. (2012). Fouling reductions in a membrane bioreactor using an intermittent electric field and cathodic membrane modified by vapor phase polymerized pyrrole. J. Membr. Sci., 394–395, 202–208.

Liu, R., A. Wilding, A. Hibberd and J. L. Zhou (2005). Partition of Endocrine - Disrupting Chemicals between Colloids and Dissolved Phase As Determined by Cross-Flow Ultrafiltration. Environmental Science & Technology 39(8): 2753 - 2761.

Liu, R., Huang, X., Xi, J., and Qian, Y. (2005). Microbial behavior in a membrane bioreactor with complete sludge retention. Process Biochemistry, 40(10), 3165-3170.

Liu, W. K., Brown, M. R. W, Elliott, T. S. J. (1997). Mechanisms of the bactericidal activity of low amperage electric current (DC). Journal of Antimicrobial Chemotherapy. 39, 687-695

Liu, Y., Fang, H.H.P. (2003). Influence of extracellular polymeric substance (EPS) on flocculation, settling and dewatering of activated sludge. Crit. Rev. Environ. Sci. Technol., 33, 237–273.

Liu, Z.-H., Y. Kanjo and S. Mizutani (2009). Removal mechanisms for endocrine disrupting compounds (EDCs) in wastewater treatment -- physical means, biodegradation, and chemical advanced oxidation: A review. Science of The Total Environment 407(2): 731-748.

Lloyd, D., L. Boddy and K. J. P. Davies (1987). Persistence of bacterial denitrification capacity under aerobic conditions: The rule rather than the exception. FEMS Microbiology Letters 45(3): 185-190.

Loghavi L, Yousef, A. E. (2007). Effect of moderate electric field frequency on growth kinetics and metabolic activity of Lactobacillus acidophilus. Biotechnol Prog. 4(1), 148-53

Loghavi, S.K.S.,Yousef A.E.. (2007). Effect of moderate electric field on the metabolic activity and growth kinetics of Lactobacillus acidophilus. Biotechn. Bioengin. 98 (4), 872-881.

Lojkine, M.H., Field, R.W., Howell, J.A. (1992). Crossflow microfiltration of cell suspensions: a review of models with emphasis on particle size effects. Transitions in Chemical Engineering, 70, 149-164.

Lowery C.A, Salzameda N.T, Sawada D. (2010). Medicinal chemistry as a conduit for the modulation of quorum sensing. J Med Chem. 53:7467-7489

Lowry, O.H., Rosebourgh, N.J., Farr, A.R., Randall, R.J. (1951). Protein measurement with the folin phenol reagent. Journal of Biological Chemistry, 193, pp 265–275.

Lubbecke, S., Vogelpohl, A., Dewjanin, W. (1995). Wastewater treatment in a biological high-performance system with high biomass concentration. Water Research, 29, pp 793–802.

Luo Q, Wang H, Zhang X, Qian Y. (2005). Effect of direct electric current on the cell surface properties of phenol-degrading bacteria. Appl Environ Microbiol. 71(1), 423-7

Lyko, S., T. Wintgens and T. Melin (2005). Estrogenic trace contaminants in wastewater - possibilities of membrane bioreactor technology. Desalination 178(1-3): 95-105.

Lyko, S., Wintgens, T., Al-Halbouni, D., Baumgarten, S., Tacke, D., Drensla, K., Janot, A., Dott, W., Pinnekamp, J., Melin, T., (2008). Long-term monitoring of a full-scale municipal membrane bioreactor-Characterisation of foulants and operational performance. J. Mem. Sci. 317 (12), 78 - 87.

Ma, C., Yu, S. L., Shi, W. X. Heijman, S. G. J., Rietveld, L.C. (2013). Effect of different temperatures on performance and membrane fouling in high concentration PAC-MBR system treating micro-polluted surface water. Bioresource Technology 141, 19-24

Ma, Z., Wen, W. H., Zhao, F., Xia, Y., Huang, X., Waite, D., Guan, J. (2013). Effect of temperature variation on membrane fouling and microbial community structure in membrane bioreactor. Bioresource Technology 133, 462-468

Madaeni, S.S., Fane A.G., and Grohmann G.S. (1995). Virus removal from water and wastewater using membranes. J. Membr. Sci., 102, 65-75.

Madaeni, S.S., Fane, A.G., Wiley, D.E. (1999). Factors influencing critical flux in membrane filtration of activated sludge. J. Chem. Technol. Biotechnol., 74, pp 539 - 543.

Maher, W., Woo, L., (1998). Procedures for the storage and digestion of natural waters for the determination of filterable reactive phosphorus, total filterable phosphorus and total phosphorus. Analytica Chimica Acta 375, 5-47.

Maillacheruvu, K., and Alshawabkeh, A. N. (2000). Anaerobic microbial activity under electric fields. In Emerging Technologies in Hazardous Waste Management VIII. New York: Kluwer Academic/Plenum Publishers.

Malakootian, M., Mansoorian, H. J., Moosazadeh, M. (2010). Performance Evaluation of Electrocoagulation P Using Iron-Rod Electrodes for Removing Drinking Water. Desalination, 255(1-3), 67-71.

Manem, J., Sanderson, R. (1996). Membrane Bioreactors. Water Treatment Membrane Processes. AWWARF/Lyonnaise des Eaux/WRC, McGraw-Hill, New York, USA.

Mangold, M., Ginkel, M., and Gilles, E. D. (2004). A model library for membrane reactors implemented in the process modelling tool PROMOT. Comput. Chem. Eng., 28, 319–332.

Manser, R., W. Gujer and H. Siegrist (2005). Consequences of mass transfer effects on the kinetics of nitrifiers. Water Research 39(19): 4633-4642.

Mara, D., Mills, S., Pearson, H. W., and Alabaster, G. P. (1992). Waste Stabilization ponds: A viable alternative for small community treatment systems. Journal of Water and Environmental Management. 6(1): 72-78.

Marriott, J., and Sørensen, E. (2003). A general approach to modeling membrane modules." Chem. Eng. Sci., 58, 4975–4990.

Marriott, J., and Sørensen, E. (2003). The optimal design of membrane systems. Chem. Eng. Sci., 58,4991–5004.

Matsunaga, T., S. Nakasono, and S. Masuda. (1992). Electrochemical sterilization of bacteria absorbed on granular activated carbon. FEMS Microbiol. Lett. 72:255-259.

Matsunaga, T., S. Nakasono, T. Takamuku, J. G. Burgess, N. Nakamura, and K. Sode. (1992). Disinfection of drinking water by using a novel electrochemical reactor employing carbon-cloth electrodes. Appl. Environ. Microbiol. 58:686-689.

Matteson, M. J.; Dobson, R. L.; Glenn, R. W.; Kukunoor, N. S.; Waits, W. H., III.; Clayfield, E. (1995). J. Electrocoagulation and Separation of Aqueous Suspensions of Ultrafine Particles. Colloids Surf., 104 (1), 101-109.

Matthiessen, P. (2003). Historical perspective on endocrine disruption in wildlife. Pure Applied Chemistry 75(11-12): 2197-2206.

Mayer, C.; Moritz, R.; Kirschner, C.; Borchard, W.; Maibaum, R.; Wingender, J.; Flemming, H.-C. (2005). The role of intermolecular interactions: Studies on model systems for bacterial biofilms. Int. J. Biol. Macromol., 26, 3–16.

249

McClintock, S. A., Randall, C. W., Pattarkine, V. M., (1993). Effects of temperature and mean cell residence time on biological nutrient removal processes. Water Environ. Res. 65 (5), 110-118.

Meas Y., Ramirez, J.A., Villalon, M.A., Mario, A., Chapman T.W. (2010). Industrial wastewaters treated by electrocoagulation. Electrochemica Acta, 55, 8165-8171.

Melhem, K. B., and Elektorowicz, M. (2010). Development of a Novel Submerged Membrane Electro-Bioreactor (SMEBR): Performance for Fouling Reduction. Environ. Sci. Technol. 44, 3298-3304.

Melin, T., B. Jefferson, D. Bixio, C. Thoeye, W. De Wilde, J. De Koning, J. van der Graaf and T. Wintgens (2006). Membrane bioreactor technology for wastewater treatment and reuse. Desalination 187(1-3): 271-282.

Mendret, J., Guigui, C., Schmitz, P., Cabassud, C. (2009). In situ dynamic characterization of fouling under different pressure conditions during dead-end filtration: Compressibility properties of particle cakes. Journal of Membrane Science, 333, pp 20-29.

Meng, F., Chae, S.R., Drews, A., Kraume, M., Shin, H.S., Yang, F. (2009). Recent advances in membrane bioreactors (MBRs): membrane fouling and membrane material. Water research, 43, 1489 -1512.

Meng, F., Shi, B., Yang, F., and Zhang, H. (2007). New insights into membrane fouling in submerged membrane bioreactor based on rheology and hydrodynamics concepts. Journal of Membrane Science. 302(1-2): 87 - 94.

Meng, F., Yang, F. (2007). Fouling mechanisms of deflocculated sludge, normal sludge and bulking sludge in membrane bioreactor. Journal of Membrane Science, 305, pp 48-56

Meng, F., Yang, F. (2007). Fouling mechanisms of deflocculated sludge, normal sludge, and bulking sludge in membrane bioreactor, J. Membr. Sci. 305, 48-56.

Meng, F., Yang, F., Shi, B., Zhang, H., (2007). A comprehensive study on membrane fouling in submerged membrane bioreactors operated under different aeration intensities. Separation and Purification Technology 59, 1-10.

Meng, F., Zhang, H., Yang, F., Zhang, S., Li, Y., and Zhang, X. (2006). Identification of activated sludge properties affecting membrane fouling in submerged membrane bioreactors. Separation and Purification Technology, 51(1), 95-103.

Meng, F.; Chae, S.-R.; Drews, A.; Kraumer, M.; Shin, H.-S. (2009). Recent advances in membrane bioreactors (MBRs): Membrane fouling and membrane materials. Water Res., 43,1489-1512.

Meng, F.G, Chae, S.R., Shin, H.S., Yang, F.L., Zhou, Z.B. (2012). Recent advances in membrane bioreactors: configuration development, pollutant elimination, and sludge reduction, Environ. Eng. Sci. 29: 139–160.

Meng, Q., F. Yang, L. Liu and F. Meng. (2008). Effects of COD/N ratio and DO concentration on simultaneous nitrifcation and denitrifcation in an airlift internal circulation membrane bioreactor. Journal of Environmental Sciences 20(8): 933- 939.

Merz, C., Gildemeister, R., Hamouri, B. E., and Kraume, M. (2007). Membrane bioreactor technology for the treatment of greywater from a sports and leisure club. Desalination. 215(1-3): 37-43.

Merzouk, B., Gourich, B., Sekki, A., Madani, K., and Chibane, M. (2009). Removal turbidity and separation of heavy metals using electrocoagulation–electroflotation technique A case study. Journal of Hazardous Materials. 164(1):215–222.

Merzouk, B., Madani, K., and Sekki, A. (2010). Using electrocoagulation–electroflotation technology to treat synthetic solution and textile wastewater, two case studies. Desalination. 250(2):573–577.

Metcalf & Eddy (2003). Wastewater engineering: treatment and reuse (4th international edition). McGraw-Hill, New York, USA.

Meunier, N., Drogui, P., Mercier, G., Blais, J. (2009). Treatment of metal-loaded soil leachates by electrocoagulation, Sep. Purif. Technol. 67, 110-116.

Meunier, N., Drogui, P., Montane, C., Hausler, R., Mercier, G., and Blais, J.-F. (2006). Comparison between electrocoagulation and chemical precipitation for metal removal from acidic soil leachate. Journal of Hazardous Materials. 137(1): 581-590.

Meyer, N., Parker W. J., Geel, P.J.V. and Adiga, M. (2005). Development of an electrodeionization process for removal of nitrate from drinking water Part 1: Single species testing. Desalination, 175, 153-165

Meyer, R. L., R. J. Zeng, V. Giugliano and L. L. Blackall. (2005). Challenges for simultaneous nitrification, denitrification, and phosphorus removal in microbial aggregates: mass transfer limitation and nitrous oxide production. FEMS Microbiology Ecology 52(3): 329-338.

Miettinen, I.T., Vartiainen, T., Martikainen, P.J., (1997). Phosphorus and bacterial growth in drinking water. Applied and Environmental Microbiology 63, 3242 - 3245.

Mikkelsen, L.H., Keiding, K., (2002). The shear sensitivity of activated sludge: an evaluation of the possibility for a standardised floc strength test. Water Res. 36, 2931-2940

Mills, D., (2000). "A new process for electrocoagulation." J. Am. Water Works Assoc. 92 (6), 34–43.

Miyoshi, T., Tsuyuhara, T., Ogyu, R., Kimura, K., Watanabe, Y., (2009). Seasonal variation in membrane fouling in membrane bioreactors (MBRs) treating municipal wastewater. Water Res. 43 (20), 5109-5118.

Mizuno, A., and Hori, Y. (1988). "Destruction of living cells by pulsed high voltage application." IEEE Trans. Ind. Appl., 24, 387–393.

Mo, H., Oleszkiewicz, J. A., Cicek, N., and Rezania, B. (2005). Incorporating membrane gas diffusion into a membrane bioreactor for hydrogenotrophic denitrification of groundwater." Water Science and Technology, 51(6-7), 357–364.

Mobarry, B. K., M. Wagner, V. Urbain, B. Rittmann and D. A. Stahl. (1997). Phylogenetic Probes for Analyzing Abundance and Spatial Organization of NItrifying Bacteria. Appl. Environ. Microbiol. 63(2).

Mohamed, M.N., Lawrence, J.R., Robarts, R.D., (1998). Phosphorus limitation of heterotrophic biofilms from the Fraser River, Britisch Columbia, and the effect of pulp mill effluent. Microbial Ecology 36, 121-130.

Mohamed, M.N., Robarts, R.D., (2003). Sestonic bacterial nutrient limitation in a northern temperate river and the impact of pulp-mill effluents. Aquatic Microbial Ecology 33, 19-28.

Mohammad Y.A. Mollah, Paul Morkovsky, Jewel A.G. Gomes, Mehmet Kesmez, Jose Parga, David L. Cocke. (2004). Fundamentals, present and future perspectives of electrocoagulation. Journal of Hazardous Materials, 114, 199-210

Emamjomeh, M. M., Sivakumar, M. Review of pollutants removed by electrocoagulation and electrocoagulation/flotation processes. Journal of Environmental Management 90 (2009) 1663–1679

Mohammed, T. A., Birima, A. H., Noor, M. J., Muyibi, S. A., and Idris, A. (2008). Evaluation of using membrane bioreactor for treating municipal wastewater at different operating conditions. Desalination. 221(1-3): 502-510.

Moisés, T.-P., Patricia, B. H., Barrera-Diaz, C., Gabriela, R.-M. and Natividad-Rangel, R. (2010). Treatment of industrial effluents by a continuous system: Electrocoagulation- Activated Sludge. Bioresource Technology. 101(20): 7761-7766.

Molla, S. H., Bhattacharjee S. (2005). Prevention of colloidal membrane fouling employing dielectrophoretic forces on a parallel electrode array. Journal of Membrane Science. 255, 187-199

Molla, S., and Bhattacharjee, S. (2007). Dielectrophoretic Levitation in the Presence of Shear Flow: Implications for Colloidal Fouling of Filtration Membranes. Langmuir 23, 10618-10627

Mollah, M. Y. A., Schennach, R., Parga, J. R., and Cocke, D. L. (2001). Electrocoagulation (EC) - science and applications. Journal of Hazardous Materials, B84, 29-21.

Mollah, M.Y.A., Pathak, S.R., Patil, P.K., Vayuvegula, M., Agrawal, T.S., Gomes, J.A.G., Kesmez, M., Cocke, D.L. (2004b). Treatment of orange II azo-dye by electrocoagulation (EC) technique in a continuous flow cell using sacrificial iron electrodes. J. Hazard. Mater. 109 (1-3), 165-171

Moreno, D. Cocke, J. Gomes, P. Morkovsky, J. Parga, E. Peterson, C. Garcia. (2009). Electrochemical reactions for electrocoagulation using iron electrodes. Ind. Eng. Chem. Res. 48, 2275-2282.

Moreno-Casillas, H. A., Cocke, D. L., Gomes, J. A.G., Morkovsky, P., Parga J. R., and Peterson, E. (2007). Electrocoagulation mechanism for COD removal. Separation and Purification Technology, 56 (2), 204-211.

Morris, J. M., Fallgren, P. H., and Jin, S. (2009). Enhanced denitrification through microbial and steel fuel-cell generated electron transport. Chemical Engineering Journal. 153(1-3): 37-42.

Moshe Ben Sasson, Avner Adin. (2010). Fouling mitigation by iron-based electroflocculation in microfiltration: Mechanisms and energy minimization. Water Research 44, 3973-3981

Mostefa, N. M., Tir, M. (2004). Coupling flocculation with electroflotation for waste oil/water emulsion treatment: optimization of the operating conditions. Desalination 161, 115-121

Mouedhen, G., Feki, M., Wery, M. D. P., and Ayedi, H., F. (2008). Behavior of Aluminum Electrodes in Electrocoagulation Process. Journal of Hazardous Materials, 150 (1), 124-135.

Mouedhen, G., Feki, M., Wery, M. D., and Ayedi, H. (2008). Behaviour of aluminum electrodes in electrocoagulation process. Journal of Hazardous Materials, 150(1): 124-135.

Mulder, J.W., Evenblij, H., Feyaerts, M., Geilvoet, S.P. (2007). Hybrid mbr Heenvliet-20 months of operational experience. Proceedings 7. Aachener Tagung Wasser und Membranen (pp. A23-1-A23-10). Aachen, Germany.

Mulder, M. (2000). Basic Principles of Membrane Technology. Kluwer Academic Publishers, Dordrecht.

Muller, E. B., Stouthamer, A. H., van Verseveld, H. W., and Eikelboom, D. H. (1995). Aerobic domestic waste water treatment in a pilot plant with complete sludge retention by cross-flow filtration. Water Research, 29(4), 1179-1189.

Munz, G., M. Gualtiero, L. Salvadori, B. Claudia and L. Claudio. (2008). Process efficiency and microbial monitoring in MBR (membrane bioreactor) and CASP (conventional activated sludge process) treatment of tannery wastewater. Bioresource Technology 99(18): 8559-8564.

Murugananthan, M., Raju, G.B., and Prabhakar, S. (2004). Removal of sulfide, sulfate and sulfite ions by electro coagulation. Journal of Hazardous Materials, 109 (1-3), 37-44.

Mustafa, S., Naeem, A., Murtaza, S., Rehana, N., and Samad, H. Y. (1999). Comparatice sorption properties of metal (III) phosphates. Journal of Colloid interface Science. 221(1): 63-74.

Nagaoka H. and Nemoto H. (2005). Influence of extracellular polymeric substances on nitrogen removal in an intermittently-aerated membrane bioreactor. Water Sci. Techn, 51 (11), 151-158

Nagaoka, H. (1999). Nitrogen removal by submerged membrane separation activated sludge process. Water Science and Technology 39(8): 107-114.

Nagaoka, H., Ueda, S., Miya, A. (1996). Influence of bacterial extracellular polymers on the membrane separation activated sludge process. Water Science & Technology, 34, pp 165–172.

Nagaoka, H., Yamanishi, S., Miya, A. (1998). Modeling of biofouling by extracellular polymers in a membrane separation activated sludge system. Water Science & Technology, 38, pp 497–504.

Nagaoka, H.; Yamanishi, S.; Miya, A. (1998). Modelling of biofouling by extracellular polymers in a membrane separation activated sludge system. Water Sci. Technol. 38, 497–504.

Naje, A.S., Chelliapan, S., Zakaria, Z., Abbas, S.A. (2015). Enhancement of an Electrocoagulation Process for the Treatment of Textile Wastewater under Combined Electrical Connections Using Titanium Plates. Int. J. Electrochem. Sci., 10, 4495-4512

Nakada, N., T. Tanishima, H. Shinohara, K. Kiri and H. Takada. (2006). "Pharmaceutical chemicals and endocrine disrupters in municipal wastewater in Tokyo and their removal during activated sludge treatment." Water Research 40(17): 3297-3303.

Ng, C.A., Sun, D., Zhang, J. Chua, H.C., Bing, W., Tay, S., Fane, A.G. (2005). Strategies to improve the sustainable operation of membrane bioreactors. Proceedings of the International Desalination Association Conference. Singapore.

Ng, H.Y., and Hermanowicz, S.W. (2005). Specific resistance to filtration of biomass from membrane bioreactor reactor and activated sludge: effects of exocellular polymeric substances and dispersed microorganisms. Water Environmental Research, 77(2), 187-92.

Ng, N. L. A., and Kim, S. A. (2007). A mini-review of modeling studies on membrane bioreactor (MBR) treatment for municipal wastewaters. Desalination, 212, 261-281.

Nguyen, D. D., Ngo, H. H., Yoon, Y. S. (2014). A new hybrid treatment system of bioreactors and electrocoagulation for superior removal of organic and nutrient pollutants from municipal wastewater. Bioresource Technology 153, 116-125

Nguyen, T., Roddick, F. A. and Fan, L. H. (2012). Biofouling of Water Treatment Membranes: A Review of the Underlying Causes, Monitoring Techniques and Control Measures. Membranes. 2, 804-840

Ni'am, M.F., Othman, F., Sohaili, J., and Fauzia, Z. (2007). Electrocoagulation technique in enhancing COD and suspended solids removal to improve wastewater quality. Water Science and Technology, 56(7), 47-53.

Ninova, V.K. (2003). Electrochemical treatment of mine wastewaters containing heavy metal ions, Annual Mining and Mineral Processing (part II), 46, 215–220

Nishihara, T., J. Nishikawa, T. Kanayama, F. Dakeyama, K. Saito and M. Imagawa. (2000). Estrogenic activities of 517 chemicals by yeast two-hybrid assay. Journal of Health Sciences 46: 282-98.

Ognier, S., Wisniewski, C., Grasmick, A. (2002). Membrane fouling during constant flux filtration in membrane bioreactors. Membrane Technology, 2002, pp 6-10.

Oh H.S., Yeon, K.M., Yang, C.S. (2012). Control of membrane biofouling in MBR for wastewater treatment by quorum quenching bacteria encapsulated in mi-croporous membrane. Environ Sci Technol. 46:4877-4884

Oleszkiewicz J A, Barnard J L (2006) Nutrient removal technology in North America and the European Union: A Review. Water Qual. Res. J. Canada 41, 449-462

Olmez, T. (2009). The optimization of Cr(VI) reduction and removal by electrocoagulation using response surface methodology, J. Hazard. Mater. 162, 1371-1378.

Orori, O. B., Etiegni, L., Senelwa, K., Mwamburi, M. M., Balozi, K. B., Barisa, G. K., Omutange, E. S. (2010). Electro-coagulation treatment efficiency of graphite, iron and aluminum electrodes using alum and wood ash electrolytes on a Kraft pulp and paper mill effluent. Water Sci. Technol. 62, 1526-1535.

Ouaissa, Y. A., Chabani, M., Amrane, A. & Bensmaili, A. (2014). Removal of tetracycline by electrocoagulation: Kinetic and isotherm modeling through adsorption. J Environ Chem Eng 2, 177-184.

Owen, G., Bandi, M., Howell, J.A., Churchouse, S.J. (1995). Economic assessment of membrane processes for water and wastewater treatment. Journal of Membrane Science, 102, pp 77-91.

Panter, G. H., R. S. Thompson, N. Beresford and J. P. Sumpter. (1999). Transformation of a nonestrogenic steroid metabolite to an oestrogenically active substance by minimal bacterial activity. Chemosphere 38(15): 3579-3596.

Pareilleux, A., and N. Sicard. (1970). Lethal effects of electric current on Escherichia coli. Appl. Microbiol. 19:421-424.

Parga, J.R., Cocke, D. L., Valverde, V., Gomes, J. A. G., Kesmez, M., Moreno, H., Weir, M., and Mencer, D. (2005). Characterization of electrocoagulation for removal of Cr and As. J. Chem. Eng. Technol., 28, 605–612.

Park, D.; Lee, D.S.; Park, J.M. (2005). Continuous biological ferrous iron oxidation in a submerged membrane bioreactor. Water Sci. Technol, 51, 59–68.

Park, J., Jung, Y., Han, M., Lee, S., (2002). Simultaneous removal of cadmium and turbidity in contaminated soil-washing water by DAF and electroflotation. Water Sci. Technol. 46 (11-12), 225-230

Park, J.S., Yeon, K.M., Lee, C.H. (2005). Hydrodynamics and microbial physiology affecting performance of a new MBR, membrane-coupled high performance compact reactor. Desalination, 172, pp 181-188.

Parker, D.S., Kinnear, D.J., Wahlberg, E.J. (2001). Review of folklore in design and operation of secondary clarifiers. Journal of Environmental Engineering, 127, pp 476- 484.

Paul D., Kim Y.S., Ponnusamy K. (2009). Application of quorum quenching to inhibit biofilm formation. Environ Eng Sci. 26:1319-1324

Pauwels, B., H. Noppe, H. De Brabander and W. Verstraete. (2008). Comparison of Steroid Hormone Concentrations in Domestic and Hospital Wastewater Treatment Plants. Journal of Environmental Engineering 134(11): 933-936.

Phalakornkule, C., Sukkasem, P., and Mutchimasattha, C. (2010). Hydrogen Recovery from the electrocoagulation treatment of dye-containing wastewater. International Journal of Hydrogen Energy. 35(20): 10934 - 10943.

Picard, T., Cathalifaund-Feuillade, G., Mazet, M., and Vandensteendam, C. (2000). Cathodic dissolution in the electrocoagulation process using aluminium electrodes. J. Environ. Monit., 2, 77–80.

Pochana, K. and J. Keller. (1999b). Study of Factors Affecting Simultaneous Nitrification and Denitrification (SND). Water Science and Technology 39(6): 61-68.

Pochana, K., J. Keller and P. Lant. (1999a). Model Development for Simultaneous Nitrification and Denitrification. Water Science Technology 39(1): 235-243.

Polatide, C., Kyriacou, G. (2005). Electrochemical reduction of nitrate ion on various cathodes – reaction kinetics on bronze cathode. Journal of Applied Electrochemistry. 35(5): 421–427.

Pollard, P.C. (2006). A quantitative measure of nitrifying bacterial growth. Water Research, 40(8), 1569-1576.

Polyakov, Y. S. (2006). Deadend outside-in hollow-fiber membrane filter: Mathematical model. Journal of membrane science, 279,615–624.

Ponnusamy K., Paul D., Kweon J.H. (2009). Inhibition of quorum sensing mechanism and Aeromonas hydrophila biofilm formation by vanillin. Environ Eng Sci. 26:1359-1363

Pramanik, B.K.; Roddick, F.A.; Fan, L. (2014). Effect of biological activated carbon pre-treatment to control organic fouling in the microfiltration of biologically treated secondary effluent. Water Res., 63, 147–157.

Prentice, G. (1991). Electrochemical Engineering Principles, Prentice Hall

Price, P. and T. Sowers. (2004). Temperature dependence of metabolic rates for microbial growth, maintenance, and survival. Microbiology 101(13): 4631-4636.

Priester, J.H.; Olson, S.G.; Webb, S.M.; Neu, M.P.; Hersman, L.E.; Holden, P.A. (2006). Enhanced oxoplolymer production and chromium stabilization in Pseudomonas putida unsaturated biofilms. Appl. Environ. Microbiol., 72, 1988-1996.

PRNewswire. (2015). Membranes Market by Type, Technology, Region & Application - Global Forecast 2015 to 2020. http://www.prnewswire.com/news-releases/membranes-market-by-type-technology-region--application---global-forecast-2015-to-2020-300184390.html. Accessed on Sept. 10, 2015

Psoch, C., and Schiewer, S. (2005). Critical flux aspect of air sparging and backflushing on membrane bioreactors. Desalination, 175, 61–71.

Psoch, C., and Schiewer, S. (2006). Resistance analysis for enhanced wastewater membrane filtration. Journal of membrane science, 280, 284– 297.

Purdom, C. E., P. A. Hardiman, V. J. Bye, N. C. Eno, C. R. Tyler and J. P. Sumpter. (1994). Estrogenic effects of effluents from sewage treatment works. Chemistry and Ecology 8(4): 275.

Rasier, G., J. Toppari, A. S. Parent and J. P. Bourguignon. (2006). Female sexual maturation and reproduction after prepubertal exposure to estrogens and endocrine disrupting chemicals: A review of rodent and human data. Molecular and Cellular Endocrinology 254-255: 187-201.

Refait, P., Drissi, H., Marie, Y., Génin, J.M.R. (1994). The substitution of Fe^{2+} ions by Ni^{2+} ions in green rust one compounds, Hyperfine Interact. 90, 389–394.

Refait, P., Genin, J.M.R., (1997). Mechanisms of oxidation of Ni(II)-Fe(II) hydroxides in chloride-containing aqueous media: Role of the pyroaurite-type Ni-Fe hydroxychlorides, Clay Miner. 32, 597-613.

Ren, Y.-X., K. Nakano, M. Nomura, N. Chiba and O. Nishimura. (2007). Effects of bacterial activity on estrogen removal in nitrifying activated sludge. Water Research 41(14): 3089-3096.

Ricordel, C., Darchen, A., and Hadjiev, D. (2010). Electrocoagulation-electroflotation as a surface water treatment for industrial uses. Separation and Purification Technology. 74(3): 342-347.

Ripperger S., and Altmann J., (2002). Crossflow microfiltration- state of the art. Sep. Purf. Tech., 26,19-31.

Robertson, L., E. Van Niel, R. Torremans and J. Kuenen. (1988). Simultaneous Nitrification and Denitrification in Aerobic Chemostat Cultures of Thiosphaera pantotropha. Applied and Environmental Microbiology 54(11): 2812-2818.

Roest, H.F. van der, Bentem, A.G. van, Lawrence, D.P. (2002). MBR-technology in municipal wastewater treatment: challenging the traditional treatment technologies. Water Science and Technology, 46, pp 273-2880.

Rosenberger, S., Evenblij, H., Poele, S. te, Wintgens, T., Laabs, C. (2005). The importance of liquid phase analyses to understand fouling in membrane assisted activated sludge processes-six case studies of different European research groups. Journal of Membrane Science, 263, pp 113–126.

Rosenberger, S., Kraume, M. (2002a). Filterability of activated sludge in membrane bioreactors. Desalination, 146, pp 373–379.

Rosenberger, S., Kruger, U., Witzig, R., Manz, W., Szewzyk, U., and Kraume, M. (2002). Performance of a bioreactor with submerged membranes for aerobic treatment of municipal waste water. Water Research, 36 (2), 413 - 420.

Rosenberger, S., Kubin, K., Kraume, M. (2002b). Rheology of activated sludge in membrane bioreactors. Engineering in Life Sciences, 2, pp 269-275.

Rosenberger, S., Laabs, C., Lesjean, B., Gnirss, R., Amy, G., Jekel, M., Schrotter, J. C., (2006). Impact of colloidal and soluble organic material on membrane performance in membrane bioreactors for municipal wastewater treatment. Water Res. 40 (4), 710-720.

Rosenberger, S.; Kraume, M. (2002). Filterability of activated sludge in membrane reactors. Desalination, 146, 373–379.

Rossini, M., Garcia, G., and Galluzo, M. (1999). Optimization of the coagulation-flocculation treatment; influence of rapid mixing parameters. Water Research, 33(8): 1817-1826.

Routledge, E. J. and J. P. Sumpter (1996). Estrogenic Activity of Surfactants and Some of Their Degradation Productions Assessed Using a Recombinant Yeast Screen. Environmental Toxicology and Chemistry 15(3): 241-248.

Routledge, E. J., D. Sheahan, C. Desbrow, G. C. Brighty, M. Waldock and J. P. Sumpter. (1998). Identification of Estrogenic Chemicals in STW Effluent. 2. In Vivo Responses in Trout and Roach. Environmental Science & Technology 32(11):1559-1565.

Rubach, S., Saur, I. F., (1997). Onshore testing of produced water by electroflocculation. Filtr. Sep. 34 (8), 877–882

Rui, L., Xia, H., Chen, L. J., Wen, X. H., and Yi, Q. (2005). Operational performance of a submerged membrane bioreactor for reclamation of bath wastewater. Process Biochem., 40 (1), 125–130.

Rutishauser, B. V., M. Pesonen, B. I. Escher, G. E. Ackermann, H.-R. Aerni, M. J. F. Suter and R. I. L. Eggen. (2004). Comparative analysis of estrogenic activity in sewage treatment plant effluents involving three in vitro assays and chemical analysis of steroids. Environmental Toxicology and Chemistry 23(4): 857-864.

S. Zodi, O. Potier, F. (2010). Lapicque and of the Industrial Wastewaters by Electrocoagulation: Op-timization of Coupled Electrochemical and Sedimen- ta-tion Processes. Desalination, 261(1-2), 186-190.

Sagle, A.C.; Van Wagner, E.M.; Ju, H.; McCloskey, B.D.; Freeman, B.D.; Sharma, M.M. (2009). PEG-coated reverse osmosis membranes: Desalination properties and fouling resistance. J. Membr. Sci., 340, 92–108.

Sakakibara, Y., and Kuroda, M. (1993). Electric prompting and control of denitrification. Biotechnol. Bioeng., 42, 535–537.

Santos, A., Ma, W., Judd, S. J. (2011). Membrane bioreactors: two decades of research and implementation, Desalination 273, 148–154.

Sarioglu, M., G. Insel, N. Artan and D. Orhon. (2009). Model evaluation of simultaneous nitrification and denitrification in a membrane bioreactor operated without an anoxic reactor. Journal of Membrane Science 337(1-2): 17-27.

Sarkar, B., De, S. (2010). Electric field enhanced gel controlled cross-flow ultrafiltration under turbulent flow conditions. Separation and Purification Technology 74, 73-82

Sarkar, M., Evans, G., and Donne, S. (2010). Bubble size measurement in electroflotation. Minerals Engineering. 23 (11-13): 1058-1065.

Sasson, M.B., Calmano, W., Adin, A. (2009). Iron-oxidation processes in an electroflocculation (electrocoagulation) cell, J. Hazard. Mater. 171, 704-709.

Satoshi, N., Norio, M., Hiroshi, S., (1997). Electrochemical cultivation of Thiobacillus ferrooxidans by potential control. Bioelectrochem. Bioenerg. 43, 61-66.

Satyawali, Y., Balakrishnan, M. (2009). Effect of PAC addition on sludge properties in an MBR treating high strength wastewater, Water Res. 43, 1577-1588.

Schoeberl, P., Brik, M., Bertoni, M., Braun, R., and Fuchs, W. (2005). Optimization of operational parameters for a submerged membrane bioreactor treating dyehouse wastewater. Sep. Purif. Technol., 44,61–68.

Şengil, I. A. and Ozacar, M. (2009). The Decolorization of C.I. Reactive Black 5 in Aqueous Solution by Electrocoa- gu-lation Using Sacrificial Iron Electrodes. Journal of Haz-ardous Materials, 161(2-3), 1369-1376.

Seo, G. T., Ahan, H. I., Kim, J. T., Lee, Y. J., and Kim I. S. (2004). Domestic wastewater reclamation by submerged membrane bioreactor with high concentration powdered activated carbon for stream restoration. Water Science and Technology, 50 (2), 173–178.

Seo, G. T., Moon, C. D., Chang, S. W., and Lee, S. H. (2004). Long term operation of high concentration powdered activated carbon membrane bioreactor for advanced water treatment. Water Science and Technology, 50 (8), 81–87.

Servos, M. R., D. T. Bennie, B. K. Burnison, A. Jurkovic, R. McInnis, T. Neheli, A. Schnell, P. Seto, S. A. Smyth and T. A. Ternes. (2005). Distribution of estrogens, 17[beta]-estradiol and

estrone, in Canadian municipal wastewater treatment plants. Science of The Total Environment 336(1-3): 155-170.

Shao, P., and Huang, R. Y. M. (2007). Review: Polymeric membrane pervaporation. Journal of membrane science, 287, 162–179.

Shareef, A., J. Wells, M. Angove and B. Johnson. (2006). Sorption of bisphenol A, 17alpha-ethynylestradiol and estrone to mineral surface. J. Colloid Interface Science 297: 62-69.

Shaw, D. J. (1992). Introduction to colloid and surface chemistry. Butterworth Heinemann, UK.

She, P., Song, B., Xing, X.-H., Loosdrecht, M.V., Liu, Z. (2006). Electrolytic stimulation of bacteria Enterobacter dissolvens by a direct current. Biochem. Eng. J. 28, 23– 29.

Shen, F., Chen, X., Gao, P., and Chen, G. (2003). Electrochemical removal of fluoride ions from industrial wastewaters. Chem. Eng. Sci., 58, 987–993.

Sheng, G.-P.; Yu, H.-Q.; Li, X.-Y. Extracellular polymeric substances (EPS) of microbial aggregates in biological wastewater treatment systems: A review. Biotechnol. Adv. 2010, 28, 882-894.

Shi, J., S. Fujisawa, S. Nakai and M. Hosomi. (2004). Biodegradation of natural and synthetic estrogens by nitrifying activated sludge and ammonia-oxidizing bacterium Nitrosomonas europaea. Water Research 38(9): 2323-2330.

Shidong, Y., Lanhe, Z., Fengguo, C., and Jun, M. (2009). Preliminary Study on Enhanced Dissolved Air Floatation by Pulsed High Voltage Discharge. IEEE Xplore.

Shimada, K., and K. Shimahara. (1985). Leakage of cellular contents and morphological changes in resting Escherichia coli B cells exposed to an alternating changes. Agric. Biol. Chem. 49:3605-3607.

Shin, H.S., Kang, S.T. (2003). Characteristics and fates of soluble microbial products in ceramic membrane bioreactor at various sludge retention times. Water Research, 37, pp 121–127.

Sincero, A. P., and Sincero, G. A. (2003). Physical- Chemical Treatment of Water and Wastewater. IWA Publishing, London.

Sliekers, A. O., N. Derwort, J. L. C. Gomez, M. Strous, J. G. Kuenen and M. S. M. Jetten. (2002). Completely autotrophic nitrogen removal over nitrite in one single reactor. Water Research 36(10): 2475-2482.

Smith, D. W., Mavinic, D. S., and Zytner, R. G. (2002). Future directions of environmental engineering in Canada. Journal Environmental Engineering Science, 1, 9-16.

Smith, P. J., Vigneswaran, S., Ngo, H. H., Ben-Aim, R., and Nguyen, H. (2005). Design of a generic control system for optimizing back flush durations in a submerged membrane hybrid reactor. Journal of membrane science, 255, 99–106.

Snyder, S. A., S. Adham, A. M. Redding, F. S. Cannon, J. DeCarolis, J. Oppenheimer, E. C. Wert and Y. Yoon. (2007). Role of membranes and activated carbon in the removal of endocrine disruptors and pharmaceuticals. Desalination 202(1-3):156-181.

Snyder, S., D. Villeneuve, E. Snyder and J. Giesy. (2001). Identification and Quantification of Estrogen Receptor Agonists in Wastewater Effluents. Environ. Sci. Technol. 35(18): 3620-3625.

Sofia, A., Ng, W.J., Ong, S.L. (2004). Engineering design approaches for minimum fouling in submerged MBR. Desalination, 160, 67-74.

Sommariva, C., Converti, A., and Borghi, M.D. (1997). Increase in phosphate removal from wastewater by alternating aerobic and anaerobic conditions. Desalination, 108 (1-3), 255–260.

Song, K-G., Kim, Y., and Ahn, K-H. (2008). Effect of coagulant addition on membrane fouling and nutrient removal in a submerged membrane bioreactor. Desalination, 221 (1-3), 467-474.

Sorensen, J. (1978). Capacity for Denitrification and Reduction of Nitrate to Ammonia in a Coastal Marine Sediment. Applied and Environmental Microbiology. 35(2): 301-305.

Spath, R.; Flemming, H. -C.; Wuertz, S. Sorption properties of biofilms. (1998). Water Sci. Technol.37, 207–210.

Sridhar, R., Sivakumar, V., Immanuel, P., Maran, J.P. (2011). Treatment of pulp and paper industry bleaching effluent by electrocoagulant process, J. Hazard. Mater. 186, 1495-1502.

Stenstrom, M.K., and Poduska, R.A. (1980). The effect of oxygen concentration on nitrification. Water Research, 14, 643–650.

Stephenson, T., Judd, S., Jefferson, B., and Brindle, K. (2000). Membrane Bioreactors for Wastewater Treatment. IWA Publishing.

Sugirato, A.T., Ito, S., Ohshima, T., Sato, M., Skalny. J. D. (2003). Oxidative decoloration of dyes by pulsed discharge plasma in water. J Electrostatics. 58:135-45.

Sun J. Y, Xiao, K., Mo, Y. H., Liang, P., Shen, Y. X., Zhu, N. W., Huang, X. (2014). Seasonal characteristics of supernatant organics and its effect on membrane fouling in a full-scale membrane bioreactor. Journal of Membrane Science 453, 168-174

Sun, D. D., Hay, C. T., and Khor, S. L. (2006). Effects of hydraulic retention time on behavior of start-up submerged membrane bioreactor with prolonged sludge retention time. Desalination, 195, 209–225.

Sun, D. D., Khor, S. L., Hay, C. T., and Leckie, J. O. (2007). Impact of prolonged sludge retention time on the performance of a submerged membrane bioreactor. Desalination. 208(1-3): 101-112.

Svenson, A., A.-S. Allard and M. Ek (2003). "Removal of estrogenicity in Swedish municipal sewage treatment plants." Water Research 37(18): 4433-4443.

Tam, L., Tang, T., Leung, W., Chen, G. and Sharma, K. (2006). A pilot study on performance of a membrane bioreactor in treating fresh water sewage and saline sewage in Hong Kong. Separation Science and Technology, 41(7), 1253-1264.

Tanneru, C. T. & Chellam, S. (2012). Mechanisms of virus control during iron electrocoagulation – Microfiltration of surface water. Water Res 46, 2111–2120.

Tansel, B.; Sager, J.; Garland, J.; Xu, S.; Levine, L.; Bisbee, P. (2006). Deposition of extracellular polymeric substances and micro-topographical changes on membrane surfaces during intermittent filtration conditions. J. Membr. Sci., 285, 225-231.

Tardieu, E., Grasmick, A., Geaugey, V., Manem, J. (1999). Influence of hydrodynamics on fouling velocity in a recirculated MBR for wastewater treatment. Journal of Membrane Science, 156, pp 131-140.

Tchamango, S., Nijki, C. P., Ngameni, E., Hadjiev, D., and Darchen, A. (2010). Treatment of dairy effluents by electrocoagulation using aluminum electrodes. Science of Total Environment. 408(4): 974-952.

Ternes, T. A., M. Stumpf, J. Mueller, K. Haberer, R. D. Wilken and M. Servos. (1999a). Behavior and occurrence of estrogens in municipal sewage treatment plants - I. Investigations in Germany, Canada and Brazil. The Science of The Total Environment 225(1-2): 81-90.

Ternes, T. A., N. Herrmann, M. Bonerz, T. Knacker, H. Siegrist and A. Joss. (2004). A rapid method to measure the solid-water distribution coefficient (Kd) for pharmaceuticals and musk fragrances in sewage sludge. Water Research 38(19):4075-4084.

Ternes, T. A., P. Kreckel and J. Mueller. (1999). "Behaviour and occurrence of estrogens in municipal sewage treatment plants -- II. Aerobic batch experiments with activated sludge." The Science of The Total Environment 225(1-2): 91-99.

Terrazas, E., Vázquez, A., Briones, R., Lázaro I., and Rodríguez. I. (2010). EC Treatment for Reuse of Tissue Paper Wastewater: Aspects That Affect Energy Consumption. Journal of Hazardous Materials, 181(1-3), 809-816.

Thorpe, K. L., R. I. Cummings, T. H. Hutchinson, M. Scholze, G. Brighty, J. P. Sumpter and C. R. Tyler. (2003). Relative Potencies and Combination Effects of Steroidal Estrogens in Fish. Environmental Science & Technology 37(6): 1142-1149.

Thrash, J.C., Coates, J.D., (2008). Review: direct and indirect electrical stimulation of microbial metabolism. Environ. Sci. Technol. 42, 3921-3931.

Tian, J.-y., Liang, H., Nan, J., Yang, Y.-l., You, S.-j., and Li, G.-b. (2009). Submerged membrane bioreactor (sMBR) for the treatment of contaminated raw water. Chemical Engineering Journal. 148(2-3)

Timmes, T. C., Kim, H. C., Dempsey, B., A. (2009). Electrocoagulation pretreatment of seawater prior to ultrafiltration: Bench-scale applications for military water purification systems. Desalination 249, 895-901

Timmes, T. C., Kim, H. C., Dempsey, B., A. (2010). Electrocoagulation pretreatment of seawater prior to ultrafiltration: Pilot-scale applications for military water purification systems. Desalination 250, 6-13

Tokuda H, Nakanishi K (1995) Application of direct current to protect bioreactor against contamination. Biosci. Biotech. Biochem. 59: 753–755.

Tongwen, X. (2002). Electrodialysis processes with bipolar membranes (EDBM) in environmental protection-a review. Conservation and Recycling, 37 (1),1-22.

Torvinen, E., Lehtola, M.J., Martikainen, P.J., Miettinen, I.T., (2007). Survival of Mycobacterium avium in drinking water biofilms as affected by water flow velocity, availability of phosphorus and temperature. Applied and Environmental Microbiology 73, 6201 - 6207.

Trompette J.L., and Vergnes H. (2009). On the crucial influence of some supporting electrolytes during electrocoagulation in the presence of aluminum electrodes. Journal of Hazardous Materials. 163(2-3): 1282-1288.

Trussell, R. S., Adham, S., and Trussell, R. R. (2005). Process Limits of Municipal Wastewater Treatment with the Submerged Membrane Bioreactor. Journal of Env. Eng., March, 410-416.

Trussell, R.S., Merlo, R.P., Hermanowicz, S.W. and Jenkins, D. (2006). The effect of organic loading on process performance and membrane fouling in a submerged membrane bioreactor treating municipal wastewater. Water Research, 40, 2675–2683.

Tsai, H.-H.; Ravindran, V.; Williams, M.D.; Pirbazari, M. (2004). Forecasting the performance of membrane bioreactor process for groundwater denitrification. J. Environ. Eng. Sci., 3, 507–521.

Tsouris, C.; DePaoli, D. W.; Shor, J. T.; Hu, M.; Ying, T. (2000). Electrocoagulation for Magnetic Seeding of Colloidal Particles. Colloids Surf. 177 (2), 223-233.

Tsuneda S., Aikawa H., Hayashi H., Yuasa A., Hirata A. (2003). Extracellular polymeric substances responsible for bacterial adhesion onto solid surface. FEMS Microbiol. Lett. 223:287-292

Tuan P.-A., J. V. (2008). Electro-dewatering of sludge under pressure and nonpressure conditions. Environmental Technology. 29(10): 1075-1084.

Tyler, C. R., S. Jobling and J. P. Sumpter. (1998). Endocrine Disruption in Wildlife: A Critical Review of the Evidence. Critical Reviews in Toxicology 28(4): 319-361.

Ueda, T., and Hata, K. (1999). Domestic wastewater treatment by a submerged membrane bioreactor with gravitational filtration. Water Research, 33 (12), 2888–2892.

263

Ueda, T., Hata, K., and Kikuoka, Y. (1996). Treatment of domestic sewage form rural settlements by a membrane bioreactor. Water Science and Technology, 34,189–96.

Ueda, T., Hata, K., Kikuoka, Y., Seino, O. (1997). Effects of aeration on suction pressure in a submerged membrane bioreactor. Water Research, 31, pp 489-494.

UNESCO. (2014). The United Nations World Water Development Report. ISBN 978-92-3-104259-1

Urase, T., C. Kagawa and T. Kikuta. (2005). Factors affecting removal of pharmaceutical substances and estrogens in membrane separation bioreactors. Desalination 178(1-3): 107-113.

Vader, J. S., C. G. van Ginkel, F. M. G. M. Sperling, J. de Jong, W. de Boer, J. S. de Graaf, M. van der Most and P. G. W. Stokman. (2000). Degradation of ethinyl estradiol by nitrifying activated sludge. Chemosphere 41(8): 1239-1243.

Valenzuela, D. P., Dubey, S. T., and Dewan, A. K. (2002). Corrosion at Metal Interfaces - A Study of Corrosion Rate and Solution Properties, Including Conductance, Viscosity, and Density. Ind. Eng. Chem. Res. 41(5): 914-921.

van den Brink, P., Satpradit, O. A., van Bentem, A., Zwijnenburg, A., Temmink, H., van Loosdrecht, M. (2011). Effect of temperature shocks on membrane fouling in membrane bioreactors Water Research 45(15), 4491-4500

Vasudevan, S., Kannan, B. S., Lakshmi, J., Mohanraj, S., Sozhan, G. (2011). Effects of alternating and direct current in electrocoagulation process on the removal of fluoride from water, J. Chem. Technol. Biotechnol. 86, 428–436.

Vik, E. A., Carlson, D. A., Eikum, A. S. & Gjessing, E. T. (1984). Electrocoagulation of potable water. Water Res 18, 1355–1360.

Villacorte LO, Kennedy MD, Amy GL, Schippers JC. (2009) The fate of transparent exopolymer particles (TEP) in integrated membrane systems: removal through pre-treatment processes and deposition on reverse osmosis membranes. Water Res 43(20):5039 5052

Villalobos, M., N. Olea, J. Brotons, M. Olea-Serrano, J. Ruiz de Almodovar and V. Pedraza. (1995). The E-Screen Assay: A Comparison of Different MCF7 Cell Stocks. Environmental Health Perspectives 103: 844-850.

Visvanathan, C., Yang, B., Muttamara S., and Maythanukhraw, R. (1997). Application of air backflushing technique in membrane bioreactor. Water Sci. Tech. 36 (12), 259–266.

von der Schulenburg, D.A. G., Vrouwenvelder, J. S., Creber S. A., Van Loosdrecht, M. C. M., Gladden, L. F., Johns, M. L. (2008). Nuclear magnetic resonance microscopy studies of membrane biofouling, Journal of Membrane Science 323 (1), 37–44.

Vrouwenvelder, J.S., Manolarakis, S.A., Veenendaal, H.R., Van Der Kooij, D., (2000). Biofouling potential of chemicals used for scale control in RO and NF membranes. Desalination 132, 1-10.

Vrouwenvelder, J.S., Picioreanu, Kruithof, C., J.C., Loosdrecht, M.C.M. van. (2010). Biofouling in spiral wound membrane systems: Three-dimensional CFD model based evaluation of experimental data, Journal of Membrane Science 346, 71–85

Vrouwenvelder, J.S., Schulenburg, D.A. G. von der, Kruithof, J.C., Johns, M.L., Loosdrecht, M.C.M. van. (2009). Biofouling of spiral wound nanofiltration and reverse osmosis membranes: a feed spacer problem, Water Research 43, 583–594

Vrouwenvelder, J.S.; Beyer, F.; Dahmani, K.; Hasan, N.; Galjaard, G.; Kruithof, J.C.; van Loosdrecht, M.C.M. (2010). Phosphate limitation to control biofouling. Water Res. 44, 3454 – 3466

Wagner, J., and Rosenwinkel, K-H. (2000). Sludge production in membrane bioreactors under different conditions. Water Science and Technology, 41 (10-11), 251-258.

Wagner, M., G. Rath, H.-P. Koops, J. Flood and R. Amann. (1996). In Situ analysis of nitrifying bacteria in sewage treatment plants. Water Science and Technolog 34(1-2): 237-244.

Wang B., He S., Wang L.,Shuo L. (2005) Simultaneous nitrification and de-nitrification in MBR. Water Sci. Techn. 52 (10-11), 435-442.

Wang, C., Chou, W., Kuo, Y. (2009). Removal of COD from laundry wastewater by electrocoagulation/electroflotation, J. Hazard. Mater. 164, 81–86.

Wang, L., Hung, Y.-T., and Shammas, N. (2005). Physicochemical Treatment Processes. In Handbook of Environmental Engineering 3: 431-500.

Wang, Y., Tng, K. H., Wu, H., Leslie, G., Waite, T. D. (2014). Removal of phosphorus from wastewaters using ferrous salts - A pilot scale membrane bioreactor study. water research 57, 140-150

Wang, Y.K., Sheng, g.P., Li, W. W., Huang, Y. X., Yu Y. Y., Zeng, R. J. and Yu, H. Q. (2011). Development of a Novel Bioelectrochemical Membrane Reactor for Wastewater Treatment. Environ. Sci. Technol., 45 (21), 9256-9261

Wang, Z., Wu, Z., Tang, S. (2010). Impact of temperature seasonal change on sludge characteristics and membrane fouling in a submerged membrane bioreactor, Sep. Sci. Technol. 45, 920-927.

Wang, Z., Wu, Z., Yu, G., Liu, J., and Zhou, Z. (2006). Relationship between sludge characteristics and membrane flux determination in submerged membrane bioreactors. Journal of Membrane Science. 284(1-2): 87-94.

Wang, Z.W., Ma, J.X., Tang, C.Y., Kimura, K., Wang, Q.Y., Han, X.M. (2014). Membrane cleaning in membrane bioreactors: A review. Journal of Membrane Science 468, 276–307

Watanabe, Y., K. Kimura, K. and Itonaga, T. (2006). Influence of dissolved organic carbon and suspension viscosity on membrane fouling in submerged MBR. Separation Science and Technology, 41, 1371 – 1382.

Wei V., Oleszkiewicz JA, M. Elektorowicz. (2009). Nutrient removal in an electrically enhanced membrane bioreactor. Water Sci. & Tech. 60, 3159-3164

Wei V., Oleszkiewicz JA, M. Elektorowicz. (2011). Influence of electric current on bacterial viability in wastewater treatment. Water Research. 45 (16), 5058-5062

Wei, V., Elektorowicz, M., and Oleszkiewicz, J. A. (2012). Electrically enhanced MBR system for total nutrient removal in remote northern applications. Water Science & Technology, 65(4) 737-742

Weigert, T., Altmann, J., Ripperger, J. (1999). Crossflow electrofiltration in pilot scale. Journal of Membrane Science 159, 253-262

Wen, X., Ding, H., Huang, X., and Liu, R. (2004). Treatment of hospital wastewater using a submerged membrane bioreactor. Process Biochemistry, 39(11), 1427-1431.

West, J. M. (1981). Basic Corrosion and Oxidation. Second edition. Wiley International Publications, New York.

Wiesner, M.R., Aptel, P. (1996). Mass transport and permeate flux and fouling in pressure driven processes. In: Water Treatment Membrane Processes. McGraw-Hill, New York, USA.

Wintgens, T., M. Gallenkemper and T. Melin. (2002). Endocrine disrupter removal from wastewater using membrane bioreactor and nanofiltration technology. Desalination 146(1-3): 387-391.

Wintgens, T., Rosen, J., Melin, T., Brepols, C., Drensla, K., and Engelhardt, N. (2003). Modeling of a membrane bioreactor system for municipal wastewater treatment. Journal of membrane science, 216, 55–65.

Wisniewski, C., and Grasmik, A. (1998). Floc size distribution in a membrane bioreactor and consequences for membrane fouling. Colloids Surface: A Physicochem Eng. Aspects, 138,403–411.

Wisniewski, C., en Grasmick, A. (1998). Floc size distribution in a membrane bioreactor and consequences for membrane fouling. Colloids and Surfaces A, pp 138, 403-411.

Wisniewski, C., en Grasmick, A., en Cruz, A.L. (2000). Critical particle size in membrane bioreactors case of a denitrifying bacterial suspension. Journal of Membrane Science, 138, pp 403-411.

Wu, J., Chen, F., Huang, X., Geng, W., and Wen, X. (2006). Using inorganic coagulants to control membrane fouling in a submerged membrane bioreactor. Desalination, 197, 124-136.

Yamamoto, H., H. M. Liljestrand, Y. Shimizu and M. Morita. (2003). Effects of Physical-Chemical Characteristics on the Sorption of Selected Endocrine Disruptors by Dissolved Organic Matter Surrogates. Environmental Science & Technology 37(12): 2646-2657.

Yamamoto, K., and Win, K. M. (1991). Tannery wastewater treatment using a sequencing batch membrane reactor. Water Science and Technology, 23(7–9), 1639–1648.

Yamamoto, K., Hiasa, M., Mahmood, T., and Matsuo, T. (1989). Direct solid-liquid separation using hollow fiber membrane in activated sludge aeration tank. Water Science and Technology, 21, 43–54.

Yamamoto, K., Hissa, M., Mahmood T., and Matsuo, T. (1994). Direct solid liquid separation using hollow fiber membrane in an activated sludge aeration tank. Water Sci. Technol., 30, 21–27.

Yamamoto, K., Hissa, M., Mahmood, T., en Matsuo, T. (1989). Direct solid liquid separation using hollow fibre membrane in an activated sludge membrane tank. Water Science & Technology, 21, 43-54.

Yamato, N., Kimura, K., Miyoshi, T., Watanabe, Y. (2006). Difference in membrane fouling in membrane bioreactors (MBRs) caused by membrane polymer materials. Journal of Membrane Science, 280, pp 911-919.

Yang, F., Shi, B., Meng, F., and Zhang, H. (2007). Membrane fouling behavior during filtration of sludge supernatant. Environmental Progress, 26 (1), 86-93.

Yang, Q., Chen, J., and Zhang, F. (2006). Membrane fouling control in a submerged membrane bioreactor with porous, flexible suspended carriers. Desalination. 189(1-3): 292-302.

Yang, W. (2009). Investigation of Endocrine Disrupting Compounds in Membrane Bioreactors and UV Processes. Biosystems Engineering. Winnipeg, University of Manitoba. Doctor of Philosophy: 153.

Yang, W. and N. Cicek. (2008). Treatment of swine wastewater by submerged membrane bioreactors with consideration of estrogenic activity removal. Desalination 231(1-3): 200-208.

Yang, W., Cicek, N., and Ilg J. (2006). State-of-the-art of membrane bioreactors: Worldwide research and commercial applications in North America. Journal of membrane science, 270(1-2), 201-211.

Yetilmezsoy, K., Ilhan, F., Sapci-Zengin, Z., Sakar, S. and Gonullu, M. T. (2009). Decolorization and COD Reduction of UASB Pretreated Poultry Manure Wastewater by Electrocoagulation Process: A Post-Treatment Study. Jour- nal of Hazardous Materials. 162(1), 120-132.

Yi, T. and J. W. F. Harper. (2007a). The effect of biomass characteristics on the partitioning and sorption hysteresis of 17[alpha]-ethinylestradiol. Water Research 41(7): 1543-1553.

Yi, T. and W. F. Harper. (2007b). The Link between Nitrification and Biotransformation of 17-alpha-Ethinylestradiol. Environmental Science & Technology 41(12): 4311-4316.

Yoon, S.-H., H.-S. Kim and I.-T. Yeom. (2004). The optimum operational condition of membrane bioreactor (MBR): cost estimation of aeration and sludge treatment. Water Research 38(1): 37-46.

Yoshimoto, T., F. Nagai, J. Fujimoto, K. Watanabe, H. Mizukoshi, T. Makino, K. Kimura, H. Saino, H. Sawada and H. Omura. (2004). Degradation of Estrogens by Rhodococcus zopfii and Rhodococcus equi Isolates from Activated Sludge in Wastewater Treatment Plants. Applied and Environmental Microbiology 70(9): 5283-5289.

Yu, H.Y., Xie, Y.J., Hu, M.X., Wang, S.Y., Wang, Z.K., Xu, Z.K. (2005). Surface modification of polypropylene microporous membrane to improve its antifouling property in MBR: CO2 plasma treatment. Journal of Membrane Science, 254, pp 219- 227.

Yu, M. J., Koo, J. S., Myung, G. N., Cho, U. K., and Cho, Y. M. (2005). Evaluation of bipolar electrocoagulation applied to biofiltration for phosphorus removal. Water Science and Technology, 51 (10), 231–239.

Yu, M. J., Ku, Y. H., Kim, Y. S., and Myung, G. N. (2006). Electrocoagulation combined with the use of an intermittently aeration bioreactor to enhance phosphorous removal. Environmental Technology, 27 (5), 483–491.

Yu, W. Z., Graham, N., Liu, H. J., Qu, J. H. (2013). Comparison of $FeCl_3$ and alum pre-treatment on UF membrane fouling. Chemical Engineering Journal 234, 158-165

Yukselen, M. A., Gregory, J. (2002). Breakage and Re-formation of Alum Flocs. Environmental Engineering Science. 19(4): 229-236

Zaloum, R., Lessard, S., Mourato, D., and Carriere, J. (1994). Membrane biological reactor treatment of oily wastewater from a mtal transformation mill. Water Science and Technology, 30(9), 21–27.

Zanello, P. (2003). Inorganic electrochemistry: theory, practice and application. Cambridge: Royal Society of Chemistry.

Zaroual, Z., Azzi, M., Saib, N., and Chainet, E. (2006). Contribution to the study of electrocoagulation mechanism in basic textile effluent. Journal of Hazardous Materials, 131(1-3), 73-78.

Zavala, M. A. L., Funamizu, N., and Takakuwa, T. (2004). Temperature effect on aerobic biodegradation of feces using sawdust as a matrix. Water Research, 38, 2406–2416.

Zeng R. J., Lemaire R, Yuan Z., Keller J. (2004). A novel wastewater treatment process: simultaneous nitrification, denitrification and phosphorus removal. Water Sci. Techn. 50 (10), 163-170.

Zeng, R. J., R. Lemaire, Z. Yuan and J. r. Keller. (2003). Simultaneous nitrification, denitrification, and phosphorus removal in a lab-scale sequencing batch reactor. Biotechnology and Bioengineering 84(2): 170-178.

Zhang, B., Y. K, S. Ohgaki and K. N. (1997). Floc size distribution and bacterial activities in membrane separation activated sludge processes for small-scale wastewater treatment/reclamation. Water Science and Technology 35: 37-44.

Zhang, B., Yamamoto, K., Ohgaki, S., en Kamiko, N. (1997). Floc size distribution and bacterial activities in membrane separation activated sludge processes for small scale wastewater treatment/reclamation. Water Science & Technology, 35, pp 37-44.

Zhang, H.F.; Sun, B.S.; Zhao, X.H.; Gao, Z.H. (2008). Effect of ferric chloride on fouling in membrane bioreactor. Sep. Purif. Technol. 63, 341–347.

Zhang, X., Bishop, P.L. (2002). Biodegradability of biofilm extracellular polymeric substances. Chemosphere, 50, pp 63 69.

Zhang, X.; Fan, L.; Roddick, F.A. (2014). Feedwater coagulation to mitigate the fouling of a ceramic MF membrane caused by soluble algal organic matter. Sep. Purif. Technol. 133, 221–226.

Zhang, X.Q., Bishop, P.L., Kinkle, B.K. (1999). Comparison of extraction methods for quantifying extracellular polymers in biofilms. Water Science and Technology, 39, pp 211–218.

Zhang, X.Q.; Bishop, P.L. (2001). Spatial distribution of extracellular polymeric substances in biofilms. J. Environ. Eng., 127, 850-856.

Zhang, Y. and J. L. Zhou. (2005). Removal of estrone and 17[beta]-estradiol from water by adsorption. Water Research 39(16): 3991-4003.

Zhao, C.H., Xua, X.C., Chen, J., Wang, G.W., Yang, F.L. (2014). Highly effective antifouling performance of PVDF/graphene oxide composite membrane in membrane bioreactor (MBR) system. Desalination. 340 (1), 59–66.

Zheng, X.-Y., Kong, H.-N., Wu, D.-y., Wang, C., and Yan Li, H.-r. Y. (2009). Phosphate removal from source separated urine by electrocoagulation using iron plate electrodes. Water Science & Technology. 60(11): 2929-2938.

Zhou, J.; Yang, F.-L.; Meng, F.-G.; An, P.; Wang, D. (2007). Comparison of membrane fouling during short-term filtration of aerobic granular sludge and activated sludge. J. Environ. Sci., 19, 1281–1286.

Zhou, S. A. and Uesaka, M. (2006). Bioelectrodynamics in living organisms. International Journal of Engineering Science 44: 67-92.

Zhou, Y.; Yu, S.; Gao, C.; Feng, X. (2009). Surface modification of thin film composite polyamide membranes by electrostatic self-deposition of polycations for improved fouling resistance. Sep. Purif. Technol., 66, 287–294.

Zhu, B., Clifford, D. A., and Chellam, S. (2005). Comparison of electrocoagulation and chemical coagulation pretreatment for enhanced virus removal using microfiltration membranes. Water Research, 39, 3098-3108.

Zhu, G.-b., Y. Peng, S.-y. Wu, S.-y. Wang and S.-w. Xu. (2007). Simultaneous nitrification denitrification in step feeding biological nitrogen removal process. Journal of Environmental Sciences 19: 1043-1048.

Zodi, S., Potier, O., Lapicque, F., and Leclerc, J.-P. (2009). Treatment of the textile wastewaters by electrocoagulation: Effect of operating parameters on the sludge settling characteristics. Separation and Purification Technology. 69(1): 29-36.

Zongo, I., Maiga, A. H., Wethe, J., Valentin, G., Leclerc, J.-P., Paternotte, G., and Lapicque, F. (2009). Electrocoagulation for treatment of textile wastewaters with Al or Fe electrodes: Compared variations of COD levels, turbidity and absorbance. Journal of Hazardous Materials. 169(1-3): 70-76.

APPENDICS

Appendix 1 Synthetic feed wastewater preparation

One. 4 L of Stock solution containing:

Chemical	g
$MgSO_4.7H2O$	16
$(NH_4)_2 SO_4$	38.55
$CaCl_2$	1.38
K_2HPO_4	15
KCl	2.63
$FeSO_4.7H_2O$	0.85
$MnSO_4.H_2O$	1.14
$NaHCO_3$	80
Glucose	100
Yeast extract	40

Two. Feed preparation: 800 mL stock solution diluted to 50L

Three. Procedure:

(1). Weigh the above amount of $MgSO_4.7H_2O$, $(NH_4)_2SO4$, $CaCl_2$, K_2HPO_4, KCl, $FeSO_4.7H_2O$, $MnSO_4.H_2O$ into a 4L container, add 3 L of hot tap water into it and mix for half hour;

(2). Weigh 80 g of $NaHCO_3$ into a 1L beaker and add 1 L of hot tape water and mix it for half hour, then pour the solution into the 4L container in (1);

(3). Weigh 100 g of glucose and 40 g of yeast into the 4L container after one hour mixing of (1) and (2)

(4). Let the final stock solution mix for two more hours

(5). Evenly distribute the stock solution in 5 portions (800 mL each) and store them in a 4 degree fridge.

Appendix 2 Protocol for TEP Analysis [Arruda et al., 2004; de la Torre et al., 2008]

Materials:

Filter Paper Schleicher & Schuell Black Ribbon

Alcian Blue solution 1% in 0.3% acetic acid (Clin Tech LTD)

Natrium Acetate (NaAc) 99%

Acetic acid (Ac) 99.8%

Preparation of Alcian Blue solution

- Prepare Alcian blue solution (1%) in 0.3% HAC solution by dissolving 1 gram Alcian Blue 8GX and 0.3 ml HAc in 100 mL flask

Preparation of acetate buffer solution (pH = 4, 0.2 M)

- 1 liter buffer solution by adding the following; dilute to 1 litre
  - 9.75 mL in Ac
  - 2.4526 g NaAC
- Adjust pH with HAc if necessary to get a pH of 4

Preparation of the Alcian Blue solution 0.055% (m/v)

- Put 5.5 ml of the alcian blue solution 1% in a 100 mL flask and make up the volume with the acetate buffer solution. Shake the flask always before use

Preparation of the calibration curve

1. Prepare a stock solution of 100 mg/L xanthan gum in acetate buffer solution
   a. This should be done day before and left on stir plate overnight
2. Prepare reference solutions from 1 to 20 mg/L xanthan gum in acetate buffer solution from the stock solution
3. Mix in a centrifuge tube:
   a. 5 mL of sample (sludge filtered through a filter paper Schleicher and Schuell Black Ribbon), 0.5 mL of the prepared alcian blue solution 0.055% (m/v) and 4.5 mL of acetate buffer solution

4. Vortex for 1 min
5. Centrifuge at 15300 rpm (23292 xg) for 10 minutes at 25C
6. Measure the absorbance of the supernatant at 602 nm DIRECTLY after centrifugation. The blank used is acetate buffer solution

Protocol for high concentrated samples (20-100 mg TEP/L)

*   Dilute the sample 5:1 by taking only 1 mL of sample instead of 5 mL and add 4 mL more of acetate buffer solution in the centrifuge tube. The concentration will be then multiplied by 5 after measuring it with the spectrophotometer

Recommendations:

*   It is recommended to use the alcian blue solution only for one month after its preparation, as the dyee aggregates and its absorbance decreases with time.
*   The use of the stock solution of 1% Alcian blue is quite useful and avoids the dilution of the alcian blue in powder form
*   The calibration curve will change depending on the alcian blue supplier and batch

Appendix 3 LIVE/DEAD® BacLight. Bacterial Viability Kits

[Modified from https://tools.thermofisher.com/content/sfs/manuals/mp07007.pdf]

1. Introduction

Molecular Probes' LIVE/DEAD® *Bac*LightTM Bacterial Viability Kits provide a novel two-color fluorescence assay of bacterial viability that has proven useful for a diverse array of bacterial genera. Conventional direct-count assays of bacterial viability are based on metabolic characteristics or membrane integrity. However, methods relying on metabolic characteristics often only work for a limited subset of bacterial groups, and methods for assessing bacterial membrane integrity commonly have high levels of background fluorescence. Both types of determinations suffer from being very sensitive to growth and staining conditions. Because of the marked differences in morphology, cytology and physiology among the many bacterial genera, a universally applicable direct-count viability assay has been very difficult to achieve. The LIVE/DEAD *Bac*Light Bacterial Viability Kits allow us to easily, reliably and quantitatively distinguish live and dead bacteria in minutes, even in a mixed population containing a range of bacterial types. The LIVE/DEAD *Bac*Light Bacterial Viability Kits utilize mixtures of SYTO® 9 green-fluorescent nucleic acid stain and the red-fluorescent nucleic acid stain, propidium iodide. These stains differ both in their spectral characteristics and in their ability to penetrate healthy bacterial cells. When used alone, the SYTO 9 stain generally labels all bacteria in a population -

those with intact membranes and those with damaged membranes. In contrast, propidium iodide penetrates only bacteria with damaged membranes, causing a reduction in the SYTO 9 stain fluorescence when both dyes are present. Thus, with an appropriate mixture of the SYTO 9 and propidium iodide stains, bacteria with intact cell membranes stain fluorescent green, whereas bacteria with damaged membranes stain fluorescent red. The excitation/emission maxima for these dyes are about 480/500 nm for SYTO 9 stain and 490/635 nm for propidium iodide. The background remains virtually nonfluorescent. Furthermore, although the dye ratios suggested for the LIVE/DEAD *Bac*Light Bacterial Viability Kits have been found to work well with a broad spectrum of bacterial types, these kits also accommodate fine tuning of the dye combinations so that optimal staining of bacteria can be achieved under a variety of environmental conditions.

A common criterion for bacterial viability is the ability of a bacterium to reproduce in suitable nutrient medium. Exponentially growing cultures of bacteria typically yield results with the LIVE/DEAD *Bac*Light bacterial viability assay that correlate well with growth assays in liquid or solid media. Under certain conditions, however, bacteria having compromised membranes may be able to recover and reproduce - such bacteria may be scored as "dead" in this assay. Conversely, some bacteria with intact membranes may be unable to reproduce in nutrient medium, and yet these may be scored as "alive." Kit L7012 to be used in this research provides separate solutions of the SYTO 9 and propidium iodide stains. Having separate staining components facilitates the calibration of bacterial fluorescence for quantitative procedures.

2. Materials

Kit Contents for Viability Kit, L7012
SYTO 9 dye, 3.34 mM (Component A), 300 µL solution in DMSO
Propidium iodide, 20 mM (Component B), 300 µL solution in DMSO
*Bac*Light mounting oil (Component C), 10 mL, for bacteria immobilized on membranes. The refractive index at 25°C is 1.517 ± 0.003. DO NOT USE FOR IMMERSION OIL.

3. Storage and Handling

For L7012, the DMSO stock solutions should be stored frozen at -20°C and protected from light. Allow reagents to warm to room temperature and centrifuge briefly before opening the vials. Before refreezing, seal all vials tightly. When stored properly, these stock solutions are stable for at least one year.

4. Culture Conditions and Preparation of Bacterial Suspensions

Note: Care must be taken to remove traces of growth medium before staining bacteria with these kit reagents. The nucleic acids and other media components can bind the SYTO 9 and propidium iodide dyes in unpredictable ways, resulting in unacceptable variations in staining. A single wash step is usually sufficient to remove significant traces of interfering media components from the bacterial suspension. Phosphate wash buffers are not recommended because they appear to decrease staining efficiency.

4.1 Take 25 mL of homogeneous biomass.

4.2 Concentrate 25 mL of the bacterial culture by centrifugation at 10,000 × g for 10 - 15 minutes.

4.3 Remove the supernatant and resuspend the pellet in 2 mL of 0.85% NaCl or appropriate buffer.

4.4 Add 1 mL of this suspension to each of two 30 - 40 mL centrifuge tubes containing either 20 mL of 0.85% NaCl or appropriate buffer (for live bacteria) or 20 mL of 70% isopropyl alcohol (for killed bacteria).

4.5 Incubate both samples at room temperature for 1 hour, mixing every 15 minutes.

4.6 Pellet both samples by centrifugation at 10,000 × g for 10 - 15 minutes.

4.7 Resuspend the pellets in 20 mL of 0.85% NaCl or appropriate buffer and centrifuge again as in step 1.6.

4.8 Resuspend both pellets in separate tubes with 10 mL of 0.85% NaCl or appropriate buffer each.

4.9 Determine the optical density at 670 nm (OD670) of a 3 mL aliquot of the bacterial suspensions in glass or acrylic absorption cuvettes (1 cm pathlength).

5. Fluorescence Microplate Readers

Staining Bacterial Suspensions with either Kit L7012
5.1 Adjust the *biomass* suspensions (live and killed) to 2 × 108 bacteria/mL (~0.06 OD670)
5.2 Mix five different proportions of *biomass* (Table 1) in 16 × 125 mm borosilicate glass culture tubes. The total volume of each of the five samples will be 2 mL.

Table 4-1 Volumes of live- and dead-cell suspensions to mix to achieve various proportions of live:dead cells for fluorescence microplate readers.

Ratio of Live:Dead Cells	mL Live-Cell Suspension	mL Dead-Cell Suspension
0:100	0	2.0
10:90	0.2	1.8
50:50	1.0	1.0
90:10	1.8	0.2
100:0	2.0	0

5.3 Mix 6 μL of Component A with 6 μL of Component B in a microfuge tube.
5.4 Prepare a 2X stain solution by adding the entire 12 μL of the above mixture to 2.0 mL of filter-sterilized H_2O in a 16 × 125 mm borosilicate glass culture tube and mix well.
5.5 Pipet 100 μL of each of the bacterial cell suspension mixtures into separate wells of a 96-well flat-bottom microplate. Prepare samples in triplicate. The outside wells (rows A and H and columns 1 and 12) are usually kept empty to avoid spurious readings.
5.6 Using a new tip for each well, pipet 100 μL of the 2X staining solution (from step 5.4) to each well and mix thoroughly by pipetting up and down several times.

5.7 Incubate at room temperature in the dark for 15 minutes.

6. Fluorescence Measurement and Data Analysis

6.1 With the excitation wavelength centered at about 485 nm, measure the fluorescence intensity at a wavelength centered at about 530 nm (emission 1; green) for each well of the entire plate.
6.2 With the excitation wavelength still centered at about 485 nm, measure the fluorescence intensity at a wavelength centered about 630 nm (emission 2; red) for each well of the entire plate.
6.3 Analyze the data by dividing the fluorescence intensity of the stained bacterial suspensions (Fcell) at emission 1 by the fluorescence intensity at emission 2.

$$\text{Ratio}_{G/R} = \frac{F_{cell,em1}}{F_{cell,em2}}$$

6.4 Plot the RatioG/R versus percentage of live cells in the *biomass* suspension (Figure 1).
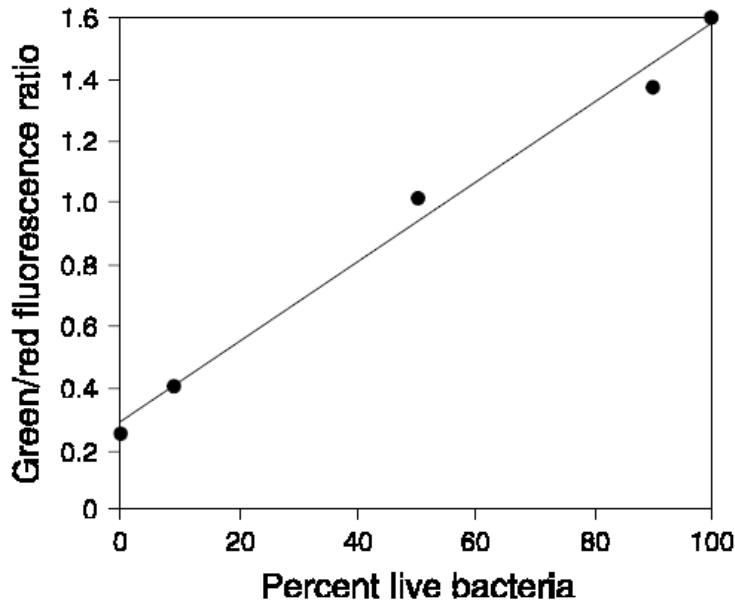
Figure 1. Analysis of relative viability of biomass suspensions in a fluorescence microplate reader. Samples of biomass were prepared and stained as outlined in the text. The integrated intensities of the green (530 ± 12.5 nm) and red (620 ± 20 nm) emission of suspensions excited at 485 ± 10 nm were acquired, and the green/red fluorescence ratios (RatioG/R) were calculated for each proportion of live/dead biomass. Each point represents the mean of ten measurements. The line is a least-squares fit of the relationship between % live bacteria (x) and RatioG/R (y).

7. Example of the microscopic images

10% live bacteria in normal biomass
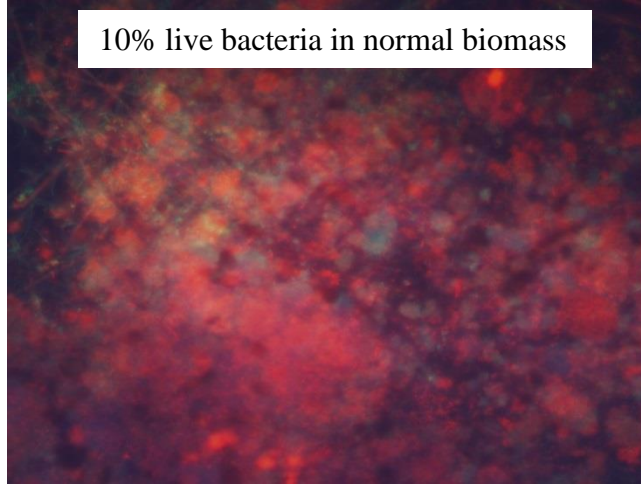
10% live bacteria in bulky biomass
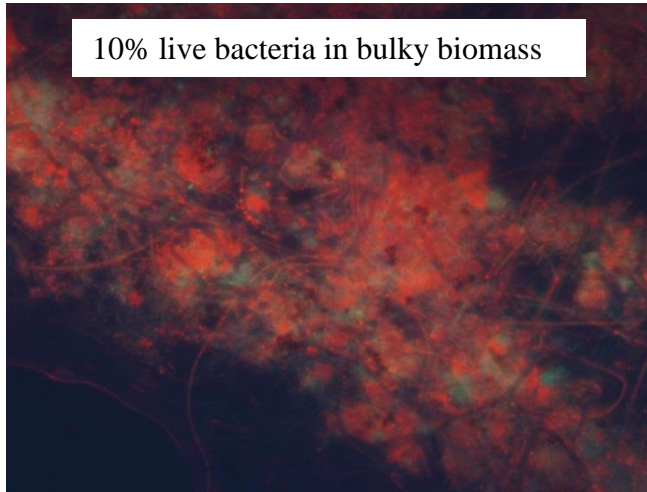
Appendix 4. Protocol of Yeast Estrogen Screen (YES) [Yang, 2009]

1. Materials and chemicals

<u>Materials</u>

1 L beaker (1)

weighing paper

balance

stirrer with heating

stirring bars

125 ml glass bottles (22)

60 ml glass bottles (20)

20 ml glass bottles (40)

200(250) beakers (5)

Autoclave (for sterilising at 121 °C)

0.2 μm pore size filter

conical flasks

pipets

50 ml graduated cylinder

orbital shaker

incubator

centrifuge

50 ml centrifuge tubes

96-well microtitre plate

microtitre plate shaker

plate reader

Chemicals

Potassium phosphate monobasic anhydrous

Ammonium sulphate

Potassium hydroxide

Magnesium sulfate

Iron (III) sulfate

L-Leucine

L-Histidine

Adenine

L-Argenine

L-Methionine

L-Tyrosine

L-Isoleucine

L-Lysine

L-Phenylalanine

L-Glutamic acid

L-Valine

L-Serine

Thiamine hydrochloride

Pyridoxine

D-Pantothenic acid hemicalcium salt

Inositol

d-Biotin

D-(+)-Glucose anhydrous; mixed anomers

L-Aspartic acid free acid

L-Threonine

Copper (II) sulfate anhydrous

Chlorophenolred-□-D galactopyranoside (CPRG)

Glycerol

β-Estradiol

2. Reagent preparation and stoarage

All glassware, spatulas, stirring bars, etc., must be thoroughly cleaned and finally rinsed twice with ethanol, and leave to air dry.

Minimal Medium (pH 7.1)

Add the following chemicals to 1L Milli-Q water and place it on heated stirrer to dissolve.

13.61 g KH_2PO_4

1.98 g $(NH4)_2SO_4$

4.2 g KOH pellets

0.2 g $MgSO_4$

1 ml $Fe_2(SO_4)3$ solution (40 mg/50 ml H_2O)

50 mg L-leucine

50 mg L-histidine

50 mg adenine

20 mg L-arginine-HCl

20 mg L-methionine

30 mg L-tyrosine

30 mg L-isoleucine

30 mg L-lysine-HCl

25 mg L-phenylalanine

100 mg L-glutamic acid

150 mg L-valine

375 mg L-serine

Dispense 45 ml aliquots into glass bottles (125 ml×22).

Sterilise at 121˚C for 15 min, and store at room temperature.

D-(+)-Glucose

Prepare a 200 ml 20% w/v solution. Add 40 g glucose to 200 ml Milli-Q water.

Sterilise in 20 ml aliquots (60 ml glass bottles × 10) at 121˚C for 15 min.

Store at room temperature.

L-Aspartic Acid

Make a 100 ml stock solution of 4 mg/ml. Add 0.4 g L-Aspartic Acid into 100 ml Milli-Q water.

Sterilise in 20 ml aliquots (60 ml glass bottles × 5) at 121˚C for 15 min.

Store at room temperature.

Vitamin Solution

Add 4 mg thiamine, 4 mg pyridoxine, 4 mg pantothenic acid, 20 mg inositol, and 10 ml biotin solution (2 mg/100 ml H_2O) to 90 ml Milli-Q water.

Sterilise by filtering through a 0.2-µm pore size disposable filter, in a laminar air flow cabinet.

Filter into sterile glass bottles in 10 ml aliquots (20 ml glass bottles $\times$ 10).

Store at 4˚C.

L-Threonine

Prepare a 50 ml solution of 24 mg/ml. Add 1.2 g L-Threonine into 50 ml Milli-Q water.

Sterilise in 10 ml aliquots (20 ml glass bottles $\times$ 5) at 121˚C for 10 min.

Store in fridge at 4˚C.

Copper (II) Sulfate

Prepare a 25 ml 3.2 mg/ml solution. Add 0.08 g $CuSO_4$ into 25 ml Milli-Q water.

Sterilise by filtering through a 0.2-µm pore size filter, in a laminar flow cabinet. Filter into sterile glass bottles (20 ml $\times$ 5) in 5 ml aliquots.

Store at room temperature.

Chlorophenol red-ß-D-galactopyranoside (CPRG)

Make a 10 ml 10 mg/ml stock solution. Add 100 mg CPRG into 10 ml MIlli-Q water.Sterilise by filtering through a 0.2-µm pore size filter into sterile glass bottle (20 ml$\times$ 1) ,in a laminar flow cabinet.

Store in fridge at 4˚C.

3. Preparation and storage of 10 x concentrated Yeast stocks

Carry out all yeast work in a type II laminar flow cabinet.

Day 1

Prepare growth medium by adding 5 ml glucose solution, 1.25 ml L-aspartic acid solution, 0.5 ml vitamin solution, 0.4 ml L-threonine solution, and 125 µl copper (II) sulfate solution to 45 ml minimal medium. Transfer to a sterile conical flask (final volume of approximately 50 ml). Add 125 µl of 10X concentrated yeast stock from cryogenic vial stored at -20˚C. Incubate at 28˚C (in water bath) for approximately 24 hour on an orbital shaker, or until turbid.

Day 2

Prepare growth medium and transfer to two conical flasks (each with a final volume of approximately 50 ml).

Add 1 ml yeast from 24-h culture to each flask.

Incubate at 28˚C for approximately 24 hour on an orbital shaker, or until turbid.

Day 3

Transfer each 24-h culture to a sterile 50-ml centrifuge tube.

Centrifuge the cultures at 4˚C for 10 min at 2,000 g.

Decant the supernatant, and resuspend each culture in 5 ml of minimal medium with 15% glycerol (add 8 ml sterile glycerol to 45 ml minimal medium).

Transfer 0.5 ml aliquots of the 10X concentrated stock culture to 1.2-ml sterile cryovials (×20).

Store at -20˚C for a maximum of 4 months.

4. Preparation of the working standard solutions

Glassware must be scrupulously cleaned since contamination may give rise to false positives. Rinse all glass bottles twice with absolute ethanol (or twice with methanol, and once with ethanol), and leave to dry.

Prepare the 17ß-estradiol (E2) stock solution in absolute ethanol, at 50 µg/L

Add 50 mg E2 in 10 ml absolute ethanol to make a 5 mg/ml solution. Add 0.1 ml 5 mg/ml solution in 9.9 ml absolute ethanol to make a 50 mg/l solution. Add 10 µl 50 mg/l solution into 10 ml absolute ethanol to make a 50 µg/L solution.

Serially dilute solutions at concentrations of 50, 100, 300, 500, 750, 1000 ng/L.

 5. Assay procedure

Carry out all yeast work in a type II laminar flow cabinet.

<u>Day 0</u>

Prepare growth medium by adding 5 ml glucose solution, 1.25 ml L-aspartic acid solution, 0.5 ml vitamin solution, 0.4 ml L-threonine solution, and 125 µl copper (II) sulfate solution to 45 ml minimal medium.

Transfer to a sterile conical flask (final volume of approximately 50 ml). Add 0.25ml of 10X concentrated yeast stock from cryogenic vial.

Incubate at 28˚C for approximately 24 hour on an orbital shaker, or until turbid.

Day 1

Prepare assay medium by adding 0.5 ml CPRG to 50 ml fresh growth medium. Seed this medium with 2 ml yeast from the 24-h culture prepared on Day 0. For every 2.5 assay plates, prepare 50 ml assay medium.

Transfer 10 µl water samples to a 96-well optically flat bottom microtitre plate. Add 200 µl of the seeded assay medium (growth medium containing CPRG and yeast) to wells using a multichannel pipette.

Each plate should contain at least one row of blanks (solvent and assay medium only), and each assay should have a 17ß-estradiol standard curve.

Seal the plates with Parafilm wrapping film and shake vigorously for 2 min on a titre plate shaker.

Incubate at 32˚C in an incubator for 72 h.

Day 4

After incubating for 3 days, shake plates (2 min) and leave for approximately 1 hour to allow the yeast to settle. Read the plates at an absorbance of 540 nm (optimum absorbance for CPRG ~575 nm) and 620 nm (for turbidity) using a plate reader.

Leave the plates at room temperature and read later if necessary.

6. Calculation

To correct for turbidity the following equation needs to be applied to the data:

Corrected value = Abs. (540 nm) - [Abs. (620 nm) – Abs_{blank}. (620 nm)]

Appendix 5 Procedure of SEM sample preparation

Procedure of SEM sample preparation in EM lab. (morphology)

Fix sample in Fixation Buffer for 4hr in room temp. or overnight in 4 ^{0}C buffer and

rinses 3X 15 min in room temp. before proceed to following steps

Buffer rinses 3X 15 min in room temp.

30% EtOH 10 min

50% EtOH 10 min

70% EtOH 10 min or overnoight

85% EtOH 20 min

95% EtOH 20 min

100% EtOH 20 min

100% EtOH 20 min or overnight

100% Acetone 20 min$

100% Acetone 20 min

Critical point drying or freeze drying

Sample on stubs

Coating Au

Observation

Note:

*Fixation Buffers (choose one):

(1) Gluteraldehyde buffer

2.5% GA + 4% PFA/0.1M phosphate or cacodylate buffer

The buffer should be pH to 7.2, store at 4□C (good for one year)

(2) Osmium tetroxide buffer

1% OsO4/0.1M phosphate or cacodylate buffer 4hr in room temp.

Make fresh - 1-2 days in advance to disolve

Use FUME HOOD! and use gloves all the time

This buffer can be used after buffer (1)

$Do not proceed to acetone step if you are not going to the drying procedure right

away, as the materials will be fragile if left in acetone for too long.

GA = gluteraldehyde

PFA = paraformaldehyde

OsO4 = osmium tetroxide

Appendix 6 Particle size data

Electrocoagulation batch test (Trial 1)

T(min)	$D_{0.1}(\mu m)$	$D_{0.5}(\mu m)$	$D_{0.9}(\mu m)$
3.5	121.8	554.4	206.4
3.6	123.2	555.6	207.4
4.4	131.6	562.1	213.2
1.9	92.8	527.8	185.4
2.2	99.2	534.2	190.1

Electrocoagulation batch test (Trial 2)

T(min)	$D_{0.1}(\mu m)$	$D_{0.5}(\mu m)$	$D_{0.9}(\mu m)$
4.2	129.5	560.6	211.8
2.7	108.8	543.3	197.1
2.2	99.7	534.8	190.5
1.7	85.1	519.3	179.4
1.5	76.0	508.3	172.2

Electrocoagulation batch test (Trial 3)

T(min)	$D_{0.1}(\mu m)$	$D_{0.5}(\mu m)$	$D_{0.9}(\mu m)$
7.1	150.4	575.9	226.4
3.4	120.7	553.5	205.6
2.0	93.8	528.7	186.1

| 1.6 | 79.8 | 513.0 | 175.2 |
| 1.6 | 80.4 | 513.7 | 175.7 |

Electrocoagulation batch test (Trial 4)

T(min)	$D_{0.1}$(µm)	$D_{0.5}$ (µm)	$D_{0.9}$ (µm)
3.7	124.4	556.6	208.2
2.5	105.7	540.4	194.9
1.7	86.5	521.0	180.6
1.5	77.1	509.6	173.1
1.1	55.5	476.5	153.8

Chemical coagulation data

Sample Name:	SOP Name:	Measured:	
Victor dosage 0 - Average	Victor Wei_EMBR Waterwater Biomass	Friday, July 16, 2010 2:52:30 PM	
Sample Source & type:	Measured by:	Analysed:	
Factory = Paris	Mastersizer 2000	Friday, July 16, 2010 2:52:31 PM	
Sample bulk lot ref:	Result Source:		
123-ABC	Averaged		
Particle Name:	Accessory Name:	Analysis model:	Sensitivity:
EMBR Waterwater Biomass	Hydro 2000S (A)	General purpose	Enhanced
Particle RI:	Absorption:	Size range:	Obscuration:
1.330	0	0.020 to 2000.000 um	11.33 %
Dispersant Name:	Dispersant RI:	Weighted Residual:	Result Emulation:
Water	1.330	18.256 %	Off
Concentration:	Span :	Uniformity:	Result units:
5938740... %Vol	7.246	2.17	Volume
Specific Surface Area:	Surface Weighted Mean D[3,2]:	Vol. Weighted Mean D[4,3]:	
2.35 m²/g	2.554 um	164.996 um	

d(0.1): 1.284 um   d(0.5): 68.168 um   d(0.9): 495.225 um

Particle Size Distribution — Control

Victor dosage 0 - Average, Friday, July 16, 2010 2:52:30 PM

Size (µm)	Volume In %	Size (µm)	Volume In %	Size (µm)	Volume In %	Size (µm)	Volume In %	Size (µm)	Volume In %	Size (µm)	Volume In %
0.010	0.00	0.105	0.24	1.096	0.79	11.482	1.43	120.226	2.57	1258.925	0.00
0.011	0.00	0.120	0.27	1.259	0.82	13.183	1.48	138.038	2.67	1445.440	0.00
0.013	0.00	0.138	0.30	1.445	0.85	15.136	1.53	158.489	2.76	1659.587	0.00
0.015	0.00	0.158	0.34	1.660	0.88	17.378	1.58	181.970	2.86	1905.461	0.00
0.017	0.00	0.182	0.37	1.905	0.92	19.953	1.64	208.930	2.95	2187.762	0.00
0.020	0.00	0.209	0.41	2.188	0.96	22.909	1.69	239.883	3.04	2511.886	0.00
0.023	0.00	0.240	0.44	2.512	0.99	26.303	1.75	275.423	3.12	2884.032	0.00
0.026	0.00	0.275	0.47	2.884	1.02	30.200	1.81	316.228	3.18	3311.311	0.00
0.030	0.00	0.316	0.50	3.311	1.06	34.674	1.88	363.078	3.21	3801.894	0.00
0.035	0.00	0.363	0.54	3.802	1.09	39.811	1.94	416.869	3.18	4365.158	0.00
0.040	0.00	0.417	0.57	4.365	1.13	45.709	2.01	478.630	3.06	5011.872	0.00
0.046	0.00	0.479	0.60	5.012	1.17	52.481	2.08	549.541	2.82	5754.399	0.00
0.052	0.04	0.550	0.63	5.754	1.21	60.256	2.16	630.957	2.35	6606.934	0.00
0.060	0.08	0.631	0.66	6.607	1.25	69.183	2.24	724.436	1.75	7585.776	0.00
0.069	0.11	0.724	0.69	7.586	1.29	79.433	2.32	831.764	0.78	8709.636	0.00
0.079	0.15	0.832	0.73	8.710	1.34	91.201	2.40	954.993	0.00	10000.000	0.00
0.091	0.20	0.955	0.76	10.000	1.38	104.713	2.49	1096.478	0.00		
0.105		1.096		11.482		120.226		1258.925			

Sample Name:
Victor dosage 20 mL - Average

Sample Source & type:
Factory = Paris

Sample bulk lot ref:
123-ABC

SOP Name:
Victor Wei_EMBR Waterwater Biomass

Measured by:
Mastersizer 2000

Result Source:
Averaged

Measured:
Friday, July 16, 2010 3:02:06 PM

Analysed:
Friday, July 16, 2010 3:02:07 PM

Particle Name:
EMBR Waterwater Biomass

Particle RI:
1.330

Dispersant Name:
Water

Accessory Name:
Hydro 2000S (A)

Absorption:
0

Dispersant RI:
1.330

Analysis model:
General purpose

Size range:
0.020 to 2000.000 um

Weighted Residual:
18.585 %

Sensitivity:
Enhanced

Obscuration:
11.25 %

Result Emulation:
Off

Concentration:
3753968... %Vol

Specific Surface Area:
0.994 m²/g

Span :
3.793

Surface Weighted Mean D[3,2]:
6.037 um

Uniformity:
1.18

Vol. Weighted Mean D[4,3]:
224.974 um

Result units:
Volume

d(0.1): 6.581 um   d(0.5): 149.310 um   d(0.9): 572.919 um

dose 27 mg/L Al^{3+},

mean floc size = 225 um

Particle Size Distribution — Volume (%) vs Particle Size (µm)

—Victor dosage 20 mL - Average, Friday, July 16, 2010 3:02:06 PM

Size (µm)	Volume In %	Size (µm)	Volume In %	Size (µm)	Volume In %	Size (µm)	Volume In %	Size (µm)	Volume In %	Size (µm)	Volume In %
0.010		0.105	0.10	1.096	0.33	11.482	1.03	120.226	3.12	1258.925	0.00
0.011	0.00	0.120	0.11	1.259	0.35	13.183	1.10	138.038	3.30	1445.440	0.00
0.013	0.00	0.138	0.12	1.445	0.37	15.136	1.18	158.489	3.49	1659.587	0.00
0.015	0.00	0.158	0.14	1.660	0.39	17.378	1.27	181.970	3.69	1905.461	0.00
0.017	0.00	0.182	0.15	1.905	0.41	19.953	1.36	208.930	3.88	2187.762	0.00
0.020	0.00	0.209	0.17	2.188	0.43	22.909	1.46	239.883	4.08	2511.886	0.00
0.023	0.00	0.240	0.18	2.512	0.45	26.303	1.56	275.423	4.26	2884.032	0.00
0.026	0.00	0.275	0.19	2.884	0.49	30.200	1.67	316.228	4.41	3311.311	0.00
0.030	0.00	0.316	0.21	3.311	0.54	34.674	1.78	363.078	4.51	3801.894	0.00
0.035	0.00	0.363	0.22	3.802	0.57	39.811	1.90	416.869	4.53	4365.158	0.00
0.040	0.00	0.417	0.23	4.365	0.62	45.709	2.03	478.630	4.43	5011.872	0.00
0.046	0.00	0.479	0.25	5.012	0.66	52.481	2.16	549.541	4.10	5754.399	0.00
0.052	0.00	0.550	0.26	5.754	0.71	60.256	2.30	630.957	3.44	6606.934	0.00
0.060	0.03	0.631	0.27	6.607	0.77	69.183	2.45	724.436	2.58	7585.776	0.00
0.069	0.04	0.724	0.29	7.586	0.83	79.433	2.61	831.764	1.15	8709.636	0.00
0.079	0.05	0.832	0.30	8.710	0.89	91.201	2.77	954.993	0.00	10000.000	0.00
0.091	0.08	0.955	0.32	10.000	0.96	104.713	2.87	1096.478	0.00		
0.105		1.096		11.482		120.226	2.94	1258.925	0.00		

Sample Name:
victor dosage 45ml - Average

Sample Source & type:
Factory = Paris

Sample bulk lot ref:

SOP Name:
Victor Wei_EMBR Waterwater Biomass

Measured by:
Mastersizer 2000

Result Source:
Averaged

Measured:
Friday, July 16, 2010 3:39:13 PM

Analysed:
Friday, July 16, 2010 3:39:14 PM

Particle Name:
EMBR Waterwater Biomass

Particle RI:
1.330

Dispersant Name:
Water

Accessory Name:
Hydro 2000S (A)

Absorption:
0

Dispersant RI:
1.330

Analysis model:
General purpose

Size range:
0.020 to 2000.000 um

Weighted Residual:
18.503 %

Sensitivity:
Enhanced

Obscuration:
11.04 %

Result Emulation:
Off

Concentration:
3137044... %Vol

Specific Surface Area:
0.784 m²/g

Span :
2.736

Surface Weighted Mean D[3,2]:
7.657 um

Uniformity:
0.844

Vol. Weighted Mean D[4,3]:
274.689 um

Result units:
Volume

d(0.1): 14.698 um   d(0.5): 221.643 um   d(0.9): 621.127 um

dose 54 mg/L Al^{3+},

mean floc size = 225 um

Particle Size Distribution — Volume (%) vs Particle Size (µm)

—victor dosage 45ml - Average, Friday, July 16, 2010 3:39:13 PM

Size (µm)	Volume In %	Size (µm)	Volume In %	Size (µm)	Volume In %	Size (µm)	Volume In %	Size (µm)	Volume In %	Size (µm)	Volume In %
0.010		0.105	0.08	1.096	0.25	11.482	0.58	120.226	3.26	1258.925	0.00
0.011	0.00	0.120	0.09	1.259	0.26	13.183	0.63	138.038	3.57	1445.440	0.00
0.013	0.00	0.138	0.10	1.445	0.26	15.136	0.69	158.489	3.88	1659.587	0.00
0.015	0.00	0.158	0.11	1.660	0.27	17.378	0.75	181.970	4.21	1905.461	0.00
0.017	0.00	0.182	0.12	1.905	0.30	19.953	0.82	208.930	4.53	2187.762	0.00
0.020	0.00	0.209	0.13	2.188	0.31	22.909	0.88	239.883	4.87	2511.886	0.00
0.023	0.00	0.240	0.14	2.512	0.32	26.303	0.96	275.423	5.18	2884.032	0.00
0.026	0.00	0.275	0.15	2.884	0.33	30.200	1.03	316.228	5.46	3311.311	0.00
0.030	0.00	0.316	0.16	3.311	0.34	34.674	1.13	363.078	5.67	3801.894	0.00
0.035	0.00	0.363	0.17	3.802	0.35	39.811	1.32	416.869	5.77	4365.158	0.00
0.040	0.00	0.417	0.18	4.365	0.37	45.709	1.51	478.630	5.68	5011.872	0.00
0.046	0.00	0.479	0.19	5.012	0.38	52.481	1.72	549.541	5.33	5754.399	0.00
0.052	0.00	0.550	0.20	5.754	0.39	60.256	1.95	630.957	4.51	6606.934	0.00
0.060	0.03	0.631	0.21	6.607	0.41	69.183	2.18	724.436	3.40	7585.776	0.00
0.069	0.04	0.724	0.22	7.586	0.43	79.433	2.43	831.764	1.52	8709.636	0.00
0.079	0.05	0.832	0.23	8.710	0.48	91.201	2.70	954.993	0.00	10000.000	0.00
0.091	0.06	0.955	0.24	10.000	0.53	104.713	2.97	1096.478	0.00		
0.105		1.096		11.482		120.226		1258.925	0.00		

Electrocoagulation batch test

Report 1

Sample Name:	SOP Name:	Measured:
Victor 5V T120 - Average	Victor Wei_EMBR Waterwater Biomass	Monday, July 19, 2010 4:00:01 PM
Sample Source & type:	Measured by:	Analysed:
Factory = Paris	Mastersizer 2000	Monday, July 19, 2010 4:00:02 PM
Sample bulk lot ref:	Result Source:	
123-ABC	Averaged	

Particle Name:	Accessory Name:	Analysis model:	Sensitivity:
EMBR Waterwater Biomass	Hydro 2000S (A)	General purpose	Enhanced
Particle RI:	Absorption:	Size range:	Obscuration:
1.330	0	0.020 to 2000.000 um	12.98 %
Dispersant Name:	Dispersant RI:	Weighted Residual:	Result Emulation:
Water	1.330	19.481 %	Off
Concentration:	Span :	Uniformity:	Result units:
1377335... %Vol	17.787	5.07	Volume
Specific Surface Area:	Surface Weighted Mean D[3,2]:	Vol. Weighted Mean D[4,3]:	
4.52 m²/g	1.327 um	91.894 um	

d(0.1): 0.529 um   d(0.5): 17.261 um   d(0.9): 307.541 um

Particle Size Distribution

- Victor 5V T0 - Average, Monday, July 19, 2010 2:01:04 PM
- Victor 5V T15 - Average, Monday, July 19, 2010 2:20:08 PM
- Victor 5V T30 - Average, Monday, July 19, 2010 2:33:50 PM
- Victor 5V T45 - Average, Monday, July 19, 2010 2:46:27 PM
- Victor 5V T60 - Average, Monday, July 19, 2010 3:00:30 PM
- Victor 5V T75 - Average, Monday, July 19, 2010 3:16:30 PM

Report 2

Sample Name:	SOP Name:	Measured:
Victor 5V T0 - Average	Victor Wei_EMBR Waterwater Biomass	Monday, July 19, 2010 2:01:04 PM
Sample Source & type:	Measured by:	Analysed:
Factory = Paris	Mastersizer 2000	Monday, July 19, 2010 2:01:05 PM
Sample bulk lot ref:	Result Source:	
123-ABC	Averaged	

Particle Name:	Accessory Name:	Analysis model:	Sensitivity:
EMBR Waterwater Biomass	Hydro 2000S (A)	General purpose	Enhanced
Particle RI:	Absorption:	Size range:	Obscuration:
1.330	0	0.020 to 2000.000 um	12.74 %
Dispersant Name:	Dispersant RI:	Weighted Residual:	Result Emulation:
Water	1.330	18.435 %	Off
Concentration:	Span :	Uniformity:	Result units:
8353315... %Vol	12.480	3.56	Volume
Specific Surface Area:	Surface Weighted Mean D[3,2]:	Vol. Weighted Mean D[4,3]:	
3.46 m²/g	1.736 um	126.277 um	

d(0.1): 0.734 um   d(0.5): 33.183 um   d(0.9): 414.868 um

Particle Size Distribution

- Victor 5V T0 - Average, Monday, July 19, 2010 2:01:04 PM

Sample Name: Victor 5V T15 - Average **SOP Name:** Victor Wei_EMBR Waterwater Biomass **Measured:** Monday, July 19, 2010 2:20:08 PM

Sample Source & type: Factory = Paris **Measured by:** Mastersizer 2000 **Analysed:** Monday, July 19, 2010 2:20:09 PM

Sample bulk lot ref: 123-ABC **Result Source:** Averaged

Particle Name: EMBR Waterwater Biomass **Accessory Name:** Hydro 2000S (A) **Analysis model:** General purpose **Sensitivity:** Enhanced

Particle RI: 1.330 **Absorption:** 0 **Size range:** 0.020 to 2000.000 um **Obscuration:** 11.66 %

Dispersant Name: Water **Dispersant RI:** 1.330 **Weighted Residual:** 18.411 % **Result Emulation:** Off

Concentration: 7903822... %Vol **Span:** 13.059 **Uniformity:** 3.72 **Result units:** Volume

Specific Surface Area: 3.54 m²/g **Surface Weighted Mean D[3,2]:** 1.694 um **Vol. Weighted Mean D[4,3]:** 122.812 um

d(0.1): 0.708 um   **d(0.5):** 31.020 um   **d(0.9):** 405.790 um
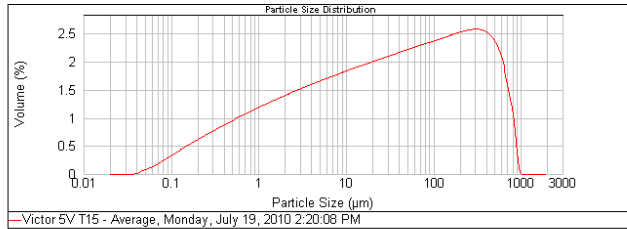
Victor 5V T15 - Average, Monday, July 19, 2010 2:20:08 PM

Size (µm)	Volume In %	Size (µm)	Volume In %	Size (µm)	Volume In %	Size (µm)	Volume In %	Size (µm)	Volume In %	Size (µm)	Volume In %
0.010		0.105	0.34	1.096	1.12	11.482	1.70	120.226	2.19	1258.925	0.00
0.011	0.00	0.120	0.39	1.259	1.15	13.183	1.73	138.038	2.22	1445.440	0.00
0.013	0.00	0.138	0.44	1.445	1.19	15.136	1.76	158.489	2.25	1659.587	0.00
0.015	0.00	0.158	0.49	1.660	1.23	17.378	1.79	181.970	2.27	1905.461	0.00
0.017	0.00	0.182	0.54	1.905	1.27	19.953	1.82	208.930	2.30	2187.762	0.00
0.020	0.00	0.209	0.59	2.188	1.30	22.909	1.85	239.883	2.32	2511.886	0.00
0.023	0.00	0.240	0.64	2.512	1.34	26.303	1.88	275.423	2.33	2884.032	0.00
0.026	0.00	0.275	0.68	2.884	1.37	30.200	1.90	316.228	2.32	3311.311	0.00
0.030	0.00	0.316	0.73	3.311	1.41	34.674	1.93	363.078	2.30	3801.894	0.00
0.035	0.00	0.363	0.78	3.802	1.44	39.811	1.96	416.869	2.24	4365.158	0.00
0.040	0.02	0.417	0.82	4.365	1.48	45.709	1.99	478.630	2.12	5011.872	0.00
0.046	0.06	0.479	0.87	5.012	1.51	52.481	2.02	549.541	1.92	5754.399	0.00
0.052	0.09	0.550	0.91	5.754	1.54	60.256	2.05	630.957	1.59	6606.934	0.00
0.060	0.13	0.631	0.95	6.607	1.57	69.183	2.08	724.436	1.17	7585.776	0.00
0.069	0.18	0.724	0.99	7.586	1.61	79.433	2.10	831.764	0.62	8709.636	0.00
0.079	0.23	0.832	1.03	8.710	1.64	91.201	2.13	954.993	0.00	10000.000	0.00
0.091	0.29	0.955	1.08	10.000	1.67	104.713	2.16	1096.478	0.00		
0.105		1.096		11.482		120.226	2.16	1258.925	0.00		

Sample Name: Victor 5V T30 - Average **SOP Name:** Victor Wei_EMBR Waterwater Biomass **Measured:** Monday, July 19, 2010 2:33:50 PM

Sample Source & type: Factory = Paris **Measured by:** Mastersizer 2000 **Analysed:** Monday, July 19, 2010 2:33:51 PM

Sample bulk lot ref: 123-ABC **Result Source:** Averaged

Particle Name: EMBR Waterwater Biomass **Accessory Name:** Hydro 2000S (A) **Analysis model:** General purpose **Sensitivity:** Enhanced

Particle RI: 1.330 **Absorption:** 0 **Size range:** 0.020 to 2000.000 um **Obscuration:** 11.58 %

Dispersant Name: Water **Dispersant RI:** 1.330 **Weighted Residual:** 18.581 % **Result Emulation:** Off

Concentration: 6391621... %Vol **Span:** 9.677 **Uniformity:** 2.82 **Result units:** Volume

Specific Surface Area: 2.84 m²/g **Surface Weighted Mean D[3,2]:** 2.111 um **Vol. Weighted Mean D[4,3]:** 144.315 um

d(0.1): 0.928 um   **d(0.5):** 47.071 um   **d(0.9):** 456.420 um

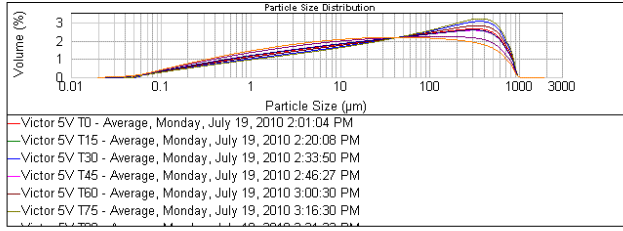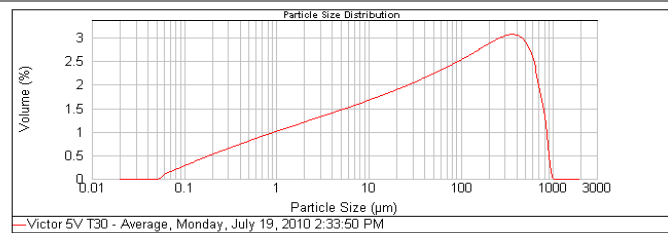Victor 5V T30 - Average, Monday, July 19, 2010 2:33:50 PM

Size (µm)	Volume In %	Size (µm)	Volume In %	Size (µm)	Volume In %	Size (µm)	Volume In %	Size (µm)	Volume In %	Size (µm)	Volume In %
0.010		0.105	0.29	1.096	0.95	11.482	1.56	120.226	2.39	1258.925	0.00
0.011	0.00	0.120	0.33	1.259	0.99	13.183	1.60	138.038	2.45	1445.440	0.00
0.013	0.00	0.138	0.37	1.445	1.02	15.136	1.64	158.489	2.51	1659.587	0.00
0.015	0.00	0.158	0.41	1.660	1.06	17.378	1.68	181.970	2.57	1905.461	0.00
0.017	0.00	0.182	0.46	1.905	1.09	19.953	1.73	208.930	2.63	2187.762	0.00
0.020	0.00	0.209	0.50	2.188	1.13	22.909	1.77	239.883	2.69	2511.886	0.00
0.023	0.00	0.240	0.54	2.512	1.16	26.303	1.81	275.423	2.73	2884.032	0.00
0.026	0.00	0.275	0.58	2.884	1.20	30.200	1.86	316.228	2.76	3311.311	0.00
0.030	0.00	0.316	0.62	3.311	1.23	34.674	1.91	363.078	2.76	3801.894	0.00
0.035	0.00	0.363	0.66	3.802	1.27	39.811	1.95	416.869	2.72	4365.158	0.00
0.040	0.00	0.417	0.69	4.365	1.30	45.709	2.00	478.630	2.60	5011.872	0.00
0.046	0.00	0.479	0.73	5.012	1.34	52.481	2.05	549.541	2.38	5754.399	0.00
0.052	0.02	0.550	0.77	5.754	1.37	60.256	2.11	630.957	1.98	6606.934	0.00
0.060	0.06	0.631	0.81	6.607	1.41	69.183	2.16	724.436	1.47	7585.776	0.00
0.069	0.11	0.724	0.84	7.586	1.45	79.433	2.21	831.764	0.65	8709.636	0.00
0.079	0.15	0.832	0.88	8.710	1.49	91.201	2.27	954.993	0.00	10000.000	0.00
0.091	0.20	0.955	0.91	10.000	1.52	104.713	2.33	1096.478	0.00		
0.105	0.24	1.096		11.482		120.226	2.33	1258.925	0.00		

Victor 5V T45 - Average

Sample Name:	SOP Name:	Measured:	
Victor 5V T45 - Average	Victor Wei_EMBR Waterwater Biomass	Monday, July 19, 2010 2:46:27 PM	
Sample Source & type:	Measured by:	Analysed:	
Factory = Paris	Mastersizer 2000	Monday, July 19, 2010 2:46:28 PM	
Sample bulk lot ref:	Result Source:		
123-ABC	Averaged		

Particle Name:	Accessory Name:	Analysis model:	Sensitivity:
EMBR Waterwater Biomass	Hydro 2000S (A)	General purpose	Enhanced
Particle RI:	Absorption:	Size range:	Obscuration:
1.330	0	0.020 to 2000.000 um	11.42 %
Dispersant Name:	Dispersant RI:	Weighted Residual:	Result Emulation:
Water	1.330	18.455 %	Off

Concentration:	Span :	Uniformity:	Result units:
7786824... %Vol	13.097	3.73	Volume
Specific Surface Area:	Surface Weighted Mean D[3,2]:	Vol. Weighted Mean D[4,3]:	
3.55 m²/g	1.691 um	122.559 um	

d(0.1): 0.706 um   d(0.5): 30.876 um   d(0.9): 405.088 um

Victor 5V T45 - Average, Monday, July 19, 2010 2:46:27 PM

Size (μm)	Volume In %	Size (μm)	Volume In %	Size (μm)	Volume In %	Size (μm)	Volume In %	Size (μm)	Volume In %	Size (μm)	Volume In %
0.010		0.105		1.096		11.482		120.226		1258.925	
0.011	0.00	0.120	0.34	1.259	1.12	13.183	1.70	138.038	2.19	1445.440	0.00
0.013	0.00	0.138	0.39	1.445	1.16	15.136	1.73	158.489	2.22	1659.587	0.00
0.015	0.00	0.158	0.44	1.660	1.19	17.378	1.76	181.970	2.24	1905.461	0.00
0.017	0.00	0.182	0.49	1.905	1.23	19.953	1.79	208.930	2.27	2187.762	0.00
0.020	0.00	0.209	0.54	2.188	1.27	22.909	1.82	239.883	2.29	2511.886	0.00
0.023	0.00	0.240	0.59	2.512	1.31	26.303	1.85	275.423	2.31	2884.032	0.00
0.026	0.00	0.275	0.64	2.884	1.34	30.200	1.88	316.228	2.32	3311.311	0.00
0.030	0.00	0.316	0.69	3.311	1.38	34.674	1.91	363.078	2.32	3801.894	0.00
0.035	0.00	0.363	0.73	3.802	1.41	39.811	1.93	416.869	2.29	4365.158	0.00
0.040	0.02	0.417	0.78	4.365	1.45	45.709	1.96	478.630	2.23	5011.872	0.00
0.046	0.06	0.479	0.82	5.012	1.48	52.481	1.99	549.541	2.11	5754.399	0.00
0.052	0.09	0.550	0.87	5.754	1.51	60.256	2.02	630.957	1.92	6606.934	0.00
0.060	0.13	0.631	0.91	6.607	1.54	69.183	2.05	724.436	1.58	7585.776	0.00
0.069	0.18	0.724	0.95	7.586	1.58	79.433	2.07	831.764	1.17	8709.636	0.00
0.079	0.23	0.832	1.00	8.710	1.61	91.201	2.10	954.993	0.52	10000.000	0.00
0.091	0.29	0.955	1.04	10.000	1.64	104.713	2.13	1096.478	0.00		
0.105		1.096	1.08	11.482	1.67	120.226	2.16	1258.925	0.00		

Victor 5V T60 - Average

Sample Name:	SOP Name:	Measured:	
Victor 5V T60 - Average	Victor Wei_EMBR Waterwater Biomass	Monday, July 19, 2010 3:00:30 PM	
Sample Source & type:	Measured by:	Analysed:	
Factory = Paris	Mastersizer 2000	Monday, July 19, 2010 3:00:32 PM	
Sample bulk lot ref:	Result Source:		
123-ABC	Averaged		

Particle Name:	Accessory Name:	Analysis model:	Sensitivity:
EMBR Waterwater Biomass	Hydro 2000S (A)	General purpose	Enhanced
Particle RI:	Absorption:	Size range:	Obscuration:
1.330	0	0.020 to 2000.000 um	11.66 %
Dispersant Name:	Dispersant RI:	Weighted Residual:	Result Emulation:
Water	1.330	18.616 %	Off

Concentration:	Span :	Uniformity:	Result units:
7053429... %Vol	11.169	3.22	Volume
Specific Surface Area:	Surface Weighted Mean D[3,2]:	Vol. Weighted Mean D[4,3]:	
3.14 m²/g	1.912 um	134.229 um	

d(0.1): 0.812 um   d(0.5): 38.801 um   d(0.9): 434.164 um

Victor 5V T60 - Average, Monday, July 19, 2010 3:00:30 PM

Size (μm)	Volume In %	Size (μm)	Volume In %	Size (μm)	Volume In %	Size (μm)	Volume In %	Size (μm)	Volume In %	Size (μm)	Volume In %
0.010		0.105		1.096		11.482		120.226		1258.925	
0.011	0.00	0.120	0.31	1.259	1.03	13.183	1.63	138.038	2.29	1445.440	0.00
0.013	0.00	0.138	0.36	1.445	1.06	15.136	1.66	158.489	2.34	1659.587	0.00
0.015	0.00	0.158	0.40	1.660	1.10	17.378	1.70	181.970	2.39	1905.461	0.00
0.017	0.00	0.182	0.45	1.905	1.14	19.953	1.73	208.930	2.43	2187.762	0.00
0.020	0.00	0.209	0.50	2.188	1.17	22.909	1.77	239.883	2.47	2511.886	0.00
0.023	0.00	0.240	0.54	2.512	1.21	26.303	1.81	275.423	2.51	2884.032	0.00
0.026	0.00	0.275	0.58	2.884	1.24	30.200	1.84	316.228	2.54	3311.311	0.00
0.030	0.00	0.316	0.63	3.311	1.28	34.674	1.88	363.078	2.56	3801.894	0.00
0.035	0.00	0.363	0.67	3.802	1.31	39.811	1.92	416.869	2.56	4365.158	0.00
0.040	0.00	0.417	0.71	4.365	1.35	45.709	1.96	478.630	2.54	5011.872	0.00
0.046	0.00	0.479	0.75	5.012	1.38	52.481	2.00	549.541	2.49	5754.399	0.00
0.052	0.08	0.550	0.79	5.754	1.42	60.256	2.04	630.957	2.37	6606.934	0.00
0.060	0.12	0.631	0.83	6.607	1.45	69.183	2.08	724.436	2.16	7585.776	0.00
0.069	0.17	0.724	0.87	7.586	1.49	79.433	2.12	831.764	1.79	8709.636	0.00
0.079	0.22	0.832	0.91	8.710	1.52	91.201	2.16	954.993	1.33	10000.000	0.00
0.091	0.26	0.955	0.95	10.000	1.56	104.713	2.21	1096.478	0.59		
0.105		1.096	0.99	11.482	1.59	120.226	2.25	1258.925	0.00		

Report 1

Sample Name: Victor 5V T75 - Average	**SOP Name:** Victor Wei_EMBR Waterwater Biomass	**Measured:** Monday, July 19, 2010 3:16:30 PM	
Sample Source & type: Factory = Paris	**Measured by:** Mastersizer 2000	**Analysed:** Monday, July 19, 2010 3:16:31 PM	
Sample bulk lot ref: 123-ABC	**Result Source:** Averaged		
Particle Name: EMBR Waterwater Biomass	**Accessory Name:** Hydro 2000S (A)	**Analysis model:** General purpose	**Sensitivity:** Enhanced
Particle RI: 1.330	**Absorption:** 0	**Size range:** 0.020 to 2000.000 um	**Obscuration:** 11.77 %
Dispersant Name: Water	**Dispersant RI:** 1.330	**Weighted Residual:** 19.373 %	**Result Emulation:** Off
Concentration: 6838625... %Vol	**Span :** 8.849	**Uniformity:** 2.6	**Result units:** Volume
Specific Surface Area: 2.73 m²/g	**Surface Weighted Mean D[3,2]:** 2.197 um	**Vol. Weighted Mean D[4,3]:** 150.523 um	

d(0.1): 1.005   um   d(0.5): 52.868   um   d(0.9): 468.824   um
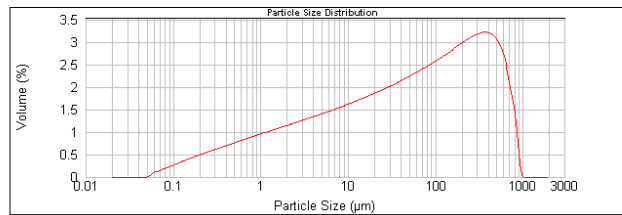
— Victor 5V T75 - Average, Monday, July 19, 2010 3:16:30 PM

Size (µm)	Volume In %	Size (µm)	Volume In %	Size (µm)	Volume In %	Size (µm)	Volume In %	Size (µm)	Volume In %	Size (µm)	Volume In %
0.010		0.105	0.27	1.096	0.90	11.482	1.52	120.226	2.44	1258.925	
0.011	0.00	0.120	0.31	1.259	0.94	13.183	1.56	138.038	2.52	1445.440	0.00
0.013	0.00	0.138	0.36	1.445	0.97	15.136	1.61	158.489	2.59	1659.587	0.00
0.015	0.00	0.158	0.39	1.660	1.00	17.378	1.65	181.970	2.66	1905.461	0.00
0.017	0.00	0.182	0.43	1.905	1.04	19.953	1.70	208.930	2.73	2187.762	0.00
0.020	0.00	0.209	0.47	2.188	1.07	22.909	1.74	239.883	2.80	2511.886	0.00
0.023	0.00	0.240	0.51	2.512	1.11	26.303	1.79	275.423	2.85	2884.032	0.00
0.026	0.00	0.275	0.55	2.884	1.14	30.200	1.84	316.228	2.85	3311.311	0.00
0.030	0.00	0.316	0.58	3.311	1.18	34.674	1.84	363.078	2.89	3801.894	0.00
0.035	0.00	0.363	0.58	3.802	1.18	39.811	1.90	416.869	2.90	4365.158	0.00
0.040	0.00	0.417	0.62	4.365	1.21	45.709	1.95	478.630	2.86	5011.872	0.00
0.046	0.00	0.479	0.66	5.012	1.25	52.481	2.00	549.541	2.74	5754.399	0.00
0.052	0.00	0.550	0.69	5.754	1.28	60.256	2.06	630.957	2.51	6606.934	0.00
0.060	0.04	0.631	0.73	6.607	1.32	69.183	2.12	724.436	2.09	7585.776	0.00
0.069	0.10	0.724	0.76	7.586	1.36	79.433	2.18	831.764	1.55	8709.636	0.00
0.079	0.15	0.832	0.80	8.710	1.40	91.201	2.24	954.993	0.69	10000.000	0.00
0.091	0.19	0.955	0.83	10.000	1.44	104.713	2.31	1096.478	0.00		
0.105	0.23	1.096	0.87	11.482	1.48	120.226	2.38	1258.925	0.00		

Report 2

Sample Name: Victor 5V T90 - Average	**SOP Name:** Victor Wei_EMBR Waterwater Biomass	**Measured:** Monday, July 19, 2010 3:31:32 PM	
Sample Source & type: Factory = Paris	**Measured by:** Mastersizer 2000	**Analysed:** Monday, July 19, 2010 3:31:34 PM	
Sample bulk lot ref: 123-ABC	**Result Source:** Averaged		
Particle Name: EMBR Waterwater Biomass	**Accessory Name:** Hydro 2000S (A)	**Analysis model:** General purpose	**Sensitivity:** Enhanced
Particle RI: 1.330	**Absorption:** 0	**Size range:** 0.020 to 2000.000 um	**Obscuration:** 11.93 %
Dispersant Name: Water	**Dispersant RI:** 1.330	**Weighted Residual:** 19.391 %	**Result Emulation:** Off
Concentration: 8085509... %Vol	**Span :** 12.994	**Uniformity:** 3.7	**Result units:** Volume
Specific Surface Area: 3.54 m²/g	**Surface Weighted Mean D[3,2]:** 1.694 um	**Vol. Weighted Mean D[4,3]:** 123.126 um	

d(0.1): 0.708   um   d(0.5): 31.229   um   d(0.9): 406.490   um
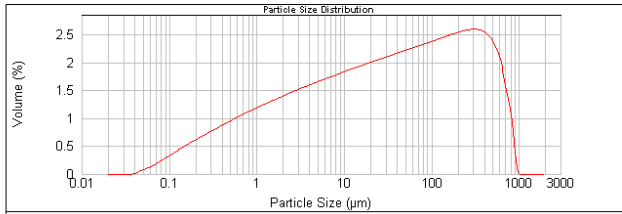
— Victor 5V T90 - Average, Monday, July 19, 2010 3:31:32 PM

Size (µm)	Volume In %	Size (µm)	Volume In %	Size (µm)	Volume In %	Size (µm)	Volume In %	Size (µm)	Volume In %	Size (µm)	Volume In %
0.010	0.00	0.105	0.34	1.096	1.11	11.482	1.69	120.226	2.19	1258.925	
0.011	0.00	0.120	0.39	1.259	1.15	13.183	1.73	138.038	2.22	1445.440	0.00
0.013	0.00	0.138	0.44	1.445	1.19	15.136	1.76	158.489	2.25	1659.587	0.00
0.015	0.00	0.158	0.49	1.660	1.23	17.378	1.79	181.970	2.28	1905.461	0.00
0.017	0.00	0.182	0.54	1.905	1.26	19.953	1.81	208.930	2.30	2187.762	0.00
0.020	0.00	0.209	0.59	2.188	1.30	22.909	1.84	239.883	2.32	2511.886	0.00
0.023	0.00	0.240	0.64	2.512	1.34	26.303	1.84	275.423	2.34	2884.032	0.00
0.026	0.00	0.275	0.68	2.884	1.37	30.200	1.87	316.228	2.33	3311.311	0.00
0.030	0.00	0.316	0.73	3.311	1.41	34.674	1.90	363.078	2.31	3801.894	0.00
0.035	0.00	0.363	0.78	3.802	1.44	39.811	1.93	416.869	2.24	4365.158	0.00
0.040	0.02	0.417	0.82	4.365	1.47	45.709	1.96	478.630	2.13	5011.872	0.00
0.046	0.06	0.479	0.86	5.012	1.51	52.481	1.99	549.541	1.93	5754.399	0.00
0.052	0.06	0.550	0.91	5.754	1.54	60.256	2.02	630.957	1.59	6606.934	0.00
0.060	0.09	0.631	0.95	6.607	1.54	69.183	2.05	724.436	1.18	7585.776	0.00
0.069	0.13	0.724	0.99	7.586	1.57	79.433	2.08	831.764	0.52	8709.636	0.00
0.079	0.18	0.832	1.03	8.710	1.60	91.201	2.11	954.993	0.00	10000.000	0.00
0.091	0.23	0.955	1.07	10.000	1.63	104.713	2.13	1096.478	0.00		
0.105	0.29	1.096		11.482	1.66	120.226	2.16	1258.925	0.00		

Victor 5V T105 - Average

Sample Name:	SOP Name:	Measured:
Victor 5V T105 - Average	Victor Wei_EMBR Waterwater Biomass	Monday, July 19, 2010 3:46:18 PM

Sample Source & type:	Measured by:	Analysed:
Factory = Paris	Mastersizer 2000	Monday, July 19, 2010 3:46:19 PM

Sample bulk lot ref:	Result Source:
123-ABC	Averaged

Particle Name:	Accessory Name:	Analysis model:	Sensitivity:
EMBR Waterwater Biomass	Hydro 2000S (A)	General purpose	Enhanced
Particle RI:	Absorption:	Size range:	Obscuration:
1.330	0	0.020 to 2000.000 um	13.24 %
Dispersant Name:	Dispersant RI:	Weighted Residual:	Result Emulation:
Water	1.330	19.170 %	Off

Concentration:	Span:	Uniformity:	Result units:
1171368... %Vol	16.301	4.61	Volume
Specific Surface Area:	Surface Weighted Mean D[3,2]:	Vol. Weighted Mean D[4,3]:	
4.23 m²/g	1.420 um	103.264 um	

d(0.1): 0.581 um   d(0.5): 21.278 um   d(0.9): 347.427 um
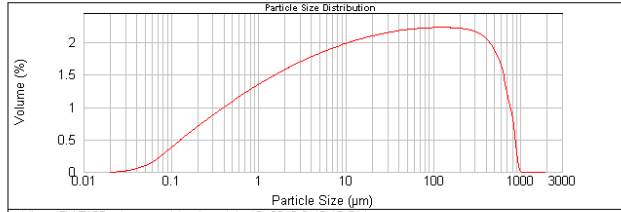
Victor 5V T105 - Average, Monday, July 19, 2010 3:46:18 PM

Size (µm)	Vol In %	Size (µm)	Vol In %	Size (µm)	Vol In %	Size (µm)	Vol In %	Size (µm)	Vol In %	Size (µm)	Vol In %
0.010		0.105		1.096		11.482		120.226		1258.925	
0.011	0.00	0.120	0.39	1.259	1.27	13.183	1.82	138.038	2.01	1445.440	0.00
0.013	0.00	0.138	0.45	1.445	1.31	15.136	1.84	158.489	2.01	1659.587	0.00
0.015	0.00	0.158	0.50	1.660	1.35	17.378	1.86	181.970	2.01	1905.461	0.00
0.017	0.00	0.182	0.56	1.905	1.39	19.953	1.88	208.930	2.00	2187.762	0.00
0.020	0.00	0.209	0.62	2.188	1.43	22.909	1.90	239.883	1.99	2511.886	0.00
0.023	0.00	0.240	0.67	2.512	1.47	26.303	1.92	275.423	1.98	2884.032	0.00
0.026	0.00	0.275	0.73	2.884	1.50	30.200	1.93	316.228	1.96	3311.311	0.00
0.030	0.01	0.316	0.78	3.311	1.54	34.674	1.95	363.078	1.93	3801.894	0.00
0.035	0.02	0.363	0.83	3.802	1.57	39.811	1.96	416.869	1.90	4365.158	0.00
0.040	0.03	0.417	0.89	4.365	1.60	45.709	1.97	478.630	1.87	5011.872	0.00
0.046	0.05	0.479	0.94	5.012	1.64	52.481	1.98	549.541	1.80	5754.399	0.00
0.052	0.08	0.550	0.99	5.754	1.67	60.256	1.99	630.957	1.68	6606.934	0.00
0.060	0.11	0.631	1.04	6.607	1.70	69.183	1.99	724.436	1.51	7585.776	0.00
0.069	0.15	0.724	1.08	7.586	1.72	79.433	2.00	831.764	1.23	8709.636	0.00
0.079	0.21	0.832	1.13	8.710	1.75	91.201	2.01	954.993	0.90	10000.000	0.00
0.091	0.27	0.955	1.18	10.000	1.77	104.713	2.01	1096.478	0.40		
0.105	0.33	1.096	1.22	11.482	1.80	120.226	2.01	1258.925	0.00		

Victor 5V T120 - Average

Sample Name:	SOP Name:	Measured:
Victor 5V T120 - Average	Victor Wei_EMBR Waterwater Biomass	Monday, July 19, 2010 4:00:01 PM

Sample Source & type:	Measured by:	Analysed:
Factory = Paris	Mastersizer 2000	Monday, July 19, 2010 4:00:02 PM

Sample bulk lot ref:	Result Source:
123-ABC	Averaged

Particle Name:	Accessory Name:	Analysis model:	Sensitivity:
EMBR Waterwater Biomass	Hydro 2000S (A)	General purpose	Enhanced
Particle RI:	Absorption:	Size range:	Obscuration:
1.330	0	0.020 to 2000.000 um	12.98 %
Dispersant Name:	Dispersant RI:	Weighted Residual:	Result Emulation:
Water	1.330	19.481 %	Off

Concentration:	Span:	Uniformity:	Result units:
1377335... %Vol	17.787	5.07	Volume
Specific Surface Area:	Surface Weighted Mean D[3,2]:	Vol. Weighted Mean D[4,3]:	
4.52 m²/g	1.327 um	91.894 um	

d(0.1): 0.529 um   d(0.5): 17.261 um   d(0.9): 307.541 um

Victor 5V T120 - Average, Monday, July 19, 2010 4:00:01 PM

Size (µm)	Vol In %	Size (µm)	Vol In %	Size (µm)	Vol In %	Size (µm)	Vol In %	Size (µm)	Vol In %	Size (µm)	Vol In %
0.010		0.105		1.096		11.482		120.226		1258.925	
0.011	0.00	0.120	0.41	1.259	1.35	13.183	1.89	138.038	1.91	1445.440	0.00
0.013	0.00	0.138	0.48	1.445	1.40	15.136	1.91	158.489	1.89	1659.587	0.00
0.015	0.00	0.158	0.54	1.660	1.44	17.378	1.93	181.970	1.87	1905.461	0.00
0.017	0.00	0.182	0.60	1.905	1.48	19.953	1.94	208.930	1.84	2187.762	0.00
0.020	0.00	0.209	0.66	2.188	1.52	22.909	1.95	239.883	1.82	2511.886	0.00
0.023	0.00	0.240	0.72	2.512	1.56	26.303	1.96	275.423	1.78	2884.032	0.00
0.026	0.00	0.275	0.78	2.884	1.60	30.200	1.97	316.228	1.74	3311.311	0.00
0.030	0.01	0.316	0.84	3.311	1.63	34.674	1.97	363.078	1.69	3801.894	0.00
0.035	0.02	0.363	0.90	3.802	1.67	39.811	1.97	416.869	1.63	4365.158	0.00
0.040	0.04	0.417	0.95	4.365	1.70	45.709	1.97	478.630	1.54	5011.872	0.00
0.046	0.06	0.479	1.01	5.012	1.73	52.481	1.97	549.541	1.43	5754.399	0.00
0.052	0.08	0.550	1.06	5.754	1.76	60.256	1.97	630.957	1.26	6606.934	0.00
0.060	0.12	0.631	1.11	6.607	1.79	69.183	1.96	724.436	1.02	7585.776	0.00
0.069	0.16	0.724	1.16	7.586	1.81	79.433	1.95	831.764	0.75	8709.636	0.00
0.079	0.22	0.832	1.21	8.710	1.83	91.201	1.95	954.993	0.33	10000.000	0.00
0.091	0.29	0.955	1.26	10.000	1.86	104.713	1.94	1096.478	0.00		
0.105	0.35	1.096	1.31	11.482	1.88	120.226	1.92	1258.925	0.00		

MBR vs EMBR

Sample Name:	SOP Name:	Measured:
Victor_LMBR	Victor Wei_EMBR Waterwater Biomass	Thursday, November 12, 2009 4:31:44 PM

Sample Source & type:	Measured by:	Analysed:
Factory = Paris	Mastersizer 2000	Thursday, November 12, 2009 4:31:45 PM

Sample bulk lot ref:	Result Source:	
123-ABC	Measurement	

Particle Name:	Accessory Name:	Analysis model:	Sensitivity:
EMBR Waterwater Biomass	Hydro 2000S (A)	General purpose	Enhanced

Particle RI:	Absorption:	Size range:	Obscuration:
1.330	0	0.020 to 2000.000 um	18.76 %

Dispersant Name:	Dispersant RI:	Weighted Residual:	Result Emulation:
Water	1.330	13.711 %	Off

Concentration:	Span :	Uniformity:	Result units:
2075357... %Vol	18.147	5.19	Volume

Specific Surface Area:	Surface Weighted Mean D[3,2]:	Vol. Weighted Mean D[4,3]:
4.59 m²/g	1.308 um	89.657 um

d(0.1): 0.519 um	d(0.5): 16.470 um	d(0.9): 299.416 um
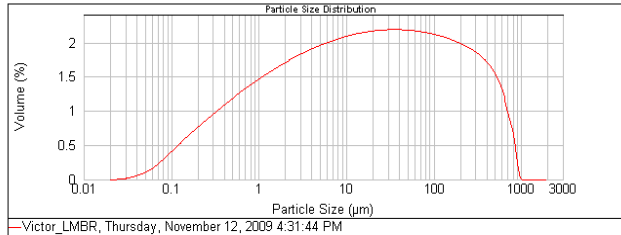
Particle Size Distribution

—Victor_LMBR, Thursday, November 12, 2009 4:31:44 PM

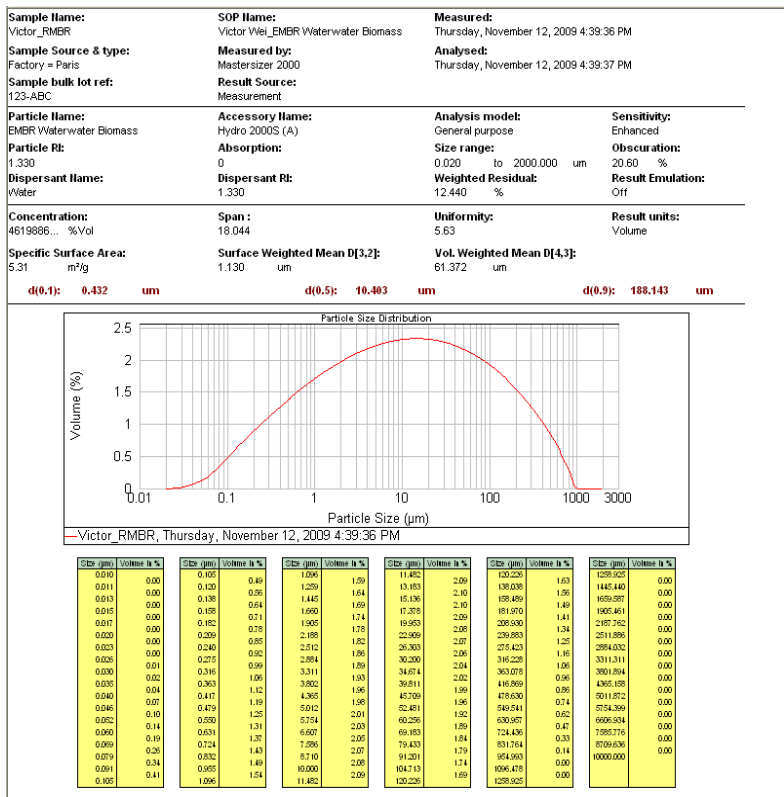| Size (µm)	Volume In %	Size (µm)	Volume In %	Size (µm)	Volume In %	Size (µm)	Volume In %	Size (µm)	Volume In %	Size (µm)	Volume In %
0.010	0.00	0.105	0.42	1.096	1.37	11.482	1.91	120.226	1.88	1258.925	0.00
0.011	0.00	0.120	0.48	1.259	1.42	13.183	1.93	138.038	1.86	1445.440	0.00
0.013	0.00	0.138	0.55	1.445	1.46	15.136	1.94	158.489	1.83	1659.587	0.00
0.015	0.00	0.158	0.61	1.660	1.51	17.378	1.95	181.970	1.80	1905.461	0.00
0.017	0.00	0.182	0.67	1.905	1.55	19.953	1.96	208.930	1.77	2187.762	0.00
0.020	0.00	0.209	0.73	2.188	1.58	22.909	1.97	239.883	1.73	2511.886	0.00
0.023	0.00	0.240	0.79	2.512	1.58	26.303	1.97	275.423	1.73	2884.032	0.00
0.026	0.00	0.275	0.85	2.884	1.62	30.200	1.97	316.228	1.69	3311.311	0.00
0.030	0.01	0.316	0.91	3.311	1.66	34.674	1.97	363.078	1.64	3801.894	0.00
0.035	0.02	0.363	0.91	3.802	1.69	39.811	1.98	416.869	1.57	4365.158	0.00
0.040	0.04	0.417	0.97	4.365	1.72	45.709	1.97	478.630	1.49	5011.872	0.00
0.046	0.06	0.479	1.02	5.012	1.75	52.481	1.97	549.541	1.38	5754.399	0.00
0.052	0.09	0.550	1.08	5.754	1.78	60.256	1.96	630.957	1.22	6606.934	0.00
0.060	0.12	0.631	1.13	6.607	1.81	69.183	1.96	724.436	0.99	7585.776	0.00
0.069	0.16	0.724	1.18	7.586	1.83	79.433	1.94	831.764	0.73	8709.636	0.00
0.079	0.22	0.832	1.23	8.710	1.85	91.201	1.93	954.993	0.32	10000.000	0.00
0.091	0.29	0.955	1.28	10.000	1.88	104.713	1.92	1096.478	0.00		
0.105	0.36	1.096	1.33	11.482	1.89	120.226	1.90	1258.925	0.00		

Sample Name:
Victor_RMBR

SOP Name:
Victor Wei_EMBR Waterwater Biomass

Measured:
Thursday, November 12, 2009 4:39:36 PM

Sample Source & type:
Factory = Paris

Measured by:
Mastersizer 2000

Analysed:
Thursday, November 12, 2009 4:39:37 PM

Sample bulk lot ref:
123-ABC

Result Source:
Measurement

Particle Name:
EMBR Waterwater Biomass

Accessory Name:
Hydro 2000S (A)

Analysis model:
General purpose

Sensitivity:
Enhanced

Particle RI:
1.330

Absorption:
0

Size range:
0.020   to   2000.000   um

Obscuration:
20.60   %

Dispersant Name:
Water

Dispersant RI:
1.330

Weighted Residual:
12.440   %

Result Emulation:
Off

Concentration:
4619886...   %Vol

Span :
18.044

Uniformity:
5.63

Result units:
Volume

Specific Surface Area:
5.31   m²/g

Surface Weighted Mean D[3,2]:
1.130   um

Vol. Weighted Mean D[4,3]:
61.372   um

d(0.1):   0.432   um   d(0.5):   10.403   um   d(0.9):   188.143   um

Particle Size Distribution

—Victor_RMBR, Thursday, November 12, 2009 4:39:36 PM

Size (µm)	Volume In %	Size (µm)	Volume In %	Size (µm)	Volume In %	Size (µm)	Volume In %	Size (µm)	Volume In %	Size (µm)	Volume In %
0.010	0.00	0.105		1.096		11.482		120.226		1258.925	0.00
0.011	0.00	0.120	0.49	1.259	1.59	13.183	2.09	138.038	1.63	1445.440	0.00
0.013	0.00	0.138	0.56	1.445	1.64	15.136	2.10	158.489	1.56	1659.587	0.00
0.015	0.00	0.158	0.64	1.660	1.69	17.378	2.10	181.970	1.49	1905.461	0.00
0.017	0.00	0.182	0.71	1.905	1.74	19.953	2.09	208.930	1.41	2187.762	0.00
0.020	0.00	0.209	0.78	2.188	1.78	22.909	2.08	239.883	1.34	2511.886	0.00
0.023	0.00	0.240	0.85	2.512	1.82	26.303	2.07	275.423	1.25	2884.032	0.00
0.026	0.01	0.275	0.92	2.884	1.86	30.200	2.06	316.228	1.16	3311.311	0.00
0.030	0.01	0.316	0.99	3.311	1.89	34.674	2.04	363.078	1.06	3801.894	0.00
0.035	0.02	0.363	1.06	3.802	1.93	39.811	2.02	416.869	0.96	4365.158	0.00
0.040	0.04	0.417	1.12	4.365	1.96	45.709	1.99	478.630	0.86	5011.872	0.00
0.046	0.07	0.479	1.19	5.012	1.98	52.481	1.96	549.541	0.74	5754.399	0.00
0.052	0.10	0.550	1.25	5.754	2.01	60.256	1.92	630.957	0.62	6606.934	0.00
0.060	0.14	0.631	1.31	6.607	2.03	69.183	1.89	724.436	0.47	7585.776	0.00
0.069	0.19	0.724	1.35	7.586	2.05	79.433	1.84	831.764	0.33	8709.636	0.00
0.079	0.26	0.832	1.43	8.710	2.07	91.201	1.79	954.993	0.14	10000.000	0.00
0.091	0.34	0.955	1.49	10.000	2.08	104.713	1.74	1096.478	0.00		
0.105	0.41	1.096	1.54	11.482	2.09	120.226	1.69	1258.925	0.00		

Appendix 7 MRI scanning program

##TITLE=Parameter List

##JCAMPDX=4.24

##DATATYPE=Parameter Values

##ORIGIN=Bruker BioSpin MRI GmbH

##OWNER=gruwelm

$$ /opt/pv/data/gruwelm/nmr/fil080410.1z1/85/method

##$Method=MSME

##$PVM_EchoTime=14.000

##$PVM_RepetitionTime=1500.000

##$PVM_NAverages=1

##$PVM_NRepetitions=1

##$PVM_ScanTimeStr=(16)

<0h8m0s0ms>

$$ @vis= Method PVM_EchoTime PVM_RepetitionTime PVM_NAverages

PVM_NRepetitions

##$PVM_UserType=Expert_User

##$PVM_DeriveGains=No

##$PVM_SliceBandWidthScale=85

##$ExcPulseEnum=hermite

$$ @vis= PVM_ScanTimeStr PVM_UserType PVM_DeriveGains PVM_SliceBandWidthScale

##$ExcPulse=(2.000, 2700.0, 90.0, 23.0, 100.00, 0.00, 100.00, LIB_EXCITATION,

<hermite.exc>, 5400.000000, 0.219734, 50.000000, 0.409600, conventional)

##$RefPulseEnum=hermite

##$RefPulse=(1.267, 2699.3, 180.0, 13.0, 100.00, 0.00, 100.00, LIB_REFOCUS, <

hermite.rfc

>, 3420.000000, 0.219734, 0.000000, 0.409600, conventional)

##$PVM_Nucleus1Enum=1H

$$ @vis= ExcPulseEnum ExcPulse RefPulseEnum RefPulse RF_Pulses

##$PVM_Nucleus1=(8)

<1H>

##$PVM_NEchoImages=1

##$constNEchoes=Yes

##$nEchoesPerEchoImage=(1)

1

$$ @vis= PVM_Nucleus1Enum PVM_Nucleus1 Nuclei PVM_NEchoImages constNEchoes

##$NEchoes=1

##$EffectiveTE=(1)

14.00

##$FitFunctionName=(32)

<No Function Defined>

##$ProcessingMacro=No

##$PVM_EffSWh=50000.0

##$PVM_ReadDephaseTime=1

$$ @vis= nEchoesPerEchoImage NEchoes EffectiveTE Echoes PVM_EffSWh

##$PVM_2dPhaseGradientTime=1

##$SliceSpoilerDuration=1.00

##$SliceSpoilerStrength=40.0

$$ @vis= PVM_ReadDephaseTime PVM_2dPhaseGradientTime SliceSpoilerDuration

##$PVM_GeoMode=GeoImaging

##$PVM_SpatDimEnum=2D

##$PVM_Isotropic=Isotropic_None

$$ @vis= SliceSpoilerStrength Sequence_Details PVM_GeoMode PVM_SpatDimEnum

##$PVM_Fov=(2)

32.000 32.000

##$PVM_FovCm=(2)

3.200 3.200

##$PVM_SpatResol=(2)

0.100 0.100

##$PVM_Matrix=(2)

320 320

##$PVM_MinMatrix=(2)

32 32

##$PVM_MaxMatrix=(2)

2048 2048

$$ @vis= PVM_Isotropic PVM_Fov PVM_SpatResol PVM_Matrix PVM_MinMatrix

##$PVM_AntiAlias=(2)

1.000 1.000

##$PVM_MaxAntiAlias=(2)

4.000 8.000

##$PVM_SliceThick=1.000

$$ @vis= PVM_MaxMatrix PVM_AntiAlias PVM_MaxAntiAlias StandardInplaneGeometry

##$PVM_ObjOrderScheme=Interlaced

##$PVM_ObjOrderList=(16)

0 2 4 6 8 10 12 14 1 3 5 7 9 11 13 15

##$PVM_NSPacks=1

##$PVM_SPackArrNSlices=(1)

16

$$ @vis= PVM_SliceThick PVM_ObjOrderScheme PVM_ObjOrderList PVM_NSPacks

##$PVM_SPackArrSliceOrient=(1)

axial

##$PVM_SPackArrReadOrient=(1)

L_R

##$PVM_SPackArrReadOffset=(1)

0.000

$$ @vis= PVM_SPackArrNSlices PVM_SPackArrSliceOrient PVM_SPackArrReadOrient

##$PVM_SPackArrPhase1Offset=(1)

-0.100

##$PVM_SPackArrPhase2Offset=(1)

0.000

##$PVM_SPackArrSliceOffset=(1)

-1.700

$$ @vis= PVM_SPackArrReadOffset PVM_SPackArrPhase1Offset

##$PVM_SPackArrSliceGapMode=(1)

non_contiguous

##$PVM_SPackArrSliceGap=(1)

0.000

##$PVM_SPackArrSliceDistance=(1)

1.000

$$ @vis= PVM_SPackArrSliceOffset PVM_SPackArrSliceGapMode

PVM_SPackArrSliceGap

##$PVM_SPackArrGradOrient=(1, 3, 3)

1.000000000000000 0.000000000000000 0.000000000000000 -0.000000000000000

1.000000000000000

0.000000000000000 0.000000000000000 0.000000000000000 1.000000000000000

##$NDummyScans=2

##$PVM_TriggerModule=Off

$$ @vis= PVM_SPackArrSliceDistance StandardSliceGeometry NDummyScans

##$PVM_FatSupOnOff=Off

##$PVM_MagTransOnOff=Off

##$PVM_FovSatOnOff=Off

##$PVM_InFlowSatOnOff=Off

$$ @vis= PVM_TriggerModule PVM_FatSupOnOff PVM_MagTransOnOff

PVM_FovSatOnOff

##$PVM_MotionSupOnOff=Off

##$PVM_FlipBackOnOff=Off

##$PVM_EchoTime1=14.0

$$ @vis= PVM_InFlowSatOnOff PVM_MotionSupOnOff PVM_FlipBackOnOff Preparation

##$PVM_EchoTime2=14.0

$$ @vis= PVM_EchoTime1 PVM_EchoTime2 MethodClass

##END

Appendix 8 FTIR method

FTIR instrument: Bruker Tensor 27

Procedure: approximately 4.5 mg of sample was mixed with approx. 150 mg of KBr and pressed into a 13mm IR pellet. A background spectra was collected prior to each sample spectra. Both background and sample spectra used scantimes of 100 scans. Spectral range was 4000 cm^{-1} to 400 cm^{-1}. All results are baseline corrected.

Samples were prepared using stock KBr that is stored in a warming oven at 100+ degrees C. One spectra was collected for each sample immediately following pellet preparation. The pellets were placed in the warming oven over the weekend to drive off any absorbed water and a second spectra was then collected for each sample.
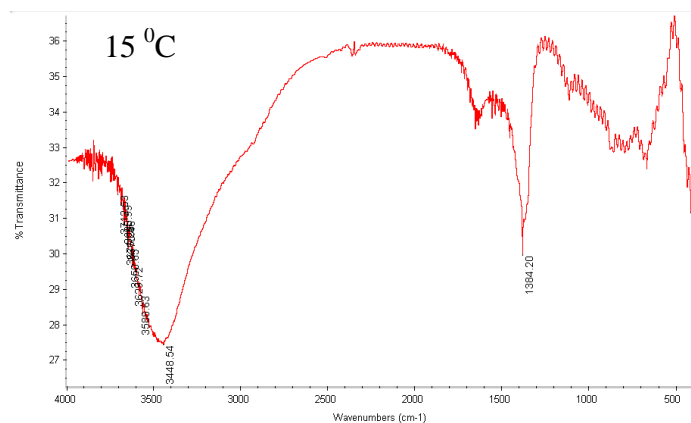
Naming conventions for the spectra files are as follows:

VW-I_KBr.dpt: sample I; baseline corrected; collected when KBr pellet was made.

VW-II_KBr.dpt: as above, for sample II.

VW-I_KBr_H.dpt: sample I; baseline corrected; spectra collected after heating ("_H")

VW-II_KBr_H.dpt: as above, for sample II
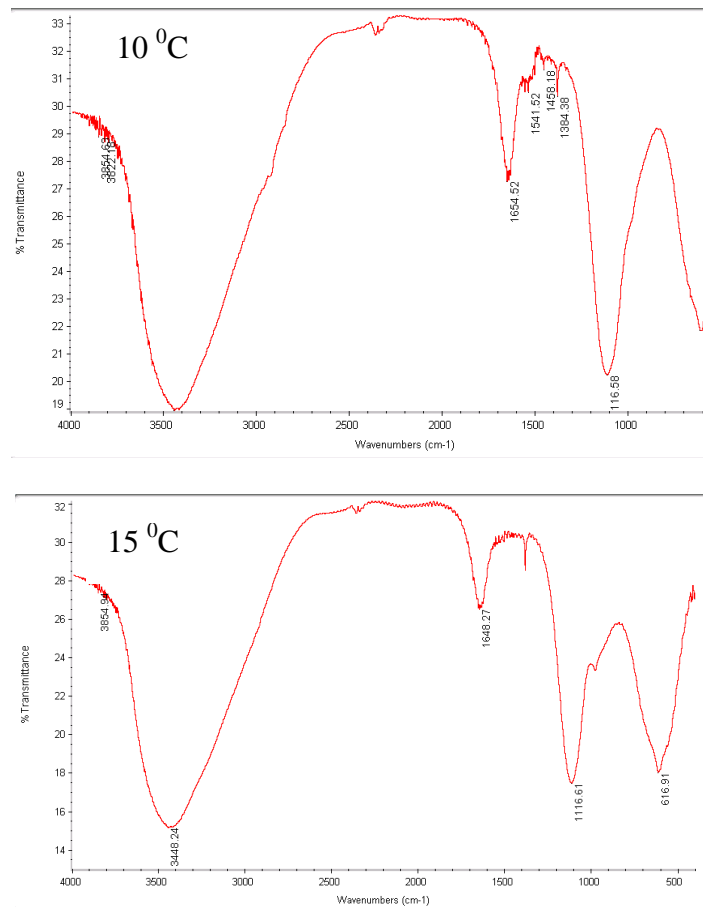
FTIR images of the electrode precipitates at different temperatures

Appendix 9 SEM Elemental analysis program

LT: 60.82   RT: 62.87   DT: 3.3 %

Calibrations:

Energy = 1.308E-08 +1.000E-02 * Ch (keV)

Efficiency = A*Exp((-T1*U1-T2*U2-T3*U3-T4*U4-DL*U5) / Cos(AI))*

(1-Exp(-DI*U5/Cos(AI)))

where E is Energy in keV

where the Ui are the appropriate linear mass absorption coefficients and

Geometry Factor (A):   1.62E-04   Be Window (T1):   0.300 um

Detector Thickness (DI)   0.250 cm   Au Window (T2):   0.020 um

Detector Dead Layer (DL): 0.300 um   Al Window (T3):   0.040 um

Det. Incident Angle (AI): 0.000 deg

Additional Detector Parameters

Det. Takeoff Angle: 40.000 deg

Detector ID: Generic Be

Detector Material: Si(Li)   Detector Shape: Planar

Detector Diameter: 0.356 cm   Source Dist.:   7.000 cm

Resolution = Sqr(23447.7 + 2242.9 * (E - 5.894)) / 1000

FWHM at 5.894 keV = 0.153 keV

Presets

Presets are :   Off

Preset Live Time: 100 secs   Preset Real Time: 180 secs

Preset Peak: 0

Preset Integral of All ROIs: 0

Tool Setup

Application Type: Electron Beam Excited

Peak Finder Mode: Low Peak to Bkg

Peak Power: 128   Peak Integral: 1024

Low Energy Cutoff: 0.000 keV   Stat Uncert. Cutoff: 0.500

Minimum Line Intensity: 0.100

ROI Width: 2.2 * FWHM   BKG Width: 1 Chan

Background Width: 1 Chan   Background Gap: 0.0 * FWHM

BKG Gap: 0 * FWHM

Energy Match Equation: 4.00E-02 + 0.000 * E

MDL Constants: Ka = 2.710   Kb = 4.650

EDS Analysis Models

Mass Absorption: Henke & Gullikson

Absorption: Philibert (w/ Duncumb & Heinrich modifications)

K Flourescence Yield: Bambynek et al. (1972)

L Flourescence Yield: Bambynek et al. (1972)

M Flourescence Yield: Bambynek et al. (1972)

Mean Ionization Pot.:   Berger & Seltzer (1969)

Stopping Power: Thomas (1964)

Jumps: ANS Database

K Shell Cross Section: Zaluzec (1978)

L Shell Cross Section: Zaluzec (1978)

Backscatter Factor: Duncumb (1991)

Peak Intensity Calc.:   Overlap Corrected Net

Hardware Parameters

Hardware Device: SYS8004:01 at Bus Address 0 Unit 0

Connected as Port: 0 using device handle 0

Device type is   100

High Voltage: 0, On   Bias Set Point: 600

Bias Control Flags: 0xFF0

Amp Coarse Gain: 32   Amp Fine Gain: 1.005

Amp Shaping Type: Triangular   Amp Shaping Time: 3.00 usec

Amp Pole Zero: 0.0 %   Amp Fast Thresh: 0.0 %

Amp Input Polarity: Pos   Amp Pile Up Rejection: Neg

Amplifier Control Flags: 0xB9

ADC Group Size: 1,024   ADC Conversion Gain: 1,024

ADC Lower Level Disc: 0.00 %   ADC Upper Level Disc: 100.00 %

ADC Digital Offset: 0   ADC Zero: 0.00 %

Dead Time Correction Mode: External   ADC Gate Mode: Off

ADC Operation Mode: PHA

ADC Conversion Mode: Linear   ADC Pile Up Rejector: Neg

ADC Sync Mode: Internal   External ADC Control Word: 0x0

Stabilizers

Type	Status	Range	Offset	Start Ch	End Ch	Assoc. ROI
Gain	Off	±12.5%	0.00	0	0	0
Gain	Off	±12.5%	0.00	0	0	0

Additional Microscope Parameters

Beam Incident Angle: 0.00   Sample X Tilt: 0.00

Working Distance: 3.90 cm   Detector Height: 3.90 cm

Beam Energy: 15.00 keV   Beam Current: 20.00 nA

Z Element Line	Compound	K-Ratio	Concentration		
			wt%	at%	Cmpd wt%
13 Al KA1 @ 1.487		0.6206	64.586	68.183	64.586
15 P KA1 @ 2.013		0.0589	8.262	7.595	8.262
16 S KA1 @ 2.307		0.2038	26.747	23.749	26.747
14 Si KA1 @ 1.740		0.0000	0.000	0.000	0.000
12 Mg KA1 @ 1.254		0.0041	0.405	0.474	0.405
		Total	100.000	100.000	100.000

Z Element Line	Gross (cps)	Bkg (cps)	Overlap (cps)	Net (cps)	Stat. Unc. (cps)	(%)
13 Al KA1 @ 1.487	282.966	26.948	0.001	256.017	2.257	0.9
15 P KA1 @ 2.013	49.671	30.714	0.001	18.957	1.150	6.1
16 S KA1 @ 2.307	93.341	28.642	0.040	64.648	1.416	2.2
14 Si KA1 @ 1.740	30.056	30.072	0.096	0.000	0.994	
12 Mg KA1 @ 1.254	22.230	20.372	0.111	1.719	0.837	48.7

Z Element Line	Z Corr	A Corr	F Corr	Tot Corr	Concentration wt%	at%
13 Al KA1 @ 1.487	1.004	1.049	0.987	1.0406	64.586	68.183 E
15 P KA1 @ 2.013	1.011	1.420	0.977	1.4032	8.262	7.595 E
16 S KA1 @ 2.307	0.987	1.330	1.000	1.3127	26.747	23.749 E

14 Si KA1 @ 1.740   0.977   1.640   0.981   1.5727   0.000   0.000 E

12 Mg KA1 @ 1.254   0.975   1.115   0.902   0.9798   0.405   0.474 E

<div align="center">Total   100.000 100.000</div>

Appendix 10 Modelling of Nitrate, Nitrite and Ammonium production Kinetics

Equations:

Nitrate $= 40 * e^{-k1 * t}$

Nitrite $= k_1 * 40 * \dfrac{e^{-k_2 * t} - e^{-k1 * t}}{k_1 - k_2}$

1. To find K1 and K2 based on the following data:

t (min)	Nitrate	Nitrite
0	40	0
5	35.9	2.3
10	31.8	3.7
15	29.3	4.7
30	18.9	5.6
45	15.4	4.4
60	11.8	3.2
75	9.5	1.9
90	8.2	1.6
105	4.8	0.8
120	3.8	0.7
135	3.4	0.8

150	1.9	0.3
165	2.9	0.4
180	2.1	0.2

Solution:

a). For Nitrate:

1). Parameter result
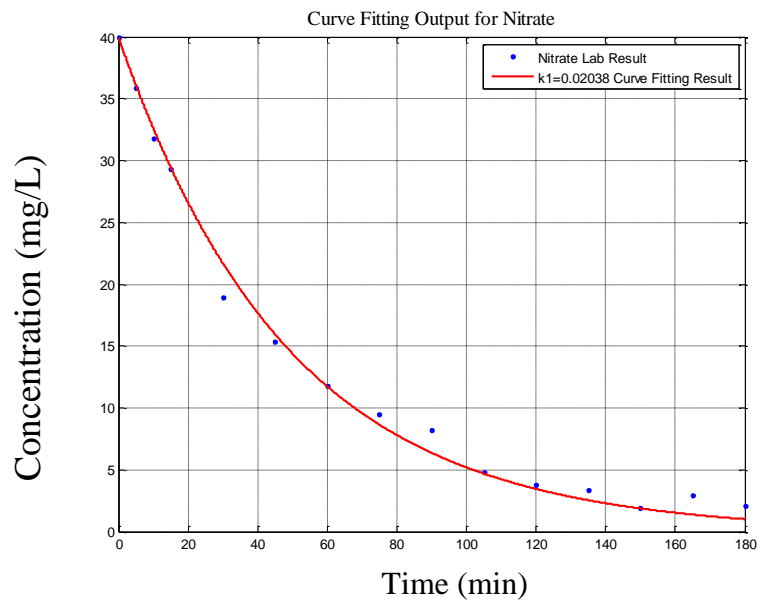
cfun(x) = 40.*exp(-k1.*x)

Coefficients (with 95% confidence bounds):

k1 =   **0.02038** (0.01906, 0.02171)

2). Curve fitting output

The related curving fitting output is showed below:

Curve Fitting Output for Nitrate

3).Related MATLAB codes:

```
a=fittype('40.*exp(-k1.*x)');
x=t;
y=nitrate;
```

```
plot(x,y,'.');
[cfun,gof]=fit(x,y,a);
x1=min(x):0.01:max(x);
yy=40.*exp(-cfun.k1.*x1);
hold on
plot(x1,yy);
```

b). For Nitrite:

1). Parameter result

If we fix the k1=0.02038 (The same as Nitrate), we can get:
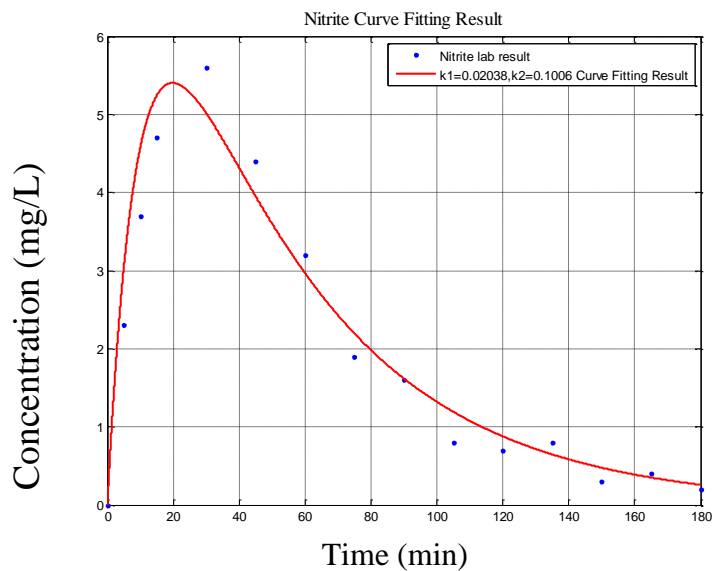
cfun =

General model:

cfun(x) = 0.02038.*40.*(exp(-k2.*x)-exp(-0.02038.*x))./(0.02038-k2)

Coefficients (with 95% confidence bounds):

k2 =   0.1006 (0.09073, 0.1104)

2). Curve fitting output

The related curve fitting output is showed below:

3) Related MATLAB codes:

```
a=fittype('0.02038.*40.*(exp(-k2.*x)-exp(-0.02038.*x))./(0.02038-k2)');
x=t;
y=Nitrite;
plot(x,y,'.');
[cfun,gof]=fit(x,y,a);
x1=min(x):0.01:max(x);
yy=0.02038.*40.*(exp(-cfun.k2.*x1)-exp(-0.02038.*x1))./(0.02038-cfun.k2);
hold on
plot(x1,yy);
```

2. To find k1 and k2 based on the following data:

T (min)	Nitrate	Nitrite
0	40	0
5	37.7	1.5
10	36.8	1.8
15	34.9	1.9
30	32.5	2.6
45	29.4	2.8
60	24.9	3.4
75	23.7	2.7
90	21.4	2.5
105	19.1	1.6
120	17.3	1.8
135	15.6	1.5
150	12.8	1.3
165	12.1	1.4

180	12.3	0.8

Solution:

a). For Nitrate:

1). Parameter result

cfun =

    General model:

    cfun(x) = 40.*exp(-k1.*x)

    Coefficients (with 95% confidence bounds):

k1 =   **0.00711** (0.006871, 0.007349)

2). Curve fitting output

The related curving fitting output is showed below:

3) Related MATLAB codes:

```
a=fittype('40.*exp(-k1.*x)');
x=t;
```
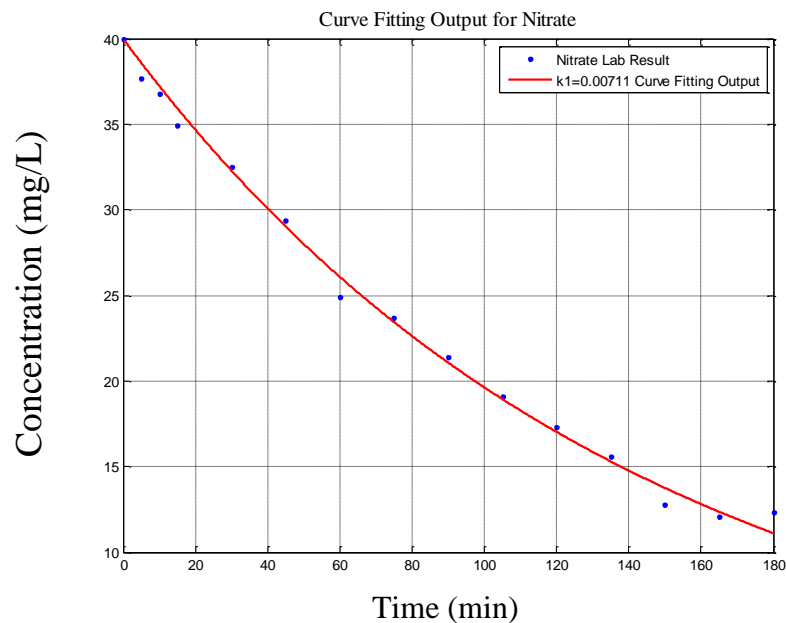
y=nitrate;
plot(x,y,'.');
[cfun,gof]=fit(x,y,a,'start',0.007);
x1=min(x):0.01:max(x);
yy=40.*exp(-cfun.k1.*x1);
hold on
plot(x1,yy);

b). For Nitrite:

1). Parameter result
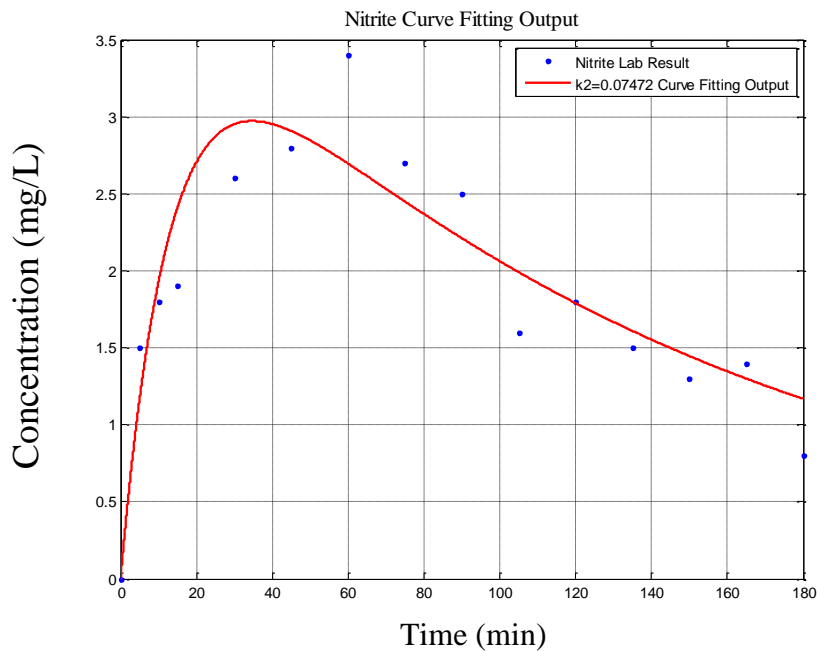
cfun =

   General model:

   cfun(x) = 0.00711.*40.*(exp(-k2.*x)-exp(-0.00711.*x))./(0.00711-k2)

   Coefficients (with 95% confidence bounds):

   k2 =   0.07472 (0.06752, 0.08193)

2). Curve fitting output

The related curve fitting output is showed below:

3) Related MATLAB codes:

a=fittype('0.00711.*40.*(exp(-k2.*x)-exp(-0.00711.*x))./(0.00711-k2)');

```
x=t;
y=Nitrite;
plot(x,y,'.');
[cfun,gof]=fit(x,y,a,'start',0.074);
x1=min(x):0.01:max(x);
yy=0.00711.*40.*(exp(-cfun.k2.*x1)-exp(-0.00711.*x1))./(0.00711-cfun.k2);
hold on
plot(x1,yy)
```